FOLLICULAR DENDRITIC CELL DISRUPTION AS A NOVEL MECHANISM OF VIRUS-INDUCED IMMUNOSUPPRESSION

Eleonora Melzi

Submitted in fulfilment of the requirements for the degree of
Doctor of Philosophy in Infection and Immunity

Institute of Infection, Immunity & Inflammation
College of Medical, Veterinary & Life Sciences
University of Glasgow

January, 2017

Abstract

Arboviruses (Arthropod-borne viruses) cause acute diseases that are increasingly affecting both human and animal health. Currently, there is a critical lack of understanding about the nature of arbovirus-host interactions in the lymph nodes (LNs), the place where the adaptive immune response is initiated and shaped. In this study, we used bluetongue virus (BTV) and its natural sheep host, to characterise the early events of an arbovirus infection with particular focus on the LNs. Our findings reveal a previously uncharacterized mechanism used by an arbovirus to manipulate host immunity. This study shows that BTV, similarly to other antigens delivered through the skin, is transported rapidly via the lymph to the peripheral lymph nodes. Here, BTV infects and disrupts the stromal network of marginal reticular cells and follicular dendritic cells composing the scaffolding of the follicular area. These cells contribute to antigen presentation and affinity maturation of B-cells for the production of antibodies. Consequently, we observed a loss of germinal centre structure, which hinders B-cell proliferation. This process results in a delayed production of high affinity and virus neutralizing antibodies that is directly related to the virulence of the BTV strain used and the severity of disease. Moreover the humoral immune response to a different antigen is also hampered in BTV-infected animals. Our data show that an arbovirus can evade the host antiviral responses by inducing an acute immunosuppression. Although transient, this immunosuppression occurs at the critical early stages of infection when a delayed host humoral immune response likely affects virus systemic dissemination and the clinical outcome of disease.

Table of contents

List of Tables

List of figures

List of accompanying material

The following publication, resulting from the work carried out in this project, is attached to this thesis:

Melzi, E., Caporale, M., Rocchi, M., Martín, V., Gamino, V., di Provvido, A., Marruchella, G., Entrican, G., Sevilla, N. and Palmarini, M. (2016) 'Follicular dendritic cell disruption as a novel mechanism of virus-induced immunosuppression', *Proceedings of the National Academy of Sciences*, 113(41), pp. E6238–E6247. doi: 10.1073/pnas.1610012113.

To my aunt Ketty,
for her example
and her fight

Acknowledgements

First and foremost I offer my sincerest gratitude to my supervisor, Prof Massimo Palmarini, who has supported me throughout my PhD with his patience, guidance and positivity whilst allowing me to follow my own intuitions.

The Centre for Virus Research became my second home and provided the equipment I have needed to produce and complete my work while the WB Martin scholarship has funded my studies. I thank all the scientists who have made this work possible. In particular, Marco Caporale at the IZS dell'Abruzzo e del Molise (Italy), and Noemi Sevilla at CISA-INIA (Spain) and their teams who handled the animals included in this study. I hope I made a good use of the lives that I have taken.

I am in debt to my co-supervisor Mara Rocchi that have incessantly believed in me and provided invaluable support and knowledge. I thank my co-supervisor Gary Entrican for his insights in veterinary immunology.

A special thanks is for Filipe Nunes and Gaelle Gonzalez, for the countless discussions about ideas, projects and issues, you have pushed forward my science and have become the North and the South Pole of my compass. Once you left, I had to learn how to sail alone.

I am grateful to all the present and past members of the Palmarini lab who have shared both hard work and fun: Mariana, Andrew, Meredith, Aislyn, Maxime, Gerald, Filipe, Karen, Matt, Alice, Ilaria, Julien, Rute, Jin, Ania, Catrina and Alex each of you taught me something, on the bench and beyond. Thanks to NS5. A personal thanks must go to Andrew for his relentless contagious optimism and his ISGs. I am also particularly grateful to the Angels, you girls have been the best companions for this adventure. I need also to thank Virginia and Keziah, who taught me to let it go. As a side note, I would also like to thank the interferon that for once decided to step aside, and let the adaptive immunity be the leading actor in virology.

In my daily work I have been blessed with a friendly and cheerful group of fellow students. Fiona, Gail and Joanna who shared the cool office (clearly named after the ventilation), which provided the warmest welcome to Glasgow and the perfect balance between friendship and research. I thank especially Caroline her strength and friendship. Navapon and Idoia for their wisdom, Kathryn for her hyperactivity that kept me going, and all the Phoenix bar users for the stimulating conversations.

I thank deeply my family, my brothers and sister, an inexhaustible source of laughter and support.

Finally, a huge 'thank you' to the man who lived all the PhD process day-by-day on my side, embarked with me on this emotional rollercoaster...and survived! For his loving support and understanding. Always managing to steal a smile. It is almost done my dear, but I will still be crazy, I am afraid.

Author's Declaration

I, Eleonora Melzi, declare that, except where explicit reference is made to the contribution of others, that this thesis is the result of my own work and has not been submitted for any other degree at the University of Glasgow or any other institution.

Printed name _____

Signature _____

Abbreviations

Ab	Antibody
ADCC	Antibody-dependent cell mediated cytotoxicity
AI	Avidity index
APC	Antigen presenting cells
ASC	Antibody secreting cells
BAFF	B-cell activating factor
BCR	B-cell receptor
BSAP	B-cell specific activator protein
BSL-3	Biosafety level 3 laboratory
BTV	Bluetongue virus
CD	Cluster of differentiation
CLSM	Confocal laser scanning microscopy
CPE	Cytopathic effect
CT	Cycle threshold
CTL	Cytotoxic T-lymphocytes
DAPI	4',6-diamidino-2-phenylindole
DAB	3,3' Diaminobenzidine
DAPI	4',6-diamidino-2-phenylindole
DC	Dendritic cell
DC-Lamp	Dendritic cell-lysosomal associated membrane protein
DIC	Disseminated intravascular coagulopathy
DMSO	Dimethyl sulfoxide

DPI	Days post-infection
DPIM	Days post-immunization
DZ	Dark zone
EDTA	Ethylenediaminetetraacetic acid
ELISA	Enzyme linked immunosorbent assay
EM	Electron microscopy
FBS	Foetal bovine serum
FDC	Follicular dendritic cells
FRC	Fibroblastic reticular cells
GC	Germinal centre
HEV	High endothelial venules
HIER	Heat induced epitope retrieval
HIGM	Hyper IgM syndrome
Hpi	Hours post-infection
ICAM-1	Intercellular Adhesion Molecule 1
ID	Intradermal
IFN	Interferon
IFNAR	Interferon alpha/beta receptor
IHC	Immunohistochemistry
IL	Interleukin
LCMV	Lymphocytic choriomeningitis virus
LN	Lymph node
LT	Lymphotoxin

LZ	Light zone
MHC-II	Major histocompatibility complex class 2
MOI	Multiplicity of infection
MRC	Marginal reticular cells
n	number
NK	Natural killer
NTC	No template control
OD	Optical density
OIE	World Organisation for Animal Health
OVA	Ovalbumin
PBMC	Peripheral blood mononuclear cells
Pi	Post infection
PCR	Polymerase chain reaction
PD50	protective dose 50
PFU	Plaque forming unit
PIER	Proteinase induced antigen retrieval
PLVAP	Plasmalemma Vesicle Associated Protein
PP	Peyer patches
qPCR	Quantitative polymerase chain reaction
RNA	Ribonucleic acid
RT	Reverse transcription
SCS	Subcapsular sinus
SMA	Smooth muscle actin

$TCID_{50}$	Median tissue culture infective dose
TH	T-cell helper
TLR	Toll-like receptor
TMB	3,3',5,5'-Tetramethylbenzidine
VIB	Viral inclusion body
VWF	Von Willebrand factor

Chapter I

Introduction

1 Introduction

1.1 Bluetongue

Bluetongue is one of the main vector-borne diseases affecting ruminants. It is caused by bluetongue virus (BTV) a double stranded RNA virus classified within the family *Reoviridae*, genus *Orbivirus*. BTV is transmitted through the bite of blood feeding insects of the *Culicoides* genus. The range of susceptible hosts to BTV includes both wild and domestic ruminants. In most cases BTV infection is asymptomatic or results in a mild clinical disease. However, in some occasions, bluetongue can evolve towards a severe haemorrhagic fever with poor prognosis.

1.1.1 History of Bluetongue

The first report of an outbreak of Bluetongue was described in South Africa in 1905 by James Spreull (Spreull 1905) when Merino sheep were introduced for the first time into the region in the late 18th century. Probably the virus had been circulating in the indigenous ruminant population for a long time. The disease was originally called “epizootic catarrh” or “malarial catarrhal fever” and only later was named bluetongue after the Afrikaans “blaauwtong”, the term used by local people to describe the cyanotic tongue presented by severely affected sheep. Until 1920s bluetongue remained confined to the African regions, then it made its first appearance in Cyprus in 1924 with recurrent outbreaks until 1943 (Gambles 1949). Soon after bluetongue was recognised as the causative agent of the “sore muzzle” in California in 1952 (Hardy & Price 1952). Thereafter, Bluetongue has been identified in in many regions of Africa, Americas, Australia and Europe. Currently only Antarctica is unaffected by Bluetongue.

Many of the initial seminal discoveries about BTV have been made at the Onderstepoort Veterinary Institute (OVI) in Pretoria, South Africa. In 1906, Sir Arnold Theiler was the first to demonstrate that the disease was caused by a filterable agent present in the blood of affected sheep, thus indicating that a virus was the etiological agent of bluetongue (Coetzee et al. 2012). Only few years later, Theiler obtained a crude blood vaccine that was obtained by passaging multiple times the virus in sheep (Theiler 1907), this attenuated virus

vaccine was extensively used in South Africa for over 40 years and could confer protection against several serotypes, although with some variability and failures.

Following the first reported infection, it was immediately clear that the disease was not contagious, as it could not be transmitted by close contact between healthy and diseased animals (Spreull 1905). However, blood, serum and spleen extracts from infected animals were recognised as a source of infection when inoculated in healthy animals, independently of the chosen routes (intravenous, subcutaneous, intradermal or intraperitoneal) (Spreull 1905). The observation that bluetongue occurred with a seasonal peak and that sheep could be protected by overnight stabling, led to the hypothesis that an arthropod vector could have been involved in the transmission cycle of the disease. In 1944 this suspecion was confirmed by Du Toit, which demonstrated that sheep developed bluetongue when inoculated with a suspension of adults *Culicoides imicola* caught in the wild. In addition, the same author also showed that the disease was reproduced when *Culicoides* were fed on infected sheep and subsequently allowed to fed on susceptible animals after an incubation period of 10 days (Du Toit 1944).

Given the unreliable protection conferred by Theiler's vaccine, the existence of a plurality of BTV serotypes was long hypothesized. However, it was demonstrated only many years later by Neitz, who established cross-protection serological test in sheep (Neitz 1948). This study confirmed that sheep, after recovering from BTV infection, acquired a lifelong protective immunity against the same serotype, but only a partial protection against different serotypes. An *in vitro* serum neutralization test was developed in the 1960s and led to the characterization of 12 different serotypes circulating in South Africa (Howell et al. 1970).

With the advent of laboratory techniques such as virus isolation and propagation in fertilised chicken eggs and later in cell culture, it become possible to start the production of more effective multivalent-vaccines, able to confer protection against different serotypes (Coetzee et al. 2012). Nowadays, the availability of reverse genetic and molecular biology techniques allow the production of recombinant vaccines (Calvo-Pinilla et al. 2014). However, despite the progress

in this area, a vaccine able to elicit a broad protection against the many existing BTV serotypes (currently 27 identified) is still not available.

1.1.2 Emergence of Bluetongue in Europe

BTV is widespread in tropical, subtropical and temperate zones of the globe. The disease is endemic mainly between latitudes 35°S and 40°N (Africa, Asia and South America), in areas where competent insect vectors are present. Several factors such as globalization, increase in international travelling and trades, movement of livestock, deforestation and climate change have been identified as facilitating the ongoing geographic expansion of competent insect vectors and the recent occurrence of bluetongue outbreaks in Northern Europe (MacLachlan et al. 2009; Mintiens et al. 2008; Purse et al. 2005). Hematophagous *Culicoides* insects are responsible for BTV transmission. More than 1000 species of *Culicoides* are present worldwide but only some of them have been identified as competent BTV vectors. The regional distribution of *Culicoides* varies and particular associations have been noticed between certain *Culicoides* species and specific BTV serotypes. The classical African-Asian vector for BTV is *Culicoides imicola*, which was absent in Europe until 1998 and it is now widely distributed in Mediterranean European regions. However, different Palearctic species, such as *Culicoides obsoletus*, *Culicoides pulicaris*, *Culicoides dewulfi*, *Culicoides scoticus*, and *Culicoides chiopterus*, seem to be responsible for BTV distribution in Northern Europe. Therefore, it is likely that the spread of BTV in Europe is the consequence of an adaptation of the virus to different vector species, living at colder temperatures. Similarly, in the Americas, BTV-10, 11, 13 and 17 are widely distributed in areas corresponding to the presence of *Culicoides sonorensis*. On the contrary, BTV-2 seems to be restricted to the Southern regions due to its adaptation to *Culicoides insignis*.

After its first description in South Africa, more than a century ago, the geographical distribution of BTV has been constantly expanding. The first severe outbreak in Europe occurred in 1956 in the Iberian Peninsula, where BTV-10 killed approximately 180,000 sheep (MacLachlan 2011; Sellers et al. 1978; Pérez de Diego et al. 2014). Following this outbreak, it became clear that BTV could become established in Europe. Therefore, as a precautionary measure, the World Organization for Animal Health (OIE) classified BT as a list "A" notifiable

disease, which includes veterinary diseases that have the potential for very serious and rapid spread, and which have serious socio-economic or public health consequence (OIE - World Organisation for Animal Health 2016a). This imposes severe limitation in trade and livestock movement in the affected country, in order to prevent the spread of the disease.

Before 1998, brief recurrent BT outbreaks have been observed in the Mediterranean regions of Europe, due mainly to livestock trade with the North African countries and wind-dispersal of infected midges across the Mediterranean Sea (Purse et al. 2005). Indeed, infected *Culicoides* can be passively disseminated with the wind for long distances (Carpenter et al. 2009). However, the pattern of BTV prevalence in Europe started to change radically in October 1998 (Figure 1-1), when BTV-9 was detected for the first time in the Greek Islands of Kos, Rhodes, Leros and Samos, close to the Turkish coast. From there, the outbreak expanded northward reaching Albania, Serbia, Bosnia, Croatia and Montenegro and westward into mainland Greece and Italy (Purse et al. 2005). BTV-1, 4 and 16 followed the same distribution route, reaching Italy, Corsica and the Balkan countries (MacLachlan 2011; Purse et al. 2005). Incursion of BTV-2 also occurred in 2000, spreading from Tunisia and Algeria into mainland Italy, and the islands of Sardinia, Sicily, Corsica and the Baleares. In addition, in 2004, BTV-4 reached the coast of Spain and Portugal from Morocco. From there on, BTV-1, BTV-2, BTV-4, BTV-9, and BTV-16 persisted in the southern European countries expanding the affected territories 800 km north from the usual localization (50°N) (Figure 1-1) (Saegerman et al. 2008).

In 2006, the first cases of Bluetongue were detected in Northern Europe, with numerous infected herds in the Netherlands and Belgium. The serotype responsible was readily identified as BTV-8, and subsequent sequence analysis indicated the presence of similarities of this strains with field isolates from the sub-Saharan Africa (Maan et al. 2008). The outbreak expanded rapidly, reaching during the same year France, Germany and Luxembourg. The outbreak halted during the winter, when the cold weather reduced the activity of *Culicoides*. However, the cold temperature did not manage to extinguish completely the outbreak and the following spring the virus resurfaced in all the affected countries as well as in Denmark, Switzerland and Czech Republic (Wilson &

Mellor 2009). In 2007 BTV made also its first appearance in the United Kingdom (Wilson & Mellor 2009).

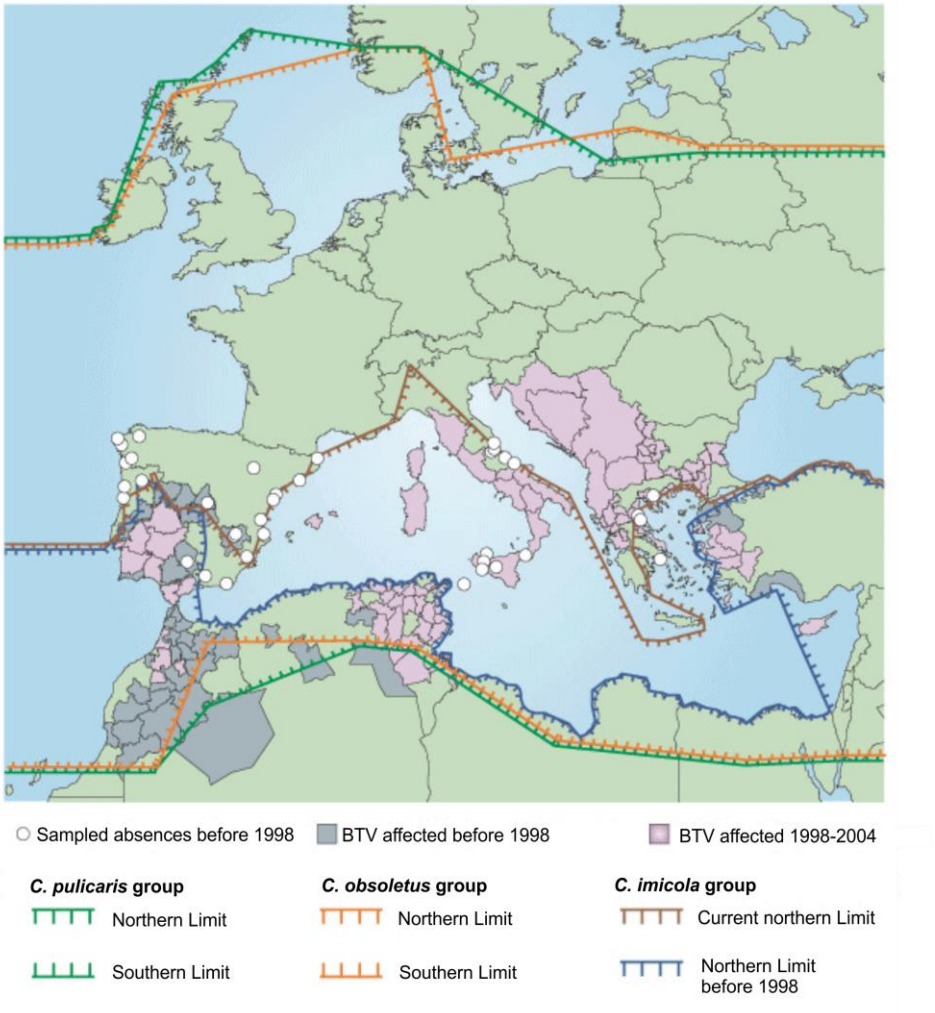

Figure 1-1 Map of *Culicoides* and BTV distribution in Europe
Map showing the distribution of BTV prior to 1998 (grey regions) and that of BTV since 1998 (up to November 2004, pink regions). Hatched lines indicate the approximate known northern and southern range limits of the three most important vector groups in Europe. Open circles indicate sites where *Culicoides imicola* was found to be absent before 1998. Picture adapted from: (Purse et al. 2005).

Inactivated vaccines against BTV-8, that were not available at the beginning of the European outbreak, started to be released on the market in early 2008 as a result of compulsory vaccination campaigns that limited significantly the propagation of disease. Only few cases of bluetongue were identified in 2008, when the virus reached Spain and Sweden (Roy et al. 2009; Wilson & Mellor 2009).

It has been estimated that the cost of the 2007-2008 outbreak in France, amounted to 1.4 billion dollars. Besides the direct economic losses due to decreased livestock productivity, the emergency containment measures imposed by the OIE to control the outbreaks had a big economic impact on the agricultural sector, generating significant economic losses to the European Union.

Many aspects of the 2007-2008 BTV-8 outbreak in Northern Europe were unusual. First, this was the first time that BTV spread and persisted for a long period of time at these latitudes. Secondly, the incursion route of this strain is still uncertain (Maan et al. 2008), since the Netherlands is located far from the BTV-8 endemic regions, and therefore it could not originate from the classical routes of introduction previously described for Mediterranean Countries. The possibility of its introduction with trade of African flowers and plants, carrying infected *Culicoides*, or the untracked, illegal introduction of livestock are options that have been considered but never confirmed (Mintiens et al. 2008).

Moreover, the BTV-8 strain responsible of the outbreak presented some unconventional features, displaying a highly virulent phenotype in sheep and inducing disease also in 10% of affected cattle, which generally are asymptomatic (Darpel et al. 2007; Elbers et al. 2008). Many reports highlighted the ability of this specific strain to cross the placental barrier between dam and foetus, allowing vertical transmission (Darpel et al. 2009; Santman-Berends et al. 2010; Dal Pozzo et al. 2009; Van Der Sluijs et al. 2013), a trait that has been generally associated solely with tissue culture adapted strains.

1.1.3 Overwintering and unconventional transmission routes

The transmission cycle of BTV can be maintained all year round in regions with mild winters like the tropics, whereas in temperate regions Bluetongue outbreaks generally appear in late summer to autumn, the period coinciding with the time of major activity of the competent vectors (White et al. 2005).

One of the unsolved mysteries of Bluetongue is where the virus “hides” during the cold months, when the temperature drops below the threshold of activity of

the arthropod vector, and virus replication in the midge cease (White et al. 2005; Carpenter et al. 2009). In temperate regions, transmission usually resumes after several months of quiescence, a period that is considered longer than the normal phase of infectious viraemia in the mammalian host and longer than the typical lifespan of the adult vector (Wilson et al. 2008). Plausible explanations have been proposed that includes host or vector related mechanisms.

Adult *Culicoides* tend to survive no longer than 10–20 days and they are not tolerant to sub-zero conditions. Although unlikely, it is possible that BTV could persist in long-lived adult *Culicoides* that manage to survive the winter, contradicting reports describe an extended survival of this species during mild winter seasons if they can find an indoor shelter (Gerry & Mullens 2000; Wilson et al. 2008). However, most of the *Culicoides* species survive the winter as larvae; hence a logical option would be the possibility of transmission of the virus from adult midges to their offspring through a transovarian infection. Despite the detection of BTV RNA, experimental studies have failed to detect infectious virus in *Culicoides* larvae (White et al. 2005; Nunamaker et al. 1990; Wilson et al. 2008).

Persistence of the virus in the mammalian host is another logical alternative. BTV infected animals develop long lasting viraemia. In blood, virus RNA detection, by means of qPCR, can give positive results in asymptomatic animals for a period of 7-8 months after initial infection. However, isolation of infectious virus from the blood is limited to the initial 2 months (Bonneau et al. 2002; Koumbati et al. 1999; Singer et al. 2001). After this period, the blood is not anymore considered as a source of infection for *Culicoides* (Bonneau et al. 2002; MacLachlan et al. 1994). These data suggest that it is unlikely that a ruminant host could function as a virus reservoir during the long time that elapses between two outbreaks. However, the presence of a chronic or latent infection in ruminants cannot be completely excluded (Wilson et al. 2008) for example in immunoprivileged sites in the host. This could give a relapse of infection and viraemia under certain circumstances, such as stressing conditions and immunosuppressive events. During an experimental BTV infection, it has been demonstrated that the virus could be recovered from $\gamma\delta$ T cells, isolated from peripheral blood samples from day 3 to 13 pi, when these cells were cultured in

presence of IL-2 (Takamatsu et al. 2003). T-cells did not show cytopathic effect and survived for long time in culture with constant viral production, hence it was hypothesized a role of γδ T-lymphocytes in the relapse of infection. However, contrary to the *in vitro* data, it was not possible to isolate infected γδ T-lymphocytes from sheep blood after the initial two weeks (Takamatsu et al. 2003). Hence, the relevance of these observations *in vivo* would require further investigation.

BTV transplacental and sexual transmission through the semen has generally been exclusively attributed to culture-adapted strain. A study in 1979, using tissue culture adapted strains, showed that sheep infected at mid-gestation with BTV serotype 4 and 16 produced clinically normal lambs that were viraemic for 2 months after birth (Gibbs et al. 1979). Only recently, investigation of the BTV strain involved in the Northern Europe outbreak, has demonstrated transplacental transmission of BTV-8 and BTV-2 minimally passaged in tissue culture (Rasmussen et al. 2013). If confirmed, these observations indicate that vertical transmission could contribute to the long-term persistence in a asymptomatic host and the perpetuation of infection. In addition, bulls and rams can occasionally shed virus with semen, although this seems to happen only in concomitance with viraemia, and this could potentially contribute to the venereal transmission of BTV (Gu et al. 2014; Kirkland et al. 2004). Currently, trade regulations require that breeding animals test negative for BTV before the export of semen.

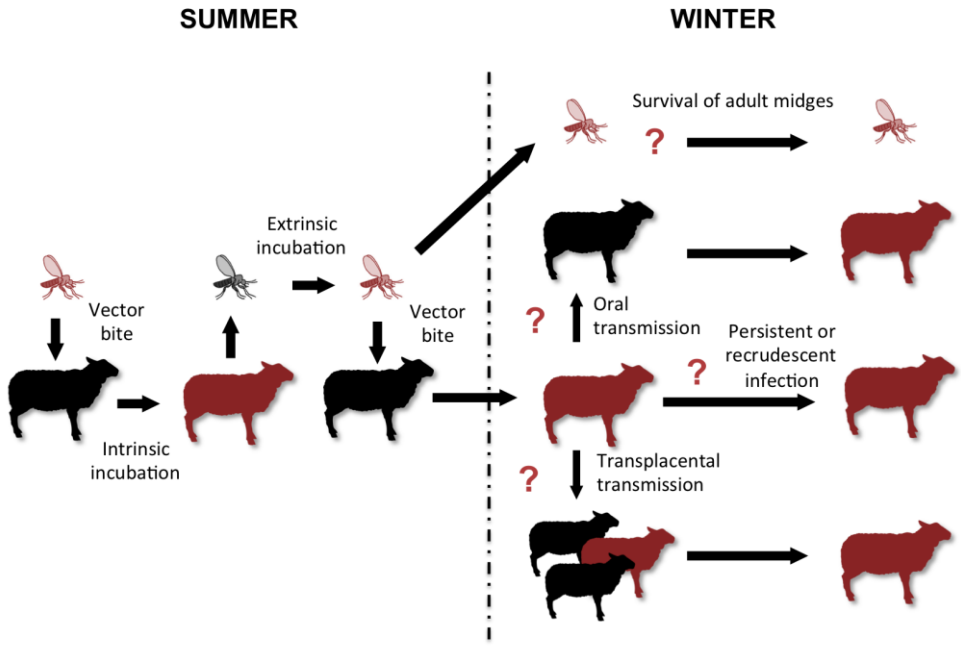

Figure 1-2 Bluetongue virus transmission in summer and winter.
In summer, there is alternative transmission between mammalian host and arthropod vector. During winter, various mechanisms of viral persistence have been hypothesised. Figure modified from (Wilson et al. 2008).

There is also the possibility that BTV overwintering relies on the presence of unidentified animal reservoirs, such as small rodents, although currently these are only speculation (MacLachlan 2011). It is important to note that BTV neutralising antibodies have been found with high prevalence in wild African carnivores, such as lions, hyenas and wild dogs, and in domestic dogs and cats (Alexander et al. 1994). These carnivores likely contracted BTV through ingestion of infected ruminants carcasses, since the lack of seroconversion in smaller predators (jackals and mongoose) sharing the same environment rules out a transmission through the arthropod vector (Alexander et al. 1994). Similarly, in 1992 a canine vaccine accidentally contaminated with BTV serotype 11 was administered to domestic dogs, causing severe disease and abortion in pregnant bitches. BTV was found in lung capillaries of the affected animals causing a lethal pulmonary ooedema (Brown et al. 1996) indicating that, under specific circumstances, this species could host the virus. However, the

epidemiological relevance of these observation together with an in depth analysis of BTV infection in carnivores is still missing.

Circumstantial evidence are available for a wide variety of overwintering mechanisms, however the lack of substantial experimental and field-collected data do not provide enough support for any of the proposed mechanism. The establishment of a proper surveillance plan would certainly help in identifying which are the risks factors and the animal species involved in BTV epidemiology.

1.2 Bluetongue virus (BTV)

BTV is an Orbivirus of the family of *Reoviridae*, a widely distributed group of viruses infecting humans and other mammals (Rotaviruses, Orbiviruses, Seadornaviruses and Orthoreoviruses), fish (Aquareoviruses), birds (Orthoreoviruses), insects (Cypoviruses and Idnoreoviruses), plants (Oryzaviruses, Fijiviruses and Phytoreoviruses) and fungi (Mycoreoviruses) (Figure 1-3) (Roy et al. 2009).

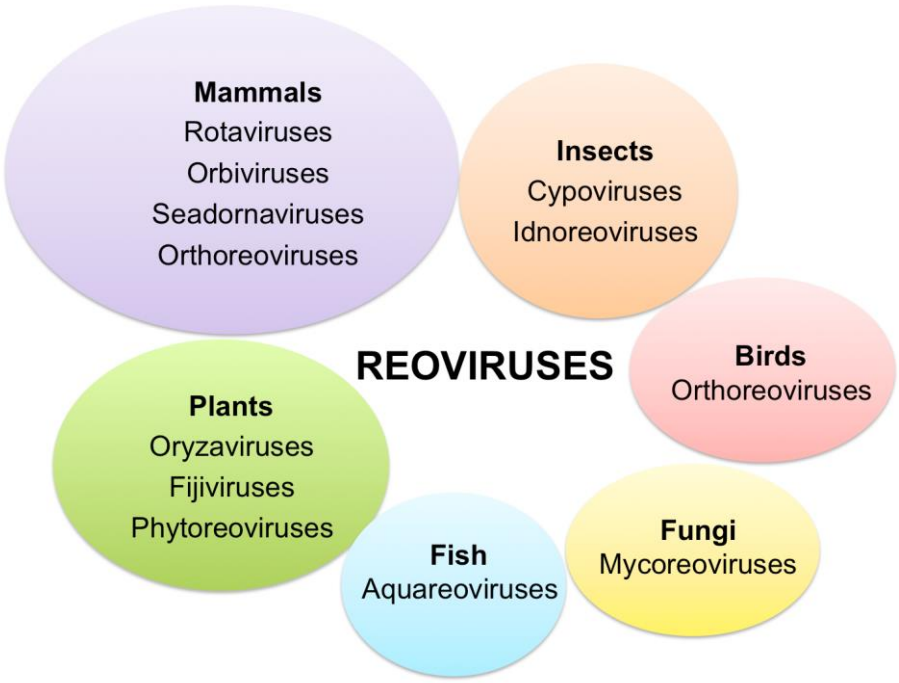

Figure 1-3 Reoviridae family, genus and host range.

Within the genus Orbivirus are included 22 virus species (representing 22 distinct virus serogroups) that have been recognized by the International Committee for the Taxonomy of Viruses (ICTV). Recently, phylogenetic comparisons of isolates from different Orbivirus species, with 'unclassified' isolate, have led to proposals to ICTV for recognition of seven additional species (Belaganahalli et al. 2015). All orbiviruses are transmitted by hematophagous arthropod vectors, which include *Culicoides*, ticks and mosquitos (Figure 1-4). The range of susceptible mammalian hosts is wide and collectively includes domestic and wild ruminants, equines, marsupials, sloths, bats, birds and humans.

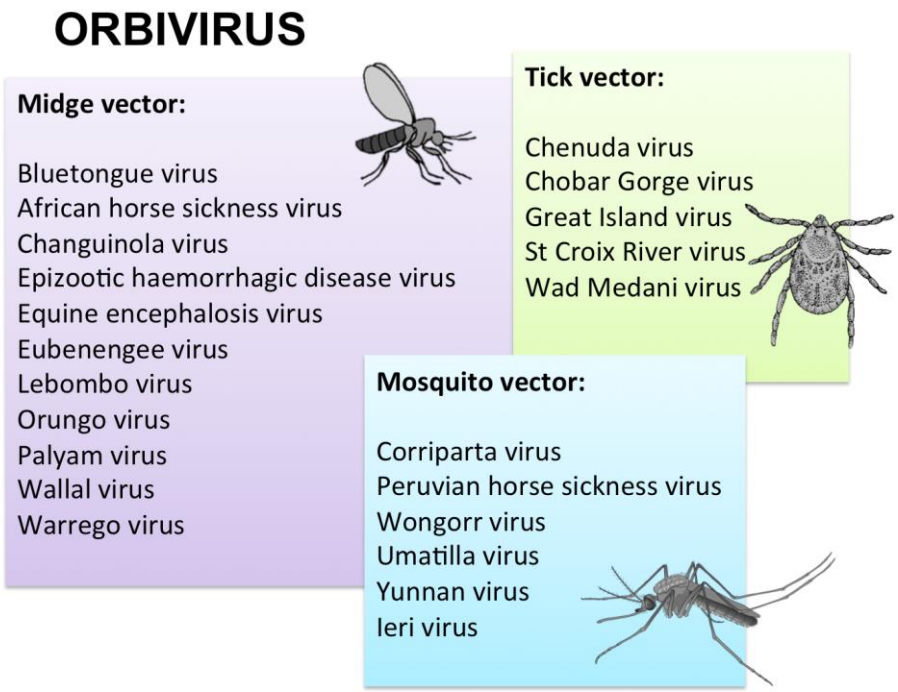

Figure 1-4 Orbiviruses and their vectors.
The genus Orbivirus includes 22 species that can be transmitted by different hematophagous arthropods vectors.

The structure of the BTV virion has been investigated in detail in several studies (Verwoerd et al. 1972; Prasad et al. 1992; Grimes et al. 1998). BTV is a non-enveloped double stranded RNA virus (dsRNA virus) with icosahedral structure, of about 80 nm in diameter. The capsid is composed of 3 protein layers containing

the genome of the virus formed by 10 linear segments of dsRNA encoding for 7 structural proteins (VP1 to VP7) and 4 non-structural proteins: NS1, NS2, NS3, NS4 (Ratinier et al. 2011) with evidences of a fifth non structural protein S10 ORF2 recently described (Figure 1-5) (Stewart et al. 2015).

VP2 and VP5 form the outer capsid and have the greater genetic variability among the BTV proteins. VP2 is responsible for the virus attachment to the cell surface and is also the main determinant of the virus serotype. Whereas VP5 form globular-shaped structures that facilitate cell-membrane penetration. So far 27 different serotypes have been identified (BTV-1 to BTV-27) (Roy et al. 2009; Schwartz-Cornil et al. 2008; Nomikou et al. 2015). The intermediate layer of the virus capsid is composed by trimers of VP7, which is also the major immunodominant protein (Figure 1-5). The inner shell, which protects the viral genome, is formed mainly by VP3 and the minor enzymatic proteins VP6 (dsRNA helicase), VP4 (RNA capping enzyme) and VP1 (RNA-dependent RNA polymerase) which are involved in transcription and replication (Figure 1-5) (Schwartz-Cornil et al. 2008).

Among the non-structural proteins of the virus, NS1 and NS2 are the most highly expressed in mammalian cells. NS1 is fundamental for virus replication; it forms multimers that assemble into cytoplasmic tubules within the infected cells and it also seems to be implicated in the cytopathic effect of BTV (Owens et al. 2004). NS2 is the principal constituent of the viral inclusion bodies, it binds ssRNA and is responsible for BTV ssRNA condensation, before its encapsidation (Kar et al. 2007; Jones et al. 1997). NS3, and its shorter version NS3a (lacking the N-terminal 13 amino acid residues), is expressed on the cellular membrane and is implicated in virus release from the cells (Beaton et al. 2002). For long time NS3 was thought to be expressed mainly in insect cells with only a minor role in mammalian cells. However, recent studies have proved that NS3 acts as interferon-antagonist in mammalian cells (Chauveau et al. 2013) and its role has been re-evaluated. Finally, the recently identified NS4 protein has been shown to localise in the nucleoli of the infected cells (Ratinier et al. 2011), as well as having a role in modulating the cell type-I interferon (IFN) response (Ratinier et al. 2016). Bioinformatics analysis has also identified the presence of a second open reading frame in segment 10 of the BTV genome, overlapping the NS3 open

reading frame in the +1 position (Sealfon et al. 2015). By using a viral expression vector, the transcript of this coding region, named S10-ORF2, localises in the cell nucleoli and seems to have a role in inhibiting gene expression, but not RNA translation (Stewart et al. 2015). The expression of this putative new protein during BTV infection is still to be confirmed.

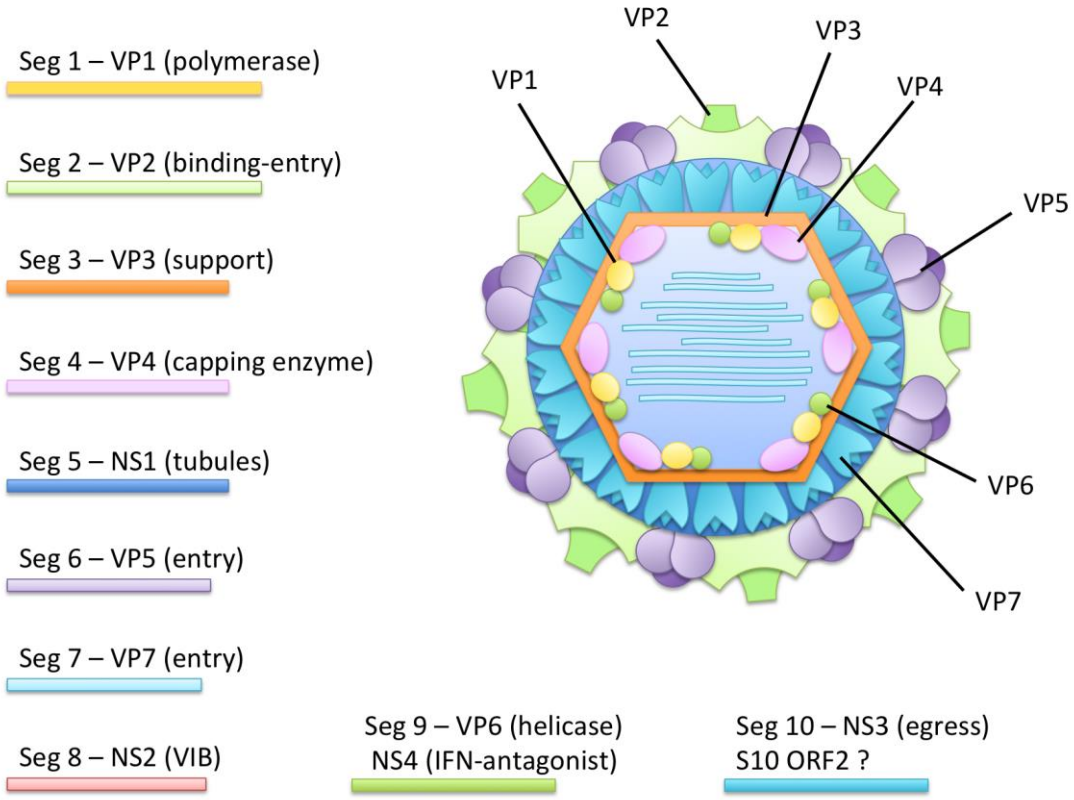

Figure 1-5 Schematic representation of a BTV particle and its genome segments.
BTV viron is assembled in three layers. The outermost capsid is formed by trimers of VP2 and VP5 proteins. The intermediate layer (core) is composed of VP7 trimers. The inner capsid (subcore) is formed by VP3 which encloses the replication protein complex (VP1, VP4, VP6) and dsRNA. The 10 segments of dsRNA forming the BTV genome, the proteins that it encodes and their main recognised role are summarised on the left.

1.2.1 Bluetongue virus replication cycle

In the mammalian host BTV interacts with the target cell membrane by means of the outer capsid protein VP2, which forms trimers that bind to the cell surface glycoproteins. In the insect cells instead, core particles (lacking the outer capsid layer) binds to the cells through VP7 trimers (Xu et al. 1997). Binding triggers a clathrin-mediated internalization of the virus particle through endocytosis

(Figure 1-6). Clathrin coated vescicles form early endosomes where the outer capsid proteins VP2 and VP5 are rapidly dissociated (Figure 1-6) (Forzan et al. 2007). pH acidification induces VP5 interaction with the endosomal membrane where VP5 acts like a fusion protein and allows the release of uncoated virus particles in the cytoplasm (Forzan et al. 2004). BTV replicates in the cytoplasm of infected cells, virus RNA transcription and replication occurs within the virus core where VP6 facilitates the separation of the two strands of viral RNA and VP1 transcribe positive sense ssRNA copies (Boyce et al. 2004). These mRNA copies are then capped at the 5' terminus by VP4 and then extruded in the cell cytoplasm through the pores formed by VP3 in the core. Viral mRNA is then translated by the host cells machinery, starting at approximately 2 hpi (Figure 1-6) (Schwartz-Cornil et al. 2008). At this stage, NS1 is implicated in the upregulation of BTV protein synthesis that by 8 hpi almost completely replace the host cells mRNA translation. Viral RNA is then directed to the viral inclusion bodies (VIB), mainly formed by NS2 (Figure 1-6) (Kar et al. 2007), where they are assembled together with VP3 forming the inner core, followed by the addition of VP7 trimers that constitutes the intermediate layer of the capsid. VP2 and VP5 are subsequently added in the cell cytoplasm when the particle exits the VIB (Figure 1-6). The method of release of virions from the infected cells varies depending of the host and type of cell involved. In insect cells BTV is release by budding, without causing membrane disruption or cell lysis, while in mammalian cells BTV release is mediated by the viroporin activity of NS3 which destabilise the cell membrane (Han & Harty 2004). This generally results in cell lysis and death with consequent release of additional viral particles (Figure 1-6) (Schwartz-Cornil et al. 2008).

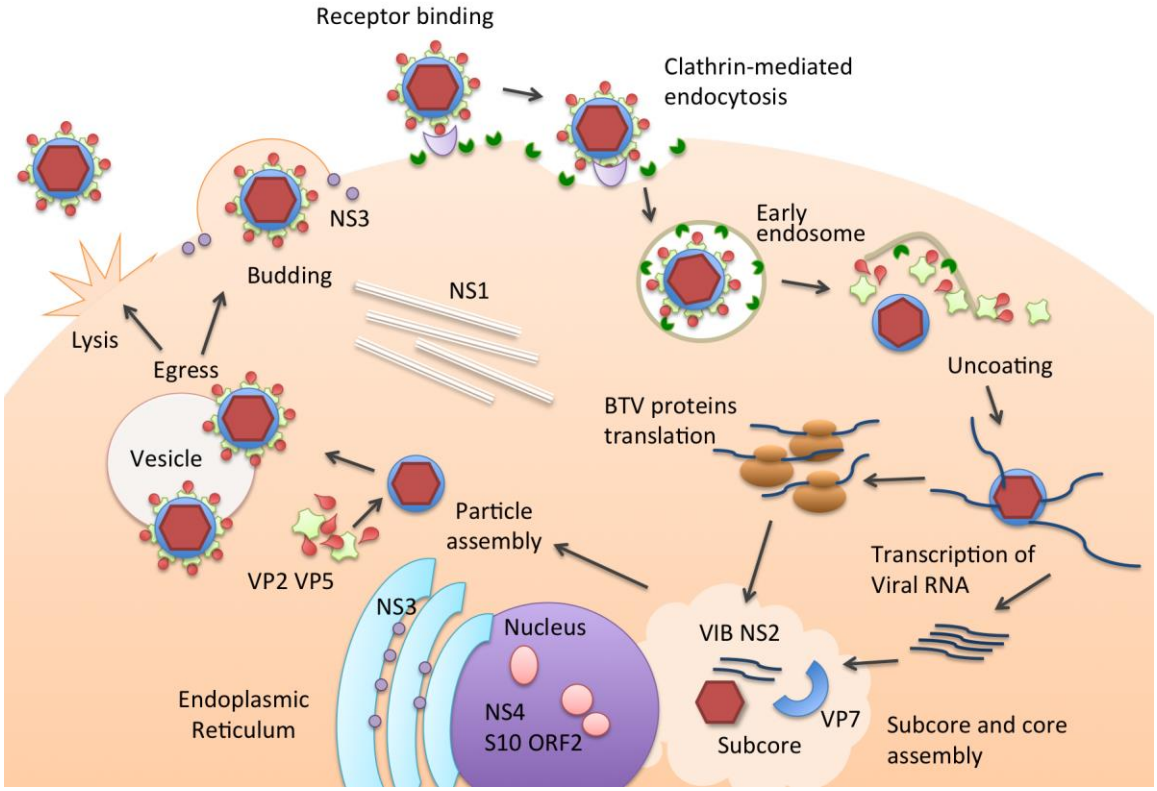

Figure 1-6 BTV replication cycle
BTV enters the cell by endocytosis in clathrin-coated pits. Acidification of early endosomes causes VP5 mediated membrane fusion. The outer capsid is dissociated from the particle and the core enters the cell cytoplasm. Inside the active core, transcription of viral RNA takes place and the ssRNA^{+} (mRNA) is extruded through the pores in the VP3 layer. BTV protein translation is performed via host cell translational machinery and viral NS1 is involved in up-regulation of BTV gene expression. Subcore and core assembly takes place in viral inclusion bodies (VIB) and it is facilitated by interactions with NS2. NS4 is transported to the cell nucleus and localises in the nucleolus where it interferes with IFN synthesis. Complete particles are formed by core association with VP2 and VP5. NS3 is involved in trafficking and egress of mature particles either by budding or by cell lysis (Mohl & Roy 2014).

1.3 Clinical outcomes of BTV infection

The outcome of BTV infection is extremely variable, ranging from a completely unapparent infection to a lethal disease. Determinants of this variability have not been completely identified. It is believed that the consequences of infection are determined by a combination of factors, including the viral serotype and strain, the infected host (species, breed, immune status and genetic background) and the surrounding environment (Caporale et al. 2011).

1.3.1 Host-related factors

The range of host species susceptible to BTV infection is very broad and includes both wild and domestic ruminants (see below). Upon infection, all ruminants can support BTV replication and tend to develop a persistent viraemia. However, a large variability in the clinical presentation of BTV infection has been recorded, with sheep and some species of wild ruminants (such as white tailed deer) being more prone to develop a severe form of the disease. In domestic ruminants, clinical bluetongue is generally characterised by a marked fever in sheep, whilst in goats and cows the infection is generally asymptomatic even if accompanied by prolonged viraemia (Caporale et al. 2014; Erasmus 1975; Richards et al. 1988; MacLachlan et al. 2009). In addition, the same BTV serotype has shown differences in virulence among various sheep breeds, and in different areas of the world (MacLachlan et al. 2009). Clinical disease in indigenous breeds in tropical and sub-tropical area is rarely observed. On the contrary, The North European breeds of sheep have been described to be very susceptible to BTV-induced disease as opposed to African or South-East Asian breeds. Strikingly, when live attenuated BTV vaccines commonly used in South Africa were tested for the first time in Dorset poll sheep, they were able to induce fever and viraemia and proved unsafe for the European market (Veronesi et al. 2010; Veronesi et al. 2005). A study that compared the effects of a standardised infection by using different sheep breeds, revealed no major differences in the outcome of infection in Mediterranean (Sardinian and Italian) and Northern European breeds (Dorset poll, generally considered highly susceptible to clinical bluetongue disease) suggesting that other factors, apart from the sheep breed, may contribute do the insurgence of disease (Caporale et al. 2014). It has to be considered that, the more severe clinical presentation of Bluetongue tend to be associated with viral strains appearing in new geographic areas or when susceptible ruminant breeds are introduced into endemic areas (Coetzee et al. 2012) as occurred during the first recorded outbreak of Bluetongue in South Africa, as a consequence of the introduction of Merino sheep (Spreull 1905), and during the recent BTV-8 outbreak in Northern Europe (Darpel et al. 2007). These observations suggest that a certain degree of herd immunity must be present in endemic areas and that viral adaptation to the residing ruminants population might also develops, thus these factors might have a major role in determining the outcome of BTV infection.

1.3.2 Virus-related factors

BTV presents a profound genetic heterogeneity. BTV exists in at least 27 serotypes, and within the same serotype strains with different virulence have been described (Nomikou et al. 2015; Caporale et al. 2014). BTV genetic diversity is the result of antigenic shift and antigenic drift. Reassortment of viral genes (antigenic shift) can take place either in the vertebrate or invertebrate host, as a result of coinfection with multiple serotypes and strains (Shaw et al. 2013; Nomikou et al. 2015). Moreover, BTV is an RNA virus and as such it has a high mutation rate (10^{-5} to 10^{-3} misincorporations per nucleotide copied) (Bonneau & Mullens 2001) (antigenic drift). In addition, RNA virus populations do not consist of a single genotype; rather, they consist of a group of related sequences, termed quasispecies by some authors (Vignuzzi et al. 2006; Domingo et al. 2012). The generation of a "cloud" of viral variants accounts for the rapid evolution and adaptability of the virus. This allows the virus to promptly change cell tropism and host range, and escape external constrains (such as immune response and antiviral agents). A combination of selection pressure and rapid viral mutations results in an accelerated form of Darwinian evolution. However, arboviruses often evolve more slowly than other RNA viruses, likely because of restrictive pressures imposed during alternating passages in arthropod and mammalian hosts (Holmes 2003; Coffey et al. 2008; Weaver et al. 1999). A decrease in population variability, and a selection of a specific minority variant in the VP2 protein, was observed in *Culicoides sonorensis* fed on BTV viremic sheep, indicating that host switching constitutes a bottleneck and that a founder effect might therefore play an important role in genetic diversification of BTV strains in nature (Bonneau & Mullens 2001). More recently, *in vitro* experiments demonstrated that isolation of BTV from infected blood, using a mammalian cell line (BHK21), in contrast with isolation using insect cells, severely impact population variability leading to a decrease in genetic diversity (Caporale et al. 2014).

Furthermore, phylogenetic analysis of the nucleotide sequence of the 10 BTV genes shows that cognate BTV genes may differ depending on the geographic origin of each virus, in a process termed topotyping. Negative selection of

individual BTV genes occurs over time following the incursion of novel viruses into new regions, creating genetically distinct region-specific clusters that might be related to the ecology of the area (Balasuriya et al. 2008; Gould & Pritchard 1990; Nomikou et al. 2015). Hence, accordingly to this phenomenon, BTV strains can be further clusters into the two major "eastern" and "western" groups, as well as several additional groups and sub-groups (Nomikou et al. 2015; Maan et al. 2008).

Although all the genetic factors described above are likely to play a role in determining disease and transmission, the genetic determinants of BTV virulence largely remain uncharacterized, as do those that are associated with emergence of the virus in new regions, and in novel vector species.

1.3.3 Environmental factors

In addition, to complicate an already intricate picture, environmental factors such as high temperature and ultraviolet radiation, seems to facilitate the onset of disease (Spreull 1905), however the mechanisms involved still need to be elucidated. It is not clear if such factors have a direct impact on the mammalian host and its response to the virus, or if, more likely, they influence the ecology of the vector.

1.3.4 Experimental procedures

Studies of the pathogenesis of BT are mainly based on observations made in experimentally infected animals. Most of these studies have been performed through the inoculation of virus with needle injection, which do not take into account additional factors related to the bite of an infected *Culicoides* vector. Various inoculation routes have been used to successfully reproduce the disease in ruminants, the most frequently used being intravenous, subcutaneous, intradermal, or a combination of these. It has been shown that the route of inoculation can significantly alter the outcome of infection (Umeshappa et al. 2011), with the intravenous route often generating a milder disease in comparison to an intradermal infection. The reasons of this variability remain to be clarified.

Similarly, the type of inoculum used affects the variability of the data obtained. Early pathogenesis studies preferentially employed the inoculation of infectious blood collected from BTV infected animals at the peak of disease (Spreull 1905; Darpel et al. 2012). However, the use of infectious blood as source of infection, did not allow to control confounding factors such as virus titre, the presence of multiple serotypes, the inoculation of donor animal immune cells and antibodies and the concomitant inoculation of unrelated blood borne pathogens. Subsequently, with the advent of cell cultures, experimental infections moved to use viral strains obtained from field-infected animals isolated and propagated in immortalised cell lines. This gave the possibility to more precisely titrate the virus and use a "cleaner" inoculum, decreasing confounding factors. However, inoculation of cell culture passaged virus fail in general to reproduce the severity of disease that is often obtained with infectious blood (Caporale et al. 2014). In a recent study, deep sequencing analysis revealed a marked decrease in the genetic diversity of the BTV population after passaging in mammalian cells, whereas virus passaging in a *Culicoides* cell line resulted in an increased of low-frequency variants compared to virus never passaged in cell culture. These observations indicate that *Culicoides* might be a source of new viral variants, and that viral population diversity can be another factor influencing BTV virulence (Caporale et al. 2014).

Thus, variability on the outcome of BTV infection can also be influenced by the experimental settings used, which could modify the course of disease in ways that have still not been fully elucidated.

1.4 Bluetongue

1.4.1 Disease in sheep

Bluetongue is mainly a disease of sheep. Despite a marked variability, all sheep breeds are susceptible to the disease (MacLachlan et al. 2009; Erasmus 1975). Contrasting results have been reported regarding the host related factors that determine this variability. In general terms, fine wool (such as Merino) and European sheep breeds are considered more susceptible than the more rustic

African breeds (Spreull 1905; Neitz 1948; Erasmus 1975). However, marked differences have also been observed within different individuals of the same breed. Hence, factors like immune status, age and genetic background can also have a role in determining the final outcome of infection (MacLachlan et al. 2009).

1.4.1.1 Clinical presentation

The disease in sheep can range from a completely asymptomatic infection, to a fulminant lethal disease. After experimental infection, the incubation period varies from 2 to 15 days, although it is more frequently of 4 to 6 days. The first sign of Bluetongue is a marked fever (41-42°C) that can last between 2 and 7 days (Spreull 1905; Erasmus 1975). Often the degree of the febrile response does not correlate with the severity of other clinical manifestations, and in most resistant sheep the febrile reaction is generally the only indication of infection (Spreull 1905). In more severe forms, a few days after the initial pyrexia, it is possible to observe hyperaemia of the oral and nasal mucosae, generally accompanied by extensive salivation and nasal discharge that can become mucus-purulent or haemorrhagic. Erosive and crust lesions are often visible on the muzzle, likely due to mechanical action of the tongue. In addition, lachrymation and hyperaemia of the eyelids are also present (Erasmus 1975).

Severely affected sheep develop ooedema of the face that can sometimes extend to the neck. Petechial lesions are often present on lips and tongue and haemorrhages at the muco-cutaneous junction of the mouth. In some cases, the tongue can appear significantly swollen and cyanotic, and protrude from the mouth, hence the name “bluetongue” given to the disease. Erosion and ulcers can be present on the mucosa of the mouth, on the gums, cheeks, palate and tongue. This results in anorexia and depression of the animal. A haemorrhagic diarrhoea can also appear which is considered as a highly unfavourable prognostic sign (Spreull 1905; Erasmus 1975).

Feet lesions can also be present; coronitis can develop and consists of hyperaemia of the coronary bands, sometimes accompanied by ulcerative lesions (Darpel et al. 2007; Erasmus 1975). The hoof can appear inflamed and, as a result of the pain, the animal is often recumbent or standing in antalgic position.

Hyperaemia can be present on the skin of various regions, on the muzzle, axilla and groin, and sometimes of the whole body. Wool growth can be affected and part of the fleece can be lost in patches. Respiratory symptoms are very frequent, ranging from an increase in the respiratory rate (tachypnoea) to a severe dyspnoea.

The mortality rate in BT can vary markedly in natural field conditions, ranging from 2 to 30%. The majority of affected animals recover even after a severe disease. In lethal cases, death occurs between 1 and 8 days after the onset of clinical signs, and it is generally the consequence of an acute pulmonary ooedema, pneumonia or in some cases the results of the prolonged debilitation caused by the disease.

1.4.1.2 Clinical pathology

Clinical pathological findings in BTV infected sheep have only rarely been assessed. A transient leukopenia between 6 and 8 dpi is a common finding during the course of BTV infection, which is generally characterised by a marked lymphopenia (MacLachlan et al. 2008; Sánchez-Cordón et al. 2015; Umeshappa, Singh, et al. 2010; Ellis et al. 1990). Lymphopenia has been described as the result of a decrease in the pool of circulating CD4, CD8 and γδ T-lymphocytes (Sánchez-Cordón et al. 2015; Umeshappa et al. 2010; Ellis et al. 1991). The mechanism underlying a decrease in the absolute number of circulating lymphocytes has not been fully identified yet. Another possible explanation is an apoptosis-induced depletion, as suggested by *in vitro* study where sheep peripheral blood mononuclear cells were infected with BTV (Umeshappa et al. 2010). In addition, other common causes of lymphopenia such as the migration of lymphocyte towards inflamed tissues or their loss through lymph extravasation should be kept into consideration. The observed lymphopenia during BTV can induce a transient immune suppression, during the early phases of infection, which has been reported to predispose the animal to secondary infection, leading to a worsening of the clinical disease (Umeshappa et al. 2010). Short after the initial lymphopenia, it is generally observed an increase in CD8 T-lymphocytes around 10-14 dpi (Sánchez-Cordón et al. 2015; Umeshappa et al. 2010; Channappanavar et al. 2012; Ellis et al. 1991).

In experimentally infected sheep, thrombocytopenia is also often reported between 5 and 10 dpi, however the decrease in platelets number does not seem to be associated with alteration in coagulation factors (McColl & Gould 1994; Sánchez-Cordón et al. 2013; Maclachlan et al. 2008). These findings rule out the hypothesis that a consumptive coagulopathy, resulting from BTV-induced endothelial damage, could be implicated in the manifestations of disease in sheep, as instead observed during the fulminant form of Bluetongue in white-tailed deer (Karstad & Trainer 1967; Howerth et al. 1988) . In sheep, the mechanism at the basis of platelet depletion and its implication in the development of disease is still to be clarified.

A recent study in experimentally infected sheep, reported for the first time a correlation between the increase of acute phase proteins (such as serum amyloid and haptoglobin) in serum and the presence of overt clinical disease, suggesting the possibility to employ these proteins as marker of tissue damage induced by BTV (Sánchez-Cordón et al. 2013). Other possible markers, present in the most severe case of BTV, have been identified in creatine phosphokinase, glutamic pyruvic transaminases and aldolase. They are all suggestive of skeletal myopathy and an increase in their serum levels have been associated with fatal cases of bluetongue probably as a consequence of a severe endothelial damage (Erasmus 1975).

1.4.1.3 Gross Pathology

Gross pathological lesions are generally associated with the clinical disease and its complications. In the digestive system, ooedema and ulcerations are present in the upper tract, mainly in the mouth and tongue, associated with the presence of necrotic tissue. A diffuse hyperaemia is commonly observed in the digestive system, including rumen and reticulum, while in the abomasum and gall bladder this is accompanied by petechial haemorrhages. In the respiratory tract the most frequent pathological finding is pulmonary ooedema, with presence of white froth extending into the trachea (Sánchez-Cordón et al. 2013; Maclachlan et al. 2008). Pneumonia is also frequent and generally the results of inhalation of ingesta or as a consequence of secondary infections that have been frequently reported during bluetongue and attributed to the debilitating and immunosuppressive effect of BTV on T-lymphocytes (Umeshappa et al. 2010). In

the cardiovascular system hyperaemia and haemorrhages are often observed in the large vessels, especially in the tunica media of the pulmonary arteries (Sánchez-Cordón et al. 2013; Erasmus 1975). Subepicardial and endocardial haemorrhages may be present, especially involving the papillary muscles of the left ventricle (Sánchez-Cordón et al. 2013; Erasmus 1975). Petechiae can also be observed on the serous membrane of heart and lungs where hydropericardium and hydrotorax can be present. The lymph nodes are commonly enlarged and present haemorrhages, especially the ones draining the area of the head and neck (Darpel et al. 2012; Erasmus 1975). Spleen and thymus could also appear enlarged and display subcapsular haemorrhages. The skin is generally characterised by an ooedematous aspect that extends to the subcutaneous layers. Hyaline degeneration of the skeletal muscles can be observed in the most severe cases, which is responsible for the emaciated aspect of the animals; at times muscular lesions are replaced by fibrous tissue in necrotic areas (Erasmus 1975). Congestion and petechial haemorrhages can also be found in the urinary tract, in the bladder, kidneys and urethra.

1.4.1.4 Histopathology

Limited information is available about the histopathological changes induced in sheep by BTV, since very few studies have assessed the microscopic aspect of the tissues following BTV infection.

In the skin, the presence of ooedema of both dermis and epidermis with multifocal perivascular petechiated haemorrhages has been described. A moderate to marked diffuse pericapillary dermal inflammation with infiltration of plasma cells, lymphocytes, eosinophils and neutrophils has also been observed in the dermis (Darpel et al. 2012; Lee et al. 2011). The presence of granulomas in the superficial dermis has been reported solely when BTV inoculation was performed through the bites of *Culicoides* (Darpel et al. 2012). In a different study, labial and oral tissues, collected 7 dpi, showed an increase in the number of perivascular mononuclear cells in the dermis and lamina propria, which reverted to normality by 14 dpi (Ellis et al. 1991)

As for gross pathological studies, histological studies report of multifocal haemorrhages and necrosis in course of Bluetongue in the heart, kidney, skeletal

muscles and lymph nodes (LNs) of sheep (Lee et al. 2011; MacLachlan et al. 2008). In the digestive tract, ulceration and necrosis were reported in the mucosa of the oral cavity, along the upper gastrointestinal tract and in the forestomachs (MacLachlan et al. 2008). In the lung it has been described the presence of ooedema and inflammation of the peribronchial connective tissue with infiltration of lymphocytes and plasmacells (Darpel et al. 2012). Mild to moderate interstitial pneumonia has also often observed (Lee et al. 2011).

The muscle fibres of the tongue, trapezius and cardiac muscle have often been found affected by perivascular ooedema and mononuclear cells infiltration accompanied by moderate degeneration of muscle fibres (Umeshappa et al. 2011). In general, it has been observed that the extensive ooedemas that occur in sheep are not accompanied by histologic evidence of destruction of small blood vessels or necrosis, suggesting that the ooedemas results from increased vascular permeability without direct endothelial damage (MacLachlan et al. 2008).

1.4.2 Bluetongue in goats

Although BTV infection was first described in goats more than 100 years ago (Spreull 1905), very few studies have been conducted in this species. Contrary to sheep, the clinical presentation of BT is generally mild in goats or completely unapparent. In 1905, Spreull firstly reported that no fever or any other visible sign occurred in naturally or experimentally infected goats, despite being able to confirm the presence of viraemia in these animals between 5 and 20 days after experimental infection by injecting goat blood into a susceptible sheep (Spreull 1905). Only few reports describe the presence of occasional clinical signs of BT in goats during naturally occurring outbreaks (Erasmus 1975). An exception is the recent outbreak of BTV-8 in Northern Europe, a particularly virulent strain that occasionally induced disease in goats with an approximate 25% case/fatality rate (Conraths et al. 2009). In experimental settings, goats tend not to present clinical disease when inoculated intradermally with the same strain and dose of BTV used to induce disease in sheep (Caporale et al. 2014; Koumbati et al. 1999), although a different study reported the presence of disease in both sheep and goats inoculated intravenously with infectious blood (Backx et al. 2007).

Regardless of the route of inoculation and the type of inoculum used, goats develop a persistent viraemia similarly to sheep.

New attention has been driven towards goats in recent years due to the discovery of new BTV serotypes that seem to preferentially replicate in this animal species. BTV-25, initially named Toggenburg virus (for the Swiss city where was first isolated), was found to circulate exclusively in the goat population in 2008 without causing disease (Hofmann et al. 2008). Subsequently, a novel BTV serotype (BTV-26) closely related to BTV-25, was isolated in Kuwait in 2010 from the blood of goats and sheep. Subsequent studies demonstrated that BTV-26 induce only mild disease in sheep and that it tends to produce an higher viraemia in experimentally infected goats compared to sheep (Batten et al. 2012). Moreover, there is evidence that goats experimentally infected with BTV-26 could transmit the virus to susceptible goats without the need of an arthropod vector (Batten et al. 2014; Batten et al. 2013). Following these reports an additional BTV serotype was isolated in 2015 in Corsica, likely constituting a putative 27th serotype, the virus was circulating once again in the goat population. Although pathogenicity studies are still missing, sequence analysis revealed similarities with the previously described BTV serotypes 25 and 26 (Jenckel et al. 2015).

1.4.2.1 Histopathology

While not many information is available on the histopathology of bluetongue in sheep, a recent studies provided insightful information about the lesions presented by goat tissues in natural occurring BTV infection with BTV-1(Sánchez-Cordón, Pedrera, et al. 2013), a serotype circulating in Spain in 2007 that was able to induce severe disease in both goat and sheep (Allepuz et al. 2010).

The authors reported a separation of connective tissue and muscle fibres as a consequence of ooedema, with mononuclear infiltrates and haemorrhages in various tissues, including skin (sampled from nostril, face, lips and coronary band), skeletal muscles of hindlimbs and tongue, cardiac muscle, lungs (with alveolar ooedema and haemorrhages), pulmonary artery, urinary bladder and along the whole gastro-intestinal system (Sánchez-Cordón, Pedrera, et al. 2013). The capillary endothelial cells of the skin were reported to appear swollen and

vacuolated, often surrounded by perivascular mononuclear infiltrates mainly comprising macrophages and lymphocytes (Sánchez-Cordón, Pedrera, et al. 2013). In the hepatic parenchyma, the authors found evidence of micro-vacuolar degeneration and congestion together with small haemorrhages and mononuclear infiltrates (Sánchez-Cordón, Pedrera, et al. 2013).

The examination of the lymph nodes (pre-scapular, submandibular, mediastinal, ileocecal and gastrohepatic) revealed distended sinuses with numerous mononuclear cells, often accompanied by cortical haemorrhages and medullary hyperaemia. Interestingly, the authors reported that both in the lymph nodes and spleen, lymphoid follicles presented clear signs of depletion that were not generally accompanied by lymphocyte destruction, such as pyknosis or cell fragmentation (Sánchez-Cordón, Pedrera, et al. 2013), however the underling cause of this depletion was not investigated.

Goats' kidneys also appeared affected by the infection, displaying glomerular congestion, with red blood cells and clumped protein present in Bowman's space and in the tubules. Interstitial mononuclear nephritis and interstitial haemorrhages were also observed (Sánchez-Cordón, Pedrera, et al. 2013).

Overall, most of the lesions described in this study appear to be re-conducible to an endothelial dysfunction, either caused by the direct cytopathic effect of the virus or by the action of inflammatory chemical mediators produced by BTV-infected cells. However, research on the pathogenesis of BTV would benefit of further in vivo studies of different BTV serotypes and in various ruminant species.

1.4.3 Bluetongue in cattle

Bluetongue in cattle generally does not induce overt clinical disease, although occasionally symptoms have been reported (Hourrigan & Klingsporn 1975). When present, the signs reported do not differ from the mild clinical form displayed by sheep. These include a rise in the body temperature, laminitis and stiffness, ulcerative lesions of the tongue, mouth and muzzle, ooedema of the lips,

hypersalivation and nasal discharge. In some cases ulcers are also present on the udders (Hourrigan & Klingsporn 1975).

Infected cattle develop a persistent viraemia that has been reported to last much longer than in sheep. Most of the circulating virus seems to be associated with platelets and red blood cells up to approximately 200 dpi. Furthermore, some species of *Culicoides* preferentially feed on cattle instead of other ruminants, making this species a perfect reservoir for BTV and the transmission of disease (MacLachlan 1994).

In a series of studies aiming to reproduce clinical disease in cattle, the animals were firstly sensitised with an inactivated BTV in combination with an immunomodulator (cimetidine hydrochloride or levamisole) and subsequently infected with the same BTV strain. The obtained results suggested that BTV signs in cattle originate from a type I hypersensitivity reaction, accompanied by the production of virus-specific IgE, histamine and prostaglandins which determine a exudative dermatitis and ulcerations (Stott et al. 1982; Anderson et al. 1987). Interestingly, the inoculation of virus without prior sensitization failed to produce disease in the tested animals. Furthermore, these studies also demonstrated that the intradermal inoculation of an hyperimmune serum together with a cell culture adapted virus was able to reproduce the disease in non-sensitised calves, indicating the role of antibodies in the pathogenesis of disease (Anderson et al. 1987). Subsequent studies identified that in cattle the main serum component responsible for this outcome, the serum IgE produced during a BTV infection, are mainly directed towards the viral VP5 (Odeón et al. 1999).

BTV infection in dams has been frequently associated with reproductive sequelae such as abortion and congenital malformations of the calves (Osburn 1994; Dal Pozzo et al. 2009). Foetuses infected in the first half of gestation develop cerebral malformations that range from hydranencephaly and cerebellar hypoplasia to poroencephaly. These malformations are thought to be the consequence of the tropism of BTV for neuronal and glial precursors in the developing brain (MacLachlan 1994).

1.4.4 Bluetongue in wild ruminants

Most wild ruminants and camelids are susceptible to BTV infection. However, they generally do not display the clinical signs of disease therefore could serve as a reservoir for BTV persistence and transmission (Falconi et al. 2011). Wild African ruminants, such as blesbock (*Damaliscus pygargus*) and mountain gazelle (*Gazelle gazelle*) present in area where BTV is endemic, are resistant to infection, and do not show clinical disease after either natural or experimental infection. Similarly, the American black tailed deer (*Odocoileus hemionus columbianus*), the North American Elk (*Cervus elaphus canadensis*) and the European red deer (*Cervus elaphus*) present a mild or asymptomatic infection.

In Europe, serological studies have highlighted the presence of BTV neutralising antibodies in many wild ungulates (free ranging or farmed) in Belgium, Spain, France and Italy. Animals tested positive included: red deer (*Cervus elaphus*), fallow deer (*Dama dama*), Spanish ibex (*Capra pyrenaica*), roe deer (*Capreolus capreolus*), mouflon (*Ovis aries musimon*), ibex (*Capra ibex*) and Southern chamois (*Rupicapra pyrenaica*) (Falconi et al. 2011). The BTV serotypes generally involved included serotype 1, 4 and 8 with the highest seroprevalence in red deer and fallow deer, both belonging to the *Cervinae* family. Numerous studies have also detected BTV RNA in the blood of red deer in Spain, France and Belgium (Linden et al. 2010; Rossi et al. 2014; García-Bocanegra et al. 2011). Infection of European wild mammals is in general completely asymptomatic and does not seem to affect the population dynamics of these species. The sole exception is represented by mouflons, which tends to develop clinical signs of inflammation of the mucous membranes, congestion, swelling and haemorrhages during BTV infection (Fernández-Pacheco et al. 2008). Mouflons are closely related to domestic sheep and their genetic similarity may therefore be implicated in the observed susceptibility (Chessa et al. 2009). The widespread and elevated antibody prevalence of BTV in wild ruminants indicate these species could serve not only as reservoir of infection but also as good BT sentinels in surveillance plans in European countries.

In the Americas, wild ruminants appear to be more susceptible to BT infection, compared to African and European species. Serological prevalence and virus isolation studies have identified infection in: black-tailed deer (*Odocoileus*

hemioneus columbianus), white-tailed deer (*Odocoileus virginianus*), American bison (*Bison bison*), pronghorn antelope (*Antilocapra americana),* mule deer (*Odocoileus hemionus),* bighorn (ovis canadensis) and North American elk (*Cervus elaphus canadensis*) (Falconi et al. 2011). Elk and black-tailed deer are relatively resistant to Bluetongue while a particularly severe form of the disease, with a high mortality rate, is generally observed in white-tailed deer and pronghorn antelopes (Thorne et al. 1988; Vosdingh et al. 1968; Karstad & Trainer 1967). Experimental infection of white-tailed deer elicits severe clinical signs, including increased temperature, erythema, facial ooedema, coronitis, and stomatitis. Widespread haemorrhages and hematomas begin to be observed at 8 dpi. These findings are associated with an alteration of the coagulation process as indicated by progressive prolongation of activated partial thromboplastin time (PTT) and prothrombin time (PT), and concomitant reduction of Factors VIII and XII plasma activities. High concentrations of fibrinogen degradation products were also detected between 3 and 6 dpi. The coagulation abnormalities are indicative of a consumptive coagulopathy that predispose to bleeding and multiple organ failure, and might therefore play a role in the most severe cases of BTV (Howerth et al. 1988). Further haematological findings include a marked thrombocytopenia starting at 6 dpi, leukopenia, lymphopenia, neutrophilia, and low total plasma protein concentration. Surprisingly, no virus-specific antibodies were detected in the deer included in the experiment.

In white-tailed deer, the histopathological changes have been well characterised (Karstad & Trainer 1967). Haemorrhages, necrosis and thrombosis were the most recurrent findings, which were principally described in the tongue, heart, spleen, kidneys and lymph nodes. Fibrin, platelets and mixed thrombi where present in several tissues and were associated with tissue necrosis and haemorrhages. In the tongue and heart, hyaline degeneration of muscle fibres was present that proceed to necrosis as a consequence of thrombosis. Haemorrhages were also frequent in the spleen and sometimes accompanied by necrosis of the follicles. In the LNs haemorrhages were reported in the medullary sinuses, accompanied with erythrophagocytosis by macrophages. In the digestive tract, haemorrhages and extensive necrosis was found in the rumen, abomasum and intestines (Karstad & Trainer 1967).

1.5 Pathogenesis of bluetongue

1.5.1 Virus dissemination in the mammalian host

Experimental infections in ruminants have been used to understand the tropism, at organ and cellular level, of BTV and its sequential dissemination in the infected host. Some of the key studies have investigated the tissue distribution of BTV after experimental inoculation (subcutaneously in the head and neck region) by euthanizing animals at intervals after infection. The presence of the virus was then evaluated in various tissues by using virus isolation techniques or BTV antigens detection (Pini 1976; Barratt-Boyes & MacLachlan 1994; Darpel et al. 2012).

The dynamics of infection appears to be similar in sheep and cattle. Once BTV is inoculated in the skin of a susceptible host, it initially replicates locally in the dermis (Darpel et al. 2012) then migrates to the regional lymph nodes where additional replications take place (Darpel et al. 2012; Pini 1976; Barratt-Boyes & MacLachlan 1994). Thereafter, the virus is likely transported by the bloodstream to peripheral tissues, which constitutes sites of secondary replication.

Therefore, the first organs to be infected after the skin are the lymph nodes, followed by the spleen (at ~4 dpi) that generally yields the higher viral titres. At 6 dpi other organs appears infected, including lungs, kidney, liver, intestinal mucosa, tongue and testicles. In some occasions BTV was also isolated from the bone marrow after the 10th dpi (Barratt-Boyes & MacLachlan 1994).

The regional lymphatic system appears to cover an important function during the early phases of infection. BTV distributes to the regional lymph node draining the site of infection with the afferent lymph. In a single study, through catheterization of the afferent lymph duct, the cells responsible of carrying the virus from the inoculation site to the draining lymph node have been identified as conventional dendritic cells (cDC), with the highest cell-associated viral load detected between 4 and 5 dpi (Hemati et al. 2009). Few infected $CD1^+$ and $CD11c^+$ cells, described as cDC, were also found in the parenchyma of the lymph node, supporting a role of these cells in carrying the virus to the regional lymph nodes (Hemati et al. 2009).

In an attempt to understand how BTV leaves the lymph node, it was noted that the cannulation of the efferent lymphatic vessel draining the site of infection, and the consequent disruption of the lymph circulation, can delay the onset of viraemia of 3-4 days (Barratt-Boyes & MacLachlan 1994). Only rare infected cells were detected in the efferent lymph, these cells leaving the lymph node were thought to be responsible for the dissemination of BTV to the peripheral tissues, but they have not been characterised (Barratt-Boyes & MacLachlan 1994).

The onset of viraemia occurs generally 48 h after the draining LNs infection. Viraemia is highly cell-associated, during the first week post-infection BTV can be detected in association with the cellular fraction of the blood, including both peripheral blood mononuclear cells (PBMC), erythrocytes and platelets but rarely in granulocytes (MacLachlan et al. 1990; Barratt-Boyes & MacLachlan 1994). BTV is generally not detectable in blood plasma. During the later stages of viraemia (after the initial 10 days) BTV tends to circulate solely in association with erythrocytes and it is no longer detectable in PBMC (Barratt-Boyes & MacLachlan 1994). Ultrastructural studies suggested that BTV particles could rapidly be sequestrated in invaginations of the erythrocytes membrane (Brewer & MacLachlan 1992; Brewer & MacLachlan 1994). Brewer and colleagues observed that erythrocytes-absorbed viral particles were not any longer labelled by immunogold staining. Hence, they postulated that, in a similar manner, neutralising antibodies are not able to reach BTV virions hidden into cell membrane invaginations (Brewer & MacLachlan 1992). Interestingly, BTV particles associated with ruminant erythrocytes often resemble morphologically viral cores, lacking the VP2 and VP5 proteins that form the outer capsid; core particles are not infectious to mammalian cells but they might still be infectious to the insect vector, as demonstrated *in vitro* (Xu et al. 1997). This mechanism would allow the virus to circulate in the presence of neutralising antibodies for long time but still remaining infectious for the insect vector. In experimentally infected animals, it has been documented that it is possible to detect BTV RNA in blood by qPCR for more than 100 days (111-222 dpi) in both sheep and cattle. This period of time appears to be consistent with the life span of ruminants red blood cells (~160 days) (Bonneau et al. 2002). However, the time in which it is possible to isolate infectious virus *in vitro* from the blood of a viremic animal is much shorter and this is also believed to be the time for which a viremic animal

is infectious to *Culicoides* midges (Bonneau et al. 2002; Singer et al. 2001). This might suggests that membrane absorbed virions lose infectivity over time. Despite the broad epidemiological consequences of this aspect, not many studies have thoroughly assessed the potential infectivity of blood. Currently, based on the available information, the World Organization for Animal Health have adopted a legislation considering 60 days as the longest period during which an affected animal can be a source of infection (OIE - World Organisation for Animal Health 2016b).

1.5.2 BTV tropism

Immunohistochemical studies of experimentally infected cattle or sheep had identified BTV infected cells mainly as endothelial cells lining small vessels, perycites and mononuclear phagocytes (MacLachlan et al. 1990; Stair 1968; Darpel et al. 2012; Mahrt & Osburn 1986; Meltzee 2016). However, attempts to identify BTV antigens in ruminant tissues have often been unsuccessful and generally have returned contrasting results, making the identification of infected cells and the evaluation of virus antigen distribution difficult to interpret.

A recent study employed confocal laser scanning microscopy (CLSM) and immunolabeling of structural (VP7) and non-structural (NS2) proteins of the virus in order to identify the cells in which BTV is replicating (Darpel et al. 2012). This study indicates that at the inoculation site, BTV replicates in endothelial cells of capillaries in the dermis at 3 dpi and at a later time (6-9 dpi) in $CD45^+$ agranular leukocytes, similarly to what previously described (Mahrt & Osburn 1986). On the contrary, VP7 but not NS2 could be detected on the membrane of erythrocytes, confirming virus adherence but lack of replication in these cells (Darpel et al. 2012).

In one study, cDCs have been identified as early targets of infection; these cells have been assumed to get infected by BTV in the skin, and have been found in the lymph draining the inoculation site (identified as $CD11c^+$ cells) in association with viral RNA between 4 to 6 dpi. Hence, cDCs have been hypothesised to be the main responsible of BTV dissemination from the skin to the peripheral LNs (Hemati et al. 2009). However, these cells have not been reported to express

viral non-structural proteins in vivo, even though, during experimental isolation and *in vitro* infection they appear to sustain BTV replication. Interestingly, the physiology of the cells does not seem to be affected by BTV. After *in vitro* infection, cDCs are activated and contrary to infected endothelial cells they do not appear to undergo apoptosis (Hemati et al. 2009). In the attempt to localise infected DCs at their arrival point, in the lymph node, the authors describe the presence of BTV NS2 in some $CD1^+$ and $CD11c^+$ cells at this site, and report the lack of infection of other cell populations such as CD4 T cells, γδ T cells, B cells and CD11b positive cells. Interestingly, the presence of infected cells that do not appear to express any of these markers was also reported, the impossibility to classify these cells in one of the most represented leukocyte populations was therefore attributed to a shutoff of surface protein synthesis induced by BTV (Hemati et al. 2009).

Lymphoid tissues of BTV infected animals often present the higher viral loads early after infection, independent of the route of infection (subcutaneous or intravenous) (Pini 1976; Barratt Boyes et al. 1992; Stair 1968; MacLachlan et al. 1990; Worwa et al. 2010). Certain subsets of leukocytes populating these tissues are therefore thought to represent primary cellular targets for the initial viral replication. Early histochemical studies described the presence of infected cells in the lymph nodes which localise in the medullary sinuses and in the paracortex (Stair 1968). In contrast, subsequent histochemical and immunofluorescence experiments only succeeded to detect few infected leukocytes at these sites together with the more prominently infected endothelial cells, however the number of infected cells present in the LNs was limited, consisting only of 3 to 10 cells per section (Darpel et al. 2012; Hemati et al. 2009).

Similarly, in the spleen the presence of BTV infected cells has only occasionally been reported (Darpel et al. 2012; MacLachlan et al. 1990). Here, the infected cells often localise at the periphery of lymphoid follicles and rarely in the red pulp (MacLachlan et al. 1990). Using subcutaneous inoculation, a recent study that employed in-situ hybridization, identified the presence of infected cells in the marginal zone and red pulp of spleen starting at 7 dpi (Lee et al. 2011). The morphology and localization of the infected cells indicates them as marginal zone macrophages. At later time, at 11 dpi, a strong positive signal was also

localised in the spleen follicles, in two different types of cell, one likely to be small lymphocytes and the other compatible for morphology with tingible body macrophages or follicular dendritic cells (FDC) (Lee et al. 2011).

In support of the data obtained in experimental infection, Sanchez-Cordon and colleagues have recently reported in detail the localization of infected cells in naturally infected animals (goats and sheep). The tested samples were collected during the BTV-1 outbreak in Spain 2010, and key elements to facilitate the detection of BTV antigens in the collected tissues were identified as the use of Bouin's fixative solution (instead of formalin) and of an appropriate antigen retrieval method (Sánchez-Cordón et al. 2010). In this work, BTV infected cells were identified in spleen as capillary endothelial cells, macrophages, lymphocytes and occasionally fibroblasts in the splenic trabeculae. In lymph nodes, infected cells were present in the medulla and in the cortex, in lymphoid follicles and interfollicular area. These cells were identified principally as endothelial cells, macrophages and some lymphocytes; furthermore the infection of an unidentified population of stellate cells, most likely stromal or reticular cells, was also reported. In other tissues where BTV was also detected (lungs, ileum, and liver), infected cells were mainly identified as endothelial cell, macrophages and stromal cells (Sánchez-Cordón et al. 2010).

The varied and conflicting results reported in these studies are difficult to interpret, and do not provide a clear picture of the tropism of BTV in skin and lymphoid tissues. It is likely that the different techniques employed offered different sensitivity for the identification of the virus in tissues. Moreover, different BTV serotypes, different routes of inoculation and the time of collection of the analysed tissues are all factors that may have contributed to varying degrees to the different results described.

Since BTV infected animals present a high and persistent viraemia, some studies focused on the identification of the cells responsible for supporting the presence of the virus in the bloodstream. A number of authors focused on determining the target cells of BTV infection in PBMC in cattle. However, PBMC demonstrated a degree of resistance to BTV infection (Ellis et al. 1993), since the virus was able to replicate only on the adherent fraction of PBMC, constituted by monocytes and the resulting macrophages (Whetter et al. 1989; Drew et al. 2010; Barratt

Boyes et al. 1992). On the contrary, infection of the non-adherent fraction of PBMC (constituted by lymphocytes) did not result in a productive infection (Barratt Boyes et al. 1992). BTV was shown to be absorbed into the cell membrane of lymphocytes 15 minutes after infection, but on the contrary to other cell types, infection did not progress beyond this stage during the following 48 h (Brewer & MacLachlan 1994). A productive infection of lymphocytes was achieved only after stimulation of these cells with IL-2 (interleukin 2) after BTV absorption (Stott et al. 1990). The phenotype of the infected cells was characterised as constituted mainly by CD4 T-lymphocytes expressing IL-2 receptor, hence indicating that only activated T-cells are permissive to BTV infection (Stott et al. 1990; Barratt Boyes et al. 1992) at least in *in vitro* experiments. On the contrary, BTV was found to infect poorly CD8 and $\gamma\delta$ T-lymphocytes even after stimulation with IL-2 or Con-A (Concanavalin A). Resting B cells do not appear to be infected by BTV but their infection after activation has not been tested.

Studies on the susceptibility of PBMC to BTV infection have only been performed in cattle and no equivalent information on these subsets is available for sheep. In sheep, studies have principally focused on $\gamma\delta$ T-lymphocytes. It has been observed that circulating and skin $\gamma\delta$ T-cells, collected during the initial 2 weeks after infection, can persistently harbour infectious viral particles. The latent infection can be converted into a lytic one through activation of lymphocytes with IL-2, by interaction with skin fibroblasts or by cross-linking the surface protein WC-1 (Takamatsu et al. 2003).

1.5.3 BTV-induced lesions

Given the virus tropism for endothelial cells, it is believed that BT associated lesions are principally the results of a direct damage of the virus to the host vasculature. Endothelial lesions can induce an increase in vascular permeability and could eventually account for the haemorrhages, ooedemas and effusions associated with the disease. When the lungs (the shock organ in ruminants) are severely involved as a result of BTV infection, respiratory distress associated with the insurgence of pulmonary ooedema can rapidly lead to the death of the animal, within a week from infection (MacLachlan et al. 2009).

BTV is a cytopathic virus, that can induce cell death (apoptosis and necrosis) in microvascular bovine and ovine endothelial cells (DeMaula et al. 2001), monocytes (Barratt Boyes et al. 1992) and activated T-cells (Takamatsu et al. 2003) *in vitro*. Induction of apoptosis as a consequence of infection has also been demonstrated *in vivo* in PBMC and spleen (Umeshappa, Singh, et al. 2010). The mechanism of viral uncoating seems to be sufficient to trigger the apoptosis cascade (Mortola et al. 2004). Accordingly to this model the level of virus replication and the extent of the damage induced to the infected cells should be proportional to the degree of clinical disease observed in the animal. However, this is not always the case, suggesting that other factors (a part from the solely cytopathic damages) are influencing the clinical outcome of disease.

It has been hypothesized that, like for other haemorrhagic fevers, a prominent role in the pathogenesis of disease could be played by a so called "cytokine storm", a cascade of cytokines released by activated or damaged cells, that can result in increased vascular permeability as a consequence of a deregulated immune response. The role of pro-inflammatory cytokines in the pathogenesis of BT has been investigated using different methods in primary cell culture.

Initial studies addressed species-specific differences during the infection of endothelial cells collected from sheep and cattle. Infection with BTV induces activation of endothelial cells and subsequent production of inflammatory mediators (Russell et al. 1996; DeMaula et al. 2002). It has been observed that upon infection, endothelial cells taken from different tracts of the respiratory system, expressed various rates of apoptosis and necrosis in sheep and cattle (DeMaula et al. 2001). Furthermore, upon BTV infection, both ovine and bovine endothelial cells express an high level of vasoactive mediators and pro-inflammatory factors, such as IL-1, IL-6, IL-8, cycloxigenase-2 (COX-2) and inducible nitric oxide synthase, together with the expression of cells adhesion molecules (like for example E-selectin) (DeMaula et al. 2001). However, in cattle it was observed a higher production of prostacyclin, which has an antithrombotic and vasodilator activity. It has been speculated that prostacyclin could likely counteract the adverse effect that inflammation and cell death could have in the insurgence of thrombosis, DIC (disseminated intravascular coagulation), and haemorrhagic diathesis. Thus, these factors could confer a certain resistance to

the cattle to the consequences of microvascular injury (DeMaula et al. 2002). *In vivo*, the presence of IL-1α and TNF-α in tissues taken from naturally infected goats, was assessed by immunohistochemistry and it appeared to be enhanced in the presence of viral protein expression (Sánchez-Cordón et al. 2013). Overall, the contribution of inflammation and related mediators may play an important role in the pathogenesis of bluetongue but no conclusive data have been presented so far during *in vivo* infection.

1.6 Host immune response to BTV infection

Currently there is a limited knowledge of the host immune response to BTV infection. Animals that recover from BT have a long lasting protection to re-infection with homologous serotypes of BTV that is attributed to both humoral and cellular immunity (Schwartz-Cornil et al. 2008; Jeggo 1986).

1.6.1 Innate immune response

Innate immune response constitutes the first line of defence against a viral incursion. Scarce information is available on the innate immune response against the virus *in vivo*. Bluetongue virus is considered a strong inducer of type-I IFN production both *in vitro* and *in vivo*, however its involvement in restricting viral replication in the ruminant host is still largely unknown, considering that viraemia continues beyond the detection of IFN in serum (MacLachlan 1994). In experimentally infected sheep, IFN starts to be detectable in serum around 4 dpi and it rapidly disappear at ~10 dpi. The peak of IFN has been registered between 4 and 8 dpi, which is in correspondence of the peak of viraemia (Foster et al. 1991). In cattle, a similarly transient IFN response is detected during the early phases of infection preceding the peak of viraemia; therefore it is reasonable to assume its implication in controlling viral spread. Increased levels of type-I IFN were also observed in lymph draining the skin of sheep inoculated intradermally with BTV-2 and BTV-8, with a peak detected at 5-6 dpi (Ruscanu et al. 2012). In sheep infected with BTV, the cells responsible for the higher production of α/ß-IFN in blood and lymph have been identified as a population of B^-/$CD11c^-$ /$CD45RB^+$ cells, and identified as plasmacytoid DCs (pDCs), a small subset of DC present in blood and lymphoid tissues (Ruscanu et al. 2012). In pDCs BTV

internalization and endo/lysosomal acidification was required to trigger type-I IFN production, and this was achieved even in the presence of inactivated virus (Ruscanu et al. 2012).

DCs are "professional" antigen presenting cells, representing the key link between innate and adaptive immunity. Historically, mononuclear cells capable of supporting BTV replication have been exclusively identified as monocytes and activated lymphocytes (Whetter et al. 1989; Barratt-Boyes et al. 1992). However, more recently, due to increased availability of new ovine-specific antibodies it has become possible to investigate the role of sheep dendritic cells in the pathogenesis of this disease.
Recent studies have shown that mononuclear cells, present in the efferent lymph coming from the area of inoculation of the virus, can be infected and support BTV replication, these cells have been identified has cDCs (Hemati et al. 2009). This study suggests that cDCs are among the first cell type to become infected by BTV in the efferent lymph and that they could have a pivotal role in virus diffusion, contacting the virus at the entry site and then spreading to the rest of the body.

Due to the stimulation of an inflammatory reaction, in response to the insect bite or the virus presence, the initial BTV infection could also act as a chemoattractant for DCs, since an increase in the percentage of cDCs in skin and (draining) lymph has been detected after virus inoculation (Hemati et al. 2009). In contrast to endothelial cells, cDCs can support viral infection without undergoing apoptosis and maintaining their functionality (DeMaula et al. 2001; Hemati et al. 2009), indeed expression of surface co-stimulatory molecules and production of IL-1ß, IL-6 and IL-12 is increased *in vitro* after BTV infection, denoting their activation. Infected cDCs also seem capable to trigger the proliferation of CD4 and CD8 T-cell and stimulate the synthesis of IFN-γ and IL-10 (Hemati et al. 2009). No difference was found in the DCs response to infection with either wild type or attenuated BTV strains, suggesting that the behaviour of these cells is not modified by the virulence of the virus.

Gene expression profile of pDCs and cDCs has been evaluated in sheep experimentally infected with BTV. Results indicate a possible involvement of these cells in the inflammatory process. In particular, circulating DCs presented

a proinflammatory signature that could potentially be implicated in the systemic inflammation and vascular permeability observed during pathology (Ruscanu et al. 2013).

1.6.2 Humoral immune response

Antigen specific antibodies can target viral proteins to limit virus infectivity and to activate effector cells. Upon BTV infection, infected ruminants develop a prompt humoral immune response towards both structural and non-structural viral proteins (Huismans & Erasmus 1981; Richards et al. 1988). Passive serum transfer studies showed that neutralizing antibodies, which normally appear between 7 and 14 dpi, are able to confer serotype-specific protection, and can completely prevent the onset of viraemia (Jeggo, Wardley & Taylor 1984; Letchworth & Appleton 1983). Virus neutralising epitopes are mainly expressed on VP2, which is one of the components of the virus outer capsid (Huismans et al. 1987; DeMaula et al. 2000). Some of the VP2 targeted epitopes appear to be conformational dependent and are due in part to VP2 folding and in part to the interaction between VP2 and VP5 (DeMaula et al. 2000). VP2 and VP5 are the proteins implicated in cell membrane binding and BTV entry, hence it is logical to think that neutralization antibodies would provide a steric obstruction that prevent membrane attachment.

The outer capsid proteins are the most variable viral proteins and are therefore considered the main determinants of BTV serotype. This means that antibodies raised against a specific serotype generally do not provide protection against heterologous serotypes. However, the presence of common neutralization epitopes has been proved by serological cross-reactivity between certain viral serotypes, furthermore animals sequentially immunised with multiple serotypes can develop a broader neutralising antibodies against a previously unchallenged serotype (Rossitto & MacLachlan 1992; Gould & Pritchard 1990). Unfortunately, the simultaneous immunisation with a combination of serotypes has proven ineffective to elicit a similar broad neutralising response, providing protection only towards some of the serotypes used.

Studies using a synthetic biology approach or reverse genetic system have achieved methods to express recombinant BTV proteins used alone or in association with core proteins to immunise animals. These experiments further confirmed that serotype specific protection and neutralising antibodies can be achieved through the immunisation of the animals with only the outer core proteins VP2 and VP5 (Boone et al. 2007; Stewart et al. 2012; Nunes et al. 2014).

Neutralising antibodies do not have the capacity to clear BTV from the blood of infected animals, indeed neutralizing antibodies are present in conjunction with viraemia for several weeks (Richards et al. 1988; Caporale et al. 2014). As mentioned before, it has been reported that BTV can be absorbed into invagination of the cells membrane in resting lymphocytes, platelets and erythrocytes. This mechanism could limit the capacity of neutralising antibodies to bind viral particles hence delaying the clearance of virus associated with cells membrane (Brewer & MacLachlan 1992).

Ruminants also develop antibodies towards a variety of other BTV proteins; in particular VP7 and NS1 have epitopes that are shared among the different serotypes. Currently, competitive ELISA tests are available on the market and widely used to detect VP7 antibodies to screen the seropositivity of suspected animals. Despite the role of non-neutralising antibodies in the host immune response is still obscure, there is evidence suggesting that they could have a protective role. Animals immunized with virus like particles expressing the core protein VP3 and VP7 presented a mild illness and a lower viraemia upon challenge compared to unvaccinated animals (Stewart et al. 2012). Similarly, animals vaccinated with a capripoxvirus expressing BTV VP7 showed partial protection against challenge with heterotypic virus (Wade-Evans et al. 1996). It is possible that non-neutralising antibodies are implicated in a process of complement activation or antibody-dependent cell-mediated cytotoxicity (ADCC), thus activating effector cells (such as natural killer and macrophages) to lyse the labelled infected cells. Only few unsuccessful attempts have been performed to demonstrate ADCC (Jeggo, Wardley & Taylor 1984). However, since limited experiments have been performed to evaluate the concomitant role of cell-mediated immunity in protection and its contribution to the development of

a specific humoral immune response, no final interpretation of these studies can be made.

1.6.3 Cellular immune response

Cell-mediated immunity can limit viral spread by targeting and eliminating infected cells. The role of effector T-cells during the course of BTV infection has not been widely investigated. The presence of BTV specific CD8 T-cells has been demonstrated following infection both in sheep and mouse models, and contrary to antibodies they demonstrate a certain degree of cross-reactivity with heterologous serotypes (Takamatsu & Jeggo 1988; Jeggo & Wardley 1982; Ghalib et al. 1985). An increase of circulating CD8 T-cell population is generally noted around 10-15 dpi (Umeshappa et al. 2010; Sánchez-Cordón et al. 2015). Indeed, sheep develop short-term cytotoxic T-lymphocytes (CTL) anti-BTV that peak at 12-14 dpi. Jeggo and colleagues, in order to study the *in vivo* role of CTL, performed the adoptive transfer of lymphocytes, taken from the thoracic duct of sheep at 7 and 14 days after experimental BTV infection, into monozygotic susceptible sheep (Jeggo, Wardley & Brownlie 1984). This experiment demonstrated the capacity of lymphocytes present at 14 dpi (but not at 7 dpi) to confer a partial protection to infection in recipient sheep. Sheep that received lymphocytes presented an earlier production of neutralising antibodies and a marked reduction of pyrexia and viraemia when challenged with a homologous BTV serotype. Furthermore, these animals showed complete protection (i.e. neither viraemia nor pyrexia) when challenged with a different BTV serotype. This observation reinforced the idea of an heterotypic protection conferred by CTL (Jeggo, Wardley & Brownlie 1984). However, since the cells transferred in this study were not characterised, it was not possible to completely rule out the presence and influence on the acquired protection of other subset of lymphocytes and of antibody producing plasma cells that were probably present among the transferred cells.

VP2 and NS1 have been identified as major CTL immunogens in sheep, with NS1 specific CTL being the main responsible for cross-protection (Andrew et al. 1995; Janardhana et al. 1999). On the contrary, in mice experimentally infected with BTV, cross protective CTL are developed against NS1 and NS2 (Jones et al. 1997; Jeggo & Wardley 1982). The difference in epitopes targeted by sheep and mouse

CTL indicate that is present a certain degree of species-specificity in the immune response.

1.7 Mouse models of infection

Studies on the pathogenesis of bluetongue can benefit from the use of the natural target specie of infection to reproduce the disease. However, large animal experiments have limitations imposed by the number of animals that is ethically acceptable to include in the study, elevated costs, the limited knowledge and the lack of tools for the analysis of the ruminant immune system. Therefore, more practical models of infection have been investigated and used for various purposes.

Neonatal mice have been used as a model to study the virulence of BTV strains (Waldvogel et al. 1986; Waldvogel et al. 1987; Caporale et al. 2011; Narayan & Johnson 1972). The initial purpose of these studies was to define a model to replicate sheep foetal infection and related cerebral malformations. In newborn mice, after intracranial inoculation, BTV replicates selectively in immature cells of the subventricular zone of the forebrain and spread along cell migratory pathways to the olfactory bulbs, caudate/putamen, hippocampus and areas of cerebral cortex (Narayan & Johnson 1972). Infection of foetal mice led to more severe cerebral malformation, while infection of 2-week-old mice results in very limited infection, demonstrating an affinity of BTV for undifferentiated cells that are gradually lost after birth (Narayan & Johnson 1972). Subcutaneous BTV infection of newborn Balb/c mice caused fatal necrotising encephalitis when virulent strains were used. Further studies, clarified that virulence was not due to the capacity of the viral strain to infect neural cells, but rather to their capacity to gain access to the brain from the skin inoculation site (Waldvogel et al. 1986; Waldvogel et al. 1987). This model was further used to determine the genetic determinants of BTV neuroinvasiveness, likely associated with VP5 and virus tropism (Carr et al. 1994). Intracerebral inoculation of neonatal mice proved useful in comparing BTV strain virulence, and attenuated vaccine safety (Franchi et al. 2008), however they do not reflect the viral dissemination and the associated pathology as it happens in the natural host.

Adult mice are resistant to BTV infection and viraemia is not observed in mice when inoculated either intravenously or subcutaneously (Ortego et al. 2014). However, blocking IFN-α/ß activity in mice has been proved useful in increasing dramatically their sensitivity to many viruses. Hence, recently a mouse model of IFNAR$^{(-/-)}$ mice was developed for BTV. These mice are lacking IFN-α/ß receptor and therefore cannot respond to IFN production. Mice with a C57BL/6 genetic background (Calvo-Pinilla, Rodríguez-Calvo, Anguita, et al. 2009) proved susceptible to various BTV serotypes, but only when inoculated intravenously. Whereas interestingly, IFNAR$^{(-/-)}$ mice with a SV129 genetic background showed the same susceptibility to BTV infection when inoculated subcutaneously, intravenously or even orally (Calvo-Pinilla et al. 2010).

Infected mice present clinical signs characterized by ocular discharges, anorexia and apathy and the disease progression led to animal death. In general, the strain virulence observed in the field in the ruminant hosts can be representatively reproduced in this mouse model, as the animal mortality rate gives an indication of the degree of BTV serotype/strain pathogenicity (Ortego et al. 2014; Caporale et al. 2011; Ratinier et al. 2011; Calvo-Pinilla, Rodríguez-Calvo, Anguita, et al. 2009; Janowicz et al. 2015). For this reason, recent studies have done extensive use of IFNAR$^{(-/-)}$ mice to help identifying the molecular determinants of BTV virulence (Caporale et al. 2011; Janowicz et al. 2015).

BTV distribution in IFNAR$^{(-/-)}$ mice mimics BTV infection in cattle and sheep. After intravenous infection BTV can be detected in spleen at 24 hpi, before its dissemination to other organs such as lungs, thymus, lymph nodes and blood (Calvo-Pinilla, Rodríguez-Calvo, Anguita, et al. 2009). The presence of viraemia after BTV inoculation is dependent on the viral dose administered, with only mice infected with high viral dose presenting viraemia, appearing at 2 dpi (24h after spleen infection) and peaking at 4 dpi (Calvo-Pinilla, Rodríguez-Calvo, Anguita, et al. 2009).

Histological analyses of BTV infected mice at 48 hpi showed many similarities with lesions described in natural hosts. Widespread oedema, petechiae and haemorrhages can be observed, especially in spleen and lungs. A bronchointerstitial pneumonia it is often present. The enlargement of secondary lymphoid organs, which can indicate immune activation, is accompanied by a

severe lymphoid depletion, that has not been further characterized, and a loss of the architecture of thymus (Calvo-Pinilla, Rodríguez-Calvo, Anguita, et al. 2009).

IFNAR$^{(-/-)}$ mice proved useful also in vaccine protection studies, since upon immunization they develop neutralizing antibodies and cytotoxic T-cells targeting varies viral proteins, and are protected against lethal challenge with virulent BTV strains (Calvo-Pinilla, Rodríguez-Calvo, Sevilla, et al. 2009; Marín-López et al. 2014).

Chapter 2

Aims

2 Aims

The aims of this research project were to investigate the early events of BTV infection in experimentally infected animals and determine how they affect viral pathogenesis and the clinical outcome of disease.

More specifically we aimed to:

1. Identify the sites (both at the tissue and cellular level) where BTV replicates in experimentally infected sheep.

2. Characterise immunopathological changes induced by BTV in experimentally infected sheep.

3. Characterise the humoral immune and immunopathology in sheep and goats infected with different strains of BTV.

Chapter 3

Material and Methods

3 Material and Methods

3.1 Cell Culture

3.1.1 Maintenance of cell culture

Sterile standard conditions of tissue culture were maintained throughout the experiments.

African green monkey kidney (Vero), Baby hamster kidney (BHK-21) cells and BSR cells (a variant of BHK-21 cells) were maintained in Dulbecco's Modified Eagle's Medium (DMEM, Thermo Scientific) supplemented with heath inactivated 10% (v/v) foetal bovine serum (FBS) (Thermo Scientific), 4 mM stabilized L-glutamine (GlutaMAX, Gibco), 25 mM dextrose, 1 mM pyruvate, 100 U/ml penicillin and 100 μg/ml streptomycin (Thermo Scientific).

Ovine choroid plexus cells (CPt-Tert) are sheep cells immortalised with simian virus 40 (SV40) T antigen and human telomerase reverse transcriptase (Arnaud et al. 2010; Caporale et al. 2014); cells were maintained in Iscove's Modified Dulbecco's Medium (IMDM, Thermo Scientific) supplemented as above for DMEM.

Culicoides sonorensis (KC) cell line (Wechsler et al. 1989) was grown in Schneider's Insect Medium (Thermo Scientific) supplemented with 15% FBS (Thermo Scientific).

Mammalian cells were maintained in incubators at 37 °C with 5% CO_2 humidified atmosphere, while insect cells were maintained at 28 °C without CO_2. Cells were routinely grown in 225 cm^2 flasks and passaged when reaching confluence. For propagation, cell monolayer was rinsed twice with phosphate buffered saline (PBS), and then incubated with a 0.05% trypsin solution containing 200 mg/L Ethylenediaminetetraacetic acid (EDTA), for 10 min at 37 °C (Thermo Scientific). Once detached cells were re-suspended in fresh media and transferred to a new sterile flask or used for assays.

For long term storage in liquid nitrogen, harvested cells were pelleted at 400x*g* for 10 minutes and re-suspended in 90% (v/v) FBS, 10% (v/v) dimethyl sulfoxide (DMSO) (Thermo Scientific). The suspension was divided in 1 ml aliquots ($1x10^6$

cells/vial), gradually brought at -80°C over 24 hours before being transferred to liquid nitrogen.

3.1.2 Viruses

Experiments were performed using different isolates of BTV serotype 8 (BTV-8).

BTV-$8_{NET2006}$ (Pirbright Institute for Animal Health, reference collection number NET2006/04) is a virulent strain isolated from a naturally infected sheep in the Netherlands, during an outbreak occurring in Northern Europe in April 2006 and previously described (Caporale et al. 2014; Ratinier et al. 2011). Here it will be referred to simply as BTV-8.

BTV-$8_{NET2007(blood)}$ is whole blood obtained from the spleen of a sheep experimentally infected with blood derived from a naturally infected cow in the Netherlands during the 2007 BTV-8 outbreak as previously described (Caporale et al. 2014). Here it will be referred to as $BTV8_{blood}$.

BTV-8_{IT2008} is a naturally attenuated strain, circulating in Italy during 2008 and isolated from an asymptomatic sheep and has been already described (Caporale et al. 2014). Here this will be referred to as $BTV8_{ita}$.

BTV-8_{p65} is an *in vitro* attenuated strain, produced by 65 sequential passages of BTV-$8_{NET2006}$ in BSR cells that has been previously described (Janowicz et al. 2015). Here this will be referred to as $BTV8_H$ (H for "highly passaged").

All viruses sourced from the field (naturally infected animals) were initially isolated on KC cells and subsequently passaged on BHK-21 cells. Afterwards, virus stocks were grown in BHK-21 cell lines. BHK-21 cells were grown in 175 cm^2 flasks until 90% confluent, then growth media (DMEM) was removed and the cell monolayer washed once with DMEM without FBS. Next, 100 µl of stock virus were diluted in 20 ml of DMEM (without serum and antibiotics) and added to the cells which were incubated at 37 °C for 4 to 5 days, until complete destruction of the cellular monolayer. Supernatant was harvested and centrifuged at 500x*g* for 10 minutes to remove cellular debris, then transferred to tubes for storage at 4 °C.

All viruses used in this study for animal infection, a part from $BTV8_H$, have the same passage history (1 passage in KC cells and two passages in BHK-21 cells) unless indicated otherwise.

3.1.3 Virus titration

Virus titre was determined by plaque assay or by end point dilution assay as previously described (Caporale et al. 2014; Nunes et al. 2014; Ratinier et al. 2011).

3.1.3.1 Plaque Assay titration

Plaque assay allows the determination of virus titre by scoring the number of plaque forming unit (PFU) generated by a virus stock in a standardised tissue culture. Each BTV-8 virus stock use in this work was quantified in triplicate. Tenfold serial dilutions of virus stock were prepared in serum-free DMEM, from 10^{-1} to 10^{-7}. 250 µl of each dilution was added to an 80% confluent monolayer of Vero cells ($5x10^5$ cells/well) in a 6 well plate and incubated for 1 hour at 37 °C to allow virus absorption. After virus removal and a wash with PBS, the cells were covered with a semisolid overlay medium prepared with a 50/50 dilution of 2.4% (w/v) Avicell (FMC BioPolymer, Belgium) with 2x Minimum Essential Media (MEM) supplemented with 4% (v/v) FBS. Plates were incubated for 72 hours at 37 °C, 5% (v/v) CO_2 to allow the appearance of cytopathic effect (CPE). Cells were then fixed with 4% formaldehyde in PBS for 20 minutes followed by staining with Crystal Violet, 0.1% (w/v) in PBS to visualize plaques. Plaques were counted in the wells showing the best discrimination and their dilution taken in account to calculate the virus titre. Virus titre was determined as the number of plaque forming units per ml (PFU/ml) of virus.

3.1.3.2 End point dilution assay

Tissue Culture Infectious Dose 50 ($TCID_{50}$) is an endpoint dilution assay that allows virus quantification, in which the virus is required to produce a cytopathic effect in 50% of inoculated tissue cultures. It is generally expressed as $TCID_{50}$/ml. Each virus stock used was titrated in quadruplicate. Serial tenfold dilutions of the virus stock were performed from 10^{-1} to 10^{-8} in DMEM in a flat bottom 96 well plate; to these, 100 µl of a suspension of Vero cells containing

$2.5x10^4$ cells in DMEM with 10% FBS were added and incubated at 37 °C with 5% CO_2 atmosphere. After 4 days the CPE was assessed with the use of an inverted microscope, with BTV infected cells rounding up and detaching from the bottom of the wells, showing partially or completely confluent foci of destruction in the monolayer. Positive well (showing CPE foci) and negative wells (presenting an intact cells monolayer) were recorded. Virus titre was determined using the Reed-Muench method (Reed & Muench 1938) and expressed as $\log_{10}$ tissue culture infectious dose 50 per ml of virus ($\log_{10}$ $TCID_{50}$/ml).

3.2 *In vivo* experiments

Due to the restriction imposed by animal health regulations on exotic and notifiable animal diseases (SAPO and Animal Health Act) the in vivo part of this project was carried out by collaborators in other EU countries. All the experimental infections of sheep, goats and mice were carried out by Dr. Marco Caporale at the Istituto Zooprofilattico Sperimentale dell'Abruzzo e del Molise "G. Caporale" (Teramo, Italy) and, only were specifically stated, by Dr. Noemi Sevilla at the Centro de Investigación en Sanidad Animal (Madrid, Spain) in accordance with locally and nationally approved protocols regulating animal experimental use (protocol numbers 7440; 11427; 12301 in Teramo and 10/142792.9/12, CBS2012/06 and PROEX 228/14 in Madrid). In addition, and to minimize the number of animals under experiment, some of the animal samples used for this study were sourced from previous experimental infections (Janowicz et al. 2015; Caporale et al. 2014). Experimental infections in sheep and goats were conducted in an insect-proof isolation unit (in BSL-3 facilities) supported by continuous veterinary care. Sheep and goats included in these studies were sources from local farms. Prior to the infections the animals were confirmed to be seronegative for BTV using a competitive ELISA (cELISA), and the absence of circulating virus was assessed by Real-Time Quantitative Reverse Transcription-PCR (qRT-PCR) on blood samples, as previously described (Caporale et al. 2014).

3.2.1 Viral localization studies in sheep and goats

Study 1. In order to follow the temporal dissemination of the infection in the natural host, sheep (n=23) were infected intradermally (ID) with a total of $2x10^6$ PFU of BTV8 in 5 ml of cell culture media (MEM, Thermo Fischer Scientific) by multiple inoculations (100 µl per inoculation) in four different areas in the inner legs and in the forearm, in areas drained by the corresponding inguinal and prescapular LNs. Control animals (n=8) were infected with 5 ml of mock-infected cell culture supernatant (MEM). Animals were monitored daily for clinical signs and body temperature recorded every day until the end of the experiment. Blood samples were collected (in EDTA) daily in order to detect viremia. Animals were humanely euthanized at 4, 8, 24, 48, 72, 96, 120 and 168 hpi (n=3 per each time point with exception of 96 h were n=2). Tissue samples of tongue, heart, aorta, spleen, lung, kidney, liver, skin and various lymph nodes (mediastinal, prescapular, inguinal, popliteal, retromandibular) were collected during post-mortem examination and fixed in 10% (v/v) neutral buffered formalin or zinc salts solutions (BD Pharmigen) and embedded in paraffin for further histological assays, while tissues used for RNA extraction and detection of viral nucleic acid were stored at -20°C in RNAlater (Thermo Fisher) until processed. In order to assess the effects and localization of an inactivated virus, two additional control sheep were inoculated with $2x10^6$ PFU of UV-inactivated BTV8 and euthanized respectively at 24 and 48 hours post infection (hpi).

Study 2. In order to follow the tissue dissemination of BTV-8 in goats, domestic goats (n=18) were inoculated with BTV8 as detailed above and euthanized at 8, 24, 48, 72, 96 and 168 hpi (n=3). Blood and tissue samples were collected as above.

Study 3. In order to follow the tissue dissemination of an attenuated strain of BTV-8, sheep (n=13) were inoculated with $BTV8_H$ (Janowicz et al. 2015) as detailed above and euthanized at 8, 24, 48, 72, 96 and 168 hpi (n=2, except from 168 h were n=3). Blood and tissue samples were collected as above for detection virus localization by qPCR and for histological assays.

3.2.2 Virus localization studies in mouse model

In order to limit the number of sheep and goats to include in the study, we tested weather a mouse model of BTV infection could recapitulate the localization of the virus in the draining lymph nodes as observed in ruminants. Adult NIH Swiss mice and transgenic mice (129sv IFNAR$^{-/-}$, B&K Universal Ltd.), deficient in type I interferon-alpha/beta receptor (IFNAR) described to be susceptible to BTV infection (Calvo-Pinilla, Rodríguez-Calvo, Anguita, et al. 2009; Caporale et al. 2011) were maintained at biosafety level 3 at the IZS (Teramo, IT). In order to identify BTV localization in the LNs in mouse models of BTV infection, groups of adult mice (n=6 for NIH Swiss and n=8 for IFNAR$^{-/-}$), age and sex-matched, were inoculated subcutaneously in the thighs with 300 PFU of BTV8 in 200 μl of cell culture media (100 μl each injection) or an equivalent volume of mock infected cell culture medium as a control. Mice were examined for clinical signs daily until the experiment was terminated (day 2) and/or the animals euthanized. Two challenged and one control mouse per group were euthanized at 4 (IFNAR$^{-/-}$ mice only), 8, 24 and 48 hours post-inoculation, inguinal lymph nodes draining the site of inoculation were collected and fixed in 10% neutral buffered formalin for histological assessment and for virus detection by confocal microscopy (as described below).

3.2.3 Long-term serological studies in sheep and goats

Study 1. In order to compare antibody responses in goats and sheep infected with virulent and attenuated strains of BTV-8, 3 sheep and 3 goats were inoculated with 2x10^6 PFU of BTV8 and an additional group of 3 sheep was inoculated with 2x10^6 PFU of BTV8$_{ita}$. Animals were monitored for 28 days, body temperature recorded, and blood samples collected as above at day 7, 14, 21 and 28 post infection for detection of virus RNA and viremia assessment. Serum samples were collected daily until day 14 and then at day 21 and 28 and were used to evaluate BTV-specific antibody response by ELISA, neutralization titres and serum avidity.

Study 2. In order to expand the range of our observations on specificity and avidity of antibody responses to BTV infection to a larger number of animals and to limit the number of newly infected animals, we analysed serum samples

collected during previously published studies (Caporale et al. 2014; Janowicz et al. 2015). In the first study, a group of 5 Sardinian sheep were inoculated with 5 ml of infected blood ($BTV8_{blood}$) and serum samples collected daily until day 28 post infection. In a second study a group of 5 Sardinian sheep, were inoculated with $5x10^5$ PFU of $BTV8_H$ and serum from these animals collected at day 7, 14, 21, 28. In both experiments serum was stored at -80 °C after collection and tested for the presence of BTV neutralising antibodies, and BTV specific IgG and IgM and their avidity by ELISA (see 3.5).

Study 3. Performed at the Centro de Investigación en Sanidad Animal (Madrid, Spain). In order to assess the B-cell response against a second antigen during the course of BTV infection, two groups of sheep (n=5 per group) were inoculated with BTV-8 as detailed above then immunised with 20 mg of ovalbumin (OVA) at either 24 or 72 hpi respectively. Ova is a T-dependent antigen and therefore requires the presence of T-helper cells and the initiation of a GC reaction for the production of antibodies. Hence, OVA was chosen to test the function of GCs in infected animals. The administered concentration of OVA was determined by preliminary immunisation experiments that assessed the capacity of OVA to induce antibody titres detectable by ELISA, without the use of adjuvants. OVA was inoculated via the intradermal route a few centimetres apart from the area of BTV inoculation to prevent confounding effects that could originate from BTV infection in the skin. A third group of sheep (n=5) was immunized with OVA (20 mg) with no prior BTV infection and served as a control. Blood and serum samples were collected at 7, 14, 21 and 28 days post-OVA immunization. The number of OVA-specific antibody producing cells (ASC) in the peripheral circulation was quantified by B cell ELISPOT (see below) and OVA-specific IgM, IgG and their avidity was quantified by ELISA (see below).

3.3 Nucleic acids extraction, quantification and amplification

3.3.1 RNA purification

RNA was extracted and purified from blood and tissue samples collected from sheep and goats experimentally infected with BTV as described below.

3.3.2 Extraction of RNA from blood samples using "High Pure Viral Nucleic Acid Kit"

To lyse red blood cells and release viral particles, 1 ml of distilled water was added to 0.5 ml of whole EDTA blood. Samples were vortexed and incubated 10 minutes on ice before centrifuging at 13,000x*g* for 10 minutes. The pellet was re-suspended in 200 µl of Binding Buffer provided with the High Pure Viral Nucleic Acid Kit (Roche, UK). Lysates where then processed accordingly to the recommended manufacturer protocol. Briefly, 200 µl of Binding Buffer supplemented with Poly(A) carrier RNA and 50 µl Proteinase-K were added to the samples. In addition, to control extraction efficiency, 5 µl of a 1:100 dilution of Armored RNA, West Nile Virus HNY1999 (Asuragen) NS5-2region were added to each sample. Samples were then incubated at 72 °C for 10 minutes before being mixed with further 100 µl of binding buffer. Samples were then transferred to a High Pure Filter tube and the RNA bound to the column membrane by centrifugation at 8000x*g* for 1 minute. After washing the column once with 500 µl of Inhibitor Removal Buffer and twice with 450 µl of Wash Buffer, the RNA was eluted by centrifugation in 50 µl of Elution Buffer.

3.3.2.1 Extraction of RNA from tissue samples using TRIzol® and purification with Qiagen RNeasy mini Kit®

Tissue sections were collected and trimmed immediately after euthanasia in the post mortem room, transferred to RNA-later® stabilization solution (Thermo Fisher Scientific) and stored at -20 °C until extraction. After defrosting, one-hundred and fifty (150) mg of tissue were transferred to a 2 ml tube containing 1.5 ml of TRIzol® Reagent (Thermo Fisher Scientific) and lysed using glass beads in a Precellys® 24 homogeniser at 6800 rpm, until complete dissolution. Debris were removed by centrifugation at 12,000x*g* for 10 minutes at 4 °C; supernatant

was collected and transferred to a new tube containing 300 µl of chloroform and mixed for 15 seconds. After a 3 minutes incubation at room temperature samples were centrifuged at 12,000x*g* for 15 minutes at 4°C, after which the mixture separates into a lower red phenol-chloroform phase, a white interphase, and a colourless upper aqueous phase containing RNA. The upper phase was collected and transferred to a new tube for RNA precipitation by addition of 500 µl of 100% isopropanol.

RNA purification was performed accordingly to the RNeasy mini kit (Qiagen®) protocol. Briefly, samples were loaded into RNeasy mini-spin columns and RNA bound to the column membrane by centrifugation at 8000x*g* for 30 sec. The membrane was washed once with 700 µl of Buffer WT1 and twice with 500 µl Buffer RPE (provided with the kit). The RNA was then eluted into a new microcentrifuge tube with 50 µl RNase-free water pipetted directly onto the silica-gel membrane of the column and centrifuged at 13000xg.

3.3.3 RNA quantitation and storage

RNA eluted from the columns (3.3.2 and 3.3.2.1) was quantified using a spectrophotometer (NanoDrop™ 1000, Thermo Scientific). The ratio of absorbance at 260 nm and 280 nm were used to assess the purity of RNA. A ratio of ~2.0 was considered acceptable for "pure" RNA. Extraction was repeated if the elute did not meet the expected standard. Samples were then stored in RNAse-free, low binding tubes at -80°C until further use.

3.3.4 Quantitative real time PCR

Quantification of virus copy number in tissues of animals experimentally infected with BTV was determined by quantitative real time polymerase chain reaction (qRT-PCR) using a previously described method (Jimenez-Clavero et al. 2006; Caporale et al. 2014).

To standardise qRT-PCR reactions, a standard curve was prepared using tenfold dilutions of BTV segment-1 RNA, from 10^1 to 10^8 copies per 2 µl, aliquots for each dilution were prepared and stored at -80°C until needed. The standard dilutions were included in triplicates in plate.

Primers and TaqMan® probes were designed to recognise highly conserved regions of the target sequences (BTV seg-1, West Nile Armored RNA seg-5 and mammalian ß-actin). A list of primers and probes used for this study are detailed in Table 3-1.

Table 3-1 - List of primers and probes used for qRT-PCR
6-carboxyfluorescein (FAM), tetramethylrhodamine (TAMRA). HEX™ (from Eurofins Scientific). BTNS1 (bluetongue virus segment-1), WNNS5 (West Nile virus segment-5), B-ACT (β-actin),

Sequence		Name	Oligonucleotides
BTV seg-1	Probe	BTNS1-P	FAM–5'-CGC TTT TTG AGA AAA TAC AAC ATC AGT GGG GAT–3'-TAMRA
	Forward primer	BTNS1-F	5'-TGG CAA CCA CCA AAC ATG G-3'
	Reverse primer	BTNS1-R	5'-CCA AAA AAG TCC TCG TGG CA-3'
West Nile Armored RNA seg-5	Probe	WNNS5-2P	HEX-5'-CCA ACG CCA TTT GCT CCG CTG -3'-TAMRA
	Forward primer	WNNS5-2F	5'- GAA GAG ACC TGC GGC TCA TG -3'
	Reverse primer	WNNS5-2R	5'- CGG TAG GGA CCC AAT TCA CA -3'
ß-actin (GenBank: FQ232650.1)	Probe	B-ACT-P	HEX-5'-CCT GGC CTC ACT GTC CAC CTT CCA-3'-TAMRA
	Forward primer	B-ACT-F	5'- TCT GTG TGG ATT GGT GGC TCT A-3'
	Reverse primer	B-ACT-R	5'- CTG CTT GCT GAT CCA CAT CTG -3'

A duplex reaction was set up to quantify at the same time virus copy number and an internal (β-Actin, housekeeping) or external (West Nile Armored RNA) control reference gene. No template controls (NTC), including all reagents except RNA template, were included in each plate to exclude accidental contamination.

The PCR assays were performed with a one-step qPCR kit, where reverse transcription and PCR amplification are carried out in the same tube. RT-PCR reactions were set up in 25 µl using the SuperScript™ III Platinum® One-Step Quantitative RT-PCR System (Thermo Fisher Scientific, UK), accordingly to manufacturer's instructions. Reaction mix was prepared as described in Table 3-2.

Table 3-2 - Reaction mix prepared for the detection of BTV seg1 (BTNS1) copy number and internal (β-actin, B-ACT) or external control (West Nile seg.5, NS5)

Reagent	Initial Concentration	Final Concentration	Volume per Reaction
2X Reaction Mix	2X	1X	12.5 µl
SSIII/Platinum TaqMix	-	-	0.5 µl
Probe BTNS1-P	50 µM	250 nM	0.13 µl
Primer BTNS1-F	100 µM	450 nM	0.1 µl
Primer BTNS1-R	100 µM	450 nM	0.1 µl
Probe NS5-2P or B-ACT-P	20 µM	150 nM	0.19 µl
Primer NS5-2F or B-ACT-F	50 µM	200 nM	0.10 µl
Primer NS5-2R or B-ACT-R	50 µM	200 nM	0.10 µl
ROX dye	50X	1 nM	0.05 µl
Nuclease-free Water	-	-	1.23 µl

A fixed amount of RNA (250 ng) in nuclease free water in a final volume of 10 µl was used for each reaction. An initial (pre-PCR) heating step was carried out at 95°C for 5 minutes to denature ds-RNA molecules.

Reactions were performed in duplicate in 96-well PCR plates (Applied Biosystem) using an Applied Biosystems® 7500 Fast Dx Real-Time PCR Instrument with the cycling program detailed in Table 3-3.

Table 3-3 - Thermal cycle used for qRT-PCR

	Function	Temperature	Time	Cycles
First Step	cDNA synthesis	50°C	15 min	Hold
		95°C	2 min	
Second Step	Denaturation	95°C	15 sec	45 Cycles
	Annealing	60°C	30 sec	

The threshold was set up at 10 times the standard deviation of the baseline, in the region of the exponential growth of PCR product. Threshold cycle (Ct) values were automatically calculated using the AB SDS® software for each sample and defined as the point where the amplification curve crossed the threshold line

(Figure 3-1). Assuming equal PCR efficiency, Ct values are inversely correlated to the logarithm of the initial copy number. For the calibrators, a Ct value of 35±2 was expected and no amplification was expected from NTC samples. If these parameters were not met, the samples were re-tested. For the BTV seg-1 (BTNS1) reaction, samples with a Ct value >40 were considered negative, because under the detection limit of $1x10^2$copies/reaction. Valid Ct values were interpolated by the software with the standard curve to calculate quantitative values; results were expressed as $\log_{10}$ copy number per 1 μg of total RNA (Figure 3-2).

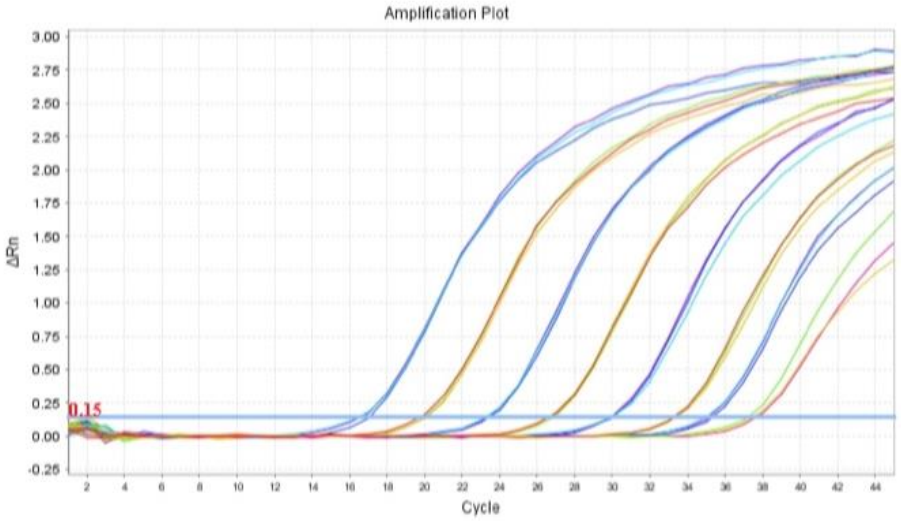

Figure 3-1 Amplification plot of qRT-PCR standard curve for BTV segment 1.
Rn is the fluorescence of the reporter dye divided by the fluorescence of the passive reference dye (ROX). ΔRn is Rn minus the baseline. ΔRn is plotted against PCR cycle number.

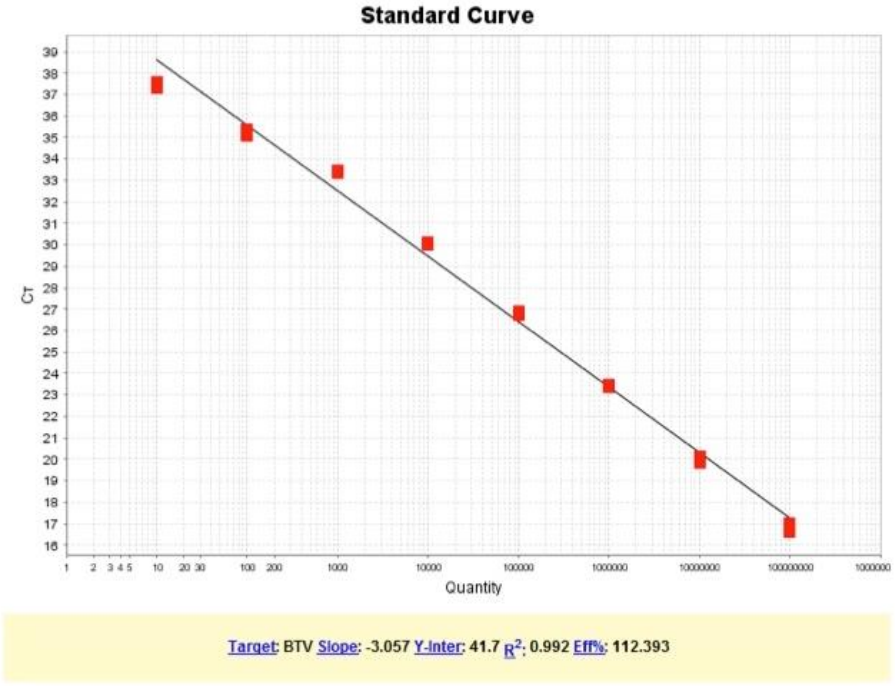

Figure 3-2 Standard curve alignment for BTV segment 1

3.4 Microscopy

3.4.1 Preparation of animal tissues for microscopy

Tissue samples were collected immediately after euthanasia in the post mortem room as described above. For immunohistochemical analysis fresh samples were trimmed to 0.5 cm in thickness for 1 cm square, and placed into processing cassettes.

3.4.1.1 Fixation

Cassettes containing tissue samples were immersed for 48 hours in a 10% neutral buffered formalin solution before further processing. For zinc salt fixation, cassettes with tissues were instead placed directly in 1% zinc fixative solution (BD Pharmingen) and allowed to sit for 24-48 hours at room temperature before processing.

3.4.1.2 Dehydration, clearing and embedding

After 48 hours, tissues were removed from formalin or zinc fixative solution and dehydrated in increasing concentration of ethanol (from 0 to 100%) then cleared in xylene and embedded in paraffin blocks as per standard histology protocols.

3.4.2 Immunohistochemistry

3.4.2.1 Sectioning

Tissue sections were cut with a microtome (4 μm thickness) and mounted on microscope slides. Sections were dewaxed with multiple passages in xylene, and re-hydrated in decreasing concentration of ethanol: 100%, 95%, 75%, 50%, and finally rinsed in water.

3.4.2.2 Antigen Retrieval Technique

Formalin fixation induces protein cross-linking which can results in conformational changes of antigenic epitopes, leading to an absent or decreased antibody reactivity. To restore the immunoreactivity of the epitopes and break formalin-induced methylene bridges, two methods are currently available: heat induced epitope retrieval (HIER) and protease induced epitope retrieval (PIER). Different types of antigen retrieval techniques were tested on formalin fixed, paraffin embedded tissues to unmask specific epitopes.

3.4.2.3 Citrate buffer - HIER

Heat induced antigen retrieval was performed in the pathology department of the School of Veterinary Medicine Diagnostic Services at the University of Glasgow. Sections were treated with Access Retrieval Unit (Menarini) in Buffer Sodium Citrate pH6, for 1 min 30 sec at 125ºC at full pressure. Then rinsed in Tris buffer pH7.5.

3.4.2.4 Proteinase K - PIER

Proteolytic digestion of formalin-fixed tissues was performed using a ready-to-use solution of proteinase-K in 0.05 M Tris-HCl, 0.015 M sodium azide, pH 7.5

(Dako, UK). Tissues were incubated for 10 minutes at 37 °C with the pre warmed solution of proteinase K, and then rinsed with PBS.

3.4.2.5 Trypsin - PIER

For Trypsin-PIER antigen retrieval treatment slides were held in water a 37 °C until transferred to a pre-warmed (37 °C) trypsin solution (0.05% trypsin, 1% $CaCl_2$, and 0.05% chymotrypsin, pH 7.8 (all reagents form Sigma, UK) and digested for 20 minutes then rinsed with PBS.

3.4.2.6 Sample labelling for immunohistochemistry (IHC)

After antigen retrieval, the tissue sections were permeabilised with a PBS solution of 1% Triton-X (Sigma) for 10 minutes at room temperature. To quench endogenous peroxidase activity slides were then treated for 30 minutes at RT with an aqueous solution of 3% hydrogen peroxide. After four washes with PBS 0.05%/Tween 20 (PBS T20, Sigma) the sections were incubated for 80 minutes with a blocking buffer containing 5% bovine serum albumin in PBS to block unspecific binding sites. Primary antibodies specific or cross-reactive with sheep and goat antigens were diluted in blocking buffer accordingly to Table 3-4 and incubated with the tissue sections overnight at 4 °C. Excess primary antibodies were removed with several washes in PBS T20.

For primary antibody detection, sections were incubated with appropriate secondary antibodies conjugated either with horseradish peroxidase (HRP) or with alkaline phosphatase (AP), for one hour at room temperature (RT). This was followed by a 5-10 minute incubation with 3,3'-diaminobenzidine (DAB) substrate-chromogen (EnVision$^+$ System, Dako) which produces a brown coloured precipitate at the antigen site or with Permanent Red chromogen (EnVision G|2 System/AP, Dako) which develops in a red coloured precipitate. Tissues were counterstained using Mayer's haematoxylin and mounted with clear resin and coverslips for long-term storage.

Tissue sections were screened using an optical microscope at different magnifications and images captured using cell^D software (Olympus).

Table 3-4 - List of research or commercial primary antibodies used in IHC and IF.
Required antigen retrieval method (AR): Citrate HIER (C), Proteinase-K PIER (K), Trypsin PIER (T). Fixative (FIX) used: formalin (F) or zinc salt (Z). Mouse (Mo), Rabbit (Rb)

Target	Clone	Isotype	Producer	Working dilution	AR	FIX
MHCII	SW73.2	Rat	Moredun	1:100	C	F
CD3	F7.2.38	Mo IgG1	Dako	1:200	C	F
CD79a	HM57	Mo IgG1	AbD Serotec	1:100	C	F
CD163	EDHu-1	Mo IgG	AbD Serotec	1:100	C	F
WC1	CC15	Mo IgG2a	AbD Serotec	1:20	C	F
IFN-γ	7B6	Mo IgG1	AbD Serotec	1:20	C	F
Ki-67	MIB-1	Mo IgG1	Dako	1:100	C	F
CD68	EBM11	Mo IgG1	Dako	1:100	T	F
CD169 - Siglec-1	HSn 7D2	Mo IgG1	Santa Cruz Biotech	1:10	-	Z
Cleaved Caspase 3	D175-5A1E	Rb	Cell Signaling	1:200	C	F
CD1w2	CC20	Mo IgG2a	AbD Serotec	1:20	-	Z
CD45	1.11.32	Mo IgG1	AbD Serotec	1:20	-	Z
CD1	20:27	Mo IgG1	AbD Serotec		-	Z
CD83	HB15e	Mo IgG1	AbD Serotec	1:50	C	F Z
CD11b	CC126	MoIgG2b	AbD Serotec	1:20	-	Z
CD21	CC21	MoIgG1	AbD Serotec	1:50	-	Z
CD8	CC63	MoIgG2a	AbD Serotec	1:100	-	Z
Desmin	DE-U-10	Mo IgG1	Sigma-Aldrich	1: 20	C	F
Fascin	55K-2	Mo IgG1	Dako	1:20	C	F
Podoplanin	D2-40	Mo IgG1k	Dako	1:10	-	Z
VWF	-	Rb IgG	Dako	1:200	K	F
Vimentin	Vim3B4	Mo IgG2ak	Dako	1:60	C	F
B cells	Dak-Pax5	Mo IgG1	Dako	1:20	C	F
FDC	CNA.42	Mo IgM	Dako	1:20	C	F
CD208 - DC lamp	1010E1.01	Rat IgG2a	Dendritics	1:80	C	F
TLR3 - CD283	713E4.06	Mo IgG1	Dendritics	1:20	-	Z
ICAM-1 CD54	117G12	Mo IgG1	Dendritics	1:20	-	Z
Perlecan	A71	Mo IgG1	Source bio	1:40	C	F
Cleaved Caspase 3	Asp175	Rb poly	Cell Signalling	1:200	C	F Z
S100	-	Rb poly	Dako	1:100	C	F Z
PCNA	PC10	Mo IgG2a	AbD Serotec	1:100	C	F
Jam-A	-	Rb Poly	AbD Serotec	1:50	C	F
ß-actin	-	Rb IgG	AbD Serotec	1:50	-	F
SMA	1A4	Mo IgG2a	Cell signaling	1:50	C	F
CD8	38.65	Mo IgG2a	Dako	1:50	-	F Z
CD4	44.38	Mo IgG2a	AbD Serotec	1:100	-	Z

3.4.3 Immunofluorescence

Tissue sections were treated as previously described for IHC with the following modifications. After primary antibody incubation, sections were rinsed in PBS T20 and incubated with appropriate anti-mouse, rabbit or rat species or isotype-specific fluorescently labelled secondary antibodies (AlexaFluor, Thermo Fisher) (Table 3-5) for one hour at RT. Excess secondary antibodies was removed by PBS T20 washes and sections were mounted using a liquid antifade mountant (Prolong Gold, Thermo Fisher) containing 4',6-diamidino-2-phenylindole (DAPI) for the staining of chromatin. The sections were stored at 4 °C and read within a week from preparation.

Table 3-5 - List of secondary antibodies used for immunofluorescence

Target	Host species	Conjugate	Manufacturer
Mouse IgG1	Goat	Alexa Fluor 488	Thermo Fisher
Mouse IgG1	Goat	Alexa Fluor 555	Thermo Fisher
Mouse IgG1	Goat	Alexa Fluor 594	Thermo Fisher
Mouse IgG1	Goat	Alexa Fluor 633	Thermo Fisher
Mouse IgG2a	Goat	Alexa Fluor 488	Thermo Fisher
Mouse IgG2a	Goat	Alexa Fluor 555	Thermo Fisher
Mouse IgG2a	Goat	Alexa Fluor 633	Thermo Fisher
Mouse IgG2b	Goat	Alexa Fluor 488	Thermo Fisher
Mouse IgG2b	Goat	Alexa Fluor 594	Thermo Fisher
Mouse IgM	Goat	Alexa Fluor 488	Thermo Fisher
Mouse IgM	Goat	Alexa Fluor 555	Thermo Fisher
Mouse IgM	Goat	Alexa Fluor 594	Thermo Fisher
Mouse IgM	Goat	Alexa Fluor 633	Thermo Fisher
Rat IgG	Goat	Alexa Fluor 488	Thermo Fisher
Rat IgG	Goat	Alexa Fluor 555	Thermo Fisher
Rat IgG	Goat	Alexa Fluor 633	Thermo Fisher
Rabbit	Goat	Alexa Fluor 488	Thermo Fisher
Rabbit	Goat	Alexa Fluor 555	Thermo Fisher
Rabbit	Goat	Alexa Fluor 594	Thermo Fisher
Rabbit	Goat	Alexa Fluor 633	Thermo Fisher
Guinea Pig	Goat	Alexa Fluor 488	Thermo Fisher

Viral proteins were detected with the use of a tyramide signal amplification (TSA) system (Thermo Fisher). Custom produced antibodies directed against structural and non-structural BTV proteins (Table 3-6) were applied to sections

overnight at 4°C. After washing excess primary antibody off, the sections were incubated with secondary donkey anti-rabbit antibodies conjugated to HRP (GE Healthcare Life Sciences) for 1 hour at RT then washed again with PBS T20. TSA reagent was then incubated for 10 minutes at RT with the sections to create a fluorescent precipitate. Sections were mounted using Prolong Gold antifade reagent as previously described, and the coverslip sealed using nail polish for medium term storage in the dark, at 4 °C.

Table 3-6 - List of antisera raised against different BTV proteins and their concentration used in immunohistochemical and immunofluorescence studies

Target Protein	Antiserum Produced In	Working Dilution
BTV-VP7	Rabbit	1:8000
BTV-NS1	Rabbit	1:7000
BTV-NS2	Rabbit	1:7000
BTV-NS2	Guinea Pig	1:8000
BTV-NS3	Rabbit	1:7000
BTV-NS4	Rabbit	1:6000

3.4.4 Confocal Microscopy

Fluorescently labelled samples were examined using a Zeiss LSM710 confocal microscope, equipped with 405, 458, 488, 514, 561, 633 nm lasers lines and Differential interference contrast (DIC) filters. Image were captured and processed with Zeiss Zen software. Rendering of Z-stack acquisitions were elaborated using Imaris (Bitplane) and FIJI (Image J) software.

3.5 Serology

3.5.1 Serum collection and heat inactivation

Blood samples were collected and kept at room temperature for 30 minutes to promote clot formation then centrifuged at 1,500x*g* for 10 minutes at 20 °C to separate the serum; serum supernatant was collected and stored frozen at -80°C until further use. Before use, serum samples were aliquoted and heat-treated at 56 °C for 30 minutes to inactivate the complement and any residual viral

particle. Heat inactivated serum samples were used throughout the experiments.

3.5.2 Neutralization Assay

The presence of neutralizing antibodies in experimentally infected sheep was assessed by micro-neutralization assay as recommended in the OIE guidelines (OIE - World Organisation for Animal Health 2016a)

To obtain the neutralization titre, serial dilution of the sera were prepared in DMEM supplemented with 3% FBS and diluted by a factor of 2, starting from 1:4 until 1:16,384 in a total volume of 100 µl. The serum was then incubated with 100 $TCID_{50}$ of BTV-8Net2006 in 50 µl of DMEM for 1 hour at 37 °C.

In each well of a 96-well flat bottom plate, 50 µl of a suspension of Vero cells containing $4x10^5$cells/ml in DMEM/3% FBS were added to 150 µl of the serum/virus mixture prepared as above and incubated at 37 °C with 5% CO_2. After 6 days the plates were fixed with 5% formaldehyde and stained using a Crystal Violet solution (0.1%). The level of CPE was quantified for each well by eye, and a well was considered protected when displayed more than 75% CPE neutralization in the cell monolayer (accordingly to OIE guidelines) (OIE - World Organisation for Animal Health 2016a)

Each sample was tested in quadruplicates, and each experiment also included a "negative control serum" obtained from a BTV naïve animal (tested by cELISA), a "positive control serum" coming from a BTV vaccinated and experimentally challenged animal, a "CPE control" were wells contained no serum but only cells and virus, and finally a "cells only control" with Vero cells suspension only.

The neutralization titre for each sample was calculated using the Reed and Muench method (Reed & Muench 1938) and expressed as 50% protective dose (PD50), defined as the dilution of antiserum required to protect 50% of Vero cell cultures from BTV infection. Samples under the detection limit of 2.23 $\log_{10}$ PD50 were considered negative.

3.5.3 Neutralization assay on ovine choroid plexus cells

Since there are evidences that BTV can use different receptors to enter target cells, we tested the ability of the sera to neutralise virus entry on a more relevant cell line, originated from sheep (CPt-Tert). The neutralization titre of sheep and goat serum was assessed as described above replacing Vero cells, with 50 µl/well of a suspension of CPt-TERT cells containing $2.5x10^5$cells/ml in IMDM with 3% (v/v) FBS.

3.5.4 ELISA quantification of serum IgG and IgM against BTV VP7

The amount of serum IgG and IgM was quantified with an indirect enzyme-linked immunosorbent assay (ELISA). Flat bottom 96-well plates coated with recombinant VP7 protein were purchased from IDVet (Innovative Diagnostics, ID Screen® Bluetongue Milk Indirect). Plates were incubated for 30 minutes with a blocking solution of PBS T20 containing 3% (w/v) dried skimmed milk (Marvel, Premier Foods). Appropriate dilutions of serum (from 1:100 to 1:5,000) were prepared in blocking buffer and chosen in order to obtain results fitting in the linear portion of the standard curve (see below). 100 µl of the serum dilution were added to the well in duplicate and incubated for 1 hour at room temperature. Plates were washed 5 times with PBS T20.

For IgG detection 100 µl of a secondary antibody directed against sheep IgG, conjugated with HRP (polyclonal donkey anti sheep/goat IgG, AbD Serotec) and diluted 1:16,000 in PBS T20 and was added to the wells for 1 hour.

For IgM detection, 100 ul of a 1:30,000 dilution of a secondary antibody directed against sheep IgM (Rabbit anti sheep IgM, AbD Serotec), conjugated with HRP was added to the wells and incubated as above.

Plates were washed five times with PBS T20, then 100 µl of TMB (3,3', 5,5;-tetramethylbenzidine) chromogen solution (Novex) were added to each well and incubated in the dark for 25 minutes for the colour to develop. The reaction was stopped by addition of an equal amount of 1 N hydrochloric acid. Absorbance at OD_{450nm} (optical density) was assessed for each well by mean of a PHERAstar FS HTS microplate reader (BMG LABTECH).

3.5.4.1 Standard curve and quantification

To normalise data across different plates a standard curve was generated and included in duplicate in each plate. Sera from animals having a high antibody titre were selected to generate a reference standard. For the IgG ELISA a pool was made with sera obtained from five sheep, which had been vaccinated and subsequently challenged with BTV8, and sera collected at 10 days after infection. For IgM quantification, a standard curve was produced by using a pool of five sera, collected from sheep at 11 days after BTV experimental infection. Standard serum was aliquoted and stored at -20°C until required.

Standard serum was diluted in two-fold steps from 1:50 to 1:3,200 in blocking buffer. For IgG quantification, at the lowest dilution (1:50) of the standard was attributed a value of 100 ELISA units, and the values of the successive dilutions were calculated accordingly. For IgM quantification, the value of 100 ELISA units was attributed to the first dilution (1:100) and the successive dilutions were calculated accordingly. Serum from a naïve animal was used as a negative control and 2 wells did not receive any serum and were used as blank controls.

The relationship between the reciprocal of the dilution tested and its OD_{405} was used to determine the serum titre (in units), by fitting into a 4-parameter logistic (4PL) curve; when the R^2 of the standard curve fit was less than 0.997 the entire assay was repeated.

Once the titres of the standard serum were determined, the value was used to assess the relative concentration of the experimental samples tested by ELISA, using MARS data analysis software (BMG Labtech). A cut-off value was determined at 3 standard deviations (SDs) from the value of the negative control. Samples were considered negative when returned an OD value inferior to the cut-off value.

3.5.5 ELISA quantification of serum IgG and IgM against ovalbumin

ELISAs for anti-OVA antibodies were performed by Dr. Noemi Sevilla and Dr. Veronica Martin at the Centro de Investigación en Sanidad Animal (Madrid, Spain). Antibodies against OVA were detected using ELISA plates (Maxisorp,

Nunc) coated for 1h at room temperature with 100 μl/well of 20 μg/ml of OVA (Sigma-Aldrich) in 0.1 M carbonate buffer (pH 9.6). Serial dilutions of sera from inoculated sheep were added to the plates and incubated for 1 hour at room temperature, after blocking with blocking buffer (PBS with 1% Tween-20 and 4% skimmed milk) for 1h at room temperature and washing five times with 1% Tween-20 in PBS. The presence of OVA-specific IgG or IgM was detected using a secondary donkey anti-sheep IgG conjugated to horseradish peroxidase (1:2000, Serotec, Oxford, UK) or rabbit anti-sheep IgM also conjugated to horseradish peroxidase (1:20,000, Bethyl). After washing ten times with 1% Tween-20 in PBS, signal was developed using 100 µl of TMB Liquid Substrate System (Sigma) and the reaction was stopped with 100 µl of 3M sulfuric acid before reading. Optical density (OD) was determined at 450 nm on a FLUOstar Omega (BMG Labtech) ELISA plate reader. All IgG/IgM measurements were made in triplicate and assays were only considered valid when standard deviations were below 10% of the average. IgG/IgM binding to OVA was considered positive only when the OD obtained was at least twice the OD obtained with the pre-immune serum from the same sheep.

3.5.6 Avidity of the IgG directed against BTV VP7 and ovalbumin

Antibody avidity was assessed by ELISA, using previously described protocols (Nair et al. 2007; Pullen et al. 1986). Low avidity IgG binding dissociation was achieved using the chaotropic agent ammonium thiocyanate (NH_4SCN). After incubation with serum samples, as described above, plates were washed with PBS and incubated at room temperature for 15 minutes with 100 µl of increasing concentration of NH_4SCN (0.5, 1, 1.5, 2, 2.5 and 3 M). The absorbance readings in the absence of NH_4SCN were considered to represent the total binding of VP7 specific IgG, and subsequent absorbance readings in the presence of increasing concentrations of NH_4SCN were converted to the corresponding percentage of the total bound antibody. The data were fitted to a curve of percentage binding vs. molar concentration of NH_4SCN using a 4PL non-linear regression model. An avidity index (AI) was calculated as the molar concentration of NH_4SCN required to reduce by 50% the VP7-specific IgG binding. Samples with absorbance readings of <0 .4 ODs in the absence of NH_4SCN were within 3 SDs of the threshold value and were therefore excluded from avidity analysis. An identical

method was used to measure antibody avidity against ovalbumin with the exception that plates were coated with OVA as described above.

3.5.7 Quantification of anti-ovalbumin-specific IgG-secreting cells by ELISPOT

ELISPOTs were performed by Dr. Noemi Sevilla and Dr. Veronica Martin at the Centro de Investigación en Sanidad Animal (Madrid, Spain). MSIPS4510 plates (Millipore) were activated using sterile 35% ethanol for 1 min and, after thorough washing with sterile water, incubated overnight at 4°C with 20 μg/ml OVA (Sigma-Aldrich) in 0.1 M carbonate buffer pH 9.6. Plates were washed then blocked with PBS containing 4% (w/v) dried skimmed milk for 2 hours at 37°C. Fresh PBMCs were suspended at $5x10^6$ cells/ml and 1:2 dilutions were performed in RPMI medium (supplemented with L-glutamine, 1 mM sodium pyruvate, 25 mM HEPES (4-(2-hydroxyethyl)-1-piperazineethanesulfonic acid), non-essential amino acids and 10% inactivated foetal calf serum) to a concentration of $1.56x10^5$ cells/ml. 100 μl per well of each cell suspension (in triplicate) was incubated overnight at 37°C, 5% (v/v) CO_2. After discarding the cells and washing with PBS, membranes were incubated with anti-sheep IgG conjugated to horseradish peroxidase (Serotec, Oxford, UK) and incubate for 3 hours at room temperature. After 5 washes in PBS, membranes were developed using TMB substrate (Mabtech). Once spots were formed, membrane were washed with abundant distilled water and allowed to dry in the dark. Results were expressed as the number of antigen specific ASC per 10^6 PBMCs.

3.5.8 Statistical analyses

Non-parametric two-tailed Mann Whitney rank U test was used to compare two unpaired groups. Paired t-test was used to compare two paired groups. One-way ANOVA was used to compare two or more unmatched groups. Data analyses were performed using Prism 6.0 (GraphPad Software Inc. San Diego, CA, USA).

Chapter 4

Results

4 Kinetics of bluetongue virus infection in experimentally infected animals

4.1 Introduction

Skin and LNs have long been identified as sites of BTV replication at early times after infection (Pini 1976). The skin surrounding the inoculation site is described as the first site of viral replication (Darpel et al. 2012), thereafter BTV is thought to be disseminated to the draining lymph nodes (LNs) by DCs (Hemati et al. 2009; Ruscanu et al. 2012; Ruscanu et al. 2013), before disseminating further to peripheral tissues (MacLachlan et al. 2009). However, the cell populations targeted by the virus and the events taking place in the LN immediately after virus arrival during bluetongue infection remain poorly defined. Draining LNs are an important stopping point along the route followed by pathogens that gain access to the host after breaching the skin barrier before systemic dissemination. LNs are the sites where the immune response is initiated and shaped, for this reason they are crucial in limiting pathogen spread.

In the skin, the plasma fraction of the blood is filtrated from the vasculature in the capillary bed and becomes interstitial fluid. This is then percolated through the interstitium into the afferent lymphatic vessels where it becomes the afferent lymph. The fluid flow is a function of Starling's forces and the molecular architecture of the dermis. The lymphatic vessels actively pump interstitial fluid out of the tissue and, by actively keeping low the hydraulic pressure of the dermal interstitium, they guarantee an unidirectional flow from the blood vessels to the lymph vessels (Swartz 2001). The process is facilitated by the fact that unlike blood vessels, lymph vessels openly communicate with the interstitium without the presence of a continuous basal membrane to restrict the movement of solutes. The backflush of fluid is also prevented by a system of semilunar valves located at different levels in the lumen of the lymphatic vessels. This convective stream counteracts entry into the blood circulation by flushing particles away from blood vessels and conveying them directly into the subcapsular sinus (SCS) of the lymph nodes (Lämmermann & Sixt 2008).

From the skin, soluble molecules or particles can reach the draining LNs with the interstitial fluid flow or carried by cells. DCs are the principal cells that carry antigens to the LNs. Resident dendritic cells in the skin can be distinguished into Langherans cells and dermal DCs. In addition, as a consequence of inflammation, monocytes can be attracted to the skin and differentiate into a third type of DCs (called inflammatory DCs) (Zaba et al. 2009). In steady state, resident DCs survey the environment for the presence of danger signals and, if activated, can phagocytose and process antigens. The DCs then acquire a more motile phenotype accompanied by the upregulation of CCR7 that drives them towards the lymphatics expressing the CCR7 ligand (CCL21) (Randolph et al. 2005). Once in the lymphatic vessels, cells and solutes are passively transported by the flow of the afferent lymph to the LN.

For drainage to the LN, multiple afferent lymph vessels combine to the lumen of the SCS that surrounds the cortical area of the LN. From here, the lymph flows along cortical sinuses running along the connective trabecules spanning from the capsule into the cortex and dividing the LN into separate lobules (Gretz et al. 1997). The cortical sinuses are in communication with medullary sinuses that surround the medullary cords and accomplish the task of collecting the lymph from all the lobules into a single efferent lymphatic vessel exiting from the hilum of the LN. Since each afferent lymphatic collects lymph from a different drainage area, each lobule is potentially exposed to a different set of antigens, APCs and inflammatory mediators. Therefore, as a result of varying stimuli, lobules within the same lymph node may have different levels of immunological activity conferring a non-uniform appearance within the LN (Lämmermann & Sixt 2008).

Lymphoid lobules are the anatomical units of the LNs of superior mammals. Three distinct functional zones compose each lobule: the cortex, paracortex and medulla (Willard-Mack 2006). In the apical part, separated from the capsule by the SCS, is the cortical area. The cortical area is generally divided into a superficial cortex where B-cells cluster around follicular dendritic cells into spherical structures called follicles, and a deep cortex, often named the paracortex, where the majority of T-cells and DCs reside. In the area surrounding the hilum, named the medulla, lymphocytes collect before exiting

the LN (Willard-Mack 2006). The LN is therefore an important hub whose compartmentalisation favours the interactions between antigens, lymphocytes and antigen presenting cells leading to the initiation of the immune response via the activation and expansion of specific lymphocyte populations.

LNs have a highly dynamic structure where lymphocytes recirculate continually. Blood arteries enter the LN through the hilum and deliver lymphocytes to the cortical area via specialized blood vessels called high endothelial venules (HEV) (Girard et al. 2012). Lymphocytes then exit via specialized sinuses, and after reaching the medulla, leave the LN via the efferent lymphatic. The efferent lymph is then drained to the subsequent lymph nodes (if part of a lymphatic chain), or directly to the cisterna chyli and finally reaching the venous blood circulation through the thoracic duct. LNs function as fluid filter systems that constantly receive cells, antigens, pathogens, cytokines and chemokines from peripheral tissues.

In this chapter we aimed to track the distribution of BTV in experimentally infected sheep at different times post-infection. We show that after inoculation in the skin, BTV is rapidly transported to the draining LNs where it infects cells present in the subcapsular and cortical area very early after infection. We then aimed to compare the in vivo distribution of a virulent and an attenuated BTV-8 strain, showing that the LN is a gateway for the virus to reach the blood and systemic dissemination. Furthermore we compared the virus distribution in goats, a BTV natural host that generally does not develop the clinical disease. Finally, we aimed to compare the results obtained in ruminants with the localization of BTV in mouse models currently used for BTV virulence studies.

4.2 Results

4.2.1 Early localization of BTV RNA in the tissues of experimentally infected sheep

Sheep were inoculated with a virulent strain of BTV (BTV-8) in order to identify the distribution of the virus in the tissues of the infected animals over time. The *in vivo* infections, sample collection and part of the qPCR analysis were carried out at the "*Istituto Zooprofilattico Sperimentale dell'Abruzzo e del Molise*" (Teramo) by Dr. Marco Caporale. Experimental infections were performed in sheep (n=23) by multiple intradermal inoculations of BTV-8 into the shoulders and thighs (Caporale et al. 2014), areas drained by the corresponding inguinal or prescapular LNs (referred as "draining LNs" from here on), in order to mimic the pattern of insect bites in the natural environment. Rectal temperatures of infected animals were monitored for 7 days, while viremia was assessed by qRT-PCR. In order to monitor the distribution of the virus in different anatomical compartments and to identify the route followed by BTV to disseminate within the infected host, sheep were euthanized at 4, 8, 24, 48, 72, 96, 120 and 168 hpi, with n=3 per time point, except from 96 h where n=2. During the post-mortem examination, tissues were collected and either preserved in RNA-later solution for qRT-PCR analysis or fixed for histopathology, immunohistochemistry and confocal microscopy.

All of the infected sheep exhibited an increase in body temperature at 120 hpi equating to a ~2°C increase over the average body temperature that persisted for the following two days (Figure 4-1A). Low levels of BTV-8 RNA were initially detected in some of the infected animals at 24 hpi. Virus RNA levels started to increase exponentially at 72 hpi and reached a plateau at 120 to 168 dpi (~10^7 copies/µg RNA, Figure 4-1A). The increase in body temperature therefore corresponded to the peak of viremia.

Using qRT-PCR, BTV RNA was detected and quantified in several organs sampled during post-mortem examination (Figure 4-1B). BTV was detected in the skin near the inoculation site and in the corresponding draining LN as early as 4 hpi. The levels of viral RNA in the skin were relatively constant at all time points analysed (ranging between 2x10^5 and 8x10^4 copies), with only a slight decrease

at 7 dpi ($3.1x10^3$ copies). In draining LNs, BTV RNA levels reached a peak at 24 hpi ($3.12x10^4$ copies/µg of RNA in inguinal LNs on average) that was maintained until 4 dpi and then gradually decreased until reaching 10^3 copies by 168 hpi (Figure 4-1B).

At 72 hpi, corresponding to the beginning of viremia, BTV was also detected at low levels in other tissues such as the spleen and lungs (Figure 1B). Since the spleen contains large quantities of blood, BTV titres in spleen paralleled the trend observed for the viremia peaking at 5-7 dpi ($1x10^4$-$3x10^5$ copies). At 7 dpi BTV RNA was distributed in most of the peripheral tissues analysed including lungs ($2x10^2$ copies), kidneys ($3x10^2$ copies), tonsils and non-draining LN (50 copies) (Figure 4-1B).

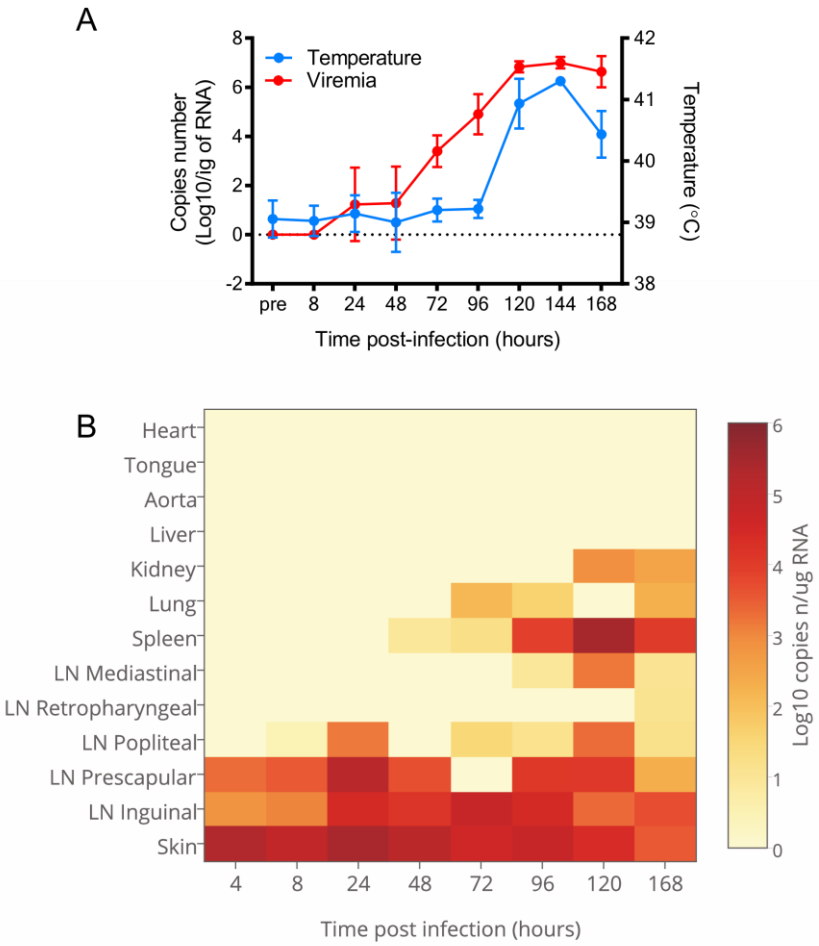

Figure 4-1 Progression of BTV-8 infection in experimentally infected sheep
Twenty-three sheep were intradermal (ID) inoculated with $2x10^6$ PFU of BTV-8 in three independent experiments and sacrificed at different times after experimental infection from 4 to 168 hours (for each time point n=3, a part from 96h where n=2). A. Graph showing body temperature and viremia in experimentally infected animals. Rectal temperature was registered daily and viremia was assessed by qRT-PCR, values shown represent average ±SD. B. Heat-map showing the tissue distribution of BTV RNA over time. Tissue samples were collected after euthanasia and viral RNA was detected by qRT-PCR, average values are expressed as Log_{10} copy number per µg of total RNA.

4.2.2 Detection of viral proteins in tissues of infected sheep

4.2.2.1 Optimization of an immunohistochemical technique for the detection of BTV proteins

Quantitative RT-PCR allowed the localization of BTV RNA in several sheep organs. However this technique does not provide evidence of virus replication and moreover does not allow the identification of infected cells. Therefore, we optimised an immunohistochemical technique to detect the presence of a non-structural protein of BTV in fixed tissues. Viral non-structural proteins are expressed in cells only during active viral replication, and therefore are excellent markers to identify infected cells.

Seven polyclonal antisera targeting different BTV proteins that were in current use in the laboratory (and had been previously shown capable of detecting viral antigens by western blot and immunofluorescence of virus-infected cultured cells) were then tested (Ratinier et al. 2011). An appropriate antibody dilution was determined through titration experiments and a working concentration was selected to achieve a robust specific signal and minimize non-specific background (Table 4-1).

Target Protein	Antiserum Produced In	Working Dilution
BTV-VP7	Rabbit	1:8000
BTV-NS1	Rabbit	1:7000
BTV-NS2	Rabbit	1:7000
BTV-NS2	Guinea Pig	1:8000
BTV-NS3	Rabbit	1:7000
BTV-NS4	Rabbit	1:6000

Table 4-1 - List of antisera raised against different BTV proteins and their concentration used in immunohistochemical studies

Detection of viral proteins in formalin fixed paraffin embedded tissue was unsuccessful without the use of an appropriate antigen retrieval process. As

described in the Material and Methods, three different types of antigen retrieval techniques were tried, including proteinase K treatment, trypsin treatment, and HIER with citrate buffer. Only the use of HIER treatment allowed detection of a strong positive signal for BTV proteins in the absence of any significant background.

As formalin fixation can affect epitope configuration, part of the tissue samples were also fixed using a zinc salts solution. As expected, the immunolabeling of viral proteins in zinc salt fixed tissue did not required antigen retrieval, however the HIER treatment of sections increased the sharpness of the signal (Figure 4-2).

To further assess the specificity of the signal for the virus proteins, sequential sections of tissue were stained with various polyclonal antibodies targeting different BTV proteins (Figure 4-2). Both structural and non-structural proteins tended to localise in the same areas of the tissue. Mock-infected animals were used as negative controls and no staining was detected in these animals in any of the tissues tested with the specific antibodies used to target BTV proteins (data not shown). Minimum background staining and the clear detection of a positive staining was obtained using the polyclonal antibodies (made in rabbits and guinea pigs) towards the BTV NS2 (Figure 4-2). Hence these antibodies were used throughout the course of this study to identify virus-infected cells.

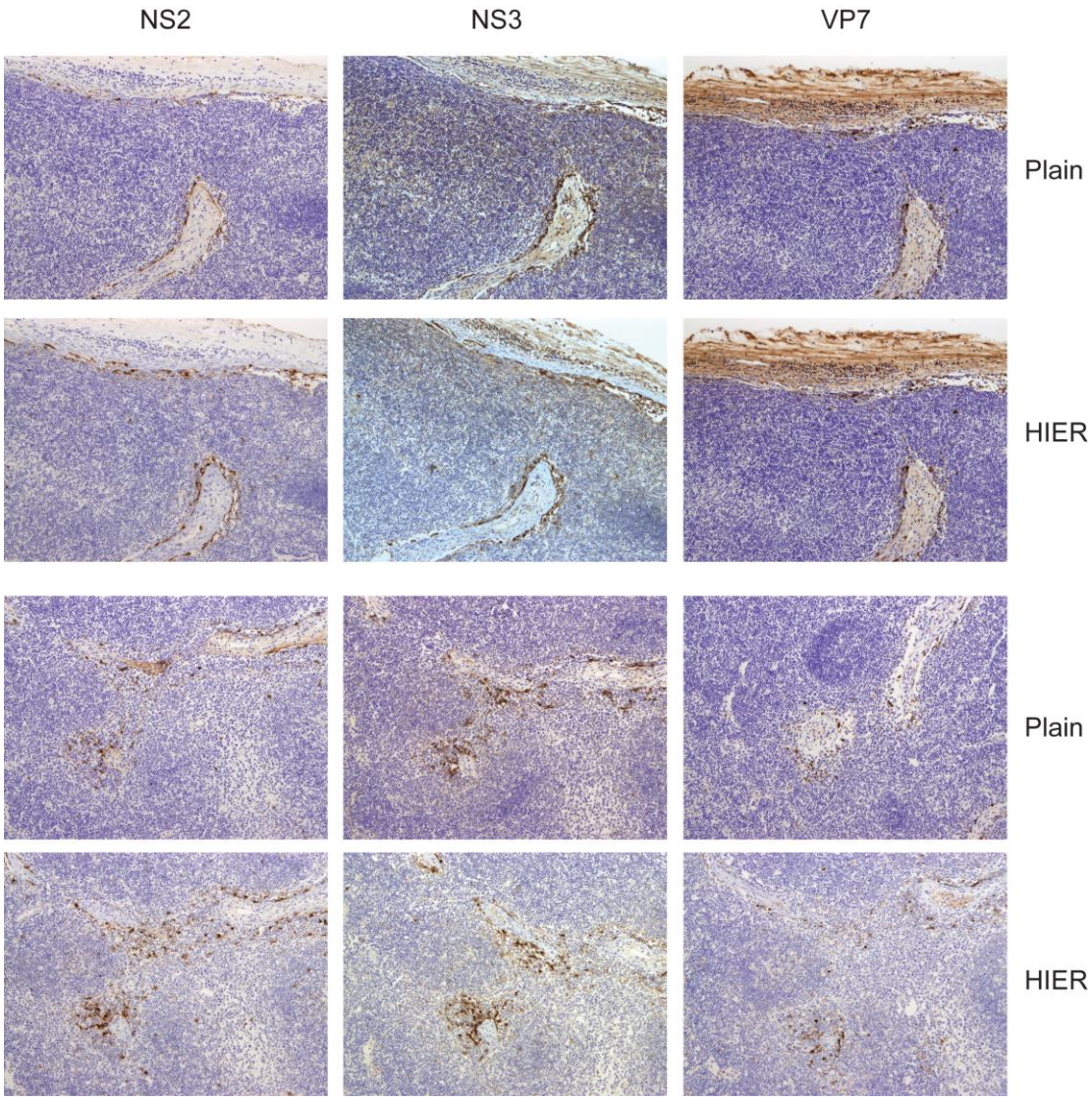

Figure 4-2 Localization of structural and non-structural BTV protein in infected tissues
Photomicrographs (x10) of IHC-stained sections, showing the localization of structural (VP7) and non-structural (NS2 and NS3) BTV proteins in LNs sequential sections obtained from sheep experimentally infected with BTV-8. LNs were fixed in zinc salt solution and the staining was tested with or without heat induced antigen retrieval (HIER). HIER treatment was not strictly required but it enhanced the specific signal. Note that both structural and non-structural proteins were expressed in similar areas. The best specific signal was obtained using antibodies targeting NS2.

4.2.3 BTV infects the lymphatic endothelial cells of the deep dermal plexus of the skin

The cells infected by BTV were characterised using IHC and confocal CLSM. We initially focused on the skin, the first site of virus replication. In all the experiments described in this study, we specifically targeted NS2, one of the BTV non-structural proteins. BTV NS2 was detected mainly in fibroblasts and in the endothelial cells of the deep dermal plexus (Figure 4-3A) in cells forming vessels with a very thin wall and lacking red blood cells in their lumen. These structures are consistent with lymphatic, rather than blood vessels (Figure 4-3A). BTV NS2 was specifically detected in endothelial cells but not in pericytes (differentiated by the expression of desmin) which are contractile cells that envelope the surface of capillaries (Figure 4-3B). BTV NS2 was detected in the skin of the sheep up to 7 dpi, with the number of infected cells gradually decreasing until being almost undetectable at 7 dpi. Infected cells did not express the pan-leukocyte marker CD45, the macrophage marker CD163 (Figure 4-4A) nor the major histocompatibility complex class II (MHC-II) (Figure 4-4B), ruling out a substantial involvement of antigen presenting cells in supporting virus replication in the skin at this stage Hence, cells of non-hematopoietic origin, likely fibroblasts and endothelial cells, are the primary target of BTV infection.

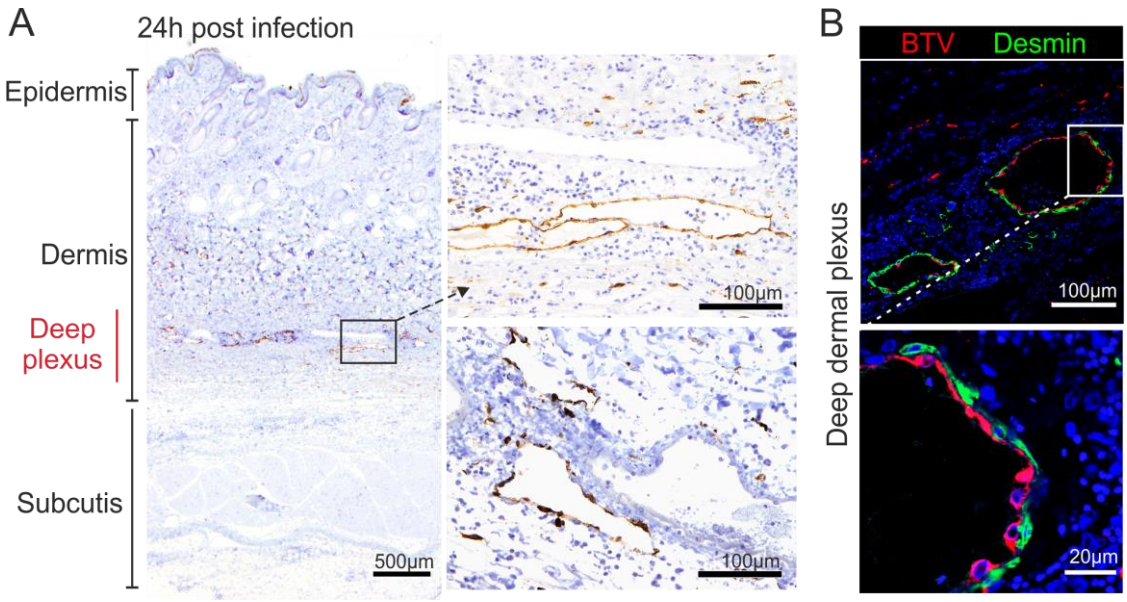

Figure 4-3 BTV infects endothelial cells in the deep dermal plexus.
A. Representative photomicrographs of IHC-stained sections showing BTV localization in skin sections of experimentally infected sheep. BTV NS2 (brown) localises in the dermis, mainly in the capillaries of the deep dermal plexus, infected vessels resemble lymphatics due to their anatomical structure. B. Representative confocal micrographs of the deep dermal plexus in skin section of experimentally infected sheep. The sections were stained for BTV NS2 (red) and desmin (green), highlighting the replication of the virus in endothelial cells surrounded by uninfected desmin^{+} perycites.

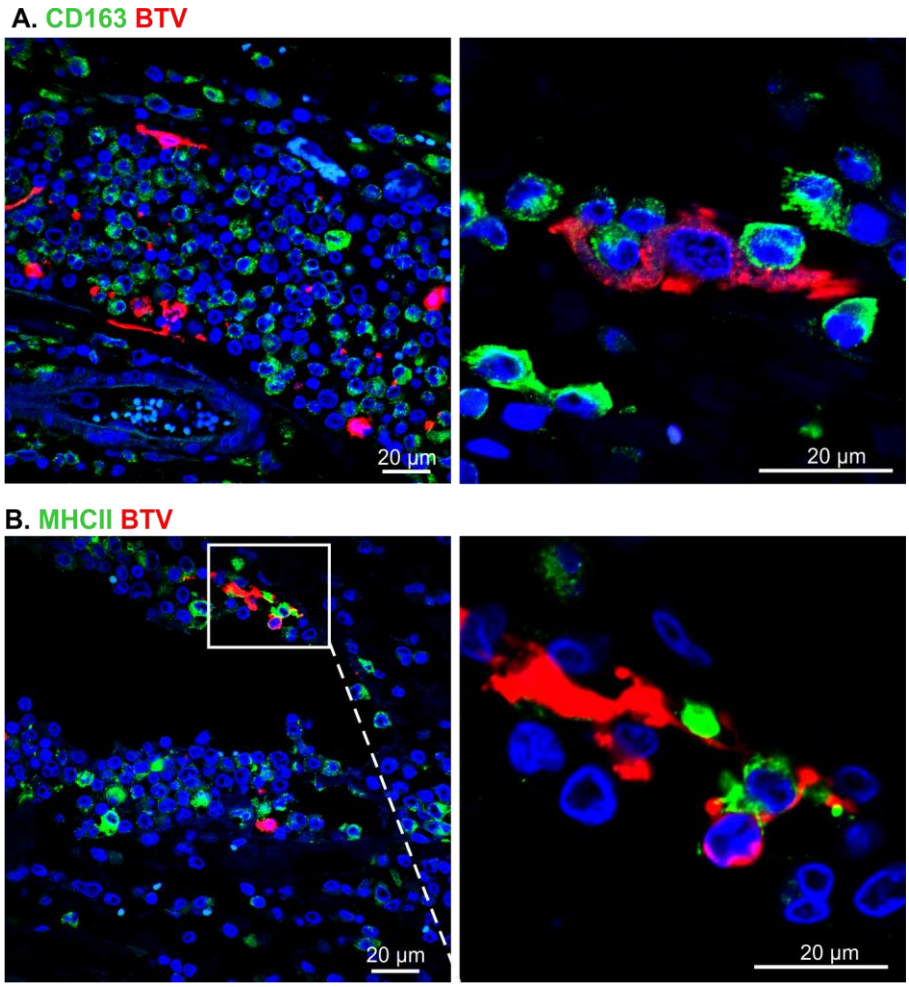

Figure 4-4 BTV does not infects antigen-presenting cells in the skin.
Representative confocal micrographs of the deep dermis of sheep skin, sections collected BTV-8 infected sheep. A. Sections were stained for monocytes and macrophages (CD163, green) and BTV NS2 (red), B. Sections were stained for MHC-II (green) and BTV NS2 (red). Numerous phagocytes arrive in the skin after infection, although in close proximity with infected cells they do not appear infected.

4.2.4 BTV rapidly infects the cortical area of the lymph nodes draining the site of infection

The qRT-PCR data shown in Figure 4-1B indicate that BTV dissemination in the draining LNs of infected animals occurs within few hours of the initial infection. Therefore, we used IHC to identify sites of viral replication within the LNs by detecting the BTV NS2 in different areas of the LNs (Figure 4-5).

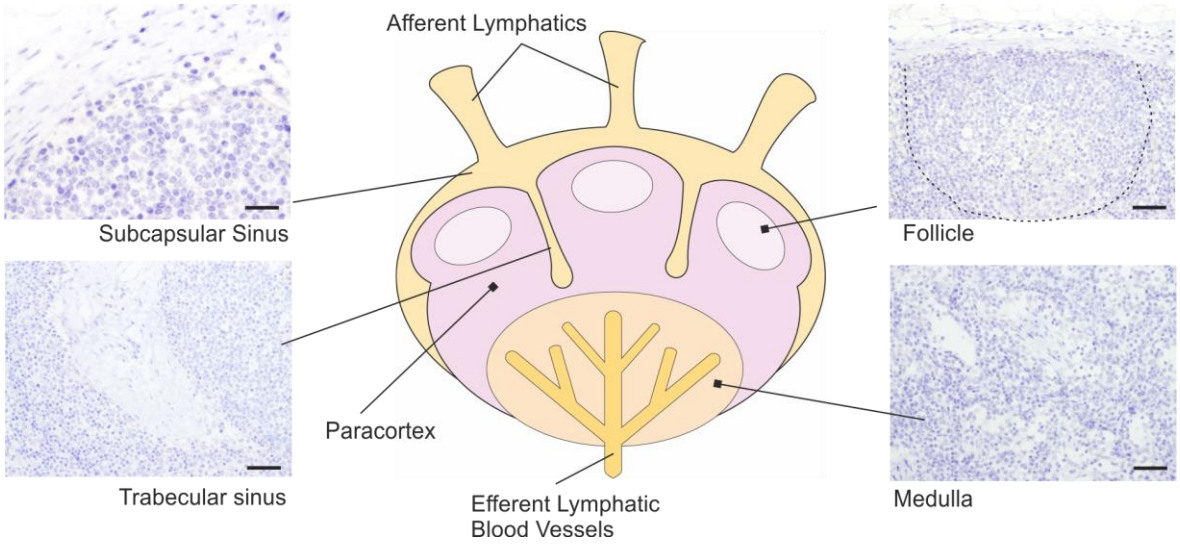

Figure 4-5 Sheep lymph node areas
Diagram showing different LN areas and IHC micrographs showing the appearance of the different areas in LN sections taken from mock-infected sheep and stained for BTV NS2 (pictures are representative of 7 animals, 6 sections per animal). No viral protein was detected in LN of control animals. Scale bars represent 50µm, for the SCS area scale bars are 20µm.

High levels of expression of BTV NS2 were detected in the cortical area of the draining LNs as early as 4 hpi (Figure 4-6). Between 4 to 8 hpi BTV NS2 was also found in the subcapsular sinus and along the trabecular sinuses that deepen inside the LN cortex (Figure 4-6). These data suggest that the virus arrives to the LN within the afferent lymphatic vessels as the sinuses collect the incoming lymph fluids. In addition, at 4 hpi only small and discontinuous segments of the SCS were infected. However the affected areas gradually expanded and at 24 hpi the majority of the SCS displayed NS2 positive cells. At the same time point, BTV infected cells were present in the parenchyma of the LN, where the virus localised around and inside the B-cell follicles of the cortex (Figure 4-6). The presence of BTV in the sinuses was detectable until 72 hpi, while at later time points BTV was detected exclusively inside the follicular area (Figure 4-6). The virus was not present in the medulla of the draining LN during the first 5 dpi. By 7 dpi no more infected cells were present inside the follicular area, however at this time BTV NS2 was detected in the medullar area, in correspondence of capillary structures (Figure 4-6).

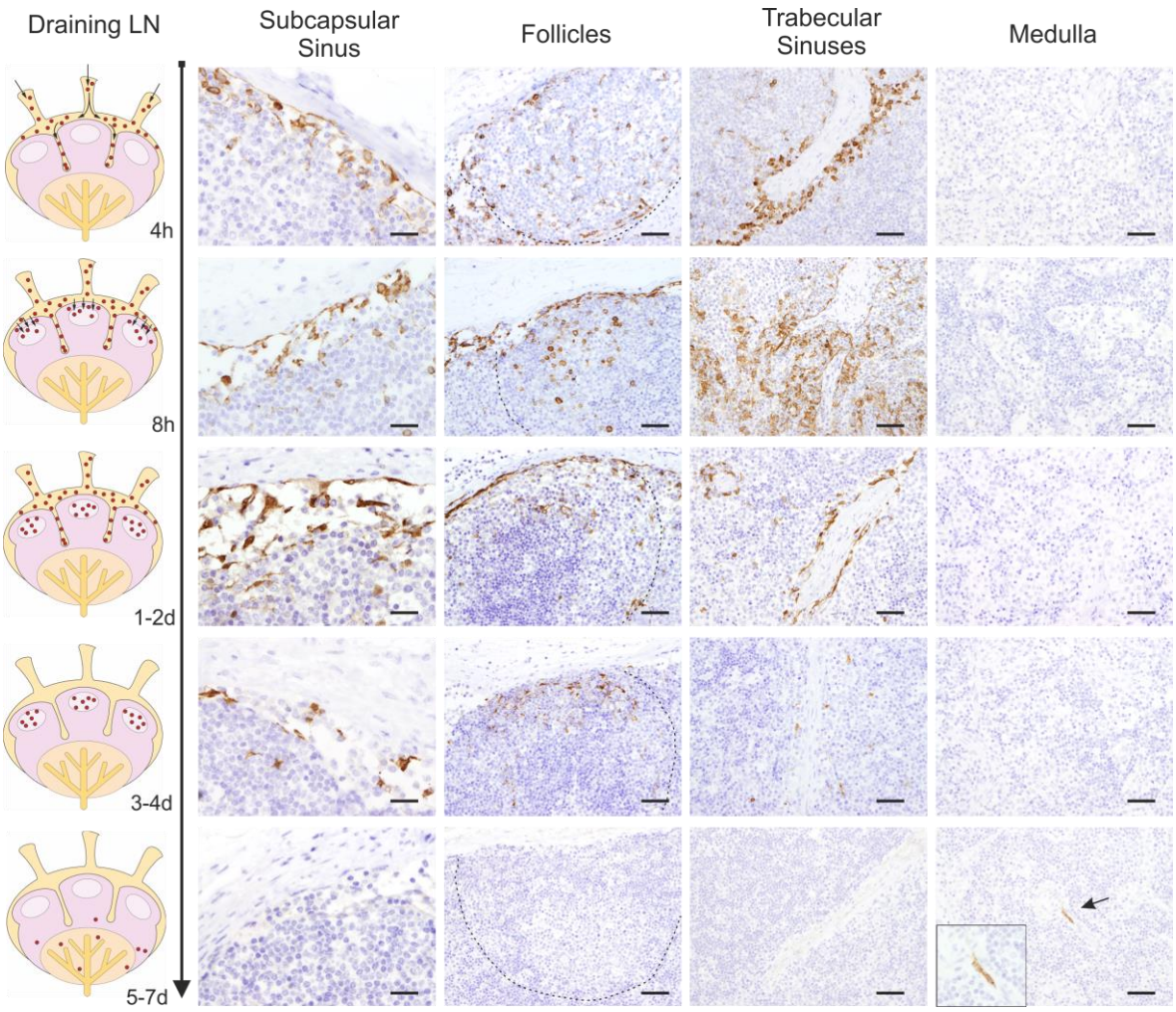

Figure 4-6 Time course of BTV infection in sheep draining lymph nodes
Immunohistochemistry micrographs showing the localization of BTV NS2 (brown), in sections of lymph nodes draining the sites of inoculation (inguinal and prescapular LNs), at different time points. BTV infected areas and likely infection route are schematically depicted in the diagrams (on the left). The BTV NS2 is highly expressed along the subcapsular sinus, trabecular sinuses and in the follicles from 4h to 2 dpi. At 3-4 dpi the sinuses are almost cleared and the virus persists in the follicular area. At 7 days the cortical and paracortical areas are cleared, and few capillaries express BTV NS2 in the medulla. Arrow indicates a positive cell in the medulla, highlighted in the inset. Scale bars represent 50µm, for the SCS area scale bars are 20µm.

BTV was not detected in the skin and draining LNs of mock-infected sheep (n=8; 1 sheep per time point) (Figure 4-7). As an additional control, in order to exclude the possibility of detecting non-replicating virus, sheep (n=2) were inoculated with UV-inactivated BTV. As expected, no BTV-8 positive cells were detected by IHC or confocal microscopy in skin or draining LNs of the inoculated sheep (Figure 4-7).

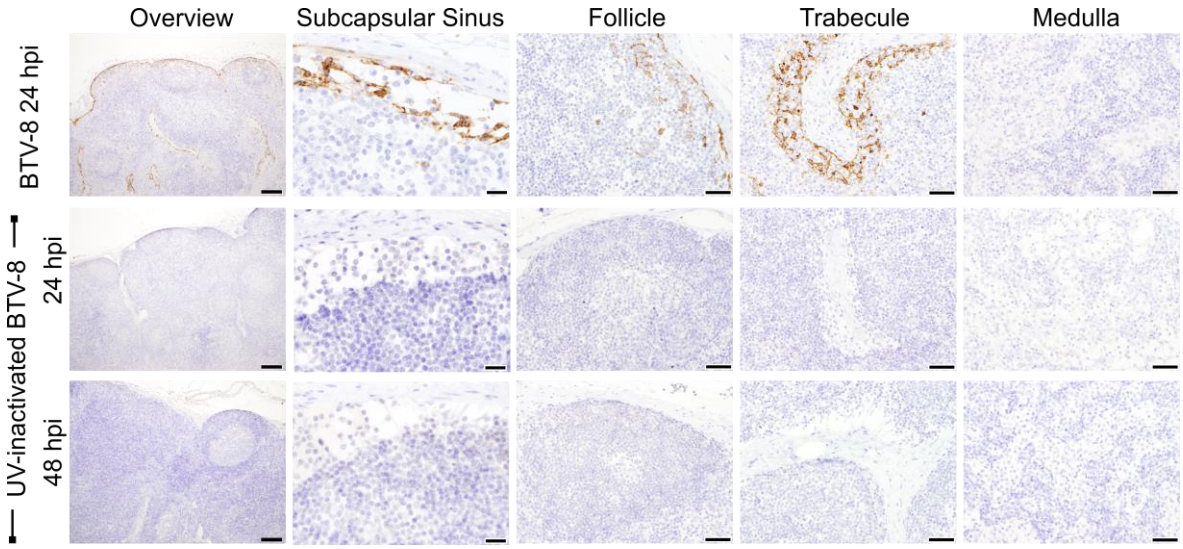

Figure 4-7 BTV NS2 was in sheep infected with UV-inactivated BTV-8
Immunohistochemistry micrographs showing detection of BTV NS2 in lymph nodes (LNs) sections from sheep infected with virulent BTV-8 or UV-inactivated BTV-8. Micrographs representative of different areas of the LN are shown. Scale bars represent 200 µm in the overview, 20 µm in the subcapsular sinus and 50 µm in all the other panels. BTV NS2 was not detected in LNs of animals infected with UV-inactivated virus at 24 and 48 hpi.

Viral infections are generally accompanied by expression of antiviral mediators such as type I interferon (IFN-I). Hence, to further confirm the presence of BTV in the LN, we assessed the production of IFN-I by testing the expression of MX-1, an interferon-induced GTPase with antiviral activity. MX-1 overexpression, as assessed by IHC, was evident as early as 4 hpi in some limited areas of the LN cortex (Figure 4-8). MX-1 was rapidly expressed in the whole parenchyma of the LN of infected animals by 24 hours and was maintained until 7 dpi. Mock-infected sheep exhibited only low levels of MX-1 expression in LNs throughout the course of the experiment (Figure 4-8). These data provide evidence for an interferon-mediated host response in the LNs draining the infected skin, simultaneously with virus arrival.

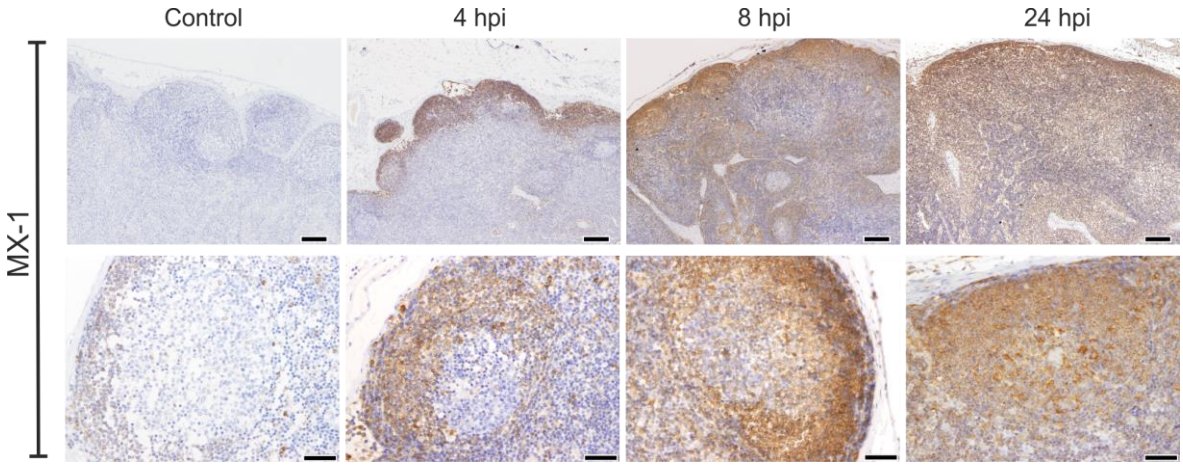

Figure 4-8 MX-1 expression in sheep draining lymph nodes
Representative immunohistochemistry micrographs showing the expression of MX-1 (brown) in draining LNs sections taken at different times from mock-infected and BTV-8 infected sheep. Note the gradual expansion of the positive areas over time. Scale bars represent 200 µm (top row) or 50 µm (bottom row).

4.2.5 The hematic dissemination of BTV leads to the infection of peripheral tissues

In agreement with qRT-PCR data, BTV NS2 was only detected in non-draining LN (far from the inoculation site, such as mediastinal LN) at later time points by immunohistochemistry (5-7 dpi). Interestingly, in these LNs the localisation of infected cells was limited to the medulla and paracortical area and, contrary to draining LNs, infected cells were not present in the sinuses or in the cortical area. The infected cells were mainly constituted by few endothelial cells lining small vessels (Figure 4-9). Thus, the localization and the timing of infection of the non-draining LNs of infected sheep suggest that BTV reaches these organs via the haematogenous, rather than lymphatic route.

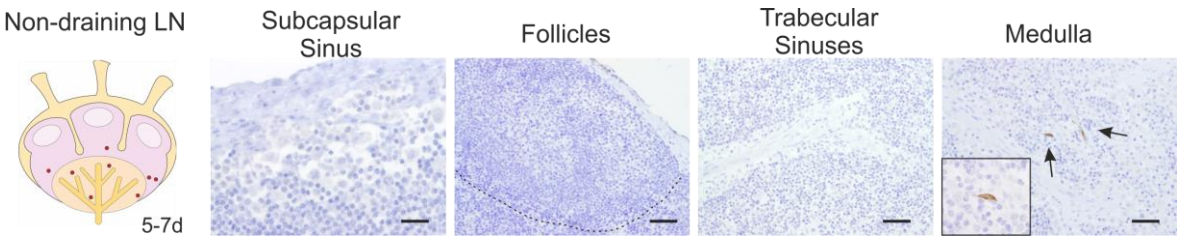

Figure 4-9 BTV infection of non-draining lymph nodes in sheep
Representative immunohistochemistry micrographs showing the localization of BTV NS2 in non-draining LNs (mediastinal, retromandibular, popliteal) sections taken from sheep inoculated with BTV-8, at 7 days pi. The images show the presence of few BTV NS2 positive capillaries in the medulla. Note that no positive cells were detectable at earlier times (pictures are representative of 3 animals, 6 sections per animal). Scale bars represent 50 µm, for the SCS area scale bars are 20 µm.

At 7 dpi BTV replication was detected in peripheral tissues (spleen, lung and kidneys) (Figure 4-10). In the spleen, the virus was found in relatively few infected cells lining small capillaries (Figure 4-10A). This is in contrast to the relatively high levels of viral RNA detected in this organ by qPCR, which suggests the presence of a large quantity of non-replicating virus in this organ. In the lungs, BTV was present mostly in capillaries and in some alveolar pneumocytes (Figure 4-10B). In the kidney, BTV was detected in small capillaries surrounding the nephrons in the cortical area (Figure 4-10C).

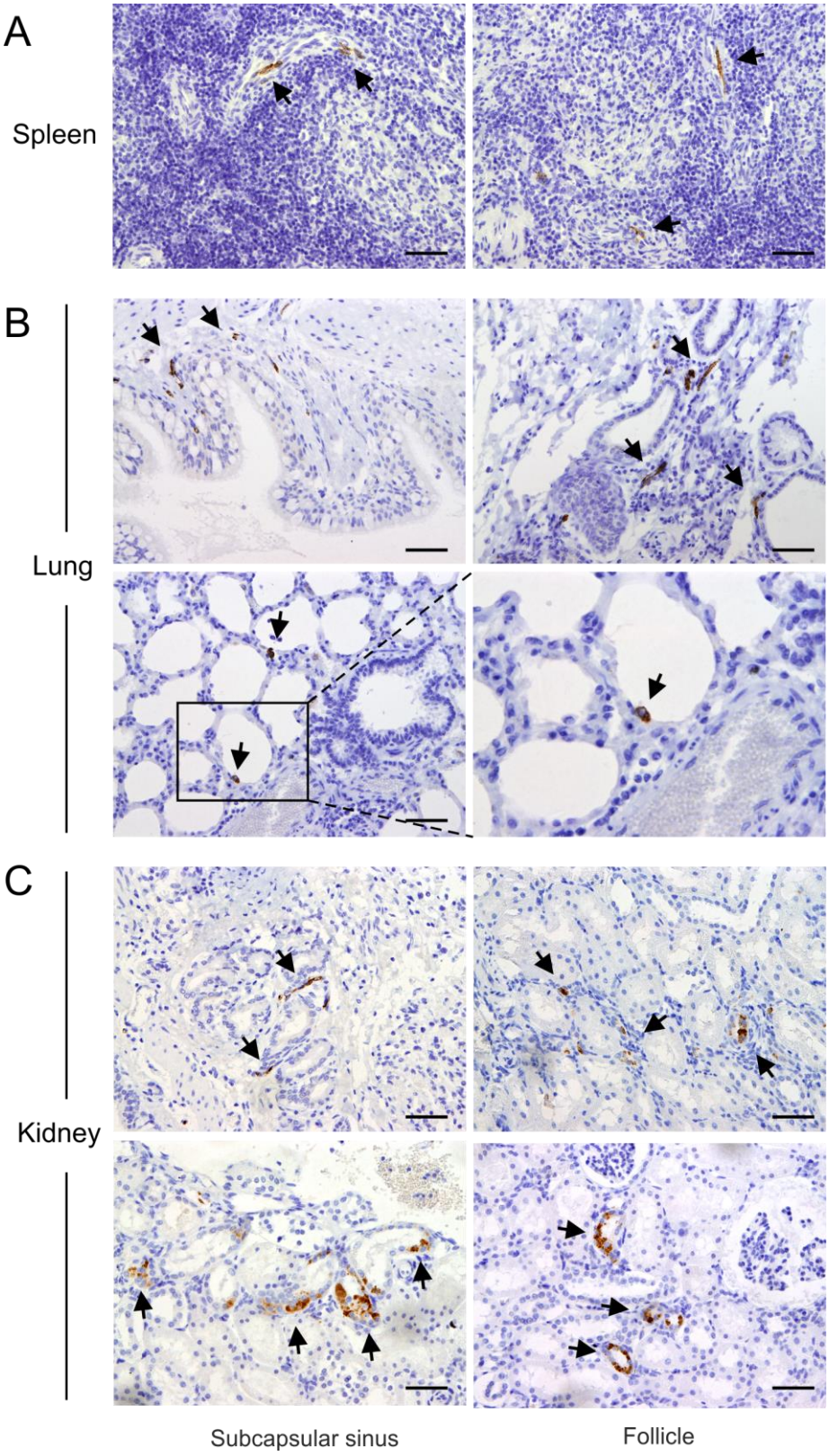

Figure 4-10 BTV infection of sheep tissues at 7 day post-infection
Representative immunohistochemistry micrographs showing the localization of BTV NS2 (brown) in (A) spleen, (B) lungs and (C) kidneys of experimentally infected sheep, at 7 dpi. (A) Few infected capillaries are present in the spleen. (B) Infected cells were identified as capillaries and pneumocytes in the alveoli of the lungs. (C) Small vessels in the cortical area of the kidney expressed BTV NS2. Arrows indicate infected cells. Scale bar is 100µm.

4.2.6 Early BTV localization in sheep experimentally infected with the attenuated strain $BTV8_H$

We next wished to determine whether an attenuated strain of BTV-8 (named $BTV8_H$) (Janowicz et al. 2015) displayed the same tropism of BTV-8 in experimentally-infected sheep. Sheep were experimentally infected with $BTV8_H$ as described before (see Material and Methods chapter). As observed in previous studies (Janowicz et al. 2015), $BTV8_H$ induced neither fever nor viremia in infected sheep (Figure 4-11A). We followed the progression of $BTV8_H$ infection by sacrificing infected sheep at different times post-infection (at 8, 24, 48, 72, 96 and 168 hpi; n=2 per time point with the exception of the 168 hpi where n=3). As assessed by qRT-PCR, we were able to detect the presence of $BTV8_H$ in the skin and in the respective draining LN at the same time-points as observed in animals infected with the BTV-8 strain (from 4 hpi to 7 dpi) (Figure 4-11B). The virus RNA levels in these tissues were similar to the ones detected in BTV-8 infected animals, with a peak between 24 and 48 hpi ($3.12x10^4$ copies). However, at 7 dpi the virus RNA levels in the draining LNs of $BTV8_H$ infected sheep were lower compared to those of BTV-8 infected sheep (20 copies compared to $5x10^3$ copies in inguinal LNs on average) (Figure 4-11B). $BTV8_H$ was not detected in any other peripheral organs since infected sheep did not develop viremia (Figure 4-11B).

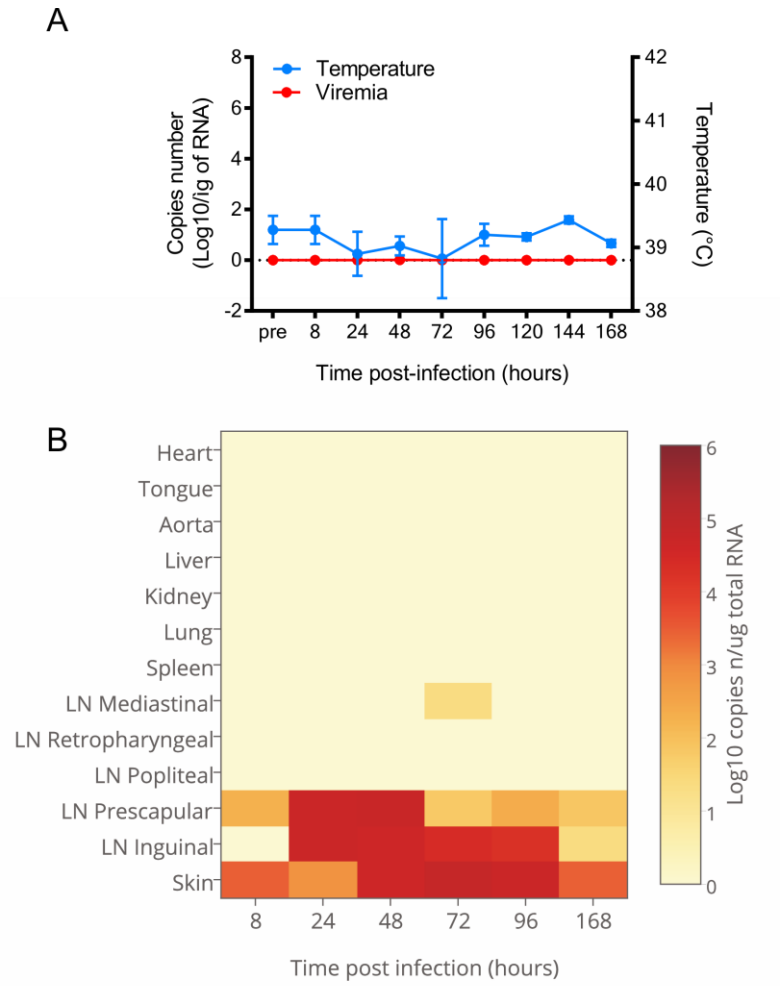

Figure 4-11 Progression of infection in sheep experimentally infected with attenuated BTV8$_H$ Thirteen sheep were ID inoculated with 5x10^5 PFU of BTV8$_H$ and sacrificed at different times after experimental infection from 8 to 168 hours (for each time point n=2, a part from 168h where n=3). (A) Graph showing body temperature and viremia in experimentally infected animals. Rectal temperature was registered daily and viremia was assessed by qRT-PCR, values shown represent average ±SD. (B) Heat-map showing the tissue distribution of BTV RNA over time. Tissue samples were collected after euthanasia and viral RNA was detected by qRT-PCR, average values are expressed as log_{10} copy number per µg of total RNA.

We checked the cellular localization of the attenuated virus in draining LN by IHC, and we detected viral proteins in a similar location as observed in BTV-8 infected animals. BTV8$_H$ was found to infect cells in the subcapsular area, the trabecular sinuses and the follicles (Figure 4-12) of the draining LNs of infected sheep. Overall these results indicate that, after inoculation via the skin, the attenuated virus maintains the capacity to reach the draining LNs, where it shows a tropism similar to the BTV-8. However, the titres of BTV8$_H$ in draining LNs decreased at 7 dpi and, strikingly, BTV8$_H$ was never detected in the

bloodstream, suggesting the presence of a bottleneck at the LN level that can restricts systemic distribution.

Collectively, these findings support the evidence that the blood stream is the main route of dissemination of BTV8 to peripheral tissues, while LNs draining the infection site are likely reached by BTV through the lymph fluids.

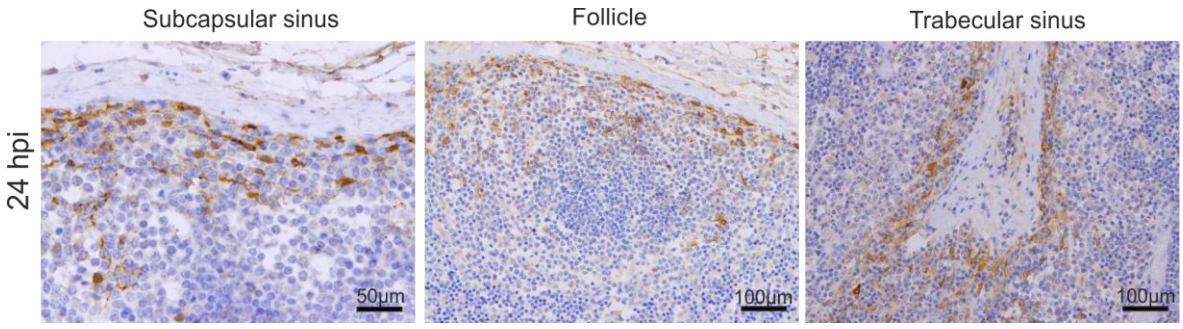

Figure 4-12 Localization of infected cells in draining lymph nodes of sheep experimentally infected with attenuated BTV8$_H$

Representative immunohistochemistry micrographs showing the localization of BTV NS2 (brown) in sections of draining LNs taken from sheep infected with attenuated BTV8$_H$, at 24 hpi. The virus localization resembles the one obtained in sheep infected with BTV-8.

4.2.7 BTV localisation in experimentally infected goats

Goats are susceptible hosts for BTV infection but they rarely develop the clinical signs of disease (Erasmus 1975; Caporale et al. 2014). In order to understand if BTV presents a different tissue tropism in distinct susceptible animal species, we experimentally infected goats (n=17) as described for sheep. After intradermal inoculation of BTV-8, we followed the progression of infection by euthanizing infected goats at different time points (8, 24, 48, 72, 96 and 168 hpi; n=3 per time point with the exception of the 8h time point where n=2). Clinically, no significant increase in the body temperature was detected in the experimentally infected goats (Figure 4-13A). BTV RNA was detectable in blood in 2 out of the 10 goats at 24 hpi but levels started to rise significantly only at 5 dpi (48h later than sheep). Goats developed lower titres of viremia compared to sheep at all the time points tested, reaching an average titre of 10^3 copies at 7 dpi (Figure 4-13A). Detection of BTV RNA in goat tissues, as assessed by qPCR, indicated that the dissemination of the virus follows different kinetics to the one observed in sheep (Figure 4-13B). Similarly to sheep, the virus rapidly localised in the skin and corresponding draining LNs at 8 hpi (first time point tested in goats),

however BTV RNA levels in draining LNs, after reaching a peak at 24 hpi (average of $3.9x10^4$ copies in draining LNs, 15 times lower than in sheep) rapidly decreased to lower titres (average $1.6x10^3$ copies in inguinal LNs) that were maintained until 7 dpi (Figure 4-13B). Furthermore, most of the peripheral tissues, including non-draining LNs, were not infected before 7 dpi, indicating a slower progression of the infection compared to sheep (Figure 4-13B). Importantly, only one of the three goats euthanized at 7 dpi presented the virus in peripheral tissues, and the same animal was the only one with high BTV levels in blood ($3.9x10^5$ compared to $8.7x10^2$ and 10^1 in the other goats), indicating a large inter-animal variability.

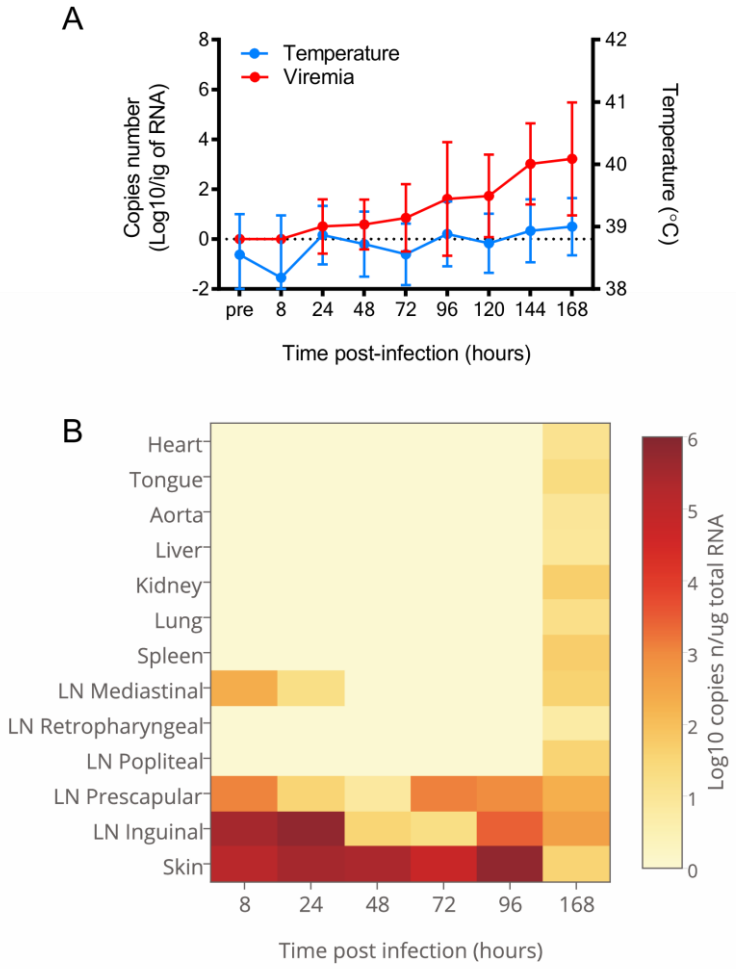

Figure 4-13 Progression of BTV-8 infection in experimentally infected goats
Seventeen goats were ID inoculated with $5x10^5$ PFU of BTV-8 in three independent experiments and sacrificed at different times after experimental infection from 8 to 168 hours (for each time point n=3, a part from 8h where n=2). (A) Graph showing body temperature and viremia in experimentally infected animals. Rectal temperature was registered daily and viremia was assessed by qRT-PCR, values shown represent average ±SD. (B) Heat-map showing the tissue distribution of BTV RNA over time. Tissue samples were collected after euthanasia and viral RNA was detected by qRT-PCR, average values are expressed as Log_{10} copy number per µg of total RNA.

We then identified sites of viral replication by immunohistochemistry in the skin and LNs of goats. In skin, BTV localised in endothelial cells of the deep dermal plexus and in fibroblast disseminated in the dermis, similar to sheep. In the draining LNs, we detected BTV infected cells along the SCS, trabecular sinuses and in the follicles, as early as 8 hpi, similar to sheep (Figure 4-14). However, contrary to what observed in sheep, in goats the lymphatic endothelial cells lining the sinus walls did not show a high degree of infection and most of the infected cells morphologically resembled phagocytes, located inside the lymphatic sinuses. In addition, numerous scattered cells were also found to be infected in the paracortical area of the goats draining LNs, contrary to observations in sheep where the paracortical area was not visibly affected by BTV infection (Figure 4-15)

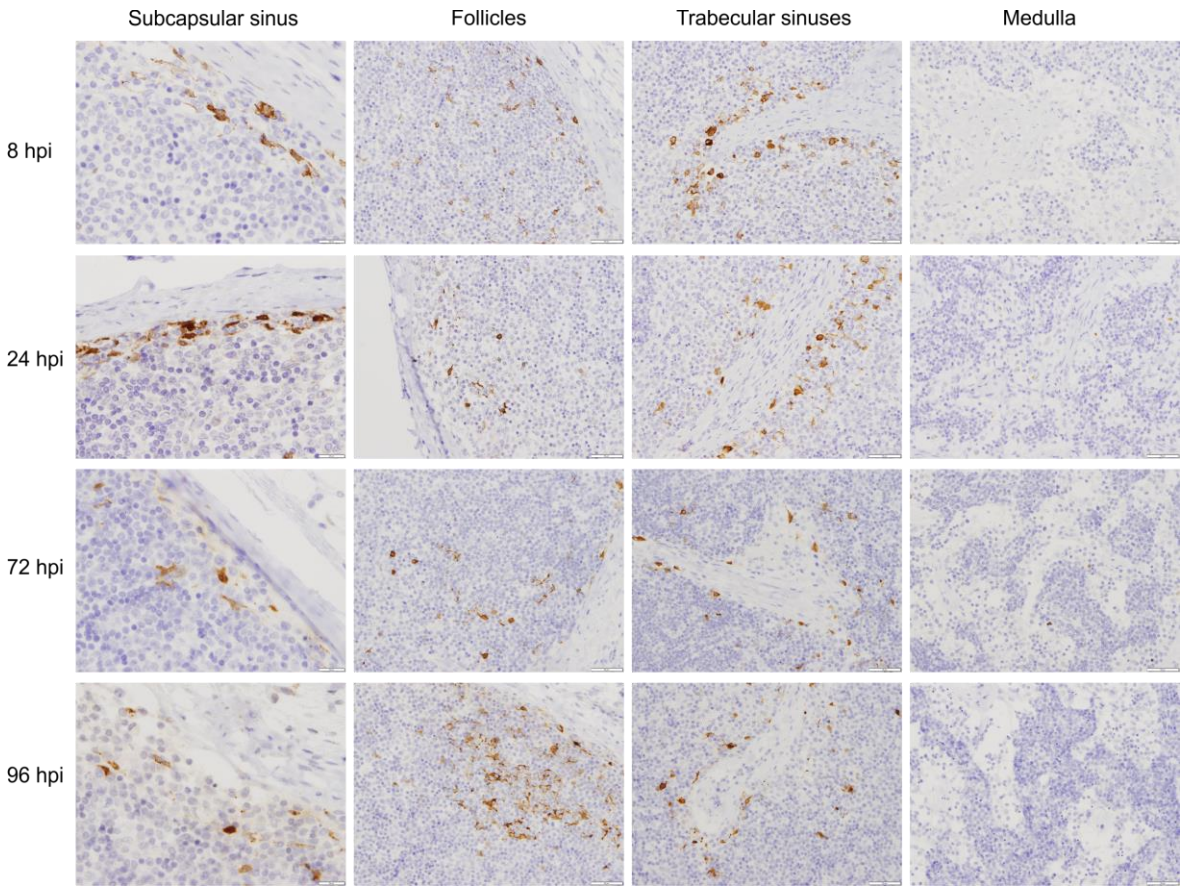

Figure 4-14 Time course of BTV infection in goat draining lymph nodes
Immunohistochemistry showing the localization of BTV NS2 (brown), in sections of lymph nodes draining the sites of inoculation (inguinal and prescapular LNs), at different time points. The BTV NS2 is highly expressed along the subcapsular sinus, trabecular sinuses and in the follicles from 4h to 96 hpi. Scale bars represent 50µm, for the SCS area scale bars are 20µm.

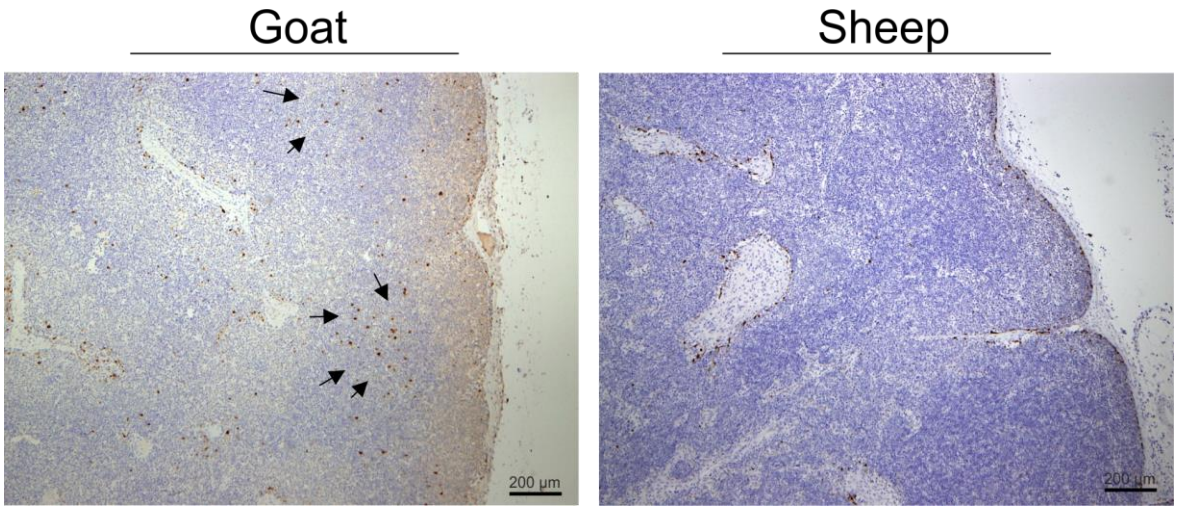

Figure 4-15 Comparison of the patter of infection in goat and sheep lymph node
Representative immunohistochemistry micrographs showing the localization of BTV NS2 (brown) in sections of draining lymph nodes in goat and sheep, at 48 hpi. In goat, many infected cells localise in the paracortical are (arrows), these cells are not infected in sheep.

4.2.8 BTV localization in mouse lymph nodes

In order to define if the localization of the virus was similar in a mouse model of disease we inoculated mice subcutaneously in the thighs with 300 PFU of BTV-8 and we collected the inguinal LNs at 8, 24 and 48 hpi. We tested two different strains of mice: NIH-Swiss and IFNAR$^{(-/-)}$ mice, lacking the ß subunit of the interferon α/ß receptor. Adult NIH-Swiss mice do not succumb to BTV infection while IFNAR$^{(-/-)}$ mice are known to support BTV replication and have been widely used for pathogenicity studies (Caporale et al. 2011; Calvo-Pinilla, Rodríguez-Calvo, Anguita, et al. 2009; Ortego et al. 2014).

Confocal microscopy of LN sections stained for BTV NS2 protein indicated that no detectable virus replication was present in NIH-Swiss mice at any time after infection (Figure 4-16). On the other hand, infected cells were detectable in the draining LNs of IFNAR$^{(-/-)}$ mice starting at 24 hpi. At this time point, infected cells localised mainly in the follicles, but also in the paracortical and medullary areas. However, no infected cells where present along the SCS, demonstrating

an important difference in comparison with sheep LN infection. At 48 hpi, infected cells constituted approximately 30% of the whole LN section and were localised both in the cortical, paracortical and medullar area (Figure 4-16). At this time we also observed a significant expansion of the size of infected LNs, compared to those of mock infected control IFNAR$^{(-/-)}$ mice and those of BTV-8 infected NIH-Swiss mice (Figure 4-16). This observation suggests that active BTV replication can trigger either an inflammatory process or lymphocyte activation and proliferation in the LNs.

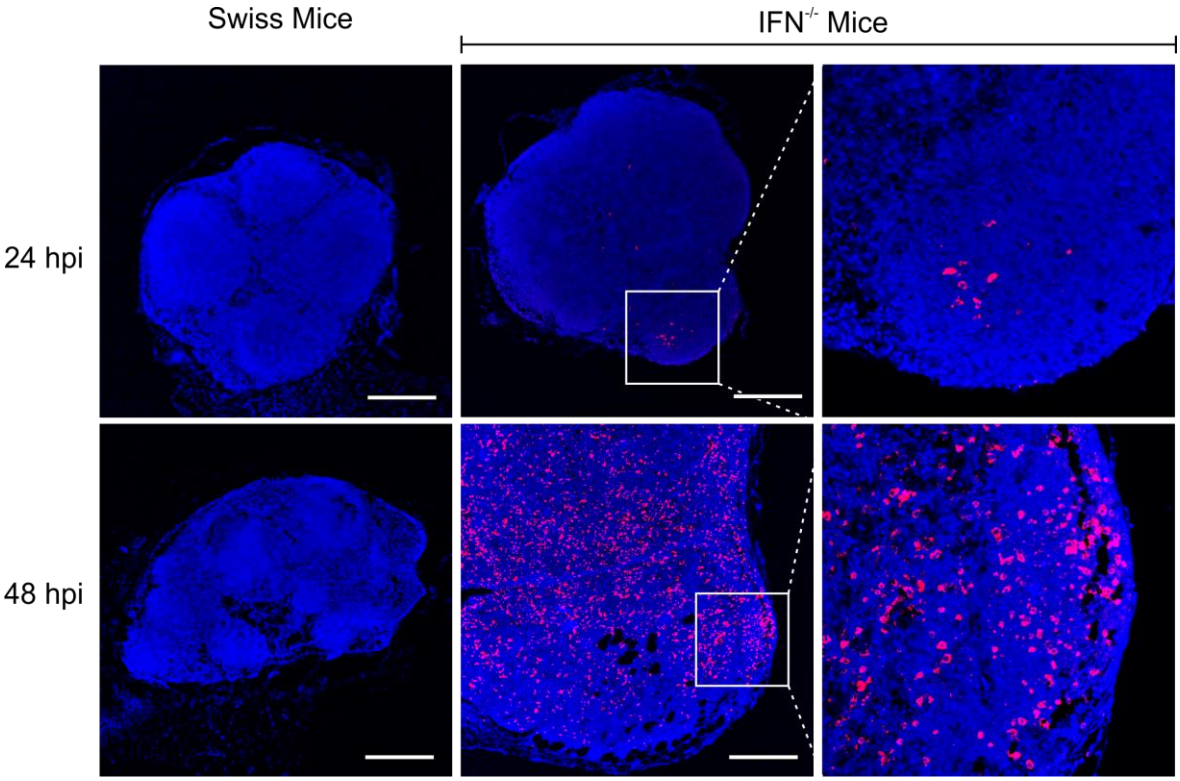

Figure 4-16 BTV-8 infection of mouse lymph nodes
Confocal images of whole LNs sections of mice subcutaneously inoculated with BTV-8. Sections were stained for BTV NS2 (red) and cell nuclei were stained with DAPI (blue). NIH Swiss mice did not support BTV replication in draining LNs between 24 and 48 hpi. On the contrary, the LNs of IFNAR$^{(-/-)}$ mice were rapidly infected by BTV and presented many positive cells both in the cortical and medullary areas. Scale bars represent 300 µm.

4.3 Discussion

In this chapter we followed the progression of BTV-8 infection in experimentally infected sheep, goats, and mice (conventional and type-I IFN α/ß-receptor deficient). We identified the distribution of the virus by qRT-PCR and localised the sites of viral replication by IHC and immunofluorescence. Our results identify the skin near the inoculation site and the corresponding draining LNs as sites of replication as early as 4 hpi.

Skin and LNs have long been recognised as sites of BTV replication by detection of viral genome or by virus isolation (Pini 1976; Barratt-Boyes & MacLachlan 1994; MacLachlan et al. 1990; Sánchez-Cordón et al. 2010; Darpel et al. 2012). Nevertheless, most of the previous histological studies failed to detect significant amounts of infected cells in LNs sections by immunohistochemistry or immunofluorescence (Hemati et al. 2009; Darpel et al. 2012). This discrepancy may be due to the time after infection when these organs were sampled, and to a different sensitivity of the techniques used in most of these studies. Indeed, we noted that an antigen retrieval process is required for the correct detection of BTV proteins in fixed tissues, in agreement with a previous study (Sánchez-Cordón et al. 2010). Furthermore, it is possible that a lack of correspondence between the presence of viral RNA and actual virus replication (with expression of non-structural proteins) in some of the tissues contributed to the observed differences. To overcome this issue, we combined qRT-PCR with an optimised IHC technique in order to identify the sites of virus replication during the in vivo infection. For example, in sheep spleen we detected high level of BTV RNA but very few infected cells; the spleen is an organ rich in blood with hemochateretic function, and BTV can be absorbed in the membrane of circulating red blood cell without active replication (Brewer & MacLachlan 1992), this observation could provide a possible explanation for the discrepancies observed by using different techniques.

Moreover, we demonstrate that the skin near the inoculation site and the corresponding draining LNs are capable of sustaining virus replication very early after infection in both sheep and goats. Our IHC results indicate that there is a

short time window in which numerous infected cells are present in the cortical area of the lymph nodes draining the infected skin (between 4 hours to 3 dpi), while at later time points only few capillaries appear to be infected in the medullary cords. Therefore, the histochemical observation of the LNs of infected animals at later time points, as done in previous studies (Darpel et al. 2012; Hemati et al. 2009; Sánchez-Cordón et al. 2010) might have missed the early phases of infection and underestimated the entity of the infection at these sites.

In sheep, by 4-8 hpi we observed numerous BTV infected cells in the cortical area of the LNs draining the infected skin, in correspondence of the subcapsular and trabecular sinuses. The cortical sinuses collect the incoming lymph from peripheral tissues. Therefore it is likely that virus particles get passively transported with the lymph fluids from the skin to the LNs.

DCs have been described as one of the key target cells infected by BTV and identified as the main carriers of BTV in the lymph (Hemati et al. 2009; Ruscanu et al. 2013). Once DCs reach the SCS, they have the capacity to cross the sinus walls and move into the T-cell area, where they finally localise. However the time required for a DC to pick up antigens in the skin, became activated and move towards the lymphatic vessels is considered to be roughly 12-18h (Itano et al. 2003; Randolph et al. 2005), which is not compatible with the time of virus arrival to the SCS observed in our study. This suggests that large part of the virus is freely transported within the lymph draining the infected skin rather than in association with DCs. Furthermore, in sheep we only rarely identify infected cells in the T-cell area (at any of the considered time points), where DCs should localise once they have accessed the LN (Braun et al. 2011).

Other organs presented infected cells only at later time points, once the viral RNA levels in the blood had increased. It is therefore evident that BTV undergoes an initial replication phase in the skin and then in the draining LNs, reached by the virus carried with the lymph flow. Subsequently, BTV reaches the bloodstream and it is distributed systemically to peripheral tissues like spleen, which contains large part of the circulating blood, and organs equipped with a capillary bed such as kidney and lung. The use of an attenuated virus ($BTV8_H$) that does not induce viremia, further strengthen this point, considering that peripheral tissues are not reached by this virus that shows a similar tropism as

BTV-8. It is therefore likely that for reaching the bloodstream the virus needs to overcome a bottleneck represented by the draining LNs, if it fails to do so, the systemic dissemination is prevented and with it the development of disease.

Different experimental settings have been used to reproduce the course of bluetongue in susceptible animals. We preferred the intradermal inoculation over the subcutaneous or intravenous route, to mimic insect bites and in order to start the infection in the anatomic compartment of the natural infection. The route of inoculation has been found to alter considerably the clinical outcome of experimental BTV infection as, for example, intravenous inoculation often fails to induce clinical signs (Umeshappa et al. 2011). These observations suggest that bypassing the skin and the LN can alter the pathogenesis of disease, and strengthen the idea that virus replication in skin and LNs is critical for the onset of disease.

Indeed, our IHC data show that the localization of BTV in non-draining LNs, that are reached by the virus between 3 to 7 dpi, during the viremic phase, is not in the sinuses or in the cortical area but in the medullar area. Therefore the tropism of the virus for specific areas of the LNs seems to be determined by the route of dissemination.

It has to be to consider that timing and localization of the virus in infected animals may have been influenced by kind of experimental setting used. For example, we did not analyse animals infected through the bite of Culicoides midges, the natural source of infection, that in previous occasions have been demonstrated to be able to enhance virus infectivity (Darpel et al. 2011) by VP2 cleavage, and to promote viremia and clinical symptoms expression (Pages et al. 2014) by delaying IFN-induced gene expression and delaying neutralizing antibody responses. Moreover, the inflammatory reaction generated by arthropod saliva has been recently identified as an important chemoattractant for cells susceptible to infection, such as mononuclear phagocytes, and it is therefore implicated in the amplification of similar arboviral diseases (Pingen et al. 2016). Furthermore, for experimental infections in sheep and goat we used $2x10^6$ PFU of BTV-8 (Caporale et al. 2014) as this dose was previously shown to be sufficient to cause disease. However, it is not currently known what is the

dose of BTV-8 inoculated by midges during the natural infection and on which extent this can be implicated on the clinical outcome.

We characterised BTV-8 distribution in experimentally infected goats, which generally do not present clinical disease (Caporale et al. 2014; MacLachlan et al. 2009). In goats, BTV RNA levels in draining LNs, after peaking at 24 hpi, rapidly decreased to lower levels compared to sheep (approximately 100 fold difference) indicating a possible difference in virus replication in goat tissues. This difference was also reflected in the delayed onset of viremia in goats, which reached significant titres only at 5 dpi and never equalled the titres observed in infected sheep (10^3 vs 10^7 copies at 7 dpi). This likely accounted for the lower level of viral distribution in peripheral tissues observed in goats. Viral replication, as assessed by IHC, was localised in similar areas of the LNs in infected sheep and goats. However, we observed some significant differences. First, the intensity of NS2 staining in lymphatic endothelial cells lining the sinuses walls was lower in goats compared to the equivalent cells in sheep. In addition, we observed numerous infected cells in the paracortical area of the LNs in goats while in sheep there were no visible infected cells in this area. A diverse tropism of the virus for different cell populations in these two animal species could explain the slower progression of infection observed in goats and possibly account for the mild or asymptomatic infection displayed in this animal species. However, the different BTV-8 tropism detected in sheep and goats could be the consequence of multiple variables, such as a different efficiency of the innate and intrinsic immunity, the virus strain specificity and adaptation, the level of expression of the cell receptor, or the presence of adaptive immunity, just to mention some possibilities. Further studies are needed to identify the weight of each factor on the final effect.

Undoubtedly, BTV studies involving the natural ruminant hosts are limited by the complexity of the system, the limited knowledge of ruminants' immune system, and the need to have a large animal facility with BSL-3. To overcome some of these issues, murine models that support BTV replication have been developed (Calvo-Pinilla, Rodríguez-Calvo, Anguita, et al. 2009). To evaluate if pathogenicity studies can be performed in a more manageable model of disease, we compared the pattern of infection and virus distribution obtained in sheep

and goats with BTV-infected mice, testing both NIH-Swiss mice and IFNAR$^{(-/-)}$ mice.

In NIH-Swiss mice, whose immune system is intact, BTV replication was not detected in draining LN, indicating that BTV is unable to replicate in mice with a fully working innate immune system. These data support the evidence that this type of mouse cannot be used for BTV studies and indicate the importance of an intact innate immune response that can restrict virus replication in non-natural species.

In IFNAR$^{(-/-)}$ susceptible mice (Calvo-Pinilla, Rodríguez-Calvo, Anguita, et al. 2009), BTV infected cells were detected in draining LNs but the anatomical localization of these cells did not resemble the one observed in infected sheep or goats. The subcapsular sinus was not infected and only few virus-positive cells were present inside B-cells follicles. Furthermore, a clear discrimination of the virus differential localisation in the cortical, paracortical or medullar area was not observed and virus-infected cells were abundantly present in each area. These data indicate that mouse models of BTV infection cannot fully replicate the viral tropism and the pathogenesis of disease that we observe in the natural ruminant hosts.

Furthermore, our results add to the notion that IFN is an important determinant of BTV susceptibility. We show that type-I IFN stimulation can completely abrogate BTV replication in a mouse model, this suggests that IFN could also be implicated in determining the range of infected cells not only in mouse but also in the target animal species, therefore interferon-stimulated genes and species-specific restriction factors may be implicated in defining host species range of BTV. Viral tropism is generally determined by a combination of two major factors: a host cell must be both permissive (allow viral replication) and susceptible (possess the receptor needed for viral entry) for a virus to establish infection. The receptor for BTV is still unknown, however, *in vitro* BTV is able to replicate in a variety of cell lines, derived from different hosts, indicating that the receptor must be widely expressed in different cells and in different animal species. This suggests that BTV can use a very evolutionary conserved receptor, or alternatively, that the virus is able to use more than one type of receptor depending on its availability in the surrounding environment. A role of heparan

sulphate in BTV-cell binding has been demonstrated (Janowicz et al. 2015; Mecham & McHolland 2010), and structural studies have also identified sialic-acid binding domains on the VP2 outer capsid protein (Zhang et al. 2010) but functional studies are still missing. Here we observed that numerous mouse cells were susceptible to BTV in absence of type-I IFN. Hence, the presence of the cellular receptor it is unlikely to be a determinant factor in restricting virus tropism in mouse, on the contrary, the permissiveness of the mouse cells seems to be determined by their innate immune response against BTV.

In summary, the data presented in this chapter show BTV distribution over time in experimentally infected sheep and goats. The results obtained underline the importance of the passive stream of free viral particles within the lymph flow at the initial stages of experimental BTV infection, and the role of the bloodstream in the systemic dissemination of the virus. We identify the draining LNs as having a crucial role during the initial stages of infection, before the onset of clinical signs. Interestingly, we found a different pattern of viral infection in goats compared to sheep LNs, and this key difference could account for the large variability in the clinical outcome of disease between these two species.

Chapter 5

Results

5 Characterization of BTV-8 infected cells in sheep lymph node

5.1 Introduction

In chapter 4, we have shown that soon after inoculation into the skin, BTV replicates in the draining LNs of the infected host. Draining LNs are essential stops along the journey of the virus toward its systemic dissemination. Inside the LN, lymphocytes encounter cognate antigens and these events lead to the initiation of the immune response. Hence, the way in which BTV interacts with the immune system inside the LN can shape the immune responses and it is of paramount importance to understand arbovirus pathogenesis.

The highly ordered architecture of the lymph node maximizes the chance that a lymphocyte will encounter antigens (Junt et al. 2008; Lämmermann & Sixt 2008). Different subsets of stromal cells (Malhotra et al. 2012) form the three-dimensional scaffolding of the LN and are responsible for the organization of distinct functional zones through secretion of specific chemokines and cytokines driving lymphocytes migration and contributing to the development of an appropriate immune response (Mueller & Germain 2009; Bajenoff et al. 2006; Link et al. 2007). For example, in the paracortical area, the place where DCs and T-cells get in contact, fibroblastic reticular cells (FRC) drive T-cells and DCs chemotaxis through secretion of chemokine ligand 19 (CCL19) and CCL21, which in turn recruit chemokine receptor 7 (CCR7) expressing cells (T-cells and DCs). On the contrary, follicular dendritic cells (FDC) and marginal reticular cells (MRC) are the stromal cells deputed to the maintenance of the B-cell follicle, producing the CXCL13 homing signal for B-cells expressing the chemokine receptor 5 (CCR5) and driving germinal centre formation and B-cell activation.

Recently, imaging studies have provided insightful information about the early events following viral infection and the initiation of immune response (Bousso & Moreau 2012). Despite most of the data described in literature are based on mouse models, and similar mechanisms in other mammalian species have been poorly characterized, some analogies can be drawn. Studies conducted in the mouse indicate that, few minutes after inoculation, free antigens and pathogens start to reach the SCS of the regional draining LN (Roozendaal et al. 2009;

Gonzalez et al. 2010; Junt et al. 2007; Braun et al. 2011; Kastenmüller et al. 2012; Gonzalez et al. 2015; Iannacone et al. 2010). The SCS forms a barrier between the lymph contents and the LN parenchyma, working like a filter to avoid uncontrolled access of potentially harmful antigens to the LN cortex. In order to access the LN cortex, antigens are screened based on theirs dimensions. Small antigens with a molecular weight lower than 70 kDa (~ 5 nm radius) are allowed free access to the LN parenchyma through a system of tubules that cross the subcapsular sinus (SCS) and deepen inside the paracortical area (Sixt et al. 2005). Antigens flowing through the conduits can then be directly sampled by resident DCs and macrophages. A less dense system of tubules was also discovered in the follicles (Roozendaal et al. 2009), deputed to deliver the antigens to follicular B-cells and FDC.

On the contrary, larger and particulate antigens (>70 kDa), such as viruses and bacteria, once they reach the SCS cannot directly access the conduits and they remain trapped in the SCS where are captured by a resident population of macrophages (Hirosue & Dubrot 2015).
Once picked up by SCS macrophages, large, unprocessed antigens can be transferred to the underlying B-cell area, where they are directly presented to follicular B-cells (Phan et al. 2009). After antigen recognition, cognate B-cells migrate either to the outer follicular zone where they present the antigens to T-cells, or to the light zone of the follicle to deliver the antigens to FDC.

Only 12-24 hours after these initial events, migratory DCs reach the LN from the skin, traverse the subcapsular sinus and head to the paracortical area bringing processed antigens (Randolph et al. 2008; Itano et al. 2003; Braun et al. 2011), initiating a second wave of antigen presentation which consolidates the initial one. In the paracortical area, T-cells have the opportunity to scan DCs for their cognate antigen. Once the antigen is recognised, a contact is established between the T-cell receptor (TCR) with peptide-MHC complexes on the surface of DC. Furthermore, T-cell-DC contact provide co-stimulatory and adhesion molecules interactions and production of soluble factors that modulate the activation of T-cells. Productive activation of naive T cells by DCs results in their clonal expansion and differentiation into effector and memory T-cells (Bousso 2008).

In this chapter we aimed to identify the cell populations infected by BTV in the lymph nodes draining the site of virus inoculation. Given the limited amount of antibodies available to target ruminant cells in formalin-fixed tissues we firstly screened a panel of antibodies to further characterise sheep lymphocytes, macrophages, DCs and lymphoid stromal cells. We then used confocal microscopy to assess virus replication in these cells at different time after infection. Our results indicate that BTV replicates in macrophages and endothelial cells lining the sinus walls. Thereafter, BTV access the cortical area of the LN by infecting B-cells and the stromal network of cells composing the lymphoid follicles where it persists until 96 hpi. Overall we discovered new viral targets in the ruminant LN and characterised the progression of BTV infection at this site.

5.2 Results

5.2.1 Characterization of cell populations in sheep lymph nodes

Research in veterinary species is negatively affected by the lack of reagents. The relatively limited knowledge of the immune system of ruminants is partially due to an incomplete characterization of their immune cell populations. Hence, the identification of monoclonal antibodies targeting specific cells populations in ruminant species is paramount for the progress of veterinary research.

5.2.1.1 Screening of antibodies to target sheep cells in paraffin embedded lymph nodes

In order to identify BTV infected cell populations in the LN of sheep we initially performed a screening of a panel of 67 antibodies (Table 5-1) to identify cell markers reacting with sheep tissues, formalin and zinc salt fixed and then paraffin embedded. The results of the screening are summarised in Table 5-1, we identified 40 antibodies that work on fixed sheep tissues, 14 of which solely work when zinc fixatives are used. The tested antibodies had various species specificity, some were specific for sheep, others were defined cross-reactive, and others have not been previously tested in sheep tissues. For clones whose cross-reactivity in ruminants was not stated by the producers, we performed a BLAST (basic local alignment search tool) search against the sheep genome of the sequence targeted by the antibody (when stated) or of the whole target protein. To blast and compare the sequences we used the PubMed online database and we sourced the protein sequences using the Uniprot database (Anon n.d.). We then tested by immunohistochemistry the efficacy of those antibodies that were raised against proteins sharing at least 70% identity with the sheep orthologues. Antibodies were tested initially in zinc fixed tissues, since the possibility to detect a specific signal was facilitated by the fact that antigen retrieval is generally not required with this type of fixation. To determine presence of a positive signal we used initially dilutions between 1:20 to 1:200. The final working concentration for each antibody was then determined based on the results obtained and it is summarised in Material and Methods. The specificity of the staining was determined by using histological insights checking if the localization of the staining in the tissue matched the likely anatomical localization of the targeted cells. However, in some cases, we

obtained specific signals in unexpected cell populations. We further characterised various cell populations by co-expression of specific markers by using a combination of two or three antibodies by confocal microscopy. Generally, we associated a well-recognised marker, or a previously characterised one, with a newly identified one. This allowed us to identify previously uncharacterised markers for sheep stromal cells and mononuclear phagocytes. Testing of antibodies in formalin fixed tissues also included the evaluation of different antigen retrieval techniques for the unmasking of formalin cross-linked epitopes (as described in Material and Methods). The use of different antibodies in multicolour immunofluorescence studies was limited by their reactivity using the same antigen retrieval technique and by the animal in which they were obtained (mouse, rabbit, rat, guinea pig or donkey) or, in case of mouse antibodies, by the isotype classes (we used IgG_1, IgG_{2a}, IgG_{2b}, IgM). The application of unrelated antibodies of the same isotype and concentration was used as a negative control to check the specificity of the positive signal.

Table 5-1 - List of antibodies tested on sheep tissues by immunohistochemistry
Results of the screening (R): no signal (red), signal in formalin fixed tissues (green), signal in zinc salts fixed tissues (blue), Inconstant results (yellow). Mo (mouse), Hu (human), Rb (rabbit), Sh (sheep), Bv (bovine), Gt (goat). PL (polyclonal).

R	Marker	Clone	Host/Target	Isotype	Manufacturer
	CD14	TUK4	Mo α Hu	IgG2a	Bio-Rad
	CD14	VPM65	Mo	IgG1	Moredun
	DEC205	CC98	Mo	IgG2b	Bio-Rad
	SIRPα	IL-A24	Mo	IgG1	Moredun
	MHC-II	SW73.2	Rat α Sh		Moredun
	CD3	F7.2.38	Mo α Hu	IgG1	Dako
	CD79a	HM57	Mo α Hu	IgG1	Bio-Rad
	CD163	EDHu-1	Mo α Hu	IgG1	Bio-Rad
	WC1	CC15	Mo α Bv	IgG2a	Bio-Rad
	IFN-Gamma	7B6	Mo α BV	IgG1	Bio-Rad
	Ki-67	MIB-1	Mo α Hu	IgG1	Dako
	CD68	EBM11	Mo α Hu	IgG1	Dako
	CD169 - Siglec-1	HSn 7D2	Mo α Hu	IgG1	Santa Cruz Biotech
	Caspase 3	74T2	Mo α Hu	IgG1	Invitrogen
	Cleaved Caspase 3	D175-5A1E	Rb	PL	Cell Signaling
	CD1w2	CC20	Mo α Bv	IgG2a	Bio-Rad
	CD45	1.11.32	Mo α Sh	IgG1	Bio-Rad
	CD1	20:27	Mo α Sh	IgG1	Bio-Rad
	CD83	HB15e	Mo α Hu	IgG1	Bio-Rad
	CD26 - WC10	CC69	Mo α Bv	IgG1	Bio-Rad
	CD11b	CC126	Mo α Bv	IgG2b	Bio-Rad
	CD21	CC21	Mo α Bv	IgG1	Bio-Rad
	CD209		Rb	PL	Bio-Rad
	CD62P	AK-6	Mo α Hu	IgG1	Bio-Rad
	CD62P	Psel.KO.2.7	Mo α Hu	IgG1	Bio-Rad
	CD8	CC63	Mo α Bv	IgG2a	Bio-Rad
	CD209	MR-1	Mo α Hu	IgG1	Bio-Rad
	LYVE-1		Gt α Hu	PL	R&D System
	Desmin	DE-U-10	Mo α Hu	IgG1	Sigma-Aldrich
	Fascin	55K-2	Mo α Hu	IgG1	Dako
	CD31	JC70A	Mo α Hu	IgG1k	Dako
	Podoplanin	D2-40	Mo α Hu	IgG1k	Dako
	Von Willebrand Factor		Rb	PL	Dako

R	Marker	Clone	Host/Target	Isotype	Manufacturer
	Von Willebrand Factor	F8/86	Mo α Hu	IgG1	Dako
	Vimentin	Vim3B4	Mo α Hu	IgG2ak	Dako
	Laminin	4C7	Mo α Hu	IgG2ak	Dako
	B-cells	Dak-Pax5	Mo α Hu	IgG1	Dako
	FDC	CNA.42	Mo α Hu	IgM	Dako
	CD21	BAQ15A	Mo α Bv	IgM	King Fisher
	CD172a	DH59B	Mo α Bv	IgG1	King Fisher
	CD11c	BAQ153A	Mo use α Bv	IgM	King Fisher
	CD208 - DC lamp	1010E1.01	Rat α Mo	IgG2a	Dendritics
	CD31	CO.3E1D4	Mo α Sh	IgG2a	Bio-Rad
	TLR3 - CD283	713E4.06	Mo α Hu	IgG1	Dendritics
	ICAM-1 CD54	117G12	Mo α Hu	IgG1	Dendritics
	ER-TR7	ER-TR7	Rat α Hu	IgG2a	Thermo
	Collagen IV	CIV22	Mo α Hu	IgG1	Dako
	JAM-2	1G4	Mo α Hu	IgG1	Sigma-Aldrich
	Fibroblasts	TE-7	Mo α Hu	IgG1	Merk Millipore
	Perlecan	A71	Mo α Bovine	IgG1	Source bioscience
	CD83		Rb	PL	Biorbyt
	CD83	HB15a	Mo α Hu	IgG2b	Biorbyt
	Desmoplakin	DP2.15	Mo α Bv	IgG1	Millipore
	Cleaved Caspase 3	Asp175	Rb	PL	Cell Signalling
	S100		Rb	PL	Dako
	PCNA (division)	PC10	Mo α Hu	IgG2a	Bio-Rad
	Sh IgG HRP		Dk anti Sh/Gt	PL	Bio-Rad
	JAM-A		Rb	PL	Invitrogen
	Lyve-1		Rb	PL	Millipore
	S100		Rb	PL	Bio-Rad
	Beta-actin		Rb α Hu	PL	Cell signaling
	Smooth muscle actin	1A4	Mo α Hu	IgG2a	Dako
	CD8	38.65	Mo α Sh	IgG2a	Bio-Rad
	CD4	44.38	Mo α Sh	IgG2a	Bio-Rad
	PLVAP	MECA-32	Rt α Mo	IgG2a	Bio-Rad
	Desmin		Rb α Mo	PL	Abcam
	CD335	EC1.1	Mo α Sh	IgG1	Bio-Rad

5.2.1.2 Identification of lymphocyte markers in sheep lymph node

To detect T-cells, we targeted **CD3** by using clone F7.2.38 (Table 5-1) (Al Saati et al. 2001) that recognizes an epitope on the intracytoplasmic portion of the ε-chain of CD3 that is well conserved in mammalian species. In sheep the anti-CD3 antibody identifies cells that localise in the paracortical area of the LN. As expected, some T lymphocytes were also present along the medullary cords but not inside the medullary sinuses. CD3 T-cells were not generally present in the SCS or along the trabecular sinuses. Antibody targeting **CD8, CD4 and WC1** were used to detect cytotoxic, helper and γδ T lymphocytes respectively. We observed these lymphocytes populations in a similar localization as it was previously described (González et al. 2001). Few scattered natural killer (NK) cells were identified in the paracortical area of the lymph node by using an antibody targeting CD335 (NCR1, natural cytotoxicity triggering receptor 1) (Olsen et al. 2015).

We also tested antibodies directed against three different markers commonly used for the identification of B-cells: CD79a, CD21 and Pax5 (Figure 5-1). **CD79a** (clone HM57) was not considered a reliable marker for B-cells identification, as the resulting staining was inconsistent. On the contrary, and as previously described, **CD21** (complement receptor 2, CR2) was expressed both by mature B-cells and FDC and by cells localised in the follicles of the cortical area of the LN. However, it was not possible to differentiate B-cells from FDC based only on the use of antibodies detecting this marker (Figure 5-1). The clone Dak-pax5 (Agostinelli et al. 2010) identifies the PAX-5 protein, also termed B-cell specific activator protein (BSAP), a member of the highly conserved paired box (PAX)-domain family of transcription factors. **BSAP** plays an essential role for B-cell commitment, since it is involved in the repression of non-B lymphoid genes and the activation of genes needed for B-cell differentiation (Agostinelli et al. 2010). BSAP is expressed in the nucleus of B-cells in all the maturation stages, but not in plasma cells. Similarly to CD21, anti-Pax5 antibody identified cells in the follicles of the LN but it does not stain FDC (Figure 5-1) and was therefore chosen as specific marker for B-cells.

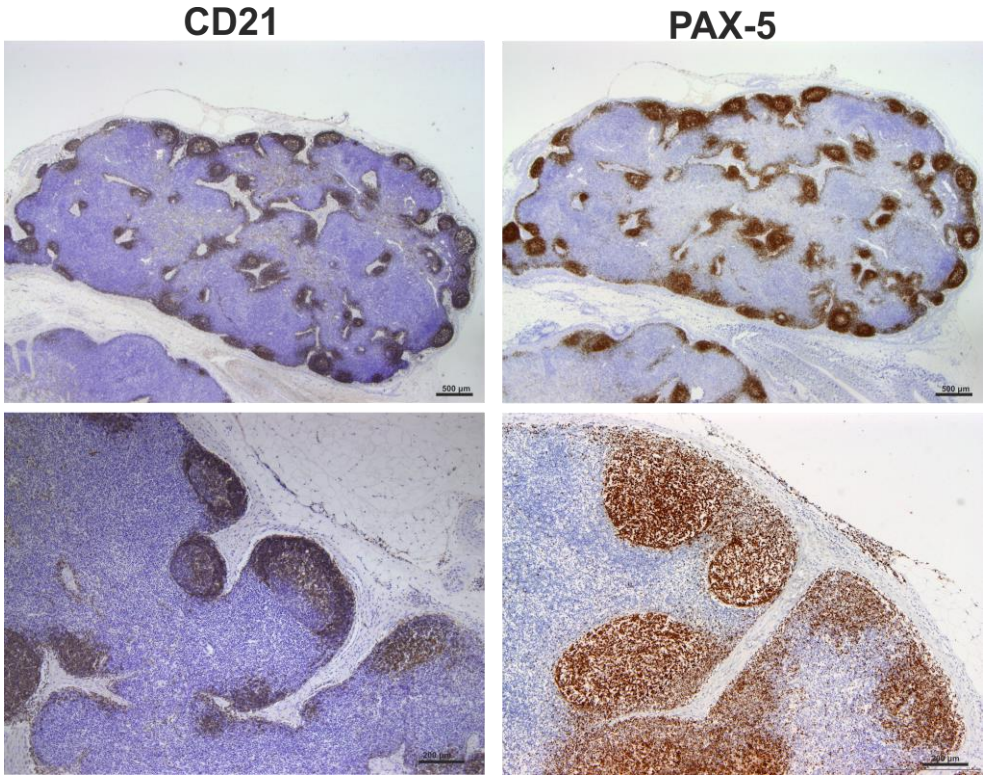

Figure 5-1 Identification of markers for sheep B-cells
Representative immunohistochemistry micrographs of sheep lymph node sections collected from uninfected control animals and fixed using zinc salt solution. Sections were stained for CD21 and

PAX-5 (BSAS protein), both markers identify sheep B-cells. Scale bars 500µm in top raw images, 200µm in the bottom raw

5.2.1.3 Identification of markers for mononuclear phagocytes (macrophages and dendritic cells) in the sheep lymph node

A broad variety of markers have helped to characterise different populations of myeloid cells in mouse and human. In ruminants species there are limited information about the mononuclear phagocytes residing in the LN. Hence, we decided to systematically test a panel of antibodies, which prove useful in other mammalian species, to identify the localization of dendritic cells and macrophages in sheep LNs. The clone SW73.2 (Hopkins et al. 1986) reacts with a monomorphic epitope on both HLA-DQ (human leucocyte antigen) and -DR beta chain of sheep and cattle MHC class II (MHC-II), which are constitutively expressed on antigen presenting cells such as dendritic cells, B lymphocytes, monocytes, macrophages and may be induced on a range of other cell types by interferon gamma. SW73.2 was used to identify antigen presenting cells: **MHC-II** was broadly expressed by cells of the cortical area, in particular by interdigitating cells present in the paracortex and at a lower level by the B-cells present in the follicles. We then screened markers considered specific for sheep macrophages. **CD163** (Figure 5-2) is a glycoprotein belonging to the scavenger receptor cysteine-rich superfamily, it is considered to be exclusively expressed by sheep macrophages and not expressed by neutrophils (unlike for example CD68) (Elnaggar et al. 2016; Herrmann-Hoesing et al. 2010). CD163 was expressed by few cells in the paracortical area and by numerous cells present along the trabecular and medullary sinuses (Figure 5-2). Another marker, **CD11b** was also expressed by cells in a similar location, along the trabecular and medullary sinuses (Figure 5-2). Therefore CD11b and CD163 likely stain the same population of macrophages, although it was not possible to use the two markers together (being both mouse IgG1 monoclonal antibodies). The sialoadhesin **CD169** is a lectin with Ig superfamily domains that binds sialic acid and is expressed exclusively by macrophages. In mouse LNs, CD169 characterises two different types of macrophages, SCS and medullary (Martinez-Pomares & Gordon 2012). These macrophages are strategically placed to allow antigen acquisition and delivery to lymphocytes. In sheep, the anti-CD169 antibody (clone HSn 72D) labelled a population of macrophages that was present along trabecular and

medullary sinuses but absent along the SCS (Figure 5-2). Hence, these results allowed the identification of 4 markers for sheep macrophages: MHCII, CD11b, CD163 and CD169.

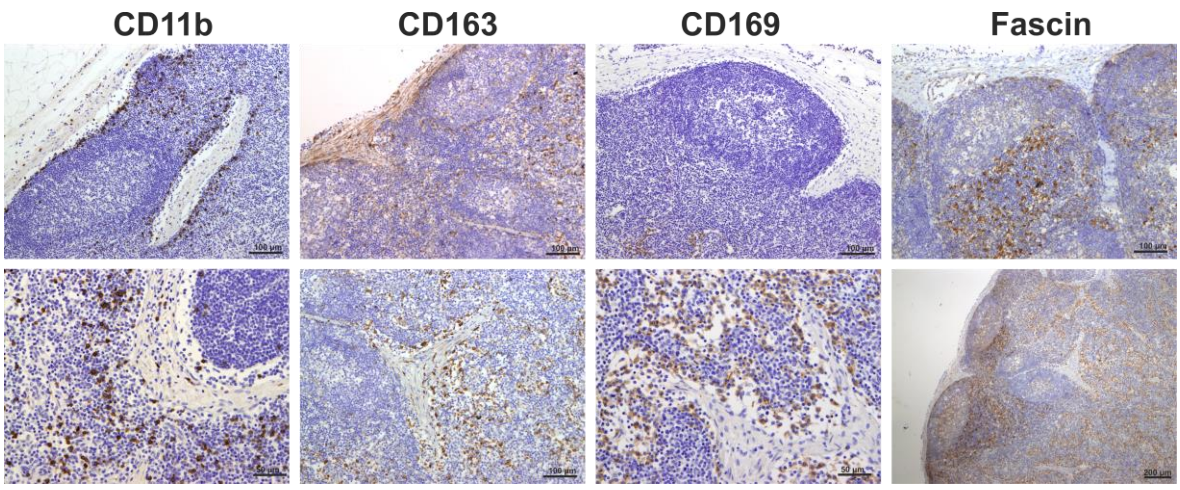

Figure 5-2 Identification of markers for sheep macrophages and dendritic cells
Representative immunohistochemistry micrographs of sheep lymph node sections collected from uninfected control animals and fixed using zinc salt solution. Tissues were stained for CD11b, CD163, CD169 and fascin. The expression of these markers in different anatomical areas of the lymph node allowed the identification of various populations of mononuclear phagocytes.

Thereafter, we screened antibodies targeting markers expressed by dendritic cells.

CD208 (dendritic cell-lysosomal associated membrane protein, DC-LAMP) is specifically expressed by DCs on activation. An anti-CD208 antibody (clone 1010E1.01) was previously used to identify bovine DCs in formalin fixed tissues (Romero-Palomo et al. 2013). In sheep, CD208 was differentially expressed by two distinct cell populations residing in the paracortical area of the LN: the first population expressed CD208 at significant high levels in the cytoplasm, while the second population showed CD208 clustered in a limited perinuclear area (likely the Golgi apparatus) (see below Figure 5-5); this second type of expression was also detected in cells present along trabecular and medullary sinuses.

Fascin has been demonstrated to be critical for the antigen presentation activity of mature mouse and human DCs (Al-Alwan et al. 2001; Ross et al. 2000) and is considered a specific marker for mature DCs that is not expressed by macrophages (Vakkila et al. 2005). In sheep LNs, fascin was highly expressed by cells present in the paracortical area, with the antibody (clone 55K-2) strongly labelling the membrane processes extending outward the main cell body (Figure

5-2, see also Figure 5-4B and Figure 5-5B). In the paracortical sinuses, fascin was expressed at much lower level (barely detectable) in round shaped cells with no visible elongations (Figure 5-2, see also Figure 5-4B and Figure 5-5B).

CD83 is a broadly used as a maturation marker for human and mouse DCs (Breloer & Fleischer 2008), however it is also expressed on a variety of different cells, including monocytes and macrophages (Cao et al. 2005), activated B and T lymphocytes (Krzyzak et al. 2016; Wolenski et al. 2003; Victora et al. 2012) and some epithelial cell populations. In sheep LNs, CD83 displayed a marked cytoplasmic localization around the nucleus in cells present in the paracortical area, while it was not present in the cells of the sinus. In addition, the anti-CD83 antibody labelled a reticulum of cells present in the B-cell follicles in the cortical area but it was absent on B-cells (Figure 5-4A)

CD1 is generally considered a specific marker for sheep DCs, however we detected its expression also on sheep B-cells as previously reported (Mwangi et al. 1991); for this reason CD1 was not used as marker for CDs in the present study. On the contrary, **CD1w** was expressed in cells present in the paracortical area, compatible with DCs, however since it was not working in immunofluorescence, it was not used extensively (Figure 5-3).

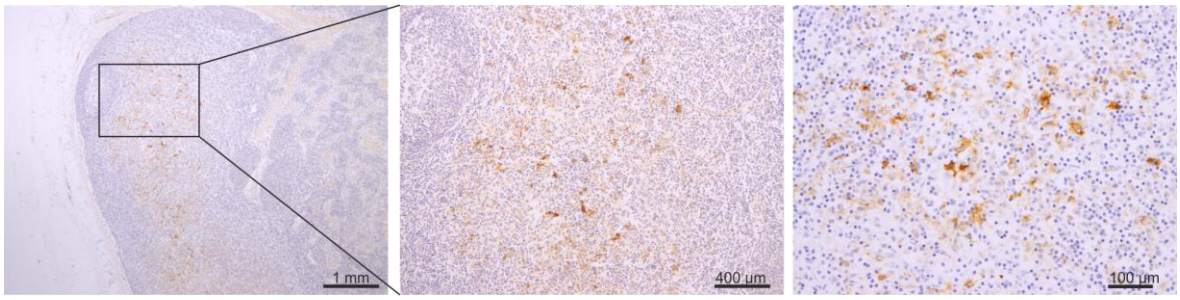

Figure 5-3 Localization of CD1w+ cells in sheep lymph node
Representative immunohistochemistry micrographs of sheep lymph node sections collected from uninfected control animals and fixed using zinc salt solution, tissues were stained for CD1w that localise in the paracortical area. Different magnification are shown.

In order to further characterise the phenotype of sheep DCs and macrophages, we performed double staining with combinations of relevant markers by using multicolour confocal microscopy (Figure 5-4 and Figure 5-5). MHCII and CD83 were both brightly expressed in cells of the paracortical area, characterised by long elongations and morphologically consistent with DCs (Figure 5-4A). MHC-II^{high} cells of the paracortical area tended to express high levels of fascin in their elongations (Fascin^{high}) (Figure 5-4B). In the follicles, MHCII positive B-cells did

not express CD83, which was instead found to be expressed by spindle shaped cells, morphologically consistent with FDC (Figure 5-4A).

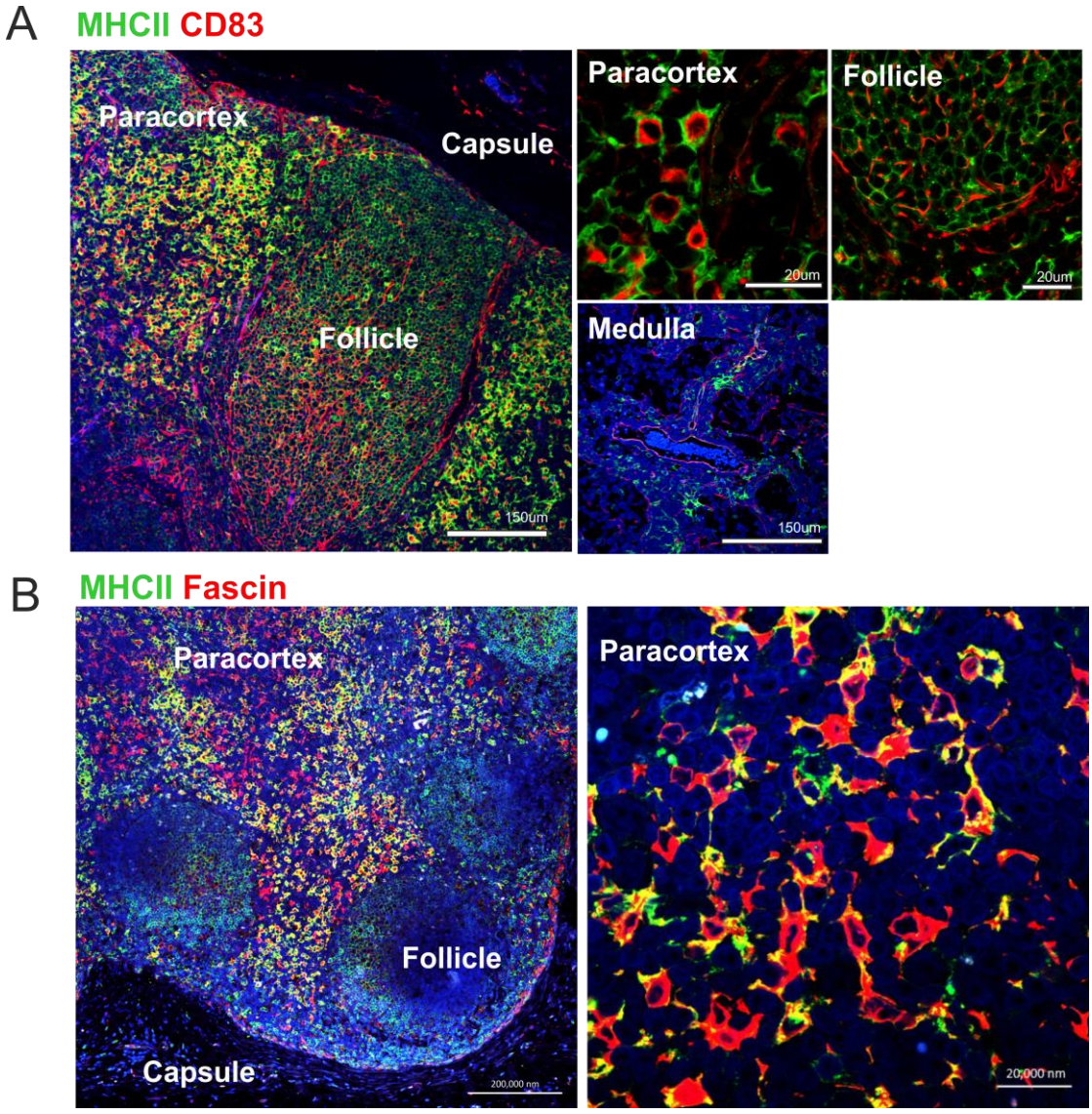

Figure 5-4 Identification of markers for sheep dendritic cells (MHCII, CD83 and fascin)
Representative confocal images of sheep lymph node sections collected from uninfected control animals. (A) Sections were stained for MHC-II (green) and CD83 (red). Insets show markers expression in different areas of the lymph node at higher magnification. (B) Sections were stained for MHC-II (green) and fascin (red) to visualise the extension of DCs in the paracortical area.

Interestingly, the high expression of CD208 and CD163 seemed to be mutually exclusive in sheep LN (Figure 5-5A). For example, in the paracortical area, cells expressing high levels of CD208 generally did not express CD163 whereas cell expressing high levels of CD163 were stained with the anti-CD208 antibody only internally in the perinuclear area ($CD208^{int}$) (Figure 5-5A), these results indicate the co-existence of various APCs populations in this area that may represent

different maturation stages of the same cells, or alternatively cells possessing different functions. A population with the same phenotype ($CD163^{+}$ $CD208^{int}$) was also present along the medullary sinuses suggesting that these cells may represent macrophages. Furthermore, $fascin^{high}$ cells also expressed CD208 at high levels in the paracortical area, while $fascin^{low}$ cells along the sinuses expressed CD208 only internally in the perinuclear area (Figure 5-5B) providing another indication that these cells are indeed macrophages.

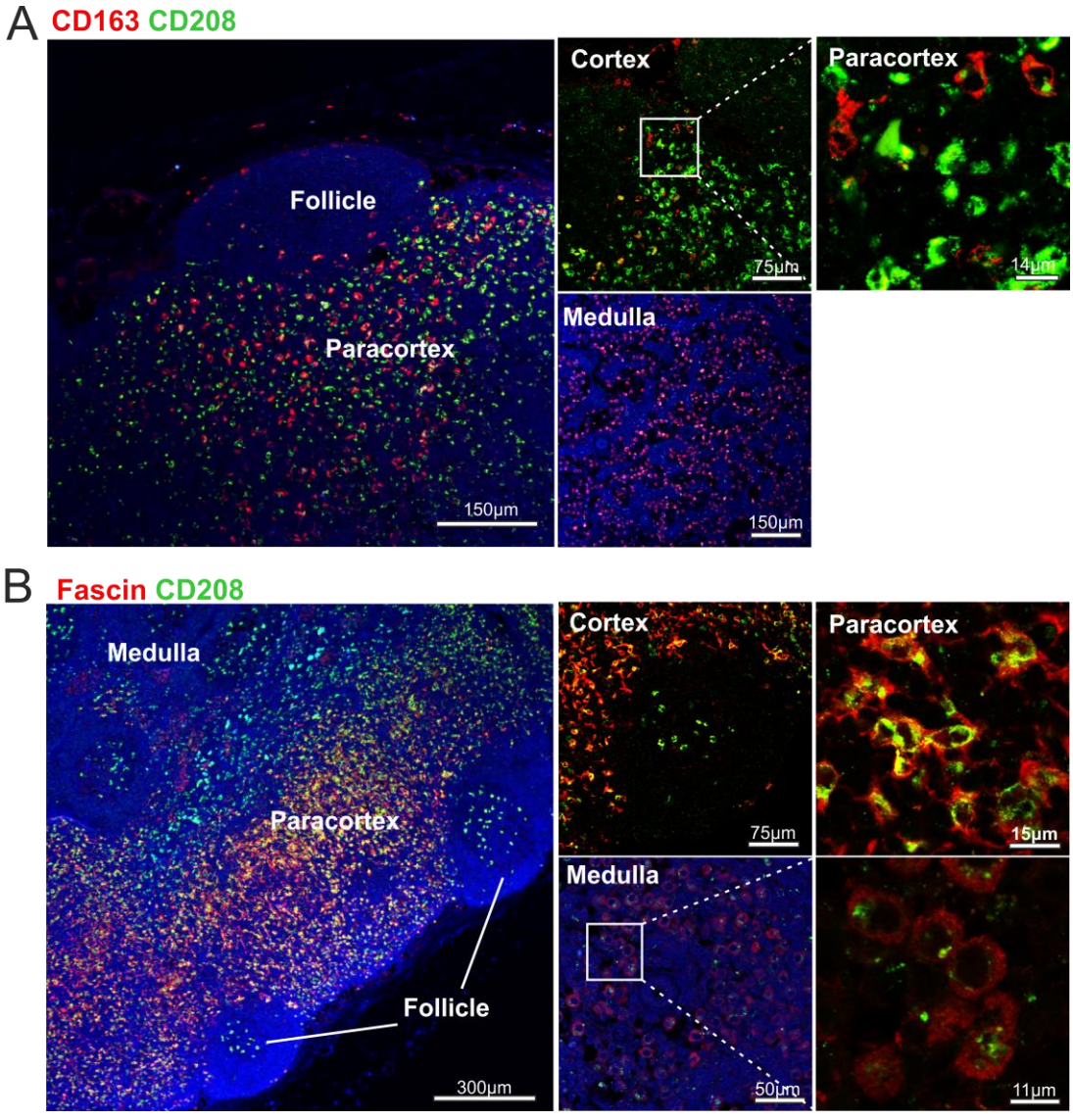

Figure 5-5 Identification of markers for sheep antigen presenting cells (CD208, fascin and CD163)
Representative confocal images of sheep lymph node sections collected from uninfected control animals. (A) Sections were stained for CD163 (red) and CD208 (green) which identify different populations of sheep phagocytes. Insets show markers expression in different areas of the lymph node at higher magnification. (B) Sections were stained for fascin (red) and CD208 (green) that were both highly expressed in cells residing in the paracortical area (dendritic cells) but not in macrophages localised not along the trabecular sinuses.

To summarise, the differential expression of combined markers lead to the characterization of a variety of APCs populations residing in the sheep LN. Along the trabecular and medullary sinuses a population of CD163^{high}/CD208^{int}/CD169^{high}/MHC-II^{+}/fascin^{low} cells represented macrophages. A similar population of macrophages has been described in the medullary sinuses in other animal species and they work by capturing antigens flowing through the LN (Gray & Cyster 2012). Dispersed in the paracortical area of the sheep LN, we identified two different populations of APCs. The first one, characterised by CD208^{high}/fascin^{high}/MHC-II^{high}/CD83^{+} cells that in some occasions displayed perinuclear CD163$^{int/-}$, presented a phenotype compatible with mature DCs that can contribute to the activation of T-cells in the paracortical area of the LN (Angel et al. 2009), while the second one, was less represented and showed a phenotype compatible with macrophage CD163^{+}/CD208^{int}/fascin^{low}. Furthermore we could localise, in the B-cell follicles, some follicular macrophages (also called tingible body macrophages), expressing both CD208 and CD163. CD208 is generally considered a specific marker for DCs but in the ruminant species has already been reported in tingible body macrophages (Romero-Palomo et al. 2013). See Table 5-2 for a summary of the populations characterised.

5.2.1.4 Identification of stromal cells markers in the sheep lymph node

Stromal cells provide the supporting network of fibres that form the LN structure; moreover, they also provide homing signals to drive leucocyte migration and have recently been assigned a role in facilitating the antigen presentation process (Hirosue & Dubrot 2015; Turley et al. 2010). New insights in the lymphoid stromal cells function shows that this is a non-homogeneous population of highly specialised cells (with defined functions and phenotype) each one specific for the different functional areas of the LN (Chang & Turley 2015). However, these phenotypic and functional specialisations have only been described in the mouse LN and, until now never been reported in other species. Here we aimed to characterise different populations of lymphoid stromal cells of the sheep LN, and to identify markers to unequivocally identify them by confocal microscopy in fixed tissues. As a result of this, some minor differences emerged in comparison with the mouse model mentioned above.

Similarly to the mouse, FRC were identified as expressing **desmin**, (Malhotra et al. 2012; Fletcher et al. 2011), delineating a network of stromal cells populating the paracortical and medullar area of the LN but absent from the follicular area (Figure 5-6). Contrary to the mouse, **smooth muscle actin** (SMA) was not expressed by sheep FRC (Malhotra et al. 2012), but only present in the LN capsule and in the pericytes surrounding HEV. Curiously, SMA was also present on a population of arc-shaped cells, which delineates the paracortical border of the follicle, which has not been previously described. It is reasonable to hypothesize that SMA^+ cells in this location were pericytes surrounding an artery feeding the follicle, but it was not possible to exclude other options.

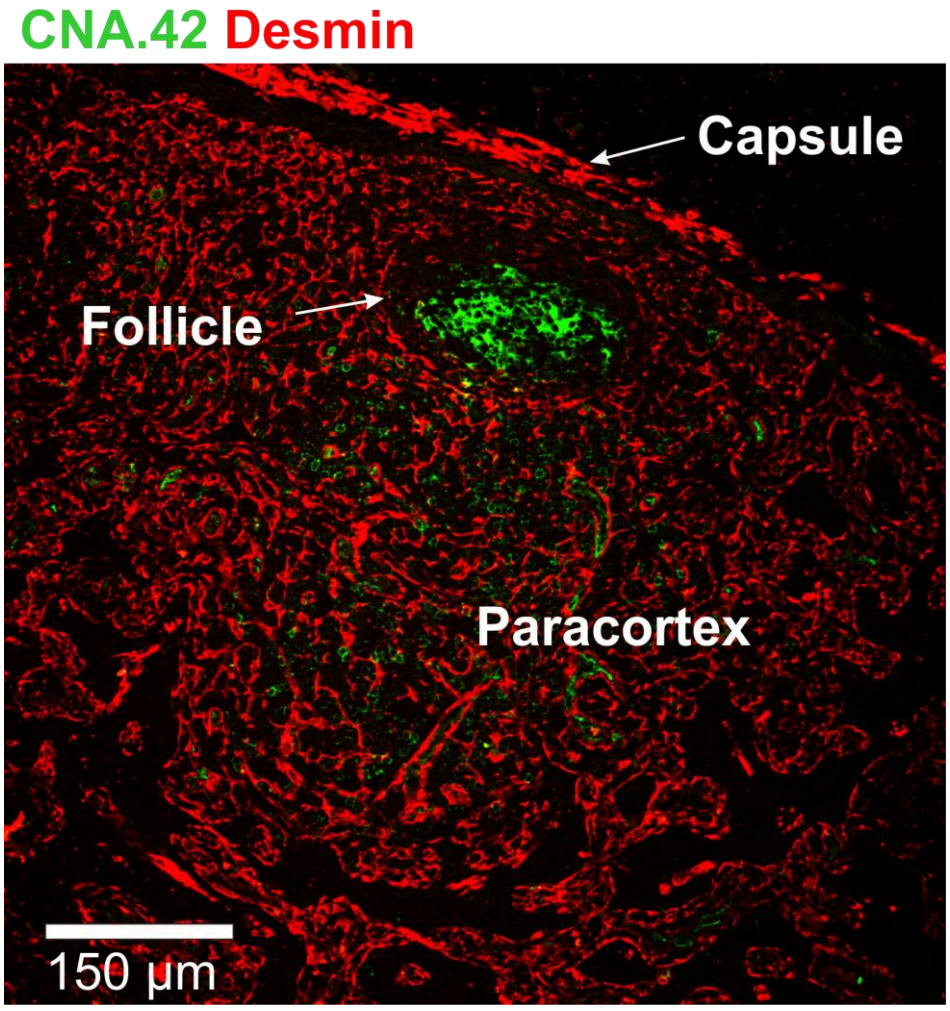

Figure 5-6 Identification of markers for sheep fibroblastic reticular cells (FRC) and follicular dendritic cells (FDC)
Representative confocal micrograph of a sheep lymph node. Section was stained for desmin (red) and CNA.42 (green) to identify fibroblastic reticular cells (FRC) and follicular dendritic cells (FDC) respectively. FRC are not present in the follicles where FDC reside

In the GCs, it is possible to distinguish two major subtypes of follicular dendritic cells (FDC) on the basis of their localization, morphology, and phenotype. FDC localised in the light zone display abundant cytoplasmic extensions with a high level of membrane-bound immune complexes, whereas in the dark zone they display fewer cytoplasmic extensions and present a low capacity to trap immune complexes (Allen & Cyster 2008).

Sheep FDC were found to react positively with the CNA.42 antibody (Figure 5-6), as already described in cattle (Romero-Palomo et al. 2013). The epitope recognized by CNA.42 antibody is a membrane-associated antigen, of 120 kd, resistant to fixation that is expressed on FDC. CNA.42 is commonly used in human diagnostic settings for the histological classification of malignancies of FDC origin (such as follicular dendritic reticulum cell sarcoma and EBV-positive inflammatory pseudotumors) (Raymond et al. 1997; Maeda et al. 2002; Troxell et al. 2005). In sheep, this antigen was also expressed by some mononuclear cells present in the paracortical area of the LN as described for human tissues (Raymond et al. 1997). We identified sheep FDC as cells forming a reticular pattern in the light zone of the germinal centres. Furthermore, FDC in the light zone were positively labelled with an antibody targeting **CD54** (Figure 5-7A). CD54 (also known as intercellular adhesion molecule 1 – ICAM-1) is a transmembrane protein expressed in endothelial cells and leucocytes which is implicated in the process of transmigration of leucocytes across lymphatic vessels (Johnson et al. 2006). Both mouse and human FDC have been described to express CD54 and this is the first report in a ruminant species (Fujiwara et al. 1999; Sukumar et al. 2006). CNA.42 and CD54 co-localise in the same cell population in the follicles present in sheep LNs (Figure 5-7A). Furthermore, to target FDC we tested the well-recognised marker **CD21** (CR2) (Figure 5-7B), which is responsible of the uptake and retention of immune complexes (Roozendaal & Carroll 2007; Herrmann et al. 2003). However, CD21 is expressed in by both FDC and follicular B-cells in sheep lymphoid tissues, similarly to other mammalian species (González et al. 2001; Breugelmans et al. 2011), due to this lack of specificity it was not used as a preferential marked for FDC.

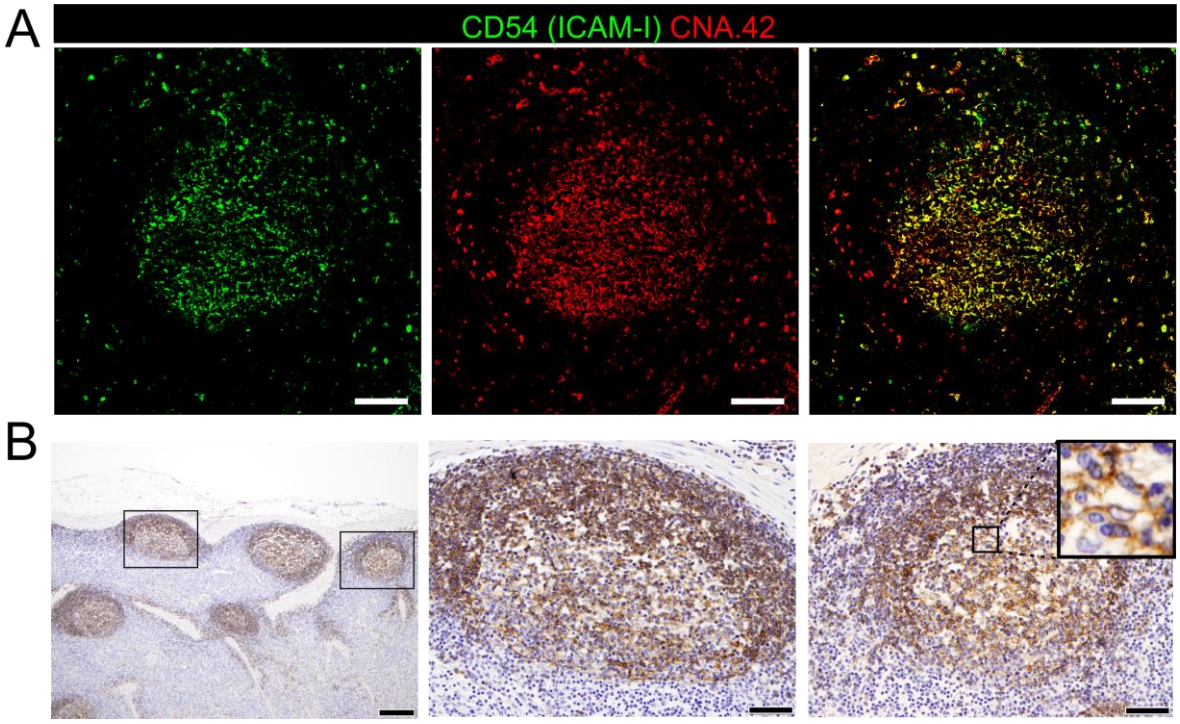

Figure 5-7 Identification of markers for sheep follicular dendritic cells
(A) Representative confocal micrograph of a sheep lymph node (LN). Sections were stained for CD54 (red) and CNA.42 (red). CD54 and CNA.42 are both markers for follicular dendritic cells (FDC) and they co-localise in the light zone of the follicle in the merge channel. Scale bars represent 100 µm. (B) Representative IHC micrographs of sheep LN sections collected from uninfected control animals and fixed in formalin. Sections were stained for CD21 (clone CC21) which is expressed both by FDC and B-cells. Scale bars represent 200 µm (left panel) or 50 µm in the insets.

In dark zone of the follicle we could identify a further population of stromal cells. These cells have been often described in literature, named “dark zone FDC” or “dark zone reticular cells”, but their function remain still obscure (Allen & Cyster 2008; Lefevre et al. 2007; Yoshida et al. 1993). We found that these cells did not express the classical FDC marker CNA.42, but were positive for **CD83** and **S100** (Figure 5-8 and Figure 5-9). CD83 was also expressed on FDC in the light zone but at a slightly lower level, and markers for FDC (such as CNA.42) and dark zone reticular cells (S100 and CD83) were co-expressed in the transition area (Figure 5-8 and Figure 5-9). This may therefore suggest that FDC in the light zone are a more specialised type of reticular cells that differentiate from the ones in the dark zone.

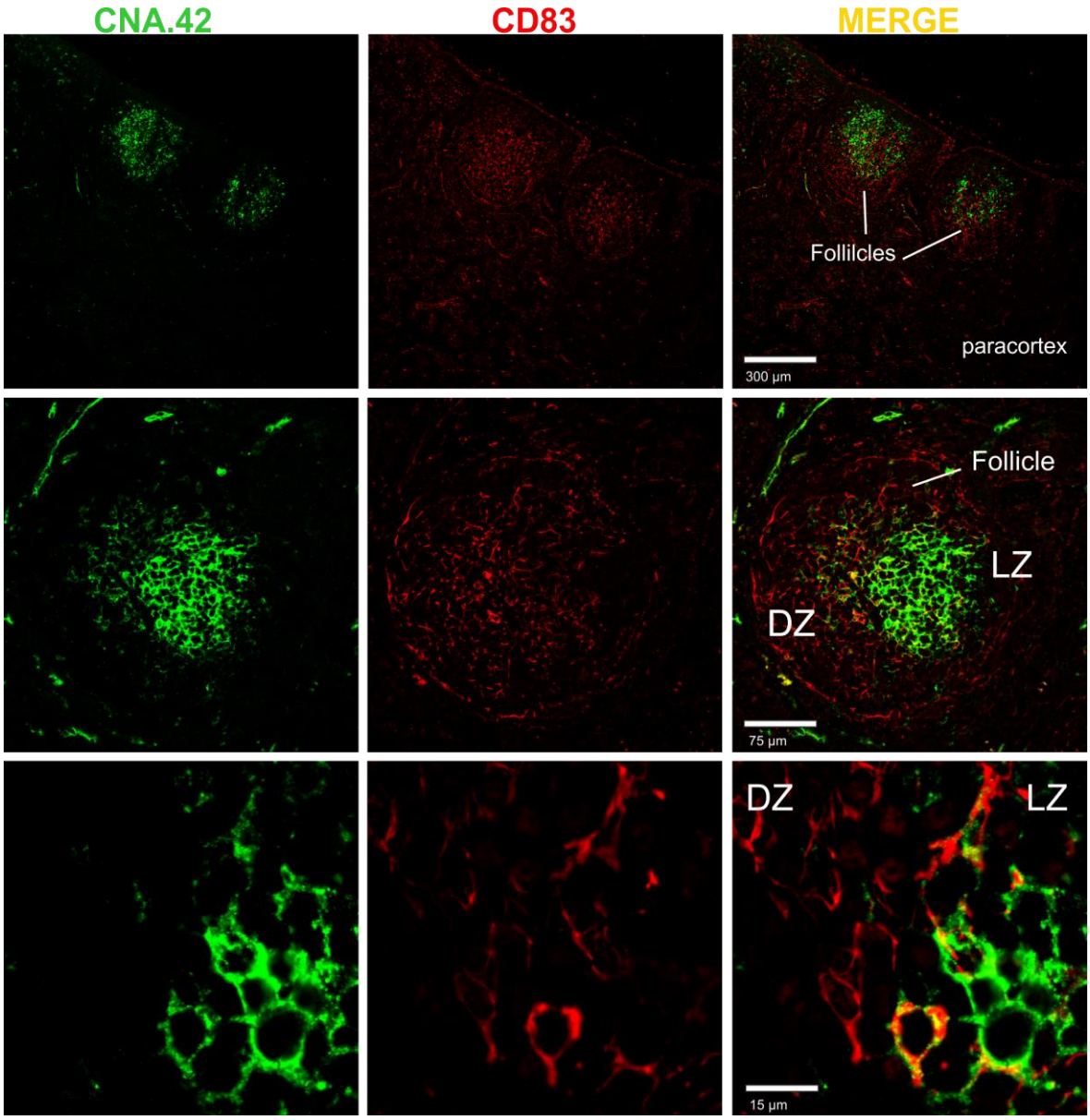

Figure 5-8 CD83 is a marker for dark zone reticular dendritic cells in sheep follicles
Representative confocal micrographs of a sheep LN. Sections were stained for CD83 (red) and CNA.42 (green). CD83 identified dark zone reticular cells present in the follicle. CNA.42 was expressed only by FDC in the light zone of the follicle. This allow to identify a dark (DZ) and a light zone (LZ) in the follicles. Note the co-expression of the two markers in cells present at the border between dark and light zone.

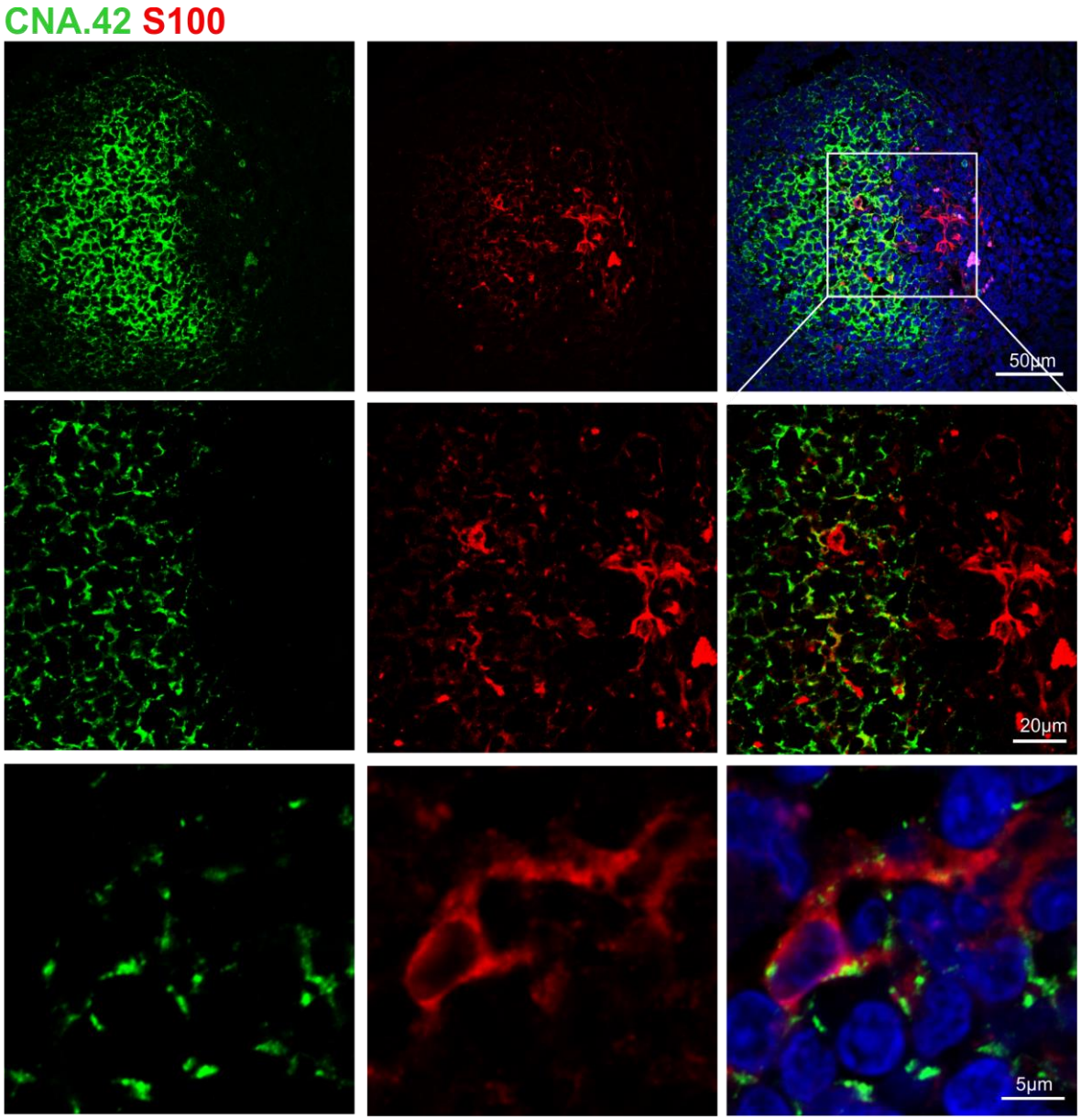

Figure 5-9 S100 is a marker for dark zone reticular cells in sheep lymph node
Representative confocal micrographs of a sheep LN. Sections were stained for CNA.42 (green) and S100 (red). S100 identified dark zone reticular cells present in the follicle. CNA.42 was expressed only by FDC in the light zone of the follicle. Note the overlap of the two markers on the same cells in the transition area between dark and light zone.

Furthermore, just below the SCS, in correspondence with the follicles, we identified an additional population of stromal cells expressing both desmin and CD83 (Figure 5-10); these double positive cells (desmin$^+$ CD83$^+$) were branching from the SCS, in continuity with sinus lining cells, until they reached the follicle area where they contacted FDC. Due to their similarities in the anatomical localization, and their expression of both FDC and FRC markers, these cells could

be identified as MRC recently described in mouse LNs (Katakai et al. 2008; Katakai 2012).

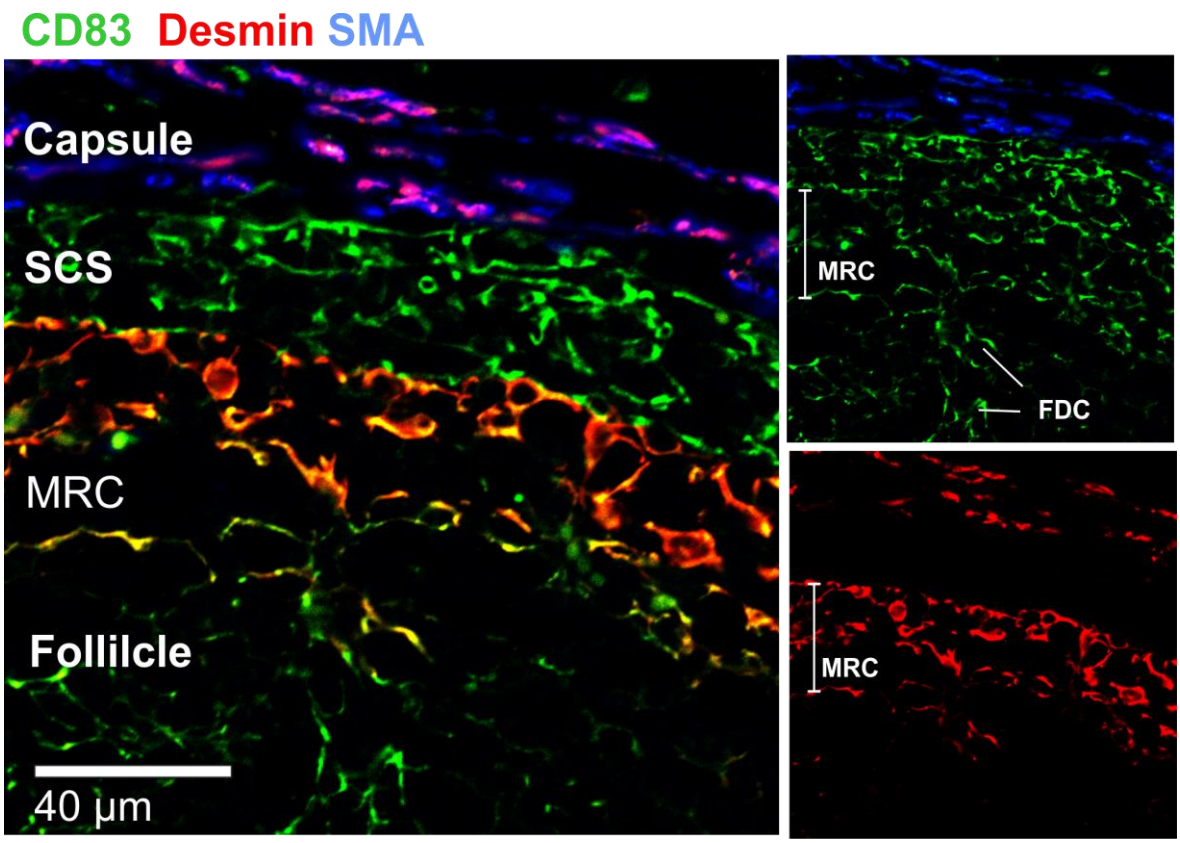

Figure 5-10 Characterization of marginal reticular cells in the sheep lymph node
Representative confocal images of sheep lymph node sections collected from uninfected control animals. Sections were stained for desmin (red), CD83 (green) and smooth muscle actin (blue). Marginal reticular cells (MRC) were identified as cells double positive for desmin and CD83 localised between the subcapsular sinus and the follicles (SCS). Desmin was not expressed by cells present in the SCS or in the follicles. On the contrary CD83 labelled the cells present inside the SCS, MRC and FDC.

Endothelial cells are also part of the stromal cells composing the LNs; both blood and lymphatic capillaries are present in the LN. We could identify blood endothelial cells expressing high level of Von Willebrand factor (VWF) protein (Figure 5-11A) and lymphatic endothelial cells along the SCS, expressing high levels of CD83 and low level of VWF (Figure 5-11A). Plasmalemma Vesicle Associated Protein (PLVAP) (Figure 5-11B) and junction adhesion molecule-A (JAM-A) were also expressed on the endothelial cell lining the sinus wall. In particular, PLVAP returned a delicate staining of a capillary network that from the SCS deepen in the underlying follicles likely identifying the initial part of the conduit system. See Table 5 2 for a summary of the populations characterised.

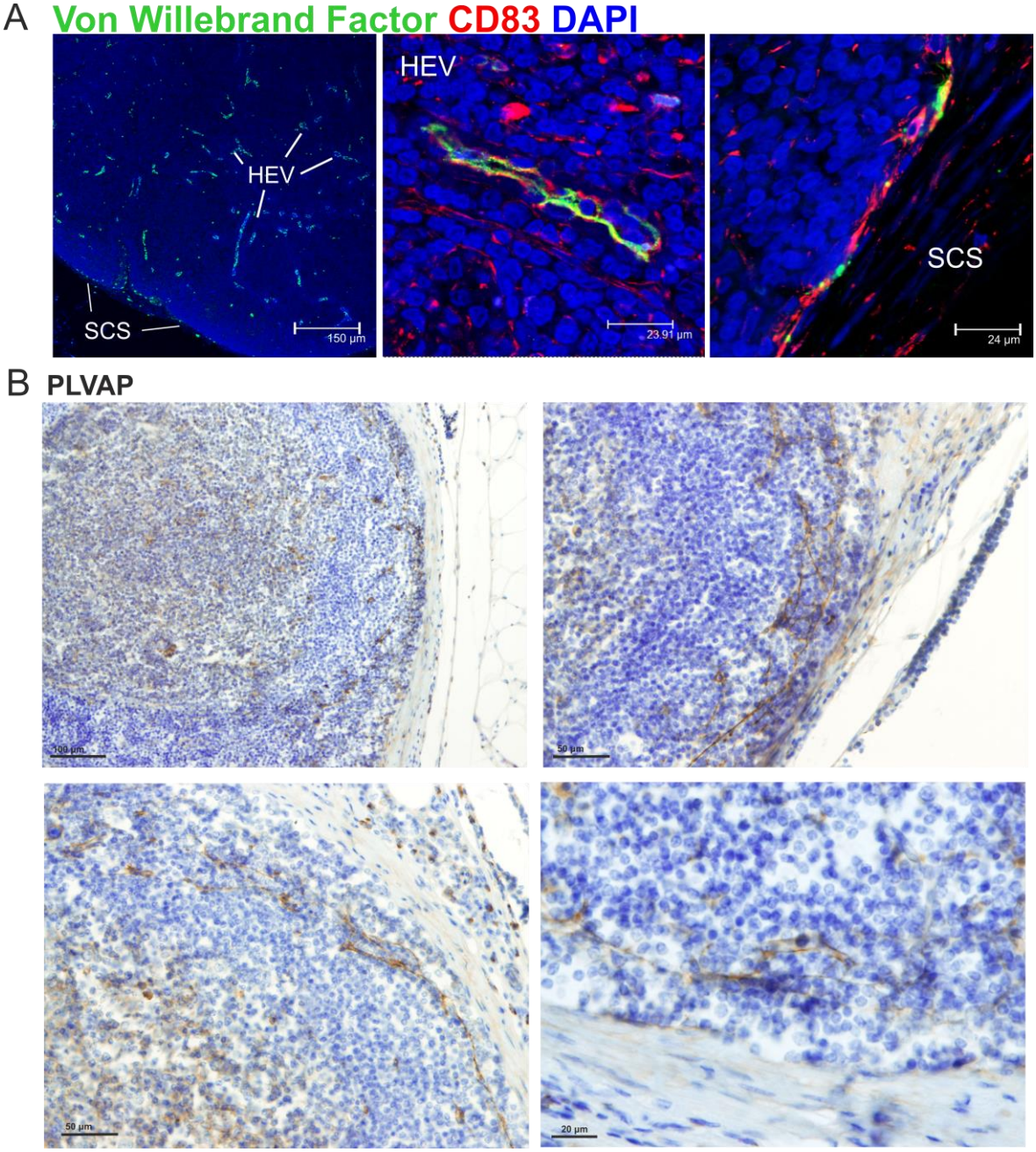

Figure 5-11 Identification of markers for sheep endothelial cells
(A) Representative confocal microscopy images of sheep lymph node showing the expression of Von Willebrand Factor (VWF, green) in the cortical area of the LN. WVF expression identified cells lining high endothelial venules and subcapsular sinus. Note co-expression with CD83. (B) Representative immunohistochemistry micrographs of sheep lymph node (LN) sections collected from uninfected control animals and fixed in formalin. Sections were stained for plasmalemma vesicle associate protein (PLVAP) that identified thin cells lining the subcapsular sinus walls and branching inside the follicles underneath.

Table 5-2 - List of cell populations identified and markers used
VWF (Von Willebrand Factor), SMA (smooth muscle actin), JAM-A (junction adhesion molecule-A). FRC (fibroblastic reticular cells), MRC (marginal reticular cells), FDC (follicular dendritic cells). *Inconsistent results.

Cell type	Markers	Localization	Identification
Lymphocytes	CD3	Largely in the paracortcal area, medullary cords and some in the follicle	T-cells
Lymphocytes	CD8 CD3	Mainly in the paracortcal area and medullary cords	Cytotoxic T-cells
Lymphocytes	WC1 CD3	Mainly in the paracortcal area and medullary cords	γδ T-cells
Lymphocytes	CD79* Pax-5 MHC-II	Follicles	B-cells
Lymphocytes	CD21 Pax-5 MHC-II CD1	Follicles	Follicular B-cells
Lymphocytes	CD335	Rare Scattered cells	Natural Killer
Antigen presenting cells	MHC-II	Expressed at different levels in various areas of the LN	Dendritic cells, Macrophages, B-cells, endothelial cells
Antigen presenting cells	CD208 MHC-II Fascin^{high} CD83 CD1w* CD1	Paracortex	Dendritic cells
Antigen presenting cells	CD163 MHC-II CD208^{int} CD169^{-}	Paracortex, few inside the SCS	Macrophages
Antigen presenting cells	CD169 CD163 MHC-II Fascin^{low}	Along trabecular and medullary sinuses	Macrophages
Antigen presenting cells	CD208 CD163	Follicle (2-4 per follicle)	Tingible body macrophages
Stromal cells	Desmin SMA	Capsule	Capsule
Stromal cells	SMA	Trabecules and around vessels	Trabecules and pericytes
Stromal cells	Desmin	Paracortex	FRC
Stromal cells	Desmin CD83	Between the SCS and the follicle	MRC
Stromal cells	CNA.42 CD21 CD54 CD83 S100	Light zone of the follicle	FDC
Stromal cells	CD83	Dark zone of the follicle	Dark zone reticular cells
Stromal cells	VWF^{high}	Paracortex and hilum	HEV and blood vessels

Stromal cells	CD83 PLVAP JAM-A VWF^{low}	Lining subcapsular sinus, lining trabecular sinuses, enveloping sinus traversing conduits	Sinus lining cells

5.2.2 Identification of sheep cells infected by BTV-8 in lymph nodes draining the sites of virus inoculation

5.2.2.1 BTV infection of subcapsular and trabecular sinuses.

In order to identify which cell populations were targeted by BTV in the LN, we used multicolour confocal microscopy and verified co-expression of BTV NS2 with specific cells markers. In accordance with the IHC data showed previously, BTV was detected in the subcapsular and trabecular sinuses at the early time points after infection (Figure 5-12). The sinuses collect the afferent lymph draining the peripheral tissues and are delimited by a layer of lymphatic endothelial cells (also called sinus lining cells) organised over a base layer of proteoglycan (Girard et al. 2012).

Initially, we defined the borders of the SCS by immunolabeling of perlecan, one of the main components of the basal membrane of the endothelium (Figure 5-13A). Thereafter, we identified in which area of the SCS BTV localised by combining NS2 detection with immunolabeling of different cell populations. Between 4 and 72 hpi the majority of the BTV NS2 signal localised in endothelial-like flat cells (characterised as JAM-A^{+}/CD83^{+}/PLVAP^{+}/Von Willebrand Factor^{low}) lining the SCS delimited by perlecan (Figure 5-13B-C). These endothelium-like cells (sinus lining cells), often extend their processes across the SCS to enwrap intraluminal conduits also called sinus traversing conduits (Rantakari et al. 2015). These structures constitute the initial part of the intricate conduit system branching inside the LN cortex (Figure 5-13C-D) (Roozendaal et al. 2008; Rantakari et al. 2015).

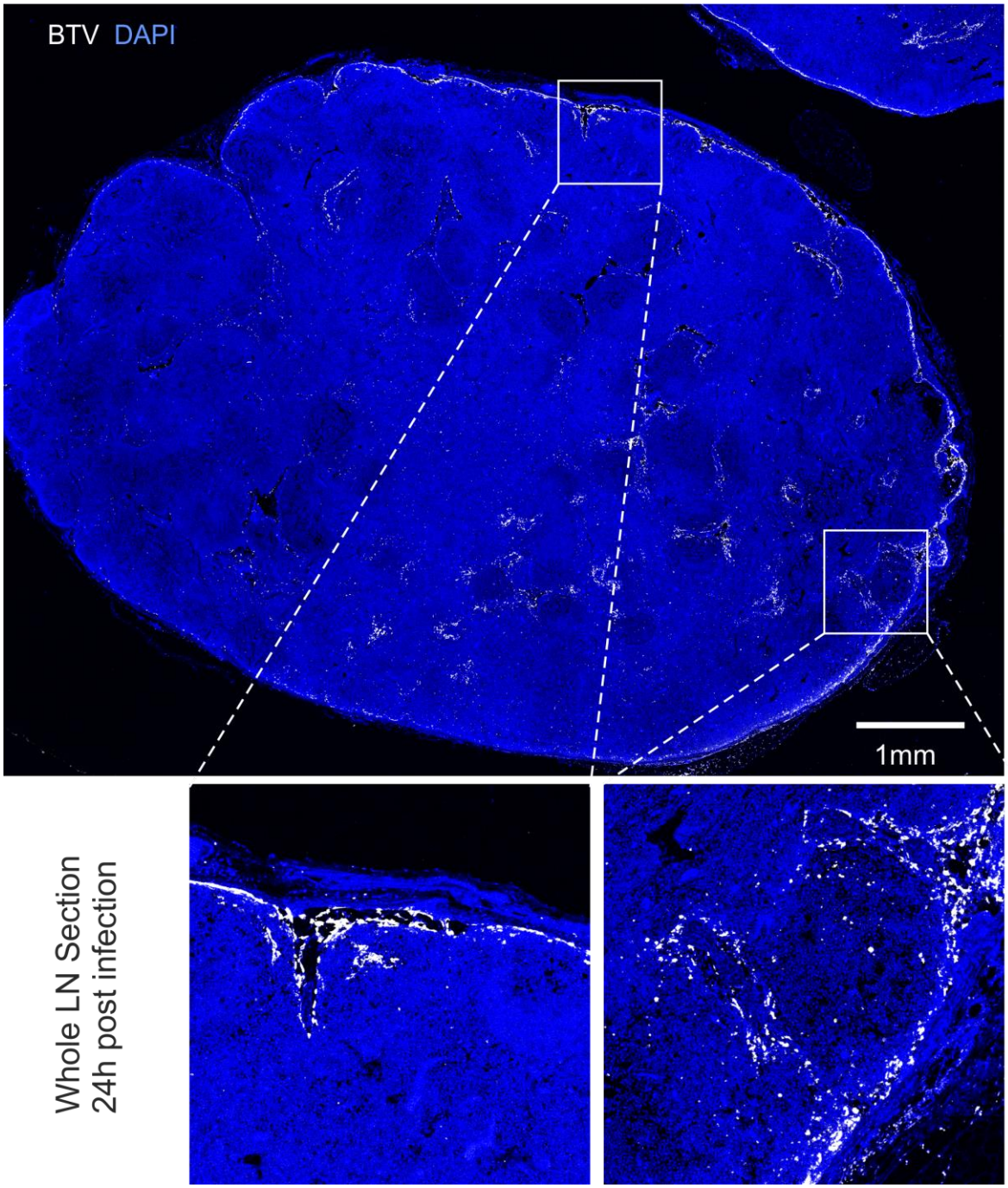

Figure 5-12 BTV infects the subcapsular area of the sheep lymph node
Confocal microscopy (stitched image of confocal tiles) of a whole sheep draining lymph node (LN) section collected from a BTV-8 infected sheep at 24 hours post-infection (hpi). BTV-infected cells are shown in white, while nuclei are stained with DAPI (blue). Note the localization of the virus along the subcapsular area. Insets show and area of the subcapsular sinus and of a follicle at higher magnification.

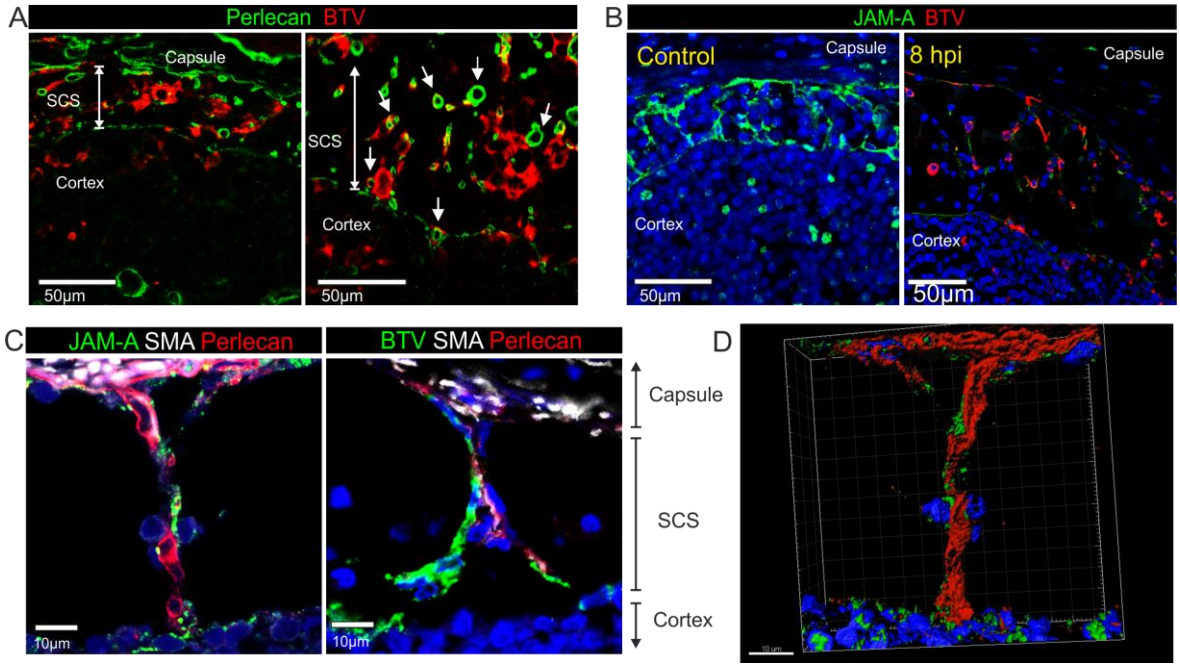

Figure 5-13 BTV infects sinus lining cells in the subcapsular sinus
(A) Confocal micrographs of LN sections stained for BTV NS2 (red). Perlecan (green) identifies the basal membrane of the subcapsular sinus (SCS). Infected cells reside mainly inside the sinus. Arrows indicate transverse section of infected conduits delimited by perlecan. Note that BTV is not detected inside the conduits but only in the surrounding cells. (B) Representative confocal images of the SCS of sheep LN showing expression of JAM-A (green) and BTV (red) in sinus lining cells and along sinus traversing conduits in infected animals (C) Confocal images of LN sections showing expression of JAM-A (green in the left image) or BTV NS2 (green in the right image), SMA (white) and perlecan (red). BTV infects the cells lining the traversing conduits. (D) Tridimensional rendering of confocal stack images highlighting the structure of the a conduit crossing the SCS of sheep LN. Section was stained for perlecan (red), JAM-A (green) and DAPI (blue).

Intermingled with the reticular fibres of the SCS, few $CD163^{+}/CD169^{-}$ macrophages were also infected although these cells did not form a compact layer of macrophages in the SCS as described in mouse (Junt et al. 2007). On the contrary, the resident population of $CD163^{+}/CD169^{+}/MHCII^{+}$ phagocytes present along the trabecular sinuses were infected by BTV until 48 hpi (Figure 5-14A-B). Given the phagocytic capacity of macrophages, to exclude the possibility that the positive signal was resulting from the phagocytosis of cellular debris, we performed a staining for BTV NS4, which localise in the nucleus of BTV infected cells. $CD163^{+}/CD169^{+}/MHCII^{+}$ macrophages localised along the trabecular sinuses were indeed actively infected by BTV as NS4 was detected in the nuclei (Figure 5-14C).

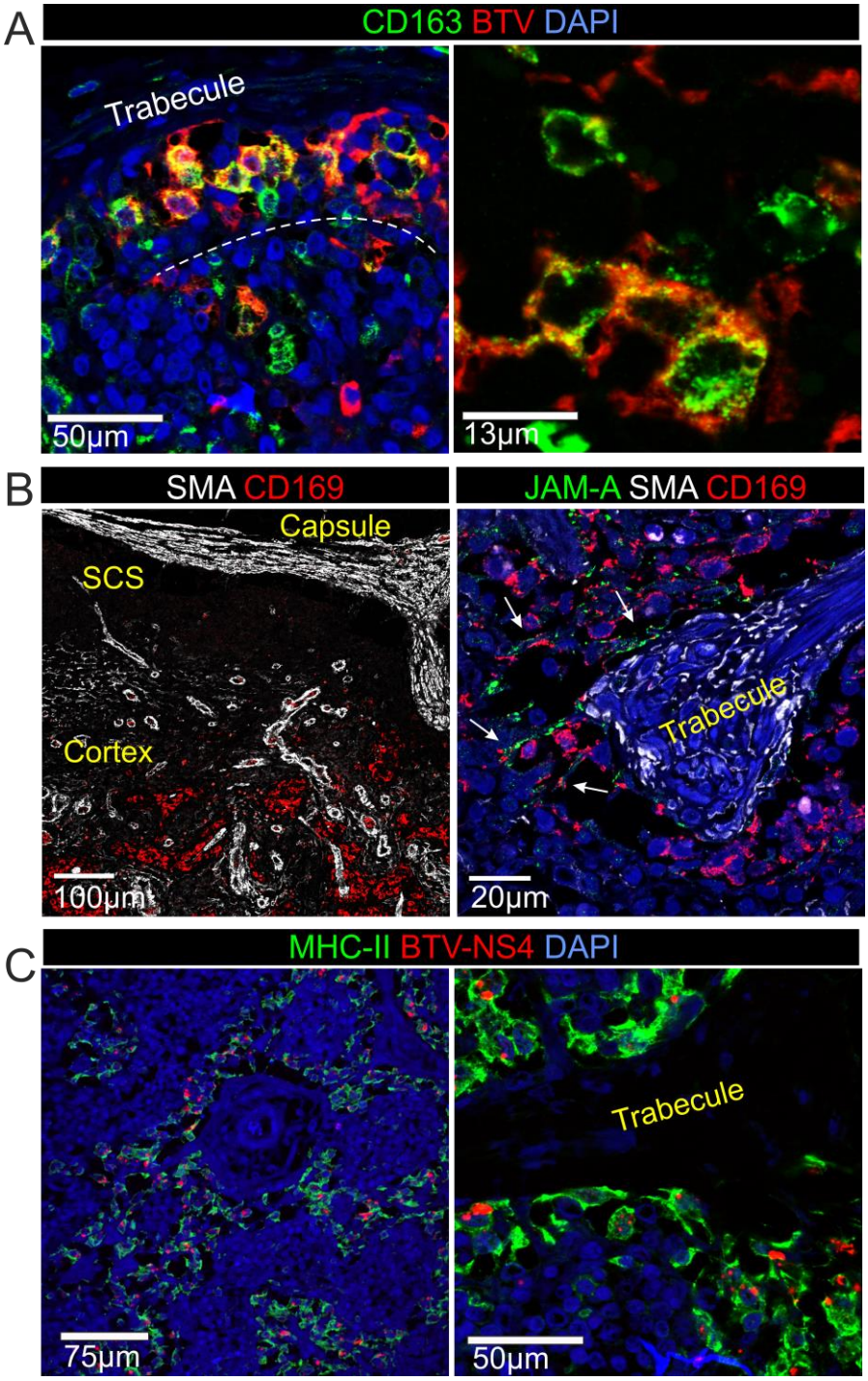

Figure 5-14 BTV infection of macrophages along the trabecular sinuses
(A) Representative confocal micrographs of the trabecular sinuses of BTV infected sheep lymph nodes (LNs). The images show BTV infection of $CD163^+$ macrophages. LN sections were stained for BTV NS2 (red) and CD163 (green). (B) Confocal images of the cortical area of an uninfected sheep LN showing the localization of $CD169^+$ macrophages (red) along trabecular sinuses. LN capsule and trabecular structures are stained with SMA (white). On the right, higher magnification images show the localization of $CD169^+$ macrophages (red) along the trabecules (SMA, white) intermingled with JAM-A^+ endothelial cells (green, arrows). (C) Representative confocal images of the trabecular sinuses of BTV infected sheep stained for MHC-II (green) and BTV-NS4 (red) showing the nuclear expression of BTV NS4 in trabecular macrophages.

5.2.2.2 BTV infects B-cell and get access to the lymph node parenchyma

BTV infectious particles are too large to freely access the LN parenchyma by using the conduit system. Nevertheless, we found infected cells in the follicles of the cortical area very rapidly after inoculation (4-8 hpi). At this early time points, in some of the follicles we could detect B-cells (identified by the expression of the nuclear B-cell-specific activator protein, BSAP) as the only infected cells (Figure 5-15A). However, in other follicles we detected BTV in B-cells as well as in spindle shaped cells (Figure 5-15B), suggesting the existence of a temporal sequence in which B-cells could be infected before the spindle cells. Approximately 70% of the infected B-cells localised in close contact with the SCS or just beneath it (Figure 5-15C), within the half part of the follicle localised in proximity of the capsule. On the other hand, less than 30% of the virus infected B-cells were localised in the portion facing the paracortex (Figure 5-15D). These data strongly indicates that the subcapsular area is the most likely source of infection for B-cell. As previously described in the mouse, B-cells can sample antigens in the subcapsular area and then carry them during their migration towards the centre of the follicle or to the border between the T/B-cells area (Cinamon et al. 2008; Phan et al. 2007).

At 24 hpi, no residual BTV infected B-cells were found in the cortical area. From 24 hpi onwards, only spindle shaped cells appeared infected in the follicles, forming a reticular pattern and remaining BTV-positive until 96 hpi. These results suggest that B-cells are likely to be the first cells to carry the virus inside the LN parenchyma from the SCS.

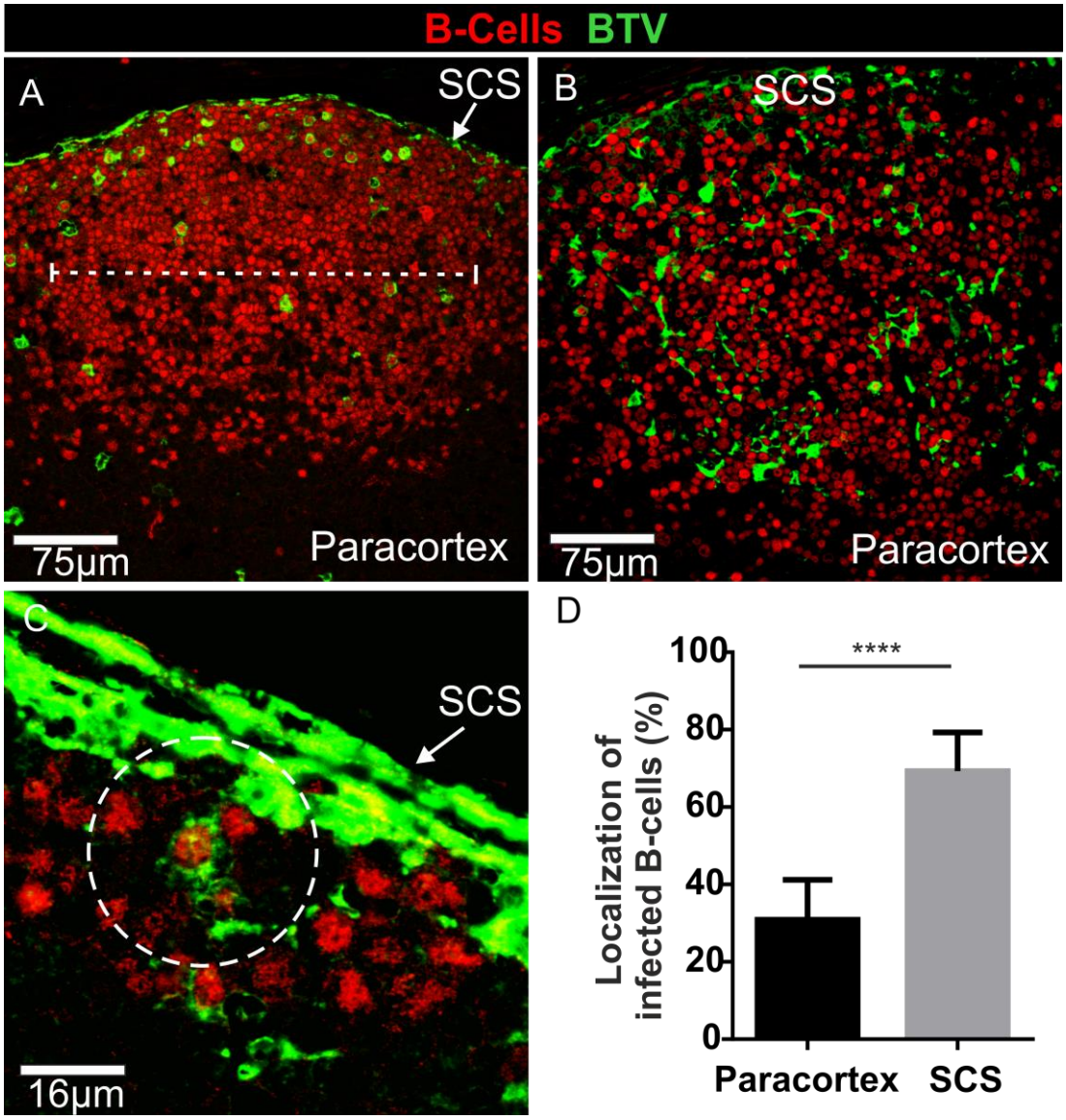

Figure 5-15 BTV infection follicular B-cells
(A-B) Confocal image of LN section collected 8 hpi showing two different patterns of BTV infection in the follicle. In (A) only B-cells are infected with BTV while in (B) BTV NS2 is detectable both in B-cells and in spindle shaped cells. Higher magnification image of the SCS area (C) shows infected B-cells in close contact with the SCS. Sections were stained for B-cells (BSAP, red) and BTV NS2 (green). (D) Localization of BTV-8 infected B-cells in the LN follicles at 8 hpi. Follicles were divided in two equal parts (dashed line), one facing the SCS and one facing the paracortical area. The number of infected B-cells in the two areas was counted in 6 LNs from 3 different animals (**** $P<0.0001$ by Mann-Whitney U-test).

5.2.2.3 BTV infects marginal reticular cells and follicular dendritic cells

The lack of expression of leucocyte markers in many of the infected cells suggested that they were probably not of lymphoid origin. Therefore, in order to characterise the infected cells that confer a reticular pattern to the infection in the follicles, we used three and four colour immunofluorescence and confocal microscopy to stain for sheep stromal cells markers and BTV proteins.

We detected BTV NS2 in correspondence of the stromal cells in the cortex of the LN, composing the B-cell area. Infected cells included MRC, dark zone reticular cells and FDC (Figure 5-16A-D). All of these cells in sheep are positively stained with the CD83 marker, indicating a possible role of this protein during the infection. On the contrary, BTV signal was absent in desmin^{+} cells (FRC) in the paracortical area of the LN; interestingly, these cells do not express the CD83 protein (as show in the previous paragraph). In addition, BTV was not found in endothelial cells composing the HEV or in pericytes, therefore it appears that the only stromal cells BTV-positive during the early stages of infection carry the CD83 marker.

We hypothesise that the temporal progression of the infection in the LNs initially affected the follicles close to the SCS, and then gradually extended to the surrounding areas, to finally deepen inside the cortical area. In support of this, we initially detected infected stromal cells at 4 hpi and at all the successive time points thereafter (until) 96 hpi and we did not detect virus in FRC or HEV or pericytes.

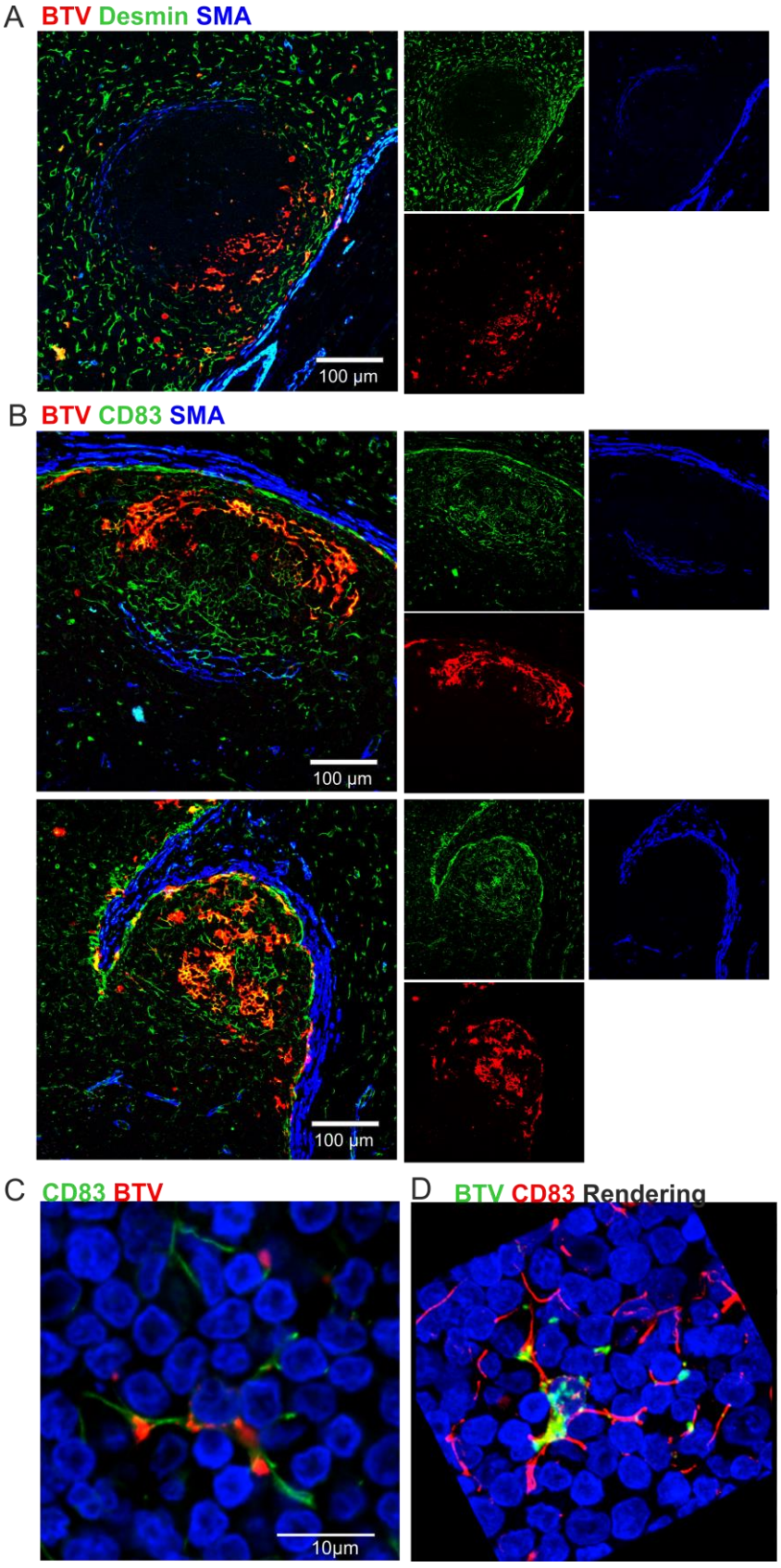

Figure 5-16 BTV infection of marginal reticular cells and follicular dendritic cells
Representative confocal photomicrographs of LN sections collected from BTV-8 infected sheep. (A) BTV NS2 (red) is expressed in MRC (desmin+, green). (B) Representative confocal images of LN sections from BTV-8 infected sheep showing infection of $CD83^{+}$ follicular dendritic cells. Sections were stained for BTV NS2 (red), CD83 (green) and SMA (blue). (C) Higher magnification of a sheep FDC stained with CD83 (green) infected by BTV (red), DAPI (blue). (D) Tridimensional rendering of confocal stack images showing the infection of a FDC. False colour staining CD83 (red) and BTV-NS2 (green), DAPI (blue).

5.2.2.4 T-lymphocytes and dendritic cells are not infected in sheep lymph nodes during BTV-8 infection

Immunofluorescence and immunohistochemistry results showed that the localization of BTV infected cells was specific for clearly defined areas, suggesting a tropism of BTV for selected cells populations. Indeed, during our initial screening, BTV NS2 was rarely found in the paracortex of the lymph node, which is an area delimited by FRCs and mainly populated by T-lymphocytes and DCs. By using immunofluorescence double labelling, we never found BTV in association with $CD3^+$ T-lymphocytes (Figure 5-17A) and only occasionally with dendritic cells, defined as $CD208^+/MHC\text{-}II^+/Fascin^{high}$ cells with dendritic morphology located in the paracortical area of the LN (Figure 5-17B).

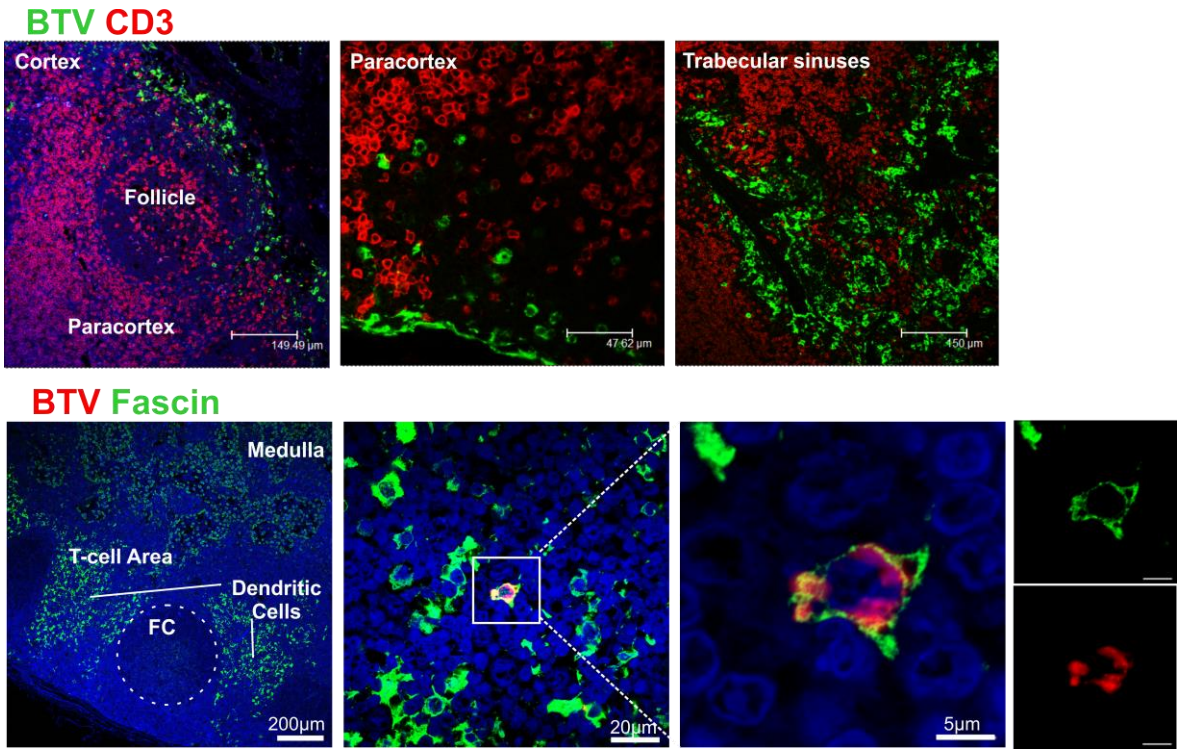

Figure 5-17 Cells in the paracortical area are rarely infected
Representative confocal images of LN sections collected from BTV-8 infected sheep. (A) Sections were stained for BTV (green) and CD3 (red). CD3+ T-lymphocytes were not infected by BTV that rarely localise in the paracortical area. (B) Sections were stained for BTV (red) and fascin (green). $Fascin^+$ dendritic cells (DCs) localise in the paracortical area of the LN, DCs are rarely infected by BTV.

5.2.3 Similar cell tropism of attenuated BTV8$_H$ and wild type BTV-8 in sheep LNs.

We next tested whether the difference in virulence between wild type and attenuated BTV strains can be linked to the tropism of these viruses for specific cell types in the LNs of infected animals. The results described in the previous chapter show that the attenuated BTV8$_H$ infects skin and draining LNs but was not detected in blood and peripheral tissues.

By confocal microscopy, BTV8$_H$ was detected in the same LN cell populations as BTV-8, including sinus lining cells, sinus macrophages and FDC (Figure 5-18). However, in animals infected with BTV8$_H$ only minor areas of the draining LN were infected. Moreover, the attenuated virus appeared to be cleared from the infected LNs earlier than the wild type virus (BTV-8). At 72 hpi only few infected cells were detectable in sections of draining LNs collected from sheep infected with the attenuated BTV8$_H$ (data not shown), whereas BTV-8 was detectable until 96 hpi. These data indicate that the tropism of the attenuated BTV8$_H$ does not differ from the virulent strain (BTV-8), at least for the cells targeted in the LN. Therefore the attenuated phenotype must be linked to other virus-related aspects, such as lower replication efficiency or impaired capacity to escape the host immune responses.

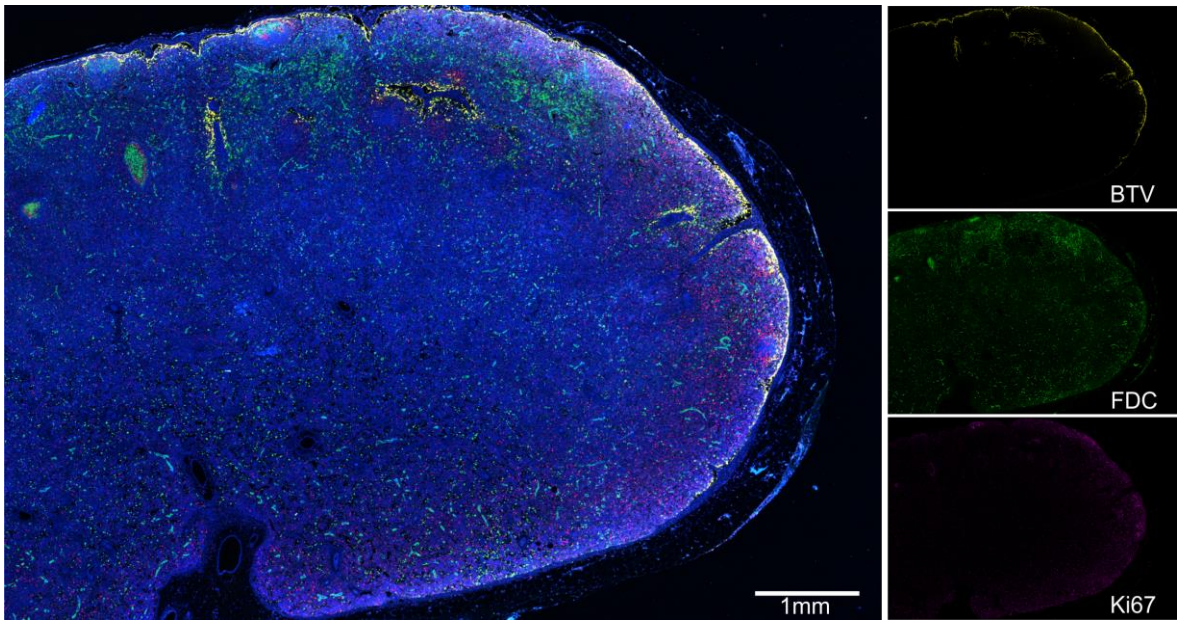

Figure 5-18 BTV8$_H$ present a similar infection pattern in sheep lymph node
Confocal microscopy (stitched image of confocal tiles) of a whole sheep draining lymph node (LN) section collected from a BTV8$_H$ infected sheep at 24 hours post-infection (hpi). BTV-infected cells are shown in yellow, follicular dendritic cells in green (CNA.42), and dividing cells in purple (Ki67), while nuclei are stained with DAPI (blue), Note the localization of the virus along the subcapsular area and in the follicles.

5.2.4 BTV infects dendritic cells in goats lymph nodes

BTV infection in goats usually results in an asymptomatic or mild disease (Spreull 1905; Erasmus 1975; Caporale et al. 2014). Indeed, in the *in vivo* studies associated with this thesis (see Chapter 4), goats experimentally infected with BTV-8 presented only a mild increase in body temperature. Observations made by IHC highlighted a different localization of BTV in goat compared to sheep LNs, with numerous infected cells present in the paracortical area. In infected sheep, BTV was localised mainly in the cortical area of the LNs. We used multicolour confocal microscopy to identify the infected cells in goat LNs. Interestingly we found a similar distribution of the virus in the sinus lining cells, follicular B-cells and sinus macrophages. However, numerous MHC-II$^+$/fascin$^+$ interdigitating DCs were infected by BTV in the paracortical area (Figure 5-19) of goat LNs. BTV-infected DCs were initially observed at 48 hpi and were present until 96 hpi. These findings highlight a major difference in the LN infection between sheep and goat, since at the same time point sheep DC do not appear infected. Moreover, infected goat DCs maintained a high expression of MHC-II (Figure 5-19), contrary to what has been hypothesized for sheep DCs (Hemati et al. 2009).

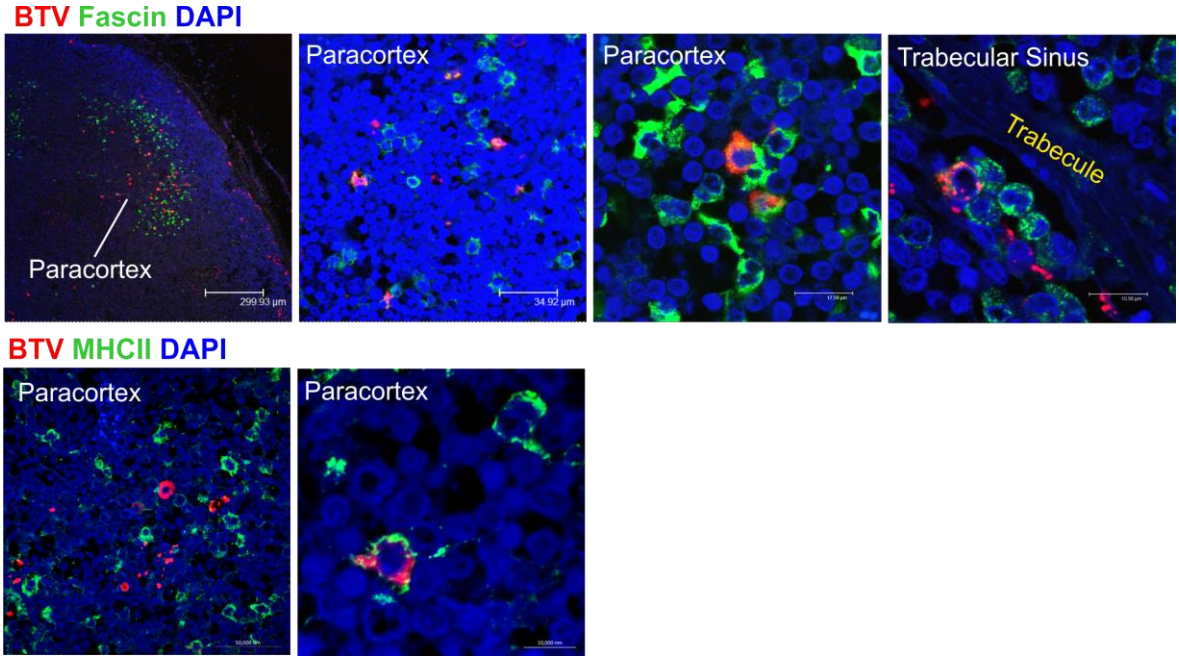

Figure 5-19 BTV infection of dendritic cells in goat lymph nodes.
First row. Representative confocal micrographs of lymph node (LN) sections collected from BTV-8 infected goats at 48 hpi. Images show the infection of dendritic cells localised in the paracortical area of the LN and of macrophages along the trabecular sinus. Sections were stained for fascin (green) and BTV (red). Bottom row. Representative confocal micrographs of LN sections collected from BTV-8 infected goats at 48 hpi. Images show the infection of MHC-II^{+} cells localised in the paracortical area of the LN. Sections were stained for MHC-II (green) and BTV (red).

5.3 Discussion

BTV is one of the major infectious diseases affecting ruminants; however little is known regarding the progression of infection, the different subsets of cells targeted by the virus in the LNs and their role in the distribution of BTV in the tissues of the infected animals.

In this chapter we specifically focused on the LN, which is with the skin one of the early sites of virus replication in BTV infected animals. We described the early arrival of BTV in the LNs and we systematically and sequentially identified the cell populations infected by the virus. In this way we were able to show that after its arrival in the subcapsular and trabecular sinuses, BTV infects a variety of cells and makes his way into the parenchyma of the LN exploiting B-cells and stromal cells interactions.

Before this study, the general understanding was that BTV replicates mainly in endothelial cells and mononuclear phagocytes in the infected host. Our data clearly indicates that other cells types, such as MRC and FDC (lymphoid stromal cells) are infected by BTV in the LN of experimentally infected sheep and goats.

Upon arrival in the SCS, BTV infects the lymphatic endothelial cells lining the sinus walls, as shown by detection of NS2 in these cells during the initial 48-72 hpi. At the same time we identified BTV infection in $CD163^+$ and $CD169^+$ phagocytes present along the trabecular sinuses of the LN. This finding suggests that invasion of the LN by BTV proceeds from the SCS over two parallel fronts: (i) by infecting B-cells in the lymphoid follicles and their stromal network where it persists up to 4 dpi, and (ii) reaching the trabecular sinuses where the virus infects sinus lining cells and macrophages and it is cleared in approximately 48 hours.

This work describes for the first time the arrival of an arbovirus in a LN in an experimental animal different from the mouse, therefore some anatomical differences should be taken into account. In mouse models, lymph borne viruses are uptaken by a layer of $CD169^+$ macrophages localised along the SCS

(Iannacone et al. 2010; Gray & Cyster 2012; Junt et al. 2007), whereas in sheep we failed to identify an homologous population of phagocytes in the same area. $CD169^+$ macrophages are populating sheep trabecular sinuses, which in ruminants are also more prominent than in mouse. Many key functions have been attributed to SCS macrophages, including filtration of lymph borne pathogens to prevent their systemic distribution (Iannacone et al. 2010; Winkelmann et al. 2014) and capture and presentation of antigens for B-cells activation (Carrasco & Batista 2007; Phan et al. 2007; Junt et al. 2007). The disruption of SCS macrophages has been associated with immunosuppression following infection and inflammation (Gaya et al. 2015; Phan et al. 2009). However, although few $CD163^+$ macrophages were detected inside the SCS, the different localization of $CD169^+$ macrophages in sheep raises questions about their function in different animal species. In sheep, $CD169^+$ macrophages are localised so far away from the follicles that their role for B-cell activation could be questioned.

The SCS forms a barrier that prevents the unrestricted passage of lymph borne antigens across the cortical area. Hence, it is interesting to note how, after the infection of the SCS, BTV reaches the FDC that are safely located at the centre of the follicle, indeed FDC have the capacity to present unprocessed antigens on their surface, and this would make them an easy target for immune activated cells. Two mechanisms have been described until now that can account for antigen transport to FDC: (a) small antigens <70kDa (~5nm) get free access to a system of conduits that open in the SCS and branches in both the T- and B-cell areas (Roozendaal et al. 2009; Gretz et al. 1996; Rantakari et al. 2015), while (b) larger antigens are sampled by follicular B-cells from the SCS and shuttled to FDC. Both systems rely on the presence of prior immunity, since only opsonised antigens can be effectively picked up by FDC (Junt et al. 2007; Aguzzi et al. 2014). Our confocal imaging data show that BTV rapidly co-localises with B-cells and FDC in naïve animals, without requirement of pre-existent antibodies or cognate B-cells. Hence a different mechanism of interaction must be involved, such as the presence of pre-existing natural antibodies recognising the virus, a complement-related opsonisation, or a direct receptor-virus interaction. BTV infectious particles are too large (~74 nm) (Prasad et al. 1992) to directly access the conduits. However we identified numerous infected cells (sinus lining and MRC) forming the walls of the conduits leading to the follicles. It is therefore

possible that the virus spreads also by contiguity along these cells until reaching the FDC. Alternatively, motile infected B-cells could contribute to the virus spread by carrying it towards the centre of the follicles during their migrations and scanning for antigens, as this is supported by the finding that BTV-8 infected B-cells were identified underneath the SCS before FDC infection occurred.

This is the first report of BTV infection of B-cells since previously the virus was identified *in vivo* only in endothelial cells and mononuclear phagocytes; their contribution, emphasized by our results, could be key in favouring virus spread in the LN. Interestingly, infected B-cells were observed only during the initial 24 hpi, suggesting that after this point they lose susceptibility to infection. Previous *in vitro* experiments failed to infect bovine B-cells with BTV (Barratt-Boyes et al. 1992) but studies of ovine B-cells have not been carried out. It is possible that a particular activation stage could be implicated in B-cells susceptibility to infection observed *in vivo*, similarly to what has been described for T-lymphocytes (Barratt-Boyes et al. 1992). The destruction of the FDC network, and the resulting shut down of the germinal centre, could be implicated in altering the B-cells phenotype and their maturation stage. Indeed we observed a visible decrease in the number of CD21 expressing cells (mature B-cells) in the marginal zone of the follicles in the infected lymph node at late time points (72-120 hpi). It would be therefore interesting to explore further this aspect of infection and its possible implication in the pathogenesis of disease.

Our data also indicate that BTV infects the stromal cells located in the B-cell area of the LN. These cells contribute to the formation of the germinal centres by providing a supporting scaffolding, driving B-cells homing (through production of CXCL13) and activation, by secreting factor such as BAFF (B-cells activating factor) and IL-6. MRC have been recently identified as precursors of LN FDC in mouse (Jarjour et al. 2014), hence it is possible that the damage produced by BTV (namely a cytopathic virus) to FDC and their precursor could negatively affect the germinal centres function, at least temporarily, inducing a certain degree of immunosuppression.

Moreover, we labelled (i) sinus lining cells, (ii) MRC and (iii) FDC with the same marker (CD83), and all these populations are targeted by BTV infection, whereas stromal cells of the T-cell area that do not express CD83, or pericytes

surrounding the HEV did not show markers of BTV replication. Interestingly the expression of CD83 changed upon infection. CD83 accomplishes numerous regulatory functions in the immune system and is implicated in B- and T-cell maturation and activation (Breloer & Fleischer 2008). The down regulation of CD83 on DCs has been described during herpes virus infections such as the one caused by varicella zoster virus (Morrow et al. 2003), human cytomegalovirus (Senechal 2004) and herpes simplex virus type 1 (Kummer et al. 2007). This process resulted in inhibition of T-cell proliferation and thus in a reduced immune response of the host (Kruse et al. 2000). Whether CD83 down regulation in specific subset of infected cells could have a major impact in the pathogenesis of BT remains still to be determined.

Migratory DCs, present in the lymph draining the BTV inoculation site, have been described to be infected in sheep (Hemati et al. 2009). However, in our experimental model, we were unable to detect infected DCs in sheep LN. On the contrary, confocal imaging data, indicated the presence of numerous DCs infected with BTV in goat LNs, demonstrating that the lack of detection was not due to a technical problem or marker downregulation. In goats, these cells did not localise in direct contact with the subcapsular or the follicular area, hence it is not clear how they get infected. In mouse, different types of DCs subpopulations have been described (Henri et al. 2001; Guilliams et al. 2010), but a similar detailed classification is not available for ruminants DCs. In the mouse LN, the paracortical area is populated by a resident population of DCs sampling antigens arriving inside the conduit system, as well as by various populations of migratory DCs that transport antigens collected from the peripheral tissues (such as the skin). Hence, there are at least two different ways in which DCs could have been infected by BTV in goats. A different effect of BTV on sheep and goat DCs could be responsible for different pattern of infection. For example, sheep migratory DCs could lose the ability to reach the paracortical area of the LN due to a down regulation of CCR7 receptor upon infection or due to a lack of homing signals produced in the LN. Alternatively, BTV could induce a more severe and rapid apoptosis of sheep DCs during their migration in the lymph, before when they reach the LN.

In addition to the data discussed above, in this chapter we have characterised previously unknown markers for the identification of different populations of sheep lymphoid stromal cells (FRC, MRC, dark zone reticular cells and sinus lining cells), and different subsets of macrophages and DCs. It was ot possible to use more conventional markers for sheep DCs in this work (such as CD1 and CD11c) as we could use, for practical reasons, only fixed tissues. However, the identification of new DCs and macrophage markers, capable to be employed on formalin fixed tissues, will be extremely useful in many diagnostic and research setting. The markers identified could open the door to new functional studies on APCs of ruminants and the host response to pathogens.

Chapter 6

Results

6 Characterisation of the humoral immune response against BTV

6.1 Introduction

The current knowledge of the host immune response following initial BTV infection is limited. As is the case with most viral infections, ruminants infected with BTV develop a variety of antiviral immune responses; these include innate and BTV-specific adaptive responses. Although both humoral and cell-mediated immunity contribute to control viral infections, passive transfer studies have demonstrated that antibodies, unlike cytotoxic T-cells (Jeggo, Wardley & Brownlie 1984), can confer full protection to BTV and prevent viremia in newly infected sheep (Jeggo, Wardley & Taylor 1984). BTV infection results in the prompt production of antibodies to both structural and non-structural viral proteins. BTV-specific neutralising antibodies can confer long-lasting resistance to reinfection with the homologous BTV serotype, which form the basis of vaccination strategies to prevent BT disease (MacLachlan et al. 2014). Neutralising epitopes for BTV are localised on the outer capsid proteins VP2 and possibly VP5, which are the main determinants of the BTV serotype (Mertens et al. 1989; DeMaula et al. 2000; Shaw et al. 2013; Roy et al. 1990). On the contrary, complement fixation function is generally attributed to the VP7 protein, which is well conserved across different serotypes (Huismans & Erasmus 1981), and is able to provide a partial cross-serotype protection (Wade-Evans et al. 1996; Stewart et al. 2012).

During BTV experimental infections, we and others have observed that a rapid onset of the antibody response in the ruminant host generally correlates with a more favourable clinical outcome (Caporale et al. 2014; Pages et al. 2014; Ratinier et al. 2016). Similar observations have been made for other arboviral infections including those caused by West Nile virus (Diamond et al. 2003), Japanese encephalitis virus (Burke et al. 1985; Libraty et al. 2002) and Crimean-Congo haemorrhagic fever virus (Shepherd et al. 1989), however the underlining mechanism accounting for the delayed onset of antibodies is still unknown. Hence, we hypothesize that the early events of arbovirus infection can influence the development of humoral immunity and play a key role in disease pathogenesis and its clinical outcome.

In the previous chapter, we have shown that in sheep and goats a large proportion of BTV infected cells is localised in the cortical area of the draining LNs, just few hours after experimental BTV inoculation into the skin. The cortical area of the LN is where most of the B-cells reside, organised in clusters denominated B-cells follicles. Our results indicate that BTV specifically infects FDC in the follicles until 96 hpi. Follicular dendritic cells are specialised stromal cells critical for the formation of the follicles, since they can attract B-cells and retain antigens in the form of immune complexes for long period of times for presentation to B-cells. Antigen presentation leads to the activation of B-cells and the initiation of the GC reaction (De Silva & Klein 2015). After contacting the antigen, B-cells undergo a proliferative burst in the dark zone of the GC. Proliferating B-cells, called centroblasts, mutate their B-cells receptors (BCR) to increase their affinity for the antigen through point mutations in the immunoglobulin V region gene; this process is called somatic hypermutation. GCs are also the site of class switch recombination, in which the immunoglobulin H constant region is replaced to generate a different antibody isotype. Then, through a stringent selective process, B-cells carrying advantageous mutations are selected to differentiate into antibody producing plasma cells or long-lived memory cells, both of which eventually leave the LN and accumulate in the bone marrow (Vinuesa et al. 2010). This process of affinity maturation drives the production of antibodies with increased affinity for a cognate antigen, ultimately improving the efficiency of the humoral immune response.

In this chapter we aimed to investigate the consequences of BTV infection on lymphoid follicles structure, cellular composition and functions. We observed a rapid depletion of FDC associated with the loss of organization of the B-cell follicles and a simultaneous shut down of centroblast division. We hypothesised that this could interfere with the development of a successful antibody response therefore we characterised the antibody response to BTV using virulent and attenuated strains. Our data indicate that the magnitude of the cytopathic insult induced by BTV on the germinal centres (GCs) varies with the virulence of the strain employed and that this in turn impairs the humoral immune response against the virus. Furthermore, the damage produced by BTV to the GCs results in a compromised capacity of B-cells to respond to subsequent antigenic challenges during a defined period of time.

6.2 Results

6.2.1 BTV disrupts the follicular dendritic cell network

We have shown in the previous chapter that BTV-8 infects FDC ad MRC. Given the central role of FDC in the formation of the GC we investigated the consequences of the infection of these cells by BTV. By using different markers for FDC in sheep LN sections, we observed that the reticular network of cells present in the follicles of infected sheep assumed an increasingly time-dependent disrupted appearance both in the light (Figure 6-1A) and in the dark zone (Figure 6-1B). By 72 hpi the presence of FDC was visibly reduced across the whole LN. As expected, FDC staining in mock-infected controls at the corresponding time-points showed FDC in most of their LN follicles (Figure 6-1A-B).

In order to assess if the lack of FDC could be attributed to the virus cytopathic effect, we assessed the presence of activated caspase 3 as a marker of apoptosis. The immunohistochemical staining of infected sheep LNs revealed the presence of numerous apoptotic cells localised in the subcapsular and trabecular sinuses and inside the follicles between 8 and 24 hpi (Figure 6-2). On the contrary, activated caspase 3 was only minimally expressed in LNs of sheep infected with UV inactivated BTV8 or in mock-infected controls (Figure 6-2). These data suggest that apoptosis in the LNs of BTV-8 infected sheep is the consequence of virus replication (Figure 6-2) and could contribute to the observed FDC depletion.

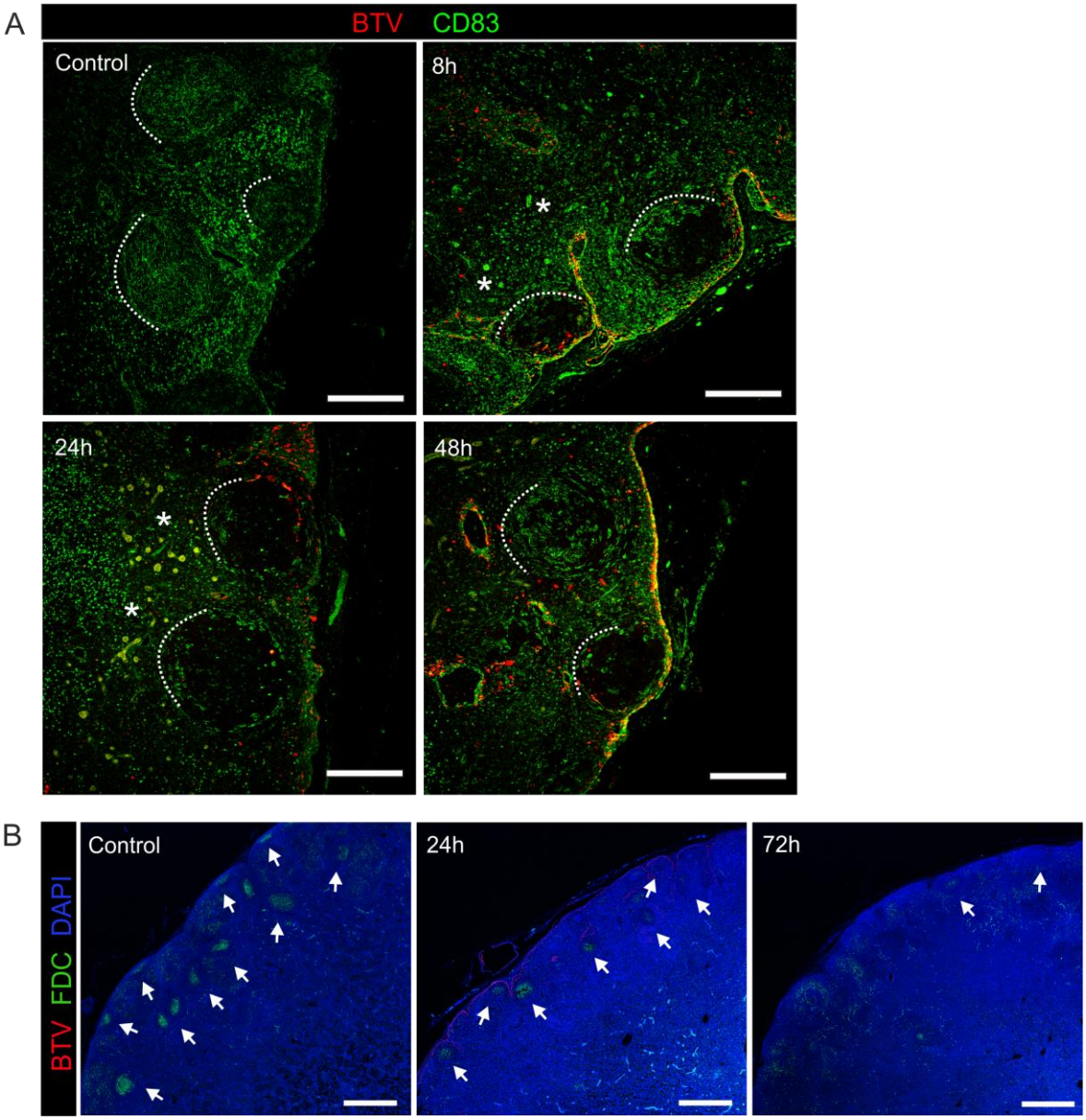

Figure 6-1 BTV induces the disruption of follicular dendritic cells in the light and in the dark zone of the follicles

(A) Confocal images of LN sections from BTV-8 infected sheep, at the indicated time post-infection (h), showing the progressive disruption of the $CD83^{+}$ reticular cell network normally present in uninfected follicles. Sections are stained for BTV NS2 (red) and CD83 (green). Dashed lines help to identify follicles. (*) Indicate the cortical area were HEVs contain autofluorescent red blood cells. Scale bars represent 300µm. (B) Confocal tile scan images of LN sections collected from BTV8 infected sheep showing the presence of FDC in the cortical area at different time points after infection. Sections were stained for BTV NS2 (red), CNA.42 (FDC, green) and DAPI (blue). Arrows indicate recognisable follicles. Scale bars represent 1mm.

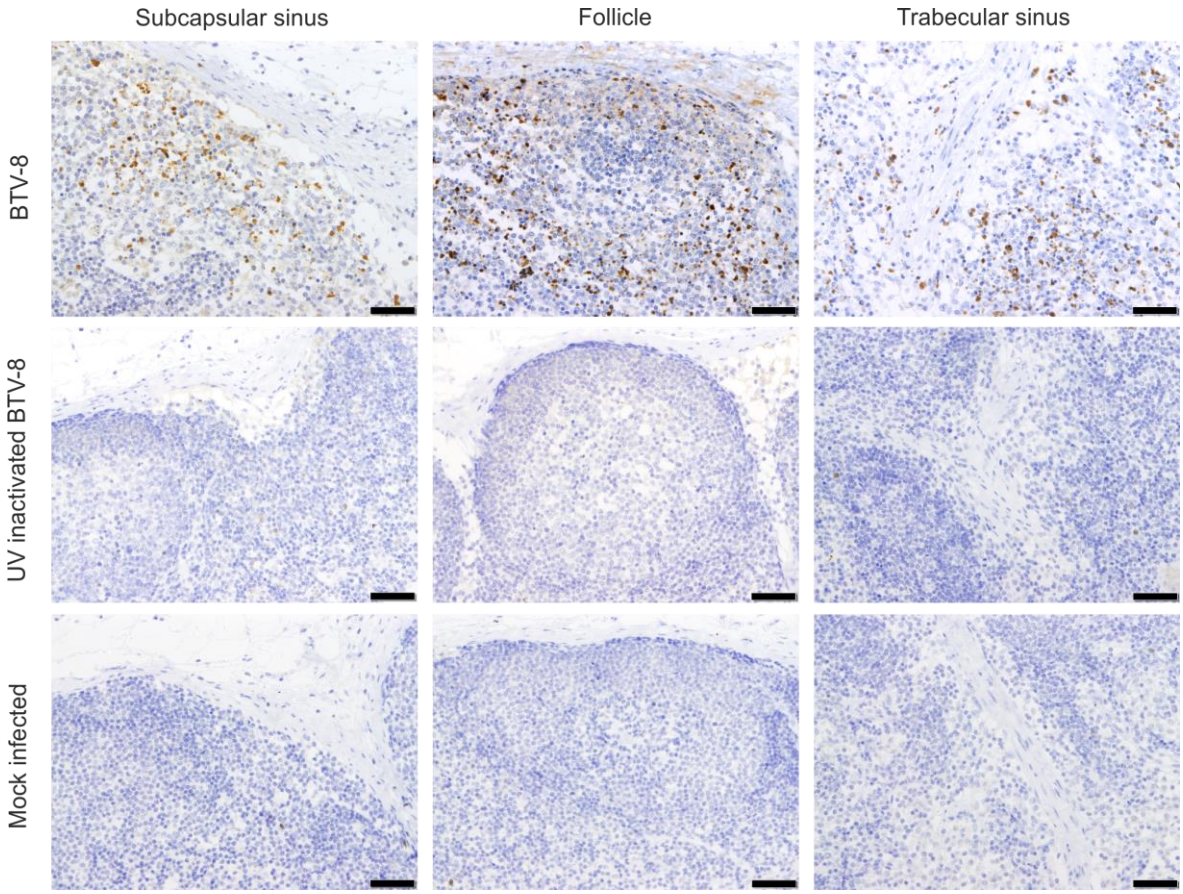

Figure 6-2 Induction of apoptosis in the cortical area of BTV8 infected lymph nodes. Representative micrographs of immunohistochemical detection of activated caspase-3 (brown) at 24 hours post infection in lymph node sections from sheep infected with BTV-8, UV-inactivated BTV8 or mock-infected controls. Micrographs representative of different areas are shown. Scale bars represent 50 µm.

6.2.2 BTV infection hampers centroblasts division

These results indicate that FDC in the LNs of infected sheep are destroyed by BTV-8 rapidly after intradermal inoculation. Considering that FDC are necessary for the recruitment of B-cells into follicles and the development of GCs (Wang et al. 2011) we proceeded to investigate if the disruption of the FDCs was associated to detectable changes in the organization of the GCs (Victora & Nussenzweig 2012).

Initially we assessed the localization of B-cells in the cortical area of the LN, where the follicles are located. Despite the relative lack of FDC in BTV-infected draining LNs, we were still able to identify B-cells clustering into follicular structures, throughout the duration of the experiment (4h to 7 dpi). However, follicles of BTV-8 infected animals presented a less compact structure, with numerous scattered B-cells, compared to mock-infected controls (Figure 6-3).

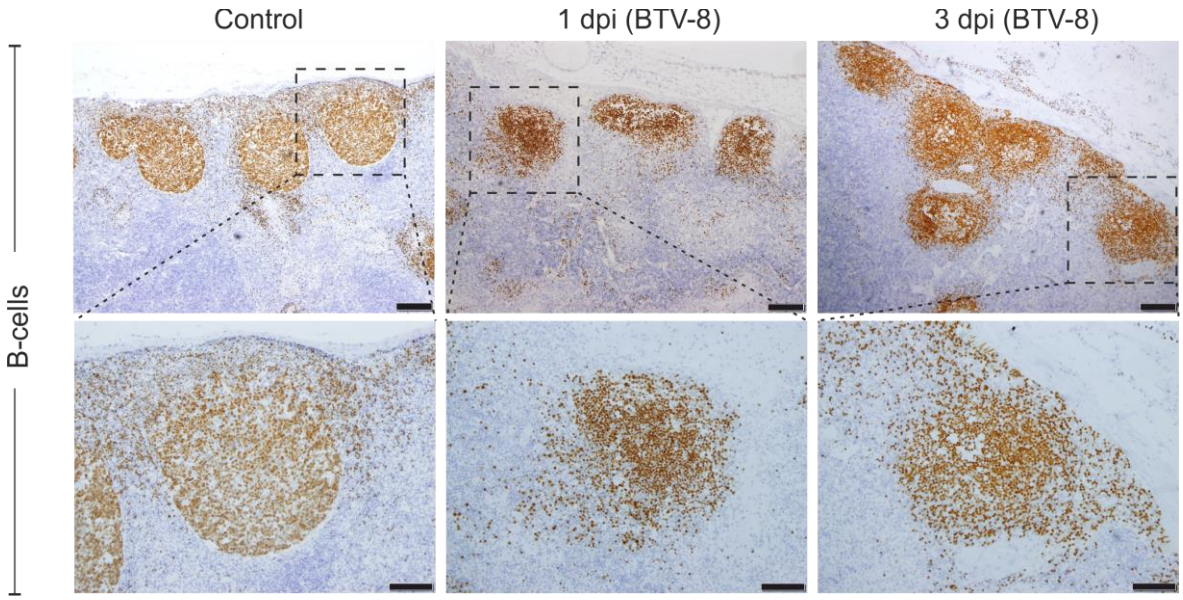

Figure 6-3 Follicular dendritic cells infection alters B-cell localization
Representative immunohistochemistry micrographs of LN sections collected from uninfected controls and BTV-infected sheep at 1 and 3 dpi. Higher magnification micrographs of individual follicles are shown in the bottom row. B-cells are stained with BSAP (brown). Scale bars represent 200 µm (top row) or 100 µm (bottom row).

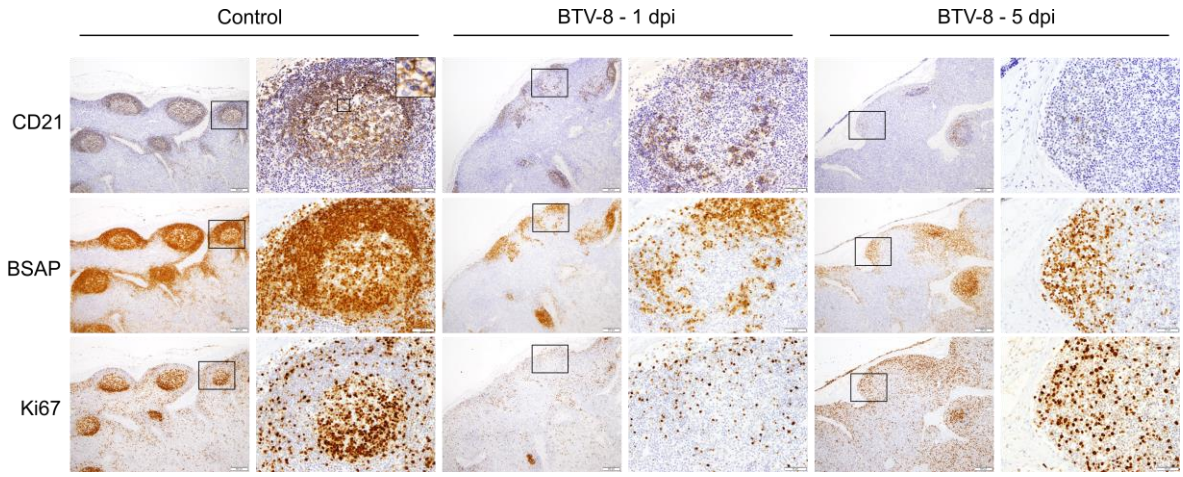

Figure 6-4 Shut down of centroblasts division is accompanied by rarefaction of B-cells
Representative immunohistochemistry micrographs of LN sections collected from uninfected controls and BTV-infected sheep at 1 and 5 dpi. Sequential sections were stained BSAP (B-cell), CD21 (B-cells and FDC) and Ki67^{+} (dividing cells). Higher magnification micrographs of individual follicles are shown on the right column for each group.

Secondly, we determined the existence of active GCs by assessing the presence of centroblasts (active B-cell) in the dark zone of the follicles, identified by the expression of the proliferation marker $Ki67^{+}$. It is important to consider that sheep included in these studies were sourced from local farms and were therefore exposed to natural environmental factors; hence we could detect the presence of numerous GCs in their LNs.

Notably, we observed a shutdown of the division of B-cells in the follicles of draining LN collected from BTV-8 infected animals already at 4-8 hpi, the lack of $Ki67^{+}$ follicles was accompanied by the rarefaction of B-cells and the down expression of the CD21 marker (Figure 6-4). This phenotype was maintained at later time points in infected sheep, while in mock infected animals it was possible to identify numerous GCs with dividing B-cells throughout the duration of the experiment (Figure 6-4). At 4 hpi in experimentally infected sheep, follicles localised near the SCS presented virus infected FDC and displayed few dividing B-cells (Figure 6-5A-i and ii). On the contrary, at the same time point, follicles localised deeper in the cortex and not in direct contact with the SCS, did not show positive staining for the virus and preserved a normal structure, with FDC in the light zone and centroblasts in division in the dark zone (Figure 6-5A-iii).

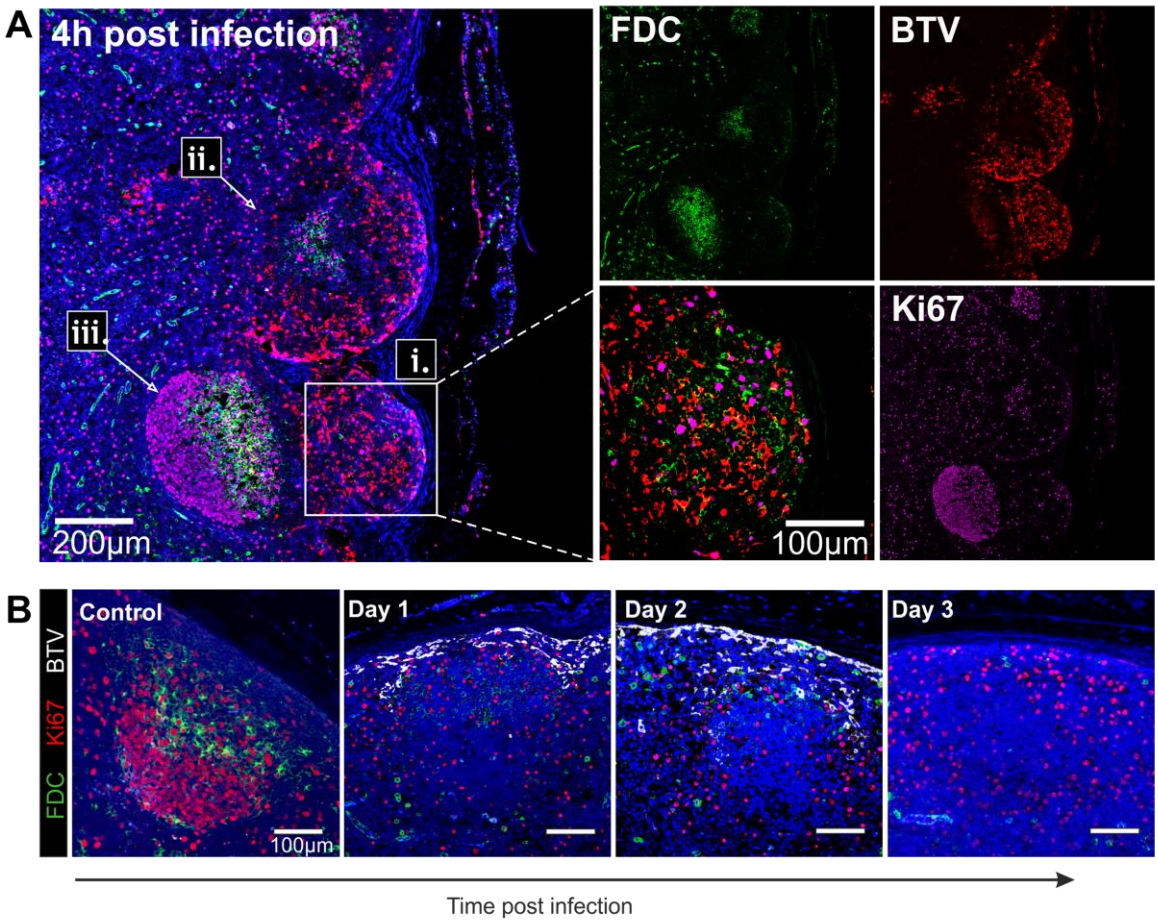

Figure 6-5 BTV infection of the follicles halts centroblasts division
(A) Representative confocal images of LN sections collected from BTV infected sheep at 4 hpi showing the progression of virus replication in the cortical area. BTV NS2 (red), CNA.42 (green) and Ki67 (purple) staining are shown. Nuclei are stained with DAPI (blue). Note the presence of (i) an infected follicle with few Ki67^{+} cells (inset and higher magnification), (ii) a partially infected follicle showing disruption of the FDC network and (iii) an uninfected follicle. Scale bars represent 200µm. (B) Representative confocal micrographs of LN sections collected from BTV-infected sheep at different time points after infection showing the arrest of centroblast division in infected follicles up to 3 dpi. Sections were stained for BTV NS2 (white), CNA.42 (green) and Ki67 (red). Nuclei are stained with DAPI (blue). Scale bars represent 100µm.

In order to determine whether there was a correlation between virus infection and block of B-cells division, we assessed the presence of Ki67^{+} B-cells in infected and uninfected follicles (Figure 6-5B). This was quantified using sequential sections of LNs taken from infected animals, considering that in the same LN section we observed both BTV infected and uninfected areas, due to the progression of the infection. The percentage of BTV-8 infected follicles containing clusters of dividing B-cells was ~50% at 4 hpi, this percentage decreased rapidly to 12.5% at 8 hpi and settled to 4-8% between 1 and 3 dpi. On

the contrary, in follicles where BTV-8 was not detectable, we observed that on average 48.6% of follicles contained clusters of dividing B-cells up to 48 hpi that decreased to 41.9% at 72 hpi (Figure 6-6). At later time points, as the virus began to be cleared from the LN, very few follicles presented BTV infected cells and therefore we could not carry out an accurate comparison between infected and uninfected follicles.

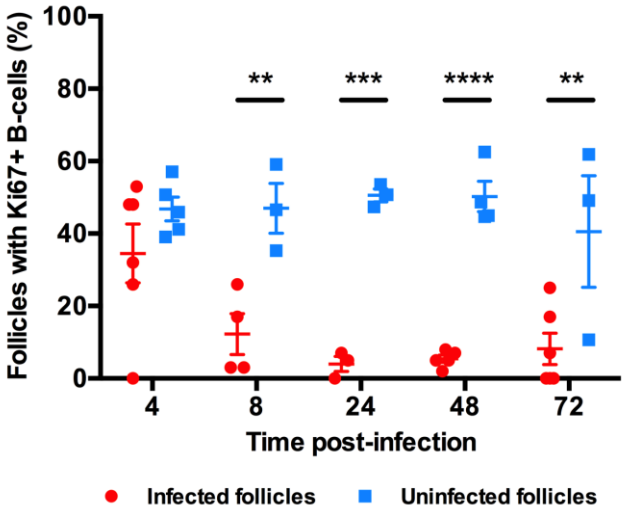

Figure 6-6 Shut down of germinal centres in sheep lymph node is associated with the presence of BTV
Graph showing the percentage of BTV-infected follicles containing dividing B-cells ($Ki67^{+}$) in comparison to uninfected follicles within the same section in sheep lymph node. Sequential LN sections were stained for B-cells, BTV NS2 and Ki67. The total number of follicles per section was quantified (range = 44 to 254 follicles/section) in a minimum of 3 draining LN per each time point. Histograms represent mean ±SD (** P<0.01, *** P<0.001, **** P<0.0001, Two-Way ANOVA).

We then compared the pattern observed in sheep with the one displayed by goats draining LNs. Similarly the presence of detectable BTV in the follicles was accompanied by a decrease in B-cell division (Figure 6-7). However, the shutdown of centroblasts appeared delayed in goats compared to sheep. Indeed at 8 hpi the percentage of infected follicles was 54.3% (not far from the percentage detected in uninfected follicles, 60.25%) and then slightly decreased to an average of 34.8% at 24 hpi. At 48 hpi no infected follicles were observed (percentage equal to zero) and this level was maintained at least until 96 hpi (Figure 6-7). It is of note that in goat LNs, BTV was still detectable at significant levels at 96 hpi infecting FDC in the follicles, while at this stage most of the virus was cleared in sheep. Interestingly, the percentage of uninfected follicles

presenting centroblasts in goat also underwent a decline going from an average of 60.25% at 8 hpi to 33.2% at 72 hpi (Figure 6).

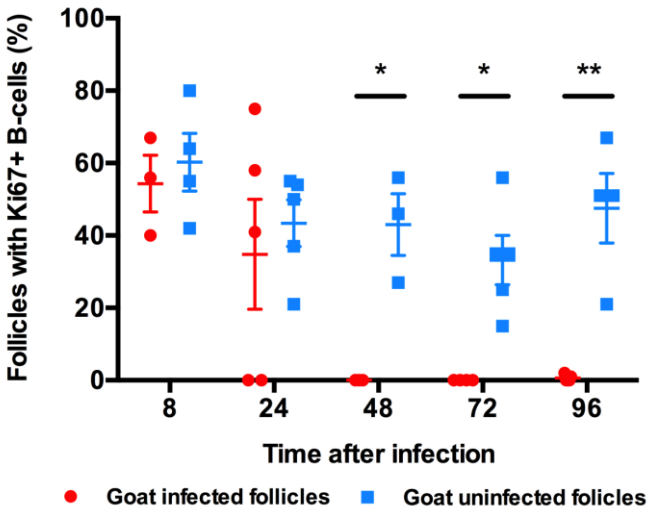

Figure 6-7 BTV induces the shutdown of germinal centres in goat lymph nodes
Graph showing the percentage of BTV-infected follicles containing dividing B-cells ($Ki67^+$) in comparison to uninfected follicles within the same section in goat lymph nodes. Sequential LN sections were stained for B-cells, BTV NS2 and Ki67. The total number of follicles per section was quantified (range = 48 to 329 follicles/section) in a minimum of 3 draining LN per each time point. Histograms represent mean ±SD. (* P≤0.05, ** P<0.01, Two-Way ANOVA).

6.2.3 Division of B-cells in germinal centres resumes more rapidly in sheep infected with an attenuated BTV-8 strain ($BTV8_H$)

The data presented above suggest that BTV-8 infection and disruption of FDC induce shutdown of B-cell division in pre-existing GCs both in sheep and in goats. Hence, we used an attenuated strain of BTV-8 ($BTV8_H$) (Janowicz et al. 2015) in order to assess if virus-induced block of B-cell division was correlated to BTV virulence. As described in the previous chapters, $BTV8_H$ replicates in the skin and draining LNs (near the inoculation sites) of the infected sheep but does not induce viremia nor does disseminates to peripheral tissues. To assess the effect of attenuation on B-cell proliferation, we infected sheep with either $BTV8_H$, BTV-8 or control tissue culture media and compared the proportion of proliferating GCs (identified by clusters of $Ki67^+$ B-cells) relative to the number of primary follicles. Clusters of B-cells and Ki67+ cells were quantified by microscopy in sequential LN sections collected at different times post-infection

(Figure 6-8). In LN collected at 3 and 4 dpi between 10 and 24% of follicles (on average) contained clusters of $Ki67^+$ B cells in sheep infected with either wild type or attenuated $BTV8_H$. In LN from mock-infected sheep however, $Ki67^+$ GCs represented the 68% of the total number of follicles throughout the duration of the experiment (Figure 6-8B). Interestingly, at 7 dpi the proportion of GCs returned to the values of mock-infected controls in animals infected with $BTV8_H$ but not in those infected with wild type BTV-8 (Figure 6-8). Hence, the extent of the cellular damage induced by $BTV8_H$ is reduced compared to wild type BTV-8, apparently resulting in an earlier recovery of B cells division in animals infected with the attenuated virus.

In addition, in order to identify a link between the recovery of the GCs structure and the severity of disease (similarly to what was observed in $BTV8_H$ infected sheep), we screened the presence of $Ki67^+$ GCs in draining LNs in goats infected with the virulent BTV-8 and in sheep infected with the $BTV8_{IT2008}$ strain (at 7 dpi only). No GCs recovery was detected in these animals, and only a low percentage of $Ki67^+$ GCs was identified in the draining LNs of both groups up to 7 dpi (the end of the experiment), similarly to what was observed in BTV-8 infected sheep (Figure 6-8B).

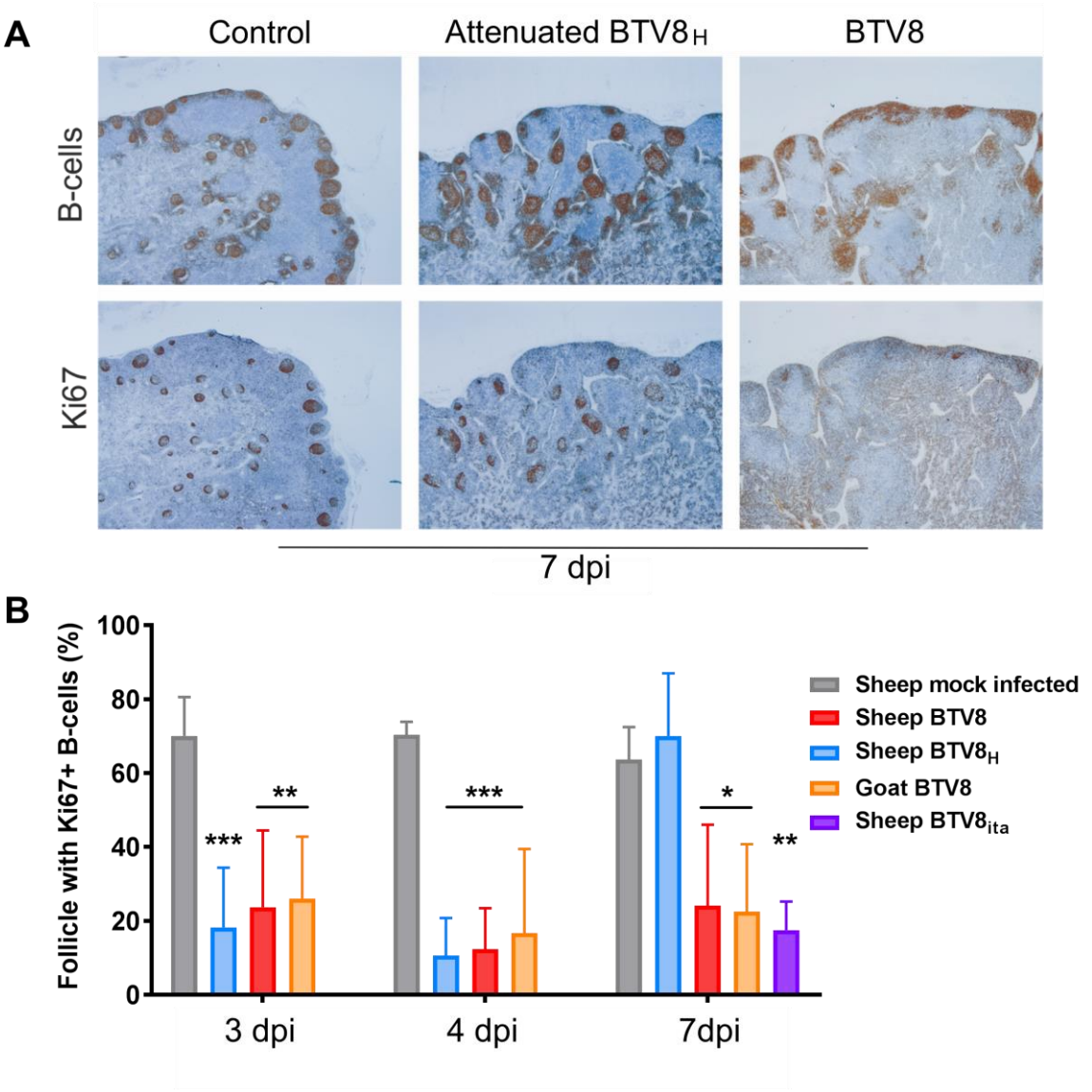

Figure 6-8 Sheep infected with $BTV8_H$ display early recovery of germinal centers (GCs) compared to sheep and goat infected with BTV8, and sheep infected with $BTV8_{ita}$
(A) Representative immunohistochemistry micrographs of lymph node sections taken from mock infected control sheep, sheep infected with BTV8 and sheep infected with the attenuated BTV8H at 7 days post-infection. Sequential sections were stained for B-cells (BSAP) and Ki67. Few GCs are visible in draining LNs collected from sheep infected with BTV8. (B) Graph showing the percentage of follicles displaying clusters of $Ki67^+$ cells in draining lymph nodes (LNs) of mock infected sheep, sheep infected with BTV8, sheep infected with $BTV8_H$, and goats infected with BTV8 at 3, 4 and 7 days post-infection (dpi). Sheep infected with $BTV8_{ita}$ were only tested at 7 dpi. The number of follicles and Ki67 clusters were quantified in sequential sections stained either for BSAP (B-cells) or Ki67 as in panel A. The total number of follicles per section was quantified (range = 44 to 254 follicles/section) in a minimum of 3 draining LN per each time point. (* P≤0.05; ** P≤0.01; *** P≤0.001 by one-way ANOVA). Bars represent the average values.

6.2.4 Antibody response differs in sheep infected with wild type or attenuated BTV-8.

Our data indicated that BTV led to the suppression of GCs, which are the site of affinity-based selection that generates high affinity antibodies and memory B-cells (Victora & Nussenzweig 2012). Therefore, we hypothesized that BTV could also affect the initiation of the host humoral immune response. In order to address our hypothesis, we characterized the antibody responses over 21 days in sheep infected with either BTV-8 (n=3) or $BTV8_H$ (n=5) (Figure 6-9).

BTV-8 infected sheep showed a raise in body temperature (40-41°C) between 5 and 7 dpi (Figure 6-9A). Animals infected with BTV-8 developed a prolonged viremia and, as seen in previous experiments (Chapter 4), the viremia peaked between 5 and 8 dpi, reaching approximately levels of 10^6 virus-copies/µg RNA, and then settling at ~10^5 copies throughout the course of the experiment, until day 28 (Figure 6-9B). Interestingly, one sheep included in this group did not show increase in body temperature (≤39.3°C), and was also the only animal that presented a delayed peak of viremia (at 7 dpi instead of 5 dpi). On the contrary, and as in previous experimental infections (Chapter 3) (Janowicz et al. 2015), $BTV8_H$ did not induce fever or viremia in any of the infected sheep (Figure 6-9A-B).

To evaluate the kinetic of the humoral immune response towards both wild-type and attenuated strains we assessed the BTV VP7 specific IgG and IgM as well as virus neutralising antibodies. VP7 is a major BTV core protein that is well conserved across different serotypes, and therefore widely used for diagnostic purposes. No significant differences were observed in the levels of IgM between the two groups of infected animals at any of the time point analysed (7, 14, 21 and 28 dpi) (Figure 6-9C). However, at 7 dpi $BTV8_H$ infected sheep produced significantly higher titres of both anti-BTV VP7 IgG and virus neutralizing antibodies compared to BTV-8 infected sheep ($P \leq 0.05$ in both cases) (Figure 6-9D-E). These differences were transitory since by 14 dpi the two groups of experimentally infected sheep showed similar levels of both anti-VP7 IgG and anti-BTV-8 neutralizing antibodies (Figure 6-9D-E). In both BTV-8 and $BTV8_H$ infected sheep, antibody (IgG) avidity increased over time. However, $BTV8_H$

infected animals consistently showed IgG of higher avidity towards VP7 at 7, 14 and 21 dpi ($P \leq 0.05$) compared to BTV-8 infected sheep (Figure 6-9F).

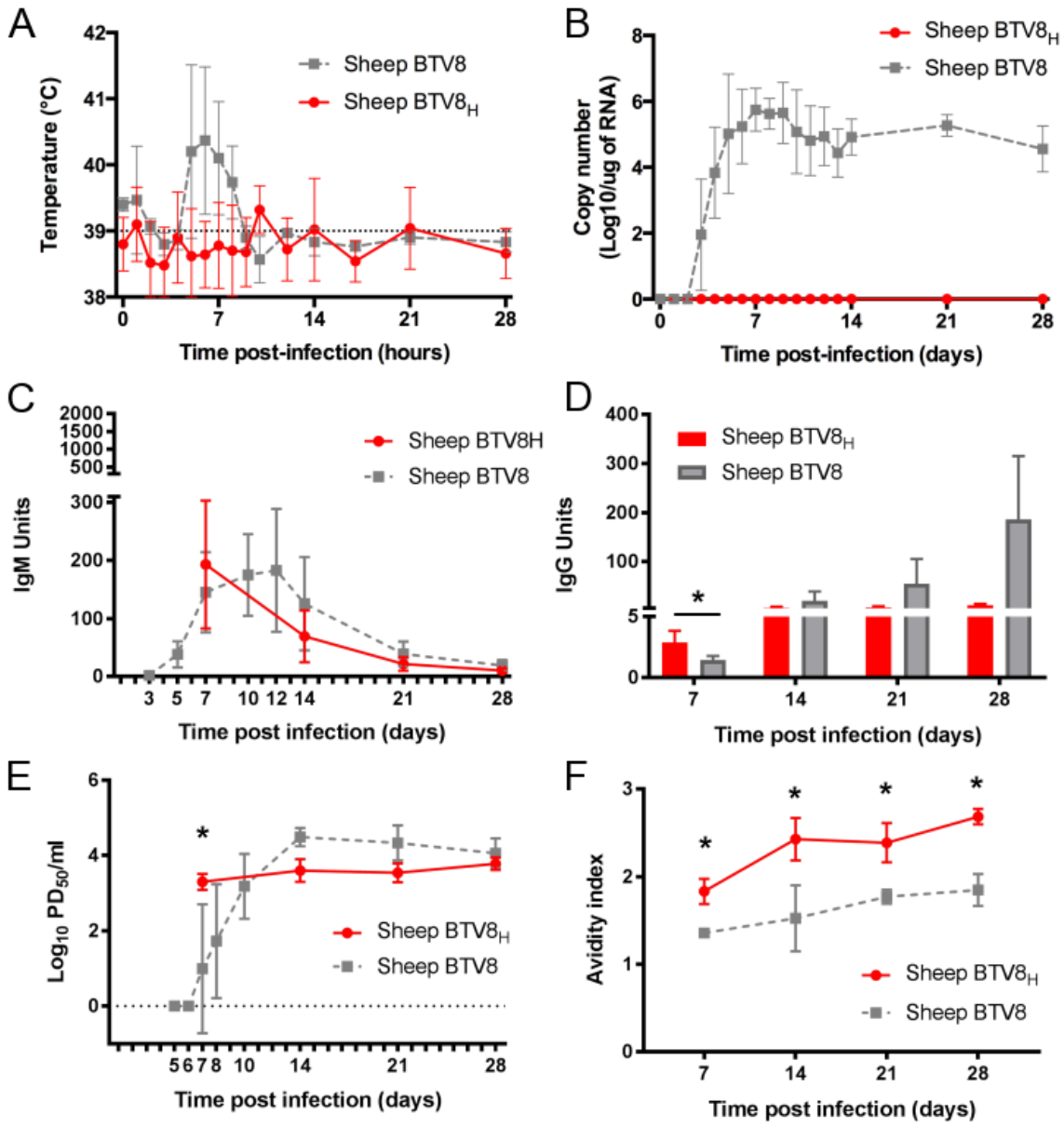

Figure 6-9 Sheep infected with attenuated BTV8$_H$ present an earlier onset of BTV specific IgG, neutralising antibodies and higher IgG avidity.
Sheep were infected with BTV8 (n=3) or attenuated BTV8$_H$ (n=5) and monitored for 28 days. (A) Graph showing rectal temperature (average ±SD) in sheep infected with either BTV8 or BTV8$_H$. Note that sheep infected with BTV8$_H$ do not present an increase in body temperature (B) Graph showing BTV RNA (average ±SD) in blood samples of experimentally infected sheep. Viral RNA was detected by qRT-PCR, and values are expressed as Log10 copy number per μg of total RNA. Note that sheep infected with BTV8$_H$ do not present viremia. (C) Graph showing BTV VP7 IgM titre in the serum of sheep infected with either BTV8 or BTV8$_H$. Serum was collected and tested by ELISA as described in Materials and Methods (D) Graph showing BTV VP7 IgG titre assessed by ELISA in sheep infected with either BTV8 or BTV8$_H$. Note that BTV8$_H$ infected sheep present higher levels of IgG at 7 dpi. (E) Graph showing BTV8 neutralization titres assessed by microneutralization assay in serum of sheep infected with either BTV8 or BTV8$_H$. Values represent

average ±SD and are expressed as Log10 of the 50% protective dose (PD_{50}). $BTV8_H$ infected sheep present higher neutralization titre at 7 dpi. (F) Graph showing BTV VP7 IgG avidity in sheep infected with either BTV8 or $BTV8_H$. Results are expressed as avidity index (AI), average ±SD. Note that antibody in $BTV8_H$ infected animals present constantly a higher avidity. (*) = P≤0.05 by Mann-Whitney U-test.

6.2.5 Antibody response of sheep infected with an Italian strain of BTV-8 ($BTV8_{IT2008}$)

We then questioned if a similar difference in neutralization and antibody avidity could be detected using a BTV strain that generally induces a mild clinical presentation in naturally infected animals, as observed in Italy in 2008 (Caporale et al. 2014). Therefore we infected intradermally 3 sheep as previously described with $6x10^2$ PFU of $BTV8_{IT2008}$. The animals were monitored for 28 days, the body temperature recorded, and blood and serum samples collected daily until day 14 and subsequently at day 21 and 28. The body temperature of $BTV8_{IT2008}$ infected sheep did not present major differences compared to those observed in BTV-8 infected animals, with an increase between 5 and 8 dpi (Figure 6-10A). In $BTV8_{IT2008}$ infected sheep, viremia started to increase exponentially at 3 dpi, reached a peak at 7 dpi (10^6 copies/µg RNA) and then plateaued at 10^5 copies/µg RNA from 10 until 28 dpi, when the experiment was terminated (Figure 6-10B), following a trend similar to what we observed in sheep infected with virulent BTV-8. No significant differences were detected in the two groups of infected animals ($BTV8_{IT2008}$ and BTV-8) regarding the titres of BTV specific IgM, IgG, neutralizing antibodies and avidity levels (Figure 6-10C-F). Overall these results did not highlight any major differences in the clinical presentation and in the humoral response generated by BTV-8 and $BTV8_{IT2008}$ in experimentally infected sheep.

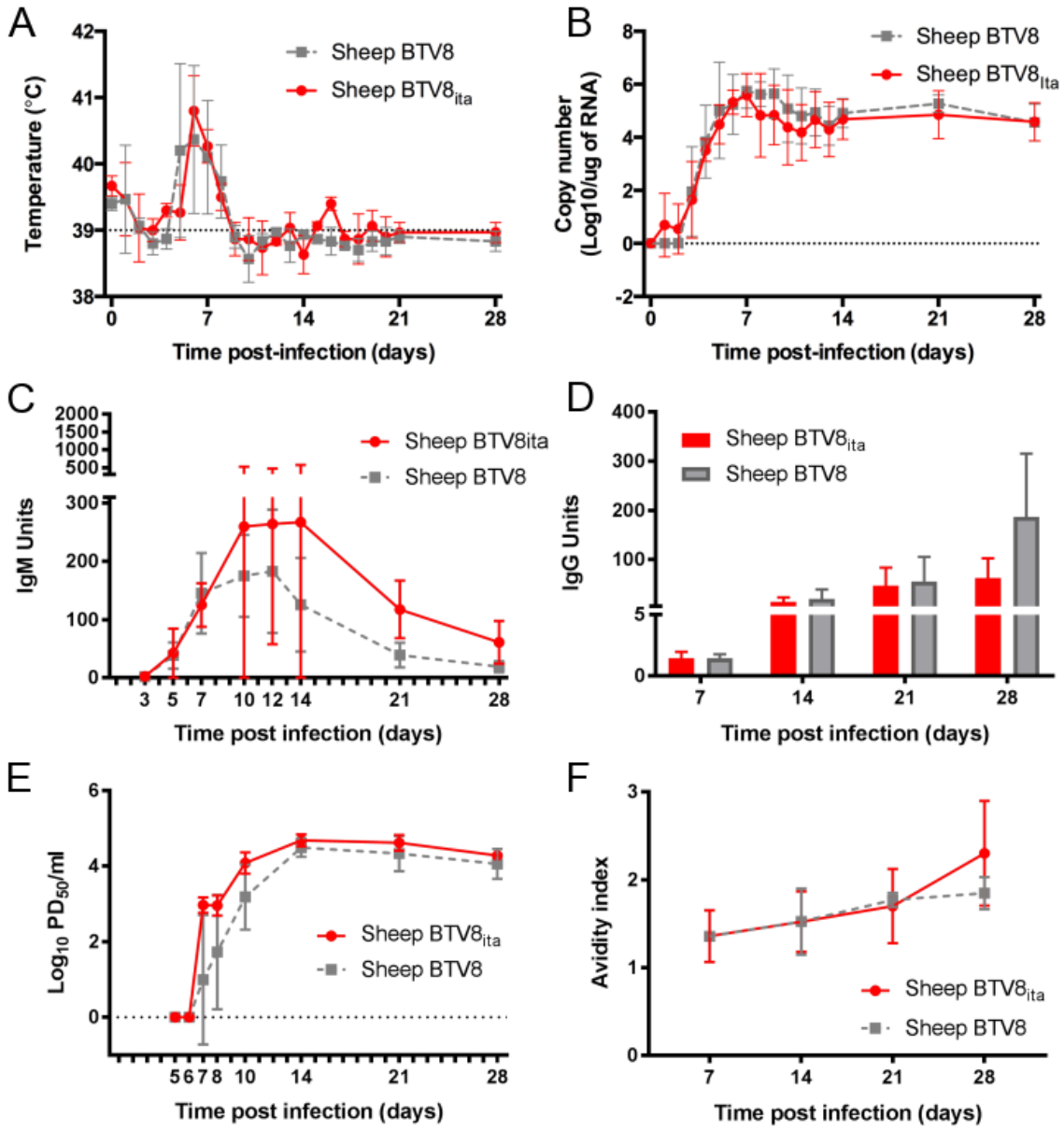

Figure 6-10 Sheep infected with attenuated BTV8$_{ita}$ and BTV8 present similar clinical presentation and antibody response in experimentally infected animals.
Sheep were infected with BTV8$_{ita}$ (n=3), a low virulence strain isolated in Italy, and monitored for 28 days. Results obtained in BTV8 infected sheep are reported for comparative purpose. (A) Graph showing rectal temperature (average ±SD) in sheep infected with either BTV8$_{ita}$ or BTV8. (B) Graph showing BTV RNA (average ±SD) in blood samples of experimentally infected sheep. (C) Graph showing BTV VP7 IgM titre in the serum of sheep infected with either BTV8$_{ita}$ or BTV8. Serum was collected and tested by ELISA as described in Material and Methods (D) Graph showing BTV VP7 IgG titre assessed by ELISA in sheep infected with either BTV8$_{ita}$ or BTV8. (E) Graph showing BTV8 neutralization titres assessed by microneutralization assay in serum of sheep infected with either BTV8$_{ita}$ or BTV8. Values represent average ±SD and are expressed as Log10 of the 50% protective dose (PD$_{50}$). (F) Graph showing BTV VP7 IgG avidity in sheep infected with either BTV8$_{ita}$ or BTV8. Results are expressed as avidity index (AI), average ±SD.

6.2.6 Antibody response of sheep infected with blood from a BTV-8 infected animal.

In a previous study, it has been showed that inoculation of infectious blood can induce more severe clinical signs compared to infection with a purified virus isolate (Caporale et al. 2014). In order to understand if an alteration of the B-cell responses and antibody production could be associated with the level of disease severity, we investigated the antibody response of 5 sheep experimentally infected with 5 ml of BTV-8 infectious blood ($BTV8_{blood}$). Serum was available from a previous experiment in which $BTV8_{blood}$ infected animals presented a higher level of viremia, sustained high body temperature and a worse clinical symptoms compared to animal infected with the BTV-8 isolated from blood and minimally passaged in cell culture (Caporale et al. 2014). Data regarding viremia and body temperature of these animals has been described in a previous study (Caporale et al. 2014). Interestingly, in these animals, we could demonstrate a complete lack of VP7 IgM response until 7 dpi (Figure 6-11A), as well as a slight delay in the reaching of the IgM peak (10-14 dpi), which however was ~7 times the titre obtained in sheep infected with cell culture isolated strain (1344.25 in blood infected animals compared to 182.94 IgM units in animal infected with isolated virus, $P \leq 0.0001$ at 10 and 12 dpi and $P \leq 0.01$ at 14 dpi) (Figure 6-11A). This delayed and more elevated peak of IgM was associated with a delay in production of IgG that were first detectable at 14 dpi (Figure 6-11B), instead of the usual 7 dpi. The onset of neutralising antibodies was also delayed in sheep infected with $BTV8_{blood}$ as they were first detected at 10 dpi and in some animals not before 14 dpi (Figure 6-11C, $P \leq 0.01$ at 8 dpi and $P \leq 0.001$ at 10 dpi). Compared to animals infected with BTV-8, no significant differences were found in the IgG avidity index at day 14, once the IgG started to be produced (Figure 6-11D).

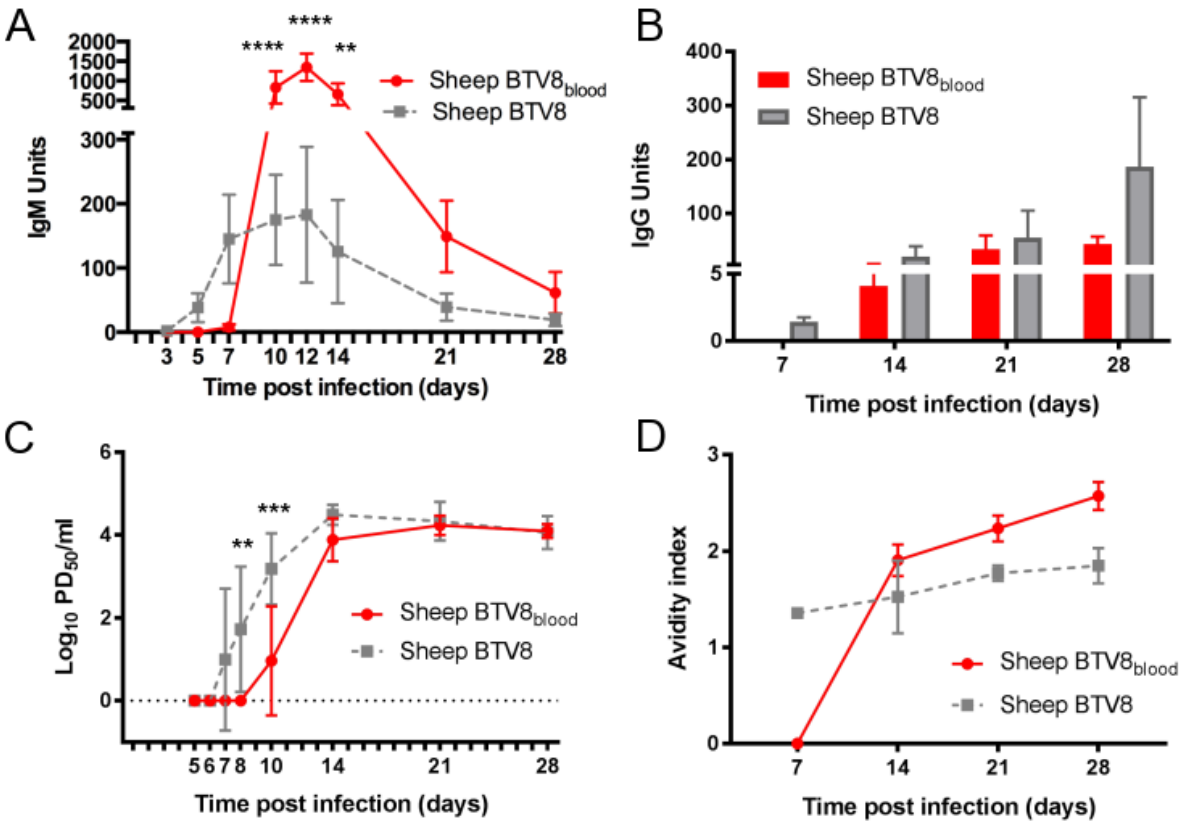

Figure 6-11 Sheep infected with BTV-8 infectious blood present a delayed onset of BTV specific immunoglobulin and neutralizing antibodies.
Serum of sheep intradermally infected with BTV8 infectious blood ($BTV8_{blood}$ n=5) was sourced from a previous experiment. Sheep infected with $BTV8_{blood}$ presented a worse clinical presentation and higher viremia compared to sheep infected with cell culture isolated BTV-8 strains. Results obtained in BTV8 infected sheep are reported for comparative purpose. (A) Graph showing BTV VP7 IgM titre in the serum of sheep infected with either $BTV8_{blood}$ or BTV8. Serum was collected and tested by ELISA as described in Material and Methods. Note that $BTV8_{blood}$ infected animals present a delayed onset of IgM followed by an higher peak at 12 dpi. (B) Graph showing BTV VP7 IgG titre assessed by ELISA in sheep infected with either $BTV8_{blood}$ or BTV8. Note the delay in IgG onset in $BTV8_{blood}$ infected animals. (C) Graph showing BTV8 neutralization titres assessed by microneutralization assay in serum of sheep infected with either $BTV8_{ita}$ or BTV8. Values represent average ±SD and are expressed as Log10 of the 50% protective dose (PD_{50}). Note the delayed onset of neutralising antibodies in $BTV8_{blood}$ infected sheep. (D) Graph showing BTV VP7 IgG avidity in sheep infected with either $BTV8_{ita}$ or BTV8. Results are expressed as avidity index (AI), average ±SD. (*) = P≤0.05, (**) = P≤0.01, (***) = P≤0.001, (****) = P≤0.0001 by Mann-Whitney U-test.

6.2.7 Antibody response of goat infected with BTV-8

Next, we infected we infected 3 goats with BTV-8 ($2x10^6$ PFU) intradermally, in order to ascertain if any differences in the antibody response against BTV were present in a species that generally do not show severe clinical signs of bluetongue. Only one of 3 infected goats presented a mild increase in body temperature between 9 and 12 dpi (reaching 40°C at 10 and 11 dpi) (Figure 6-12A). As in previous experiments (Chapter 4), the onset of viremia in goats was delayed compared to BTV-8 infected sheep ($P \leq 0.001$ at 4 and 5 dpi). BTV was firstly detected in the blood of infected goats at 5 dpi and peaked on average between 7-10 dpi, however the virus titre in goat blood remained at a significantly lower levels compared to sheep (10^4 in goats versus 10^6 copies/μg RNA in sheep, $P \leq 0.01$ at 6 dpi) (Figure 6-12B). Interestingly, the goat with increased temperature also presented a delayed peak of viremia (at 12-13 dpi instead of 7-9 dpi). Serum IgM in infected goats started to appear at 3 dpi, peaked between 7 and 12 dpi and then gradually decreased (Figure 6-12C). IgG were detected at extremely low levels at 7 dpi and gradually increased in titre throughout the remaining course of the experiment although never reached the high titres detected in sheep infected with the same virus (Figure 6-12D, $P \leq 0.01$ at 28 dpi). Moreover, the production of BTV neutralising antibodies in goats was also delayed compared to sheep infected with the same BTV-8 strain. Although non statistically significantly difference were present, it's worth noticing that In goats, neutralising antibodies were not present at 7 dpi; one of the three infected animals produced neutralising antibodies at 10 dpi (3 days after sheep) while in the other two goats we could only detect neutralising antibody production starting from 14 and 21 dpi, respectively (Figure 6-12E). Finally, in the BTV-8 infected goats IgG avidity did not differed substantially from sheep infected with the same virus (Figure 6-12F). Interestingly, the last goat to develop neutralising antibodies was the same animal that presented a delayed peak of viremia and fever. The delay in neutralising antibodies and IgG production observed in goats, do not seem to affect negatively the clinical outcome of disease as for sheep. This might indicate the presence of different protective mechanisms acting effectively in goat, such as type I IFN response or cell-mediated activity.

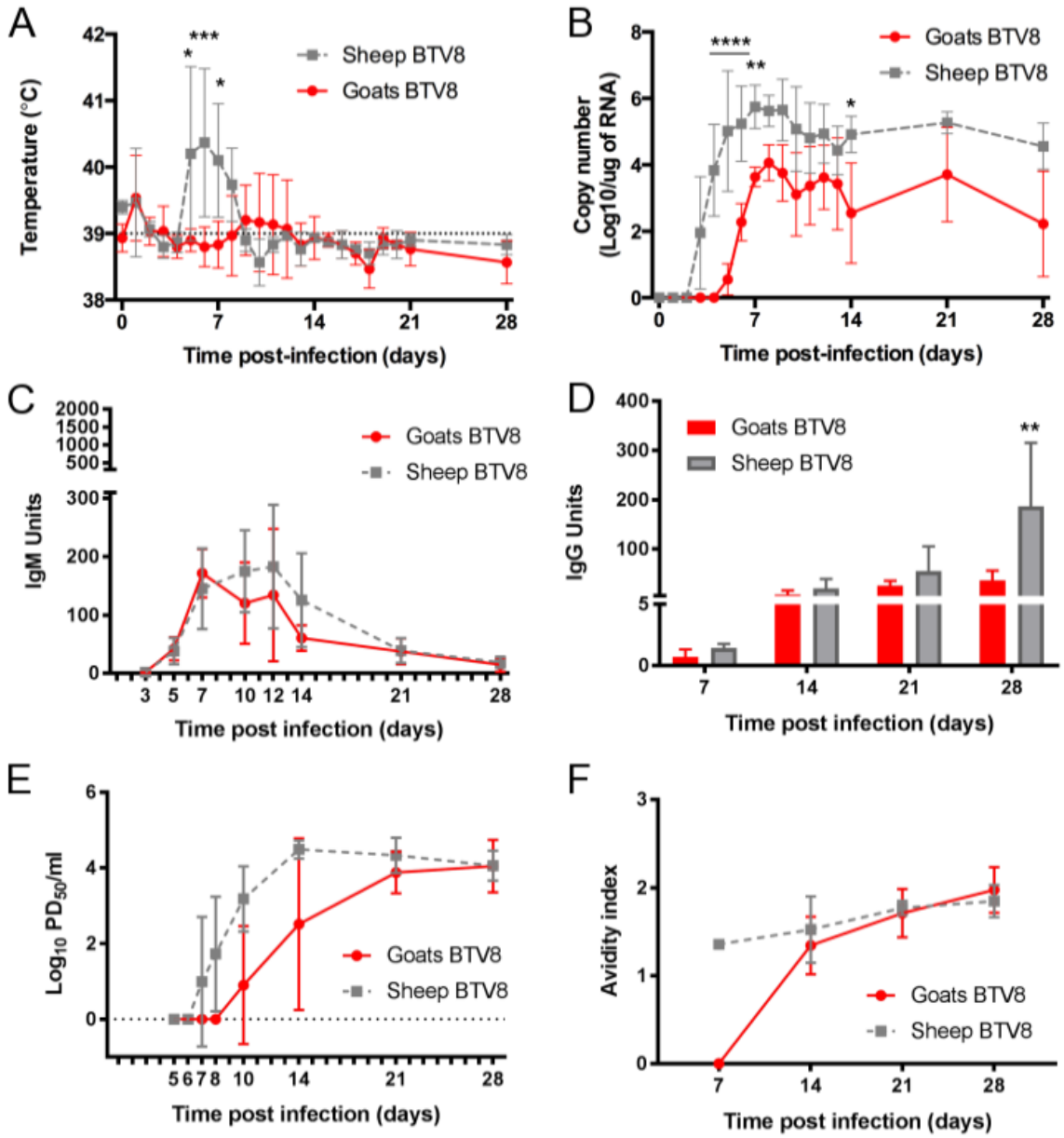

Figure 6-12 Goats infected with BTV8 present a lower viremia and a delayed onset of neutralising antibodies.

Goats were infected with BTV8 (n=3) and monitored for 28 days. Results obtained in BTV8 infected sheep are reported for comparative purpose. (A) Graph showing rectal temperature (average ±SD) in goat and sheep infected with BTV8. Goats display only a mild increase in body temperature (B) Graph showing BTV RNA (average ±SD) in blood samples of experimentally infected goats and sheep. Note that goats present a lower viremia compared to sheep. (C) Graph showing BTV VP7 IgM titre in the serum of goat infected with BTV8. Serum was collected and tested by ELISA as described in Materials and Methods (D) Graph showing BTV VP7 IgG titre assessed by ELISA in goats infected with BTV8. (E) Graph showing BTV8 neutralization titres assessed by microneutralization assay in serum of goats and sheep infected with BTV8. Values represent average ±SD and are expressed as Log10 of the 50% protective dose (PD_{50}). Note that goats present a delayed onset of neutralising antibodies compared to sheep. (F) Graph showing BTV VP7 IgG avidity in sheep infected with either $BTV8_{ita}$ or BTV8. Results are expressed as avidity index (AI), average ±SD. (*) = P≤0.05, (**) = P≤0.01, (***) = P≤0.001, (****) = P≤0.0001 by Mann-Whitney U-test.

6.2.8 BTV infection induces a temporary immunosuppression

In the previous chapters and paragraphs we have shown that BTV-8 infection of FDC induces a disruption of the follicle organisation. As a consequence, the anatomical alteration of the cortical area hampers the capacity of B-cell to effectively respond to BTV infection. Indeed, we observed a delayed onset of neutralising antibodies and in the affinity maturation process when a virulent strain was used for infection.

The presence of complicating and secondary bacterial infections has been commonly described during the course of BTV (Umeshappa, Singh, et al. 2010; Veronesi et al. 2010; Erasmus 1975) and they have been generally considered a consequence of the lymphopenia detected during the early phases of infection. We hypothesised that the follicle infection could also be partially responsible of the observed immunosuppression and that the impairment of the B-cell responses is not only specific for BTV but may have broader implications towards other antigens that reach the LN at a second time after infection.

In order to test this hypothesis, we assessed the ability of BTV-8 infected sheep to elicit a humoral response to an exogenous antigen. Hence, we used OVA as a model T-dependent antigen to test the capacity of infected follicles to respond to immunisation, T-dependent antigens require T-cell help to initiate a germinal centre reaction and to produce a high affinity class-switched serological response (Grant et al. 2012). The following experiments were planned at the CVR, in Glasgow, but were carried out by Dr Noemi Sevilla at the Instituto Nacional de Investigación y Tecnología Agraria y Alimentaria (INIA) in Madrid, Spain.

A control group of sheep (n=5) was immunised with OVA as described in material and methods, without prior BTV infection (Figure 6 13A) and served to monitor a normal humoral response in healthy animals. Two additional groups of sheep were instead infected with BTV-8 and successively immunised with OVA at either 24 (n=5) or 72 hpi (n=5). These times of immunisation were chosen to allow BTV to reach the draining LNs and induce the disruption of the existing GCs, since we

detected the most severe shutdown of Ki67+ B-cells between 24 and 96h hpi. To avoid confounding effects that might originate from BTV infection of the skin, OVA was inoculated subcutaneously, few centimetres a part from BTV inoculation sites, in areas drained by the inguinal or prescapular LNs..

Blood and serum were collected at predetermined time points (7, 14 and 21 days post-immunisation, dpim), the PBMC was isolated for detection of OVA-specific ASC by ELISPOT and OVA-specific antibodies evaluated by ELISAs.

In control sheep we detected a peak of OVA-specific IgM at 7 dpim (mean 200 Elisa units, EU) that decreased progressively at 14 and 21 dpim to reach a mean of 50 EU. Sheep immunised with OVA at 24h after BTV inoculation demonstrated a significant reduction in circulating OVA-specific IgM compared to controls at 7 dpim (mean 32.4 EU, $P<0.01$), 14 dpim (mean 23.36 EU, $P<0.01$) and 21 dpim (mean 14.48 EU, $P<0.01$).

The OVA-specific IgG response in healthy animals reached a mean of 84.76 EU at 7 dpim and increased to 101.35 EU at 14 dpim, and 110.86 EU at 21 dpim. The corresponding IgG titre in animals immunised 24h after BTV infection was significantly lower both at 7 dpim (mean 40.6 EU, $P<0.01$) and 14 dpi (mean 74 EU, $P<0.05$) compared to uninfected controls (FIGURE).

The quantity of OVA-specific antibody produced was supported by the presence of circulating OVA specific ASC, which in control animals presented a peak at 7 dpim (946.4 ASC/106 PBMC) and progressively decreased at 14 and 21dpim (114.2 and 103.8 ASC/106 PBMC respectively). Strikingly, the formation of OVA-specific ASC was almost completely ablated in BTV-8 infected animals both at 7 (2.44 ASC/106 PBMC, $P<0.01$) and 14 dpim (10.2 ASC/106 PBMC, $P<0.01$).

These data indicate that the formation of plasmacells able to produce OVA-specific IgM and IgG is impaired during the early phases of BTV infection, suggesting that the capacity of germinal centres to respond to a second antigen has been compromised.

On the other hand, animals immunized with OVA 72h after BTV infection exhibited a less substantial decrease in the levels of OVA-specific antibodies and

ASC compared to uninfected controls (Figure 6 13B). The variable results obtained at this time point might indicate a certain degree of inter-animal variability in the time required to recover GC functionality, with some of the sheep able to respond to immunization, and other sheep still non responsive. These data demonstrate that the inability of BTV infected sheep to elicit an OVA-specific antibody response is temporary.

In order to further assess the GC functionality we assessed the process of somatic hypermutation taking place in the GCs by measuring the degree of affinity maturation of OVA-specific antibodies. Specifically, we compared the avidity index (AI) of OVA-specific IgG in BTV-infected and control sheep. No differences were detected at 7 dpim. However, both groups of sheep immunised with OVA after BTV infection (24 and 72 hpi) presented reduced antibody avidity at 14 dpim (AI=1.2, $P \leq 0.05$ for animal immunised 24 hpi and AI=1.18, $P \leq 0.01$ for animal immunised 72 hpi) compared to controls (AI=1.84), indicating an impairment in the process of affinity maturation in infected LNs that become evident as time passes. This difference was maintained also at 21 dpim in animal immunised 24 hpi (AI=0.84 $P \leq 0.05$, compared to controls AI=1.48).

Overall these data indicate that BTV infection is not only able to produce a delay in virus-specific immune responses, but also capable to affect temporarily the ability of B-cells to respond to other incoming antigens. Thus, BTV induces an acute immune suppression that can favour the secondary infections described as complicating factors for the outcome of bluetongue.

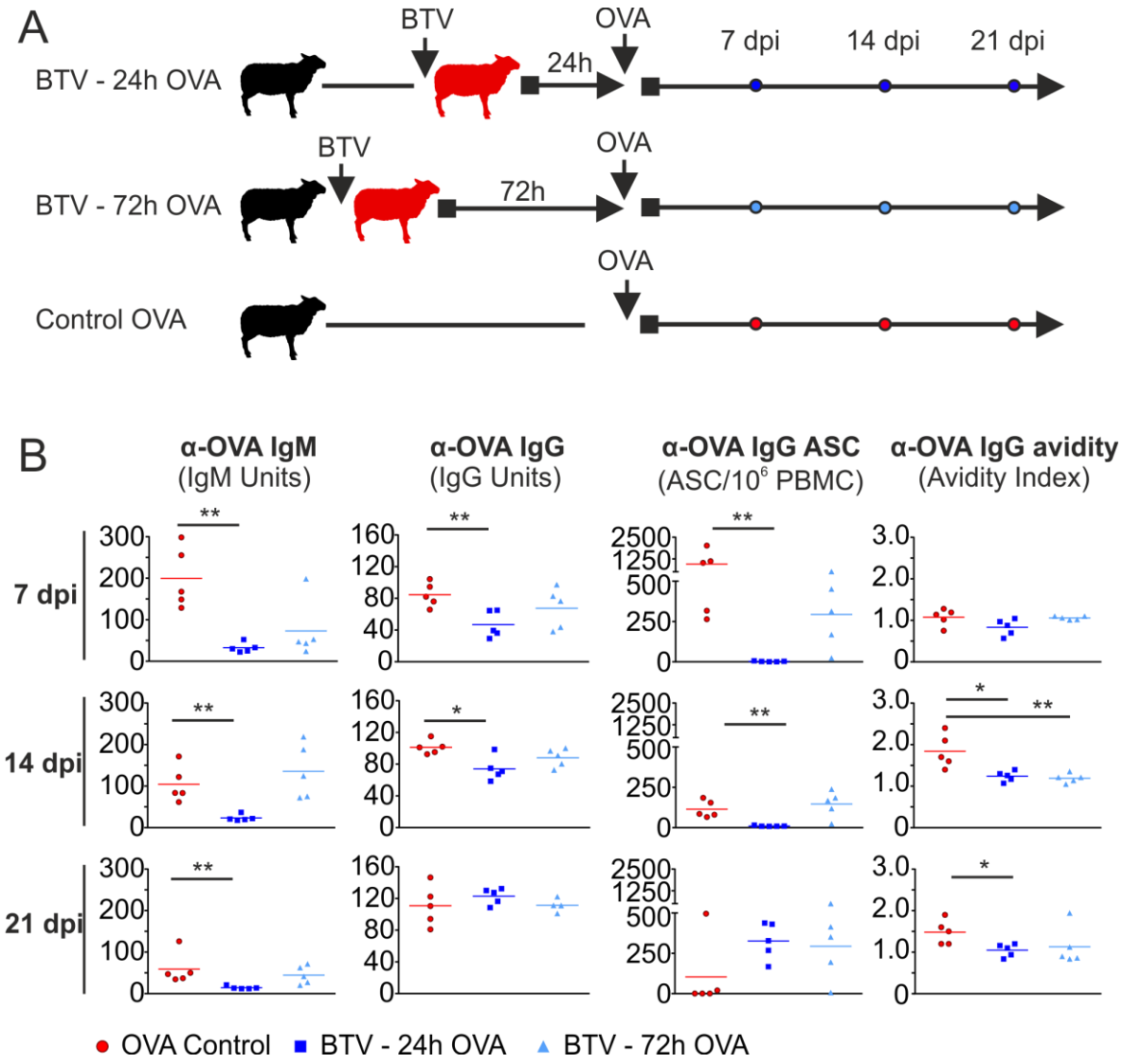

Figure 6-13 BTV infection induces a transient immunosuppression
(A) Experimental design. Sheep were divided into three groups (n=5 per group). All groups were immunized with ovalbumin (OVA). Two of the three groups were previously infected with BTV either 24h or 72h before OVA immunization. (B) Graphs showing OVA-specific IgM and IgG titres assessed by ELISA, OVA-specific antibody secreting cells (ASC) assessed by ELISPOT and IgG avidity assessed by ELISA as described in Material and Methods. Serum was collected at 7, 14 and 21 dpi. Each dot represents values for an individual sheep and bars represent the average values (* P≤0.05 and ** P≤0.01 by Mann-Whitney U-test). Note that sheep immunised with OVA 24h after BTV infection presented lower IgM and IgG titres and a marked delay in ASC production. Both groups of BTV infected animals presented a lower OVA-IgG avidity compared to uninfected controls.

6.3 Discussion

In this chapter we have shown that BTV8 rapidly infects and disrupt the FDC network present in lymphoid follicles. Our data indicate that this process induces an architectural and functional alteration of the GCs present in LNs draining the site of infection. Consequently, the early humoral immune response against BTV is impaired by the lack of FDC, as assessed by the delayed production of high affinity and neutralising antibodies which correlates with the severity of disease and the viral strain used. Furthermore, we showed that the capacity of B-cells to respond to a different antigenic stimulus is temporary hampered during BTV infection.

To our knowledge this is the first report of FDC depletion directly caused by a virus. Pathogen-related depletion of FDC has been previously described during chronic infection with HIV and Leishmania (Smelt et al. 1997; Heesters et al. 2015) as a result of CD8 T-cell mediated cytotoxic activity. Our data, on the contrary, are consistent with a direct CPE of the virus, given the rapidity of the cellular depletion (4-24 hpi), the abundant presence of BTV antigens in FDC and the increase in the number of apoptotic cells in the follicles.

The capacity of the host to respond promptly to infection, by mounting an adequate humoral response is of paramount importance for pathogen control and clearance. The data presented in this chapter demonstrate that the disruption of FDC correlates with a sudden shutdown of centroblasts replication, blocking somatic hypermutation in the dark zone of the follicles that leads to the production of high affinity antibodies.

The extent of the damage induced to the lymphoid follicles appears to be directly correlated to the virulence of the virus strain. We tested virulent and attenuated strains of BTV and we noticed that sheep infected with the attenuated $BTV8_{H,}$ that did not induce fever and viremia, presented an earlier recovery of GCs, higher neutralization titres and BTV specific antibodies with increased avidity. $BTV8_H$ possesses attenuating mutations in several viral proteins hampering optimal replication both *in vitro* in primary cells, and *in vivo* in sheep and $IFNAR^{-/-}$ mice (Janowicz et al. 2015), hence it is probably outcompeted by the immune responses of the host.

To contrast a rapidly multiplying virus any delay in the development of an appropriate antibody response could favour virus dissemination in peripheral tissues. Indeed, passive serum transfer studies demonstrated that antibodies can confer full protection in newly infected sheep (Jeggo, Wardley & Taylor 1984). However, in natural occurring BTV infections, infectious viral particles can persist in blood for up to 2 months despite the presence of circulating neutralising antibodies (Bonneau et al. 2002; Koumbati et al. 1999; Singer et al. 2001). These observations may suggest that once BTV has reached the blood, the neutralising antibodies have a limited capability to target and eliminate the virus, possibly due to the capacity of BTV to be sequestered in invaginations of the RBCs membrane where it cannot be reached by antibodies (Brewer & MacLachlan 1992). Hence, it is likely that even a slight delay in the production of neutralising antibodies and in the process of antibodies affinity maturation could confer an advantage to the systemic distribution of non-attenuated strains of BTV and might explain the differences observed with regards to the variability of clinical disease.

In this chapter we characterised the humoral immune response elicited in sheep by different strains of BTV-8. We could not detect any major differences related to the presence of GCs, neutralising antibodies, onset and levels of IgM/IgG and IgG avidity in sheep infected by the Netherlands (BTV-8) and Italian ($BTV8_{IT2008}$) strains of BTV. The latter was reported to be attenuated in both field and experimental infections (Caporale et al. 2014). However the discrepancies that we observed could reflect the small number of animals tested in this particular experiment (3 per group) that does not allow discerning subtle differences that might be visible on a larger population scale. We found instead tangible differences in the type of humoral immune response elicited in sheep inoculated with blood collected from a BTV-8 infected animal ($BTV8_{blood)}$. In this case, we noticed a significant delay of both IgM and IgG production that were associated with a more severe clinical presentation of disease and a higher viremia. It is interesting to note that these animals presented a delayed peak (but with relatively higher levels) of IgM compared to sheep infected with wild-type or attenuated BTV-8. It might be noteworthy to investigate if this was caused by an even more severe insult to the GCs, which could affect for a longer period of time the capacity of B-cells to undergo class switch recombination. A similar

process is described in the human hyper IgM syndromes (HIGM), where individuals affected present a group of primary immune deficiency disorders characterized by defective CD40 signalling by B-cells (Etzioni & Ochs 2004; Renshaw et al. 1994) which results in an altered class switch recombination and somatic hypermutation. Individuals with HIGM present decreased concentrations of serum IgG and IgA and normal or elevated IgM, leading to increased susceptibility to infections.

Interestingly, sheep infected with infectious blood ($BTV8_{blood}$) did not develop neutralising antibodies until 14 dpi, much later than sheep inoculated with tissue culture isolated BTV strains. Considering the worse disease presented by $BTV8_{blood}$ infected sheep, the complete lack of neutralising antibodies seems to have a negative impact on the clinical presentation and on the level of viremia presented by sheep. Caporale et al. have recently shown that virus passaging in tissue culture can lead to adaptive changes in the viral genotype, in particular a genetic bottleneck was observed after viral passaging in mammalian BHK21 cells which lower the degree of the population variability compared to the viral quasispecies represented in blood (Caporale et al. 2014). Hence, this and other factors could contribute to the higher virulence displayed by a non-tissue culture passaged virus and could contribute to a more severe effect of BTV on the GCs.

Curiously, while the lack of early neutralising antibodies seems to correlate with disease severity in sheep, this has not been observed in goats. Data presented show that unapparent or mild disease in goat is not accompanied by the presence of early neutralising antibodies, which tend to appear only 2 weeks after infection. Although different explanations could exist, it is possible that goats, unlike sheep, benefit of a T-helper1 (T_H1) polarised immune response that is more efficient in counteracting BTV infection, while sheep may lean towards a T-helper2 (T_H2) response that favours antibody production. However, further studies would be necessary to identify the determinants of species specificity of the immune responses and the role of T-cells in BTV infection.

It is worth noting that in essentially all the experimentally infected sheep and goats used in this study, independently from the BTV strain used for infection, we observed the appearance of IgG in concomitance with the detection of neutralising antibodies. This observation suggests that BTV specific IgM do not

possess neutralising capacity. Hence, the processes of class switching and IgG affinity maturation are critical for the selection of B-cell clones targeting BTV neutralising epitopes.

Our results demonstrated a rapid disappearance of the FDC network as a result of BTV infection. The maintenance of FDC in the follicles requires a continual interaction with B-cells expressing lymphotoxin alpha/beta (LTα/ß); indeed, it has been demonstrated that FDC can rapidly collapse from their mature state and lose their capacity of retaining immune complexes within 24 h when deprived of LTα/ß (Mackay & Browning 1998).

Studies of the function of FDC have been performed in mouse models where their ablation was achieved trough an interference with tumour necrosis factor-alpha (TNF-α) and LTα/ß signalling (Mackay & Browning 1998), or by depletion of the genes that encode for these cytokines (Alimzhanov et al. 1997; Koni et al. 1997; Matsumoto et al. 1997). These mice show an abnormal formation of the GCs and the production of low affinity antibodies (Koni & Flavell 1999). However, inference made about FDC in these studies are confounded by the fact that the lack of LTα or ß induces a variety of alterations that are not only affecting FDC but many other cells and the development of the lymphoid tissues in general. For example, mice with a disrupted LTα or LTß gene also lack LNs and Peyer's patches (PP), and show profound defects of the splenic architecture. We have shown that BTV specifically targets and eliminates FDC in sheep and goats, making this experimental platform a useful model for the study of the depletion of FDC and the derived consequences. The phenotype that we describe in sheep, following FDC depletion, is similar to the one previously described in mouse, in regards of the impairment of GC functionality and antibody response. Cyster and colleagues described that upon FDC ablation, B-cells form disorganized bands of cells around T zones (Wang et al. 2011), in our observations, the B-cell scattering was limited, and follicular structures were still somewhat recognisable throughout the course of the experiment in the cortical area of infected LNs.

GCs are generally described as dynamic anatomical structures that can be re-utilised during immune responses to unrelated antigens (Schwickert et al. 2009), meaning that they are not supposed to undergo a regressive process upon a

subsequent immunisation. Hence, it was surprisingly to observe the shut down and dispersal of B-cells during the early phases of BTV infection, since a similar effect has not been previously described in any other infection. The possibility that a pathogen could turn off these structures, manipulating host responses for its own advantage, is a novel finding and can open the door for the interpretation of similar observations made in unrelated pathological conditions.

Our data show that BTV infection and disruption of FDC impairs the capacity of B-cells to respond to a subsequent antigenic stimulus by producing high affinity antibodies. In essence, BTV induces a transitory immunosuppression. Indeed, we found the titre and avidity of serum IgG and the number of ASC towards a second antigen (OVA) to be significantly lower in the presence of BTV. Interestingly, the lack of FDC induced also a delay in the IgM response against OVA, indicating that FDC can influence B-cell responses at various levels of maturation as suggested by previous in vitro studies (Aydar et al. 2005). The subversion of the host humoral immune response during BTV infection is however transient. Infected animals become responsive to newly administered exogenous antigen after a short time frame (3 days) although they still present a delay in the affinity maturation process, which is therefore the last function of the GCs to recover after FDC insult. Although transient, this immunosuppression occurs at a key stage of infection, during which delayed antibody production is likely to affect the systemic spread of the virus and the clinical course of the disease.

Chapter 7

Conclusions

7 Conclusions

Globalization, ecological and climate changes and an increase in international travel have all favoured the geographic expansion of numerous arboviruses (arthropod-borne viruses) that now pose a considerable global burden to both human and animal health (Weaver & Reisen 2010). Similarly to other infectious agents, arboviruses induce a wide spectrum of clinical signs in the infected hosts and the clinical outcome of these infections is influenced by host- and pathogen-related factors. Consequently, the characterization of the complex interactions between virus and host are critical for better understanding the pathogenesis of arbovirus infections.

Arboviruses cause acute diseases making the study of the early stages of infection (i.e. before the onset of clinical signs) and the corresponding host responses in humans extremely difficult. Mouse models are widely used but they often fail to fully replicate the intricate interplay between host and pathogen, which is shaped by co-evolutionary adaptations. However, arboviruses naturally infect a variety of mammalian species providing opportunities to study viral infection in the natural host. In this study we used BTV, since observations made in the naturally occurring infection can be effectively reproduced in a convenient experimental setting using the same target animal species (Caporale et al. 2014). Studies on bluetongue in ruminants offer the unique perspectives of understanding arbovirus pathogenesis in the natural host.

After gaining entry into the mammalian host, an arbovirus needs to overcome host antiviral responses in order to replicate abundantly in susceptible cells and produce sufficiently high titres in the bloodstream to be infectious for competent biting insects. In this study, we tracked the distribution of BTV in the infected animals after intradermal inoculation and we noticed that during the initial 48 h, BTV resides solely in the skin (at the inoculation site) and the corresponding draining LN. Therefore, we reasoned that the early events of viral replication taking place at these sites are key in establishing a successful infection in the host and may be critical in determining the clinical outcome of bluetongue.

One of the key discoveries made during this project was that BTV infects and disrupts FDC in the peripheral LNs. In turn, the lack of FDC impairs B-cell activation and division, and leads to disorganization of the GCs. This process induces an acute immunosuppression, characterised by the temporary inability of the B-cells to respond to antigenic stimuli. Hence, we describe for the first time a new strategy used by an arbovirus to modulate host immunity and we demonstrate how the early stages of infection can influence the severity of disease.

The experimental infection of the natural host has the advantage to recapitulate the immunopathological events leading to disease in their entirety. Moreover, the sheep included in our experiments have been naturally exposed to environmental pathogens and commensals, which also contribute to shape the host immune system. Indeed, in the LNs of these sheep we found the presence of numerous GCs preceding infection with BTV. GCs are generally missing in laboratory mice kept in clean animal facilities. Therefore, the virus-induced lesions that we described in this study would have been difficult to observe in conventional murine models.

It is becoming increasingly evident that viral infections can target the stromal network of cells that compose the lymphoid organs, inducing the disruption of the anatomic integrity and loss of immunocompetence. For example, lymphocytic choriomeningitis virus (LCMV) directly infects FRC in mouse spleen and LNs. This infection results in a T-cytotoxic mediated destruction of FRC and an altered functionality of the LN conduit network that contributes to viral persistence (Mueller et al. 2007; Scandella et al. 2008). Similarly, during highly pathogenic infections of non-human primates such as Ebola virus, Marburg virus and Lassa virus it is possible to observe a severe damage to secondary lymphoid organs attributed to the infection of FRC and endothelial cells, which is accompanied by a considerable level of cell death (Davis & Anderson 1997; Steele et al. 2009; Geisbert et al. 2003). It is interesting to note that in humans, fatal cases of Ebola are characterised by impaired humoral responses, with barely detectable levels of specific IgM and no IgG. In contrast, Ebola survivors present, from the early stages of infection, increasing levels of IgG directed against viral protein, followed by clearance of circulating viral antigen and

activation of cytotoxic T cells (Baize et al. 1999; Rowe et al. 1999). A defect in adaptive immunity if often associated with the severe outcome of viral haemorrhagic fevers, such as bluetongue, and our data indicate that this is at least in part due to the virulence of the viral strain and the extent of damage that it induces to the germinal centres.

An impairment of the humoral immune response has also been observed during other arboviral infections, including those caused by West Nile virus (Diamond et al. 2003), Japanese encephalitis virus (Burke et al. 1985; Libraty et al. 2002) and Crimean-Congo haemorrhagic fever virus (Shepherd et al. 1989). However, virus infection of the lymphoid stromal cells was not linked to immunosuppression in any of the above mentioned cases.

Current observations indicate that at least four factors can impair an early neutralizing-antibody response. These include (i) a low frequency of germline-encoded immunoglobulin V-regions encoding neutralizing antibodies, (ii) active modification of the B-cell repertoire by depletion of certain B-cell subsets, (iii) induction of abnormal T_H-cell function resulting in polyclonal B-cell activation, and (iv) immunopathological changes in secondary lymphoid organs (Hangartner et al. 2006). Our findings fall into the latter category, however we cannot completely exclude the possibility that any of the other factors could also contribute to the immune dysregulation that we observed in BTV infected sheep. In particular, BTV has been described to infect DCs in the lymph draining the infected skin (Hemati et al. 2009). Antigen presentation from DCs to T_H cells in the LN is required to initiate the GC reaction and antibody production. Thus, an alteration of DCs, behaviour or density, consequent to virus infection could impact the activation of T_H-cells and the resulting antibody response. Although in extremely rare cases, we found BTV-infected DCs in sheep LNs and our data highlighted a difference in the degree of DCs infection between sheep and goats. In light of these findings, it would be of interest to characterise the outcome of DCs infection in different animal species, to evaluate how this aspect can differentially influence the host immune responses.

As observed in other studies (Ratinier et al. 2016; Caporale et al. 2014; Pages et al. 2014) we confirmed that the onset of neutralising antibodies is delayed in sheep infected with virulent strains of BTV (BTV-8 or $BTV8_{blood}$) compared to

sheep inoculated with the attenuated $BTV8_H$. Furthermore, we clearly show that the process of antibody affinity maturation is delayed in sheep infected with virulent strains. Therefore we provide a link between the immunopathology described in the infected LNs, the humoral response (neutralising antibody and affinity maturation) and the outcome of infection.

In general, it is worth noting that presence of neutralising antibodies *in vitro* does not necessarily correlate with *in vivo* protection. Indeed, it has been demonstrated that *in vivo* protection is influenced by both the concentration of neutralising antibodies and by their avidity. Antibodies below a certain threshold of avidity fail to confer protection even when administered at elevated concentrations (Bachmann 1997). Hence, it is reasonable to assume that animals infected with attenuated BTV strains would acquire an earlier protection in comparison to the ones infected with virulent strains and that this would contribute to slowing or halting viral systemic spread. Furthermore, the induction of a non-protective low avidity antibody response, under some conditions can results in enhanced disease upon reinfection, as demonstrated by vaccination against respiratory syncytial virus (Delgado et al. 2009) and measles virus (Polack et al. 2003; Polack et al. 1999) where the presence of low-avidity antibodies contributed to disease severity through the formation of immune complexes and their deposition in various tissues. Curiously, the clinical presentation of the vaccine-induced atypical measles resembles many aspects of bluetongue, being characterised by high fever, vesicular or petechial rash, severe pneumonitis accompanied by pleural effusions, hilar adenopathy, peripheral oedema, and finally shock.

The pathogenic effects of the lack of affinity maturation of BTV specific humoral responses would require further assessment (such as the evaluation of circulating immune complexes and its correlation to disease severity), in order to evaluate if an enhancement of disease could be ascribed to a deleterious effect of the impaired antibody responses. Evidence of a secondary reaction to BTV-specific antibodies, and a pathogenic process involving type I hypersensitivity have been identified in cattle but never characterised into details (Odeón et al. 1999; Anderson et al. 1987; Stott et al. 1982).

Our results show that BTV, by affecting the structural integrity of GCs, induces an acute immunosuppression in BTV infected animals, characterised by a dysregulation of B-cell responses. Sheep immunised with a different antigen (OVA) during the early phases of infection, failed to respond to immunisation and produce antibodies. This transitory immunosuppression could have serious repercussion in inducing disease complications and favouring the secondary microbial infections sometimes reported during bluetongue (Umeshappa, Singh, et al. 2010; Veronesi et al. 2010; Erasmus 1975). When planning vaccination campaigns, it will be important to consider that this immunosuppressive phase happens during the unapparent initial stages of BTV infection. Therefore, it is likely that in this condition, healthy looking animals subjected to routine herd vaccinations may return a poor immune response and results unprotected, determining vaccine failure.

It is also interesting to note that the onset and type of antibody response during BTV infection varies significantly depending on the kind of inoculum used (blood or virus isolate), the species involved (sheep or goats) and the viral strain (BTV-8, $BTV8_{IT2008}$, $BTV8_{H}$). Notwithstanding small fluctuations, that could be likely ascribed to individual susceptibility, group of animals of the same species, when infected with the same inoculum tended to present a similar humoral immune response, in term of IgM onset and peak, IgG onset and titres, production of neutralising antibodies and serum avidity. These findings highlight the presence of species-specific factors able to influence the outcome of BTV infection.

It is also important to highlight that in this study, in order to characterise the tropism of BTV, we overcame the lack of reagents available to identify sheep cell markers by screening a panel of over 60 antibodies. This allowed the novel identification of different populations of sheep antigen presenting cells and lymphoid stromal cells residing in the LN. These markers will be useful for other studies in ruminants, since we believe that an increased awareness of the diversity of the antiviral responses in different animal species would be of benefit to the fields of viral pathogenesis and immunity which have relied almost exclusively on mouse models. The use of a large animal model allowed us to dissect experimentally an arbovirus infection at the whole organism, tissue and cellular level in the natural target host. This was key in discovering the novel

effects reported in this study. Mouse models of arbovirus infection are limited by the fact that they generally lack a fully competent immune system in order to permit virus replication. Indeed, our histological analysis of infected mouse LNs after BTV infection revealed a different localization of BTV infected cells compared to sheep LN.

In conclusion, this is the first study demonstrating induction of a transient immunosuppression by an arbovirus, and this is also the first report linking immunosuppression with virus infection and destruction of FDC. Our study has therefore shown how virus infection of FDC can subvert the host humoral responses and this can inform our understanding of the pathogenesis of many other human and animal arbovirus infections. The identification of this pathogenic process opens a way to explore previously uncharacterized mechanisms of arbovirus-host interactions and pathogenesis. Virus infection of FDC can also offers new avenues in understanding the origin of these cells and the key role they play in the biology of GCs and initiation of immune response (Figure 7-1)

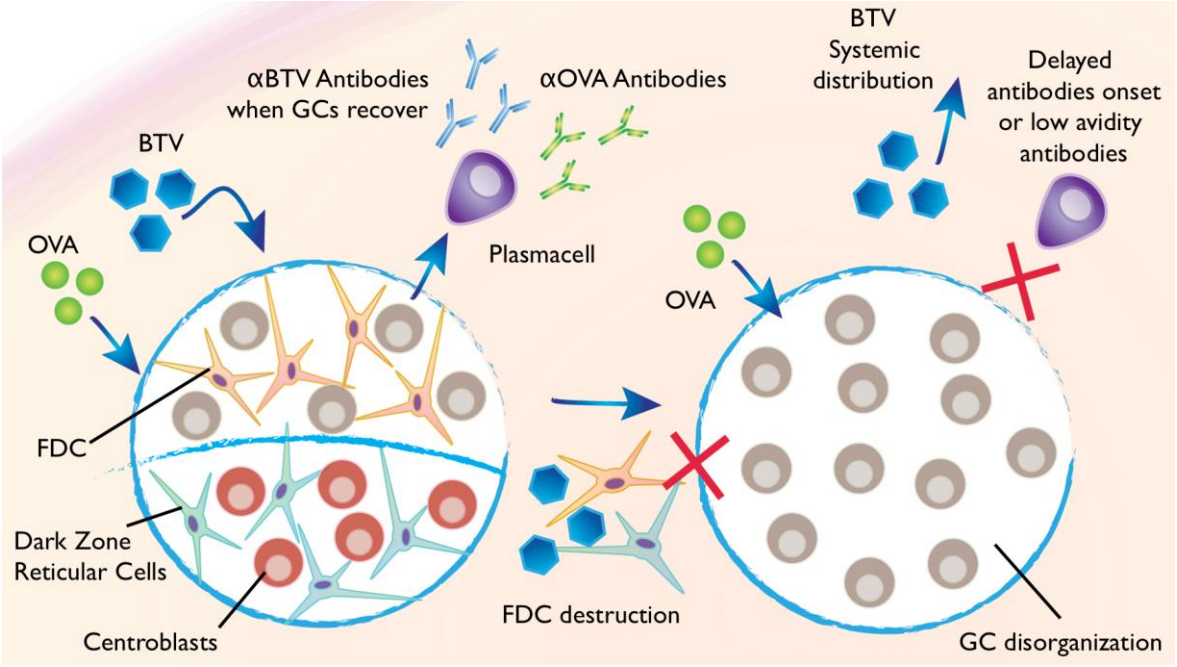

Figure 7-1 Graphic summary
Normal germinal centres (GCs) (left) present follicular dendritic cells (FDC) in the light zone and reticular cells in the dark zone. In the dark zone, dividing B-cells, called centroblasts, undergo somatic hypermutation and clones with high affinity for the antigen are selected to differentiate into plasmacells and produce antibodies. Bluetongue virus (BTV) infects and destroys follicular dendritic cells and reticular cells in the germinal centres of infected animals. As a consequence we observe GCs disorganization, characterised by a shut down of centroblasts division and B-cell dispersion. Infected GCs are not able to respond to the virus or other antigens, such as ovalbumin

(OVA), in a timely manner. A delay in high affinity and neutralising antibodies can likely favour BTV dissemination in the animal tissues.

Bibliography

Agostinelli, C. et al., 2010. Characterization of a new monoclonal antibody against PAX5/BASP in 1525 paraffin-embedded human and animal tissue samples. *Applied immunohistochemistry & molecular morphology : AIMM / official publication of the Society for Applied Immunohistochemistry*, 18(6), pp.561–72.

Aguzzi, A., Kranich, J. & Krautler, N.J., 2014. Follicular dendritic cells: origin, phenotype, and function in health and disease. *Trends in Immunology*, 35(3), pp.105–113.

Al-Alwan, M.M. et al., 2001. Fascin is involved in the antigen presentation activity of mature dendritic cells. *Journal of immunology (Baltimore, Md. : 1950)*, 166(1), pp.338–345.

Alexander, K.A. et al., 1994. Evidence of natural bluetongue virus infection among African carnivores. *American Journal of Tropical Medicine and Hygiene*, 51(5), pp.568–576.

Alimzhanov, M.B. et al., 1997. Abnormal development of secondary lymphoid tissues in lymphotoxin -deficient mice. *Proceedings of the National Academy of Sciences*, 94(17), pp.9302–9307.

Allen, C.D.C. & Cyster, J.G., 2008. Follicular dendritic cell networks of primary follicles and germinal centers: Phenotype and function. *Seminars in Immunology*, 20(1), pp.14–25.

Allepuz, A. et al., 2010. Monitoring bluetongue disease (BTV-1) epidemic in southern Spain during 2007. *Preventive Veterinary Medicine*, 96(3–4), pp.263–271.

Anderson, G.A. et al., 1987. Identification of Bluetongue Virus-specific Immunoglobulin E in Cattle. *Journal of General Virology*, 68(9), pp.2509–

2514.

Andrew, M. et al., 1995. Antigen specificity of the ovine cytotoxic T lymphocyte response to bluetongue virus. *Veterinary Immunology and Immunopathology*, 47(3–4), pp.311–322.

Angel, C.E. et al., 2009. Distinctive localization of antigen-presenting cells in human lymph nodes. *Blood*, 113(6), pp.1257–1267.

Anon, UniProt - The Universal Protein Resource. , p.http://www.uniprot.org/. Available at: http://www.uniprot.org/.

Arnaud, F. et al., 2010. Interplay between Ovine Bone Marrow Stromal Cell Antigen 2/Tetherin and Endogenous Retroviruses. *Journal of Virology*, 84(9), pp.4415–4425.

Aydar, Y. et al., 2005. The influence of immune complex-bearing follicular dendritic cells on the IgM response, Ig class switching, and production of high affinity IgG. *Journal of immunology (Baltimore, Md. : 1950)*, 174(9), pp.5358–5366.

Bachmann, M.F., 1997. The Role of Antibody Concentration and Avidity in Antiviral Protection. *Science*, 276(5321), pp.2024–2027.

Backx, A., Heutink, C. & Rooij, E. Van, 2007. Clinical signs of bluetongue virus serotype 8 infection in sheep and goats. *Veterinary Record*, 161(17), p.591.

Baize, S. et al., 1999. Defective humoral responses and extensive intravascular apoptosis are associated with fatal outcome in Ebola virus-infected patients. *Nature medicine*, 5(4), pp.423–426.

Bajenoff, M. et al., 2006. Stromal Cell Networks Regulate Lymphocyte Entry, Migration, and Territoriality in Lymph Nodes. *Immunity*, 25(6), pp.989–1001.

Balasuriya, U.B.R. et al., 2008. The NS3 proteins of global strains of bluetongue virus evolve into regional topotypes through negative (purifying) selection. *Veterinary Microbiology*, 126(1–3), pp.91–100.

Barratt-Boyes, S.M. et al., 1992. Flow cytometric analysis of in vitro bluetongue virus infection of bovine blood mononuclear cells. *The Journal of general virology*, 73 (Pt 8), pp.1953–60.

Barratt-Boyes, S.M. & MacLachlan, N.J., 1994. Dynamics of viral spread in bluetongue virus infected calves. *Veterinary Microbiology*, 40(3–4), pp.361–371.

Barratt Boyes, S.M. et al., 1992. Flow cytometric analysis of in vitro bluetongue virus infection of bovine blood mononuclear cells. *J Gen Virol*, 73(Pt 8), pp.1953–1960.

Batten, C. et al., 2014. Evidence for transmission of bluetongue virus serotype 26 through direct contact. *PLoS ONE*, 9(5), p.e96049.

Batten, C.A. et al., 2013. Bluetongue virus serotype 26: Infection kinetics, pathogenesis and possible contact transmission in goats. *Veterinary Microbiology*, 162(1), pp.62–67.

Batten, C.A. et al., 2012. Bluetongue virus serotype 26: Infection kinetics and pathogenesis in Dorset Poll sheep. *Veterinary Microbiology*, 157(1–2), pp.119–124.

Beaton, A.R. et al., 2002. The membrane trafficking protein calpactin forms a complex with bluetongue virus protein NS3 and mediates virus release. *Proceedings of the National Academy of Sciences of the United States of America*, 99(20), pp.13154–13159.

Belaganahalli, M.N. et al., 2015. Genetic characterization of the tick-borne orbiviruses. *Viruses*, 7(5), pp.2185–2209.

Bonneau, K.R. et al., 2002. Duration of viraemia infectious to Culicoides sonorensis in bluetongue virus-infected cattle and sheep. *Veterinary microbiology*, 88(2), pp.115–25.

Bonneau, K.R. & Mullens, B.A., 2001. Occurrence of Genetic Drift and Founder

Effect during Quasispecies Evolution of the VP2 and NS3/NS3A Genes of Bluetongue Virus upon Passage between Sheep, Cattle, and Culicoides sonorensis. *Journal of Virology*, 75(17), pp.8298–8305.

Boone, J.D. et al., 2007. Recombinant canarypox virus vaccine co-expressing genes encoding the VP2 and VP5 outer capsid proteins of bluetongue virus induces high level protection in sheep. *Vaccine*, 25(4), pp.672–678.

Bousso, P., 2008. T-cell activation by dendritic cells in the lymph node: lessons from the movies. *Nature reviews. Immunology*, 8(9), pp.675–84.

Bousso, P. & Moreau, H.D., 2012. Functional immunoimaging: the revolution continues. *Nature reviews. Immunology*, 12(12), pp.858–64.

Boyce, M. et al., 2004. Purified recombinant bluetongue virus VP1 exhibits RNA replicase activity. *Journal of virology*, 78(8), pp.3994–4002.

Braun, A. et al., 2011. Afferent lymph-derived T cells and DCs use different chemokine receptor CCR7-dependent routes for entry into the lymph node and intranodal migration. *Nature immunology*, 12(9), pp.879–887.

Breloer, M. & Fleischer, B., 2008. CD83 regulates lymphocyte maturation, activation and homeostasis. *Trends in Immunology*, 29(4), pp.186–194.

Breugelmans, S. et al., 2011. Immunoassay of lymphocyte subsets in ovine palatine tonsils. *Acta Histochemica*, 113(4), pp.416–422.

Brewer, A. & MacLachlan, N.J., 1994. The pathogenesis of bluetongue virus infection of bovine blood cells in vitro: ultrastructural characterization. *Archives of virology*, pp.287–298.

Brewer, A.W. & MacLachlan, N.J., 1992. Ultrastructural Characterization of the Interaction of Bluetongue Virus with Bovine Erythrocytes in vitro. *Veterinary Pathology*, 29(4), pp.356–359.

Brown, C.C. et al., 1996. Distribution of bluetongue virus in tissues of experimentally infected pregnant dogs as determined by in situ

hybridization. *Veterinary pathology*, 33(3), pp.337–40.

Burke, D.S. et al., 1985. Fatal outcome in Japanese encephalitis. *The American journal of tropical medicine and hygiene*, 34(6), pp.1203–1210.

Calvo-Pinilla, E., Rodríguez-Calvo, T., Anguita, J., et al., 2009. Establishment of a bluetongue virus infection model in mice that are deficient in the alpha/beta interferon receptor. C. A. Stoddart, ed. *PloS one*, 4(4), p.e5171.

Calvo-Pinilla, E., Rodríguez-Calvo, T., Sevilla, N., et al., 2009. Heterologous prime boost vaccination with DNA and recombinant modified vaccinia virus Ankara protects IFNAR(−/−) mice against lethal bluetongue infection. *Vaccine*, 28(2), pp.437–445.

Calvo-Pinilla, E. et al., 2014. Recombinant vaccines against bluetongue virus. *Virus Research*, 182, pp.78–86.

Calvo-Pinilla, E., Nieto, J.M. & Ortego, J., 2010. Experimental oral infection of bluetongue virus serotype 8 in type I interferon receptor-deficient mice. *Journal of General Virology*, 91(11), pp.2821–2825.

Cao, W., Lee, S.H. & Lu, J., 2005. CD83 is preformed inside monocytes, macrophages and dendritic cells, but it is only stably expressed on activated dendritic cells. *The Biochemical journal*, 385(Pt 1), pp.85–93.

Caporale, M. et al., 2011. Determinants of bluetongue virus virulence in murine models of disease. *Journal of virology*, 85(21), pp.11479–11489.

Caporale, M. et al., 2014. Virus and host factors affecting the clinical outcome of bluetongue virus infection. *Journal of virology*, 88(18), pp.10399–411.

Carpenter, S., Wilson, A. & Mellor, P.S., 2009. Culicoides and the emergence of bluetongue virus in northern Europe. *Trends in Microbiology*, 17(4), pp.172–178.

Carr, M. a et al., 1994. Association of bluetongue virus gene segment 5 with neuroinvasiveness. *Journal of virology*, 68(2), pp.1255–1257.

Carrasco, Y.R. & Batista, F.D., 2007. B Cells Acquire Particulate Antigen in a Macrophage-Rich Area at the Boundary between the Follicle and the Subcapsular Sinus of the Lymph Node. *Immunity*, 27(1), pp.160–171.

Chang, J.E. & Turley, S.J., 2015. Stromal infrastructure of the lymph node and coordination of immunity. *Trends in Immunology*, 36(1), pp.30–39.

Channappanavar, R. et al., 2012. Enhanced proinflammatory cytokine activity during experimental bluetongue virus-1 infection in Indian native sheep. *Veterinary immunology and immunopathology*, 145(1–2), pp.485–92.

Chauveau, E. et al., 2013. NS3 of bluetongue virus interferes with the induction of type I interferon. *Journal of virology*, 87(14), pp.8241–6.

Chessa, B. et al., 2009. Revealing the History of Sheep Domestication Using Retrovirus Integrations. *Science*, 324(5926), pp.532–536.

Cinamon, G. et al., 2008. Follicular shuttling of marginal zone B cells facilitates antigen transport. *Nature immunology*, 9(1), pp.54–62.

Coetzee, P. et al., 2012. Bluetongue: a historical and epidemiological perspective with the emphasis on South Africa. *Virology journal*, 9(1), p.198.

Coffey, L.L. et al., 2008. Arbovirus evolution in vivo is constrained by host alternation. *Proceedings of the National Academy of Sciences of the United States of America*, 105(19), pp.6970–6975.

Conraths, F.J. et al., 2009. Epidemiology of bluetongue virus serotype 8, Germany. *Emerging Infectious Diseases*, 15(3), pp.433–435.

Dal Pozzo, F., Saegerman, C. & Thiry, E., 2009. Bovine infection with bluetongue virus with special emphasis on European serotype 8. *The Veterinary Journal*, 182(2), pp.142–151.

Darpel, K.E. et al., 2007. Clinical signs and pathology shown by British sheep and cattle infected with bluetongue virus serotype 8 derived from the 2006

outbreak in northern Europe. *The Veterinary record*, 161(8), pp.253–261.

Darpel, K.E. et al., 2012. Involvement of the skin during bluetongue virus infection and replication in the ruminant host. *Veterinary Research*, 43(1), pp.1–16.

Darpel, K.E. et al., 2011. Saliva proteins of vector Culicoides modify structure and infectivity of bluetongue virus particles. *PLoS ONE*, 6(3), p.e17545.

Darpel, K.E. et al., 2009. Transplacental transmission of bluetongue virus 8 in cattle, UK. *Emerging Infectious Diseases*, 15(12), pp.2025–2028.

Davis, K. & Anderson, A., 1997. Pathology of experimental Ebola virus infection in African green monkeys. *Arch Pathol Lab* ….

Delgado, M.F. et al., 2009. Lack of antibody affinity maturation due to poor Toll-like receptor stimulation leads to enhanced respiratory syncytial virus disease. *Nature medicine*, 15(1), pp.34–41.

DeMaula et al., 2002. The Role of Endothelial Cell-Derived Inflammatory and Vasoactive Mediators in the Pathogenesis of Bluetongue. *Virology*, 296(2), pp.330–337.

DeMaula, C.D. et al., 2002. Bluetongue virus-induced activation of primary bovine lung microvascular endothelial cells. *Veterinary immunology and immunopathology*, 86(3–4), pp.147–57.

DeMaula, C.D. et al., 2001. Infection kinetics, prostacyclin release and cytokine-mediated modulation of the mechanism of cell death during bluetongue virus infection of cultured ovine and bovine pulmonary artery and lung microvascular endothelial cells. *The Journal of general virology*, 82(Pt 4), pp.787–94.

DeMaula, C.D., Bonneau, K.R. & MacLachlan, N.J., 2000. Changes in the outer capsid proteins of bluetongue virus serotype ten that abrogate neutralization by monoclonal antibodies. *Virus research*, 67(1), pp.59–66.

Diamond, M.S. et al., 2003. B Cells and Antibody Play Critical Roles in the Immediate Defense of Disseminated Infection by West Nile Encephalitis Virus. *Journal of Virology*, 77(4), pp.2578–2586.

Domingo, E., Sheldon, J. & Perales, C., 2012. Viral quasispecies evolution. *Microbiology and molecular biology reviews : MMBR*, 76(2), pp.159–216.

Drew, C., Heller, M. & Mayo, C., 2010. Bluetongue virus infection activates bovine monocyte-derived macrophages and pulmonay artery endothelial cells. *Veterinary immunology …*, 136(530), pp.292–296.

Elbers, A.R.W. et al., 2008. Field observations during the bluetongue serotype 8 epidemic in 2006. I. Detection of first outbreaks and clinical signs in sheep and cattle in Belgium, France and the Netherlands. *Preventive Veterinary Medicine*, 87(1–2), pp.21–30.

Ellis, J.A. et al., 1993. Prevalence of bluetongue virus expression in leukocytes from experimentally infected ruminants. *American journal of veterinary research*, 54(9), pp.1452–6.

Ellis, J.A. et al., 1990. T Lymphocyte Subset Alterations Following Bluetongue Virus Infection in Sheep and Cattle. *Veterinary Immunology and Immunopathology*, 24(1), pp.49–67.

Ellis, J. a et al., 1991. Cutaneous lymphoid traffic in sheep infected with bluetongue virus. *Veterinary pathology*, 28, pp.175–178.

Elnaggar, M.M. et al., 2016. Characterization and use of new monoclonal antibodies to CD11c, CD14, and CD163 to analyze the phenotypic complexity of ruminant monocyte subsets. *Veterinary Immunology and Immunopathology*.

Erasmus, B.J., 1975. Bluetongue in sheep and goats. *Australian veterinary journal*, 51(4), pp.165–70.

Etzioni, A. & Ochs, H.D., 2004. The hyper IgM syndrome - An evolving story.

Pediatric Research, 56(4), pp.519–525.

Falconi, C., López-Olvera, J.R. & Gortázar, C., 2011. BTV infection in wild ruminants, with emphasis on red deer: A review. *Veterinary Microbiology*, 151(3–4), pp.209–219.

Fernández-Pacheco, P. et al., 2008. Bluetongue virus serotype 1 in wild mouflons in Spain. *Veterinary Record*, 162(20), p.659.

Fletcher, A.L. et al., 2011. Reproducible isolation of lymph node stromal cells reveals site-dependent differences in fibroblastic reticular cells. *Frontiers in Immunology*, 2(SEP), p.35.

Forzan, M., Marsh, M. & Roy, P., 2007. Bluetongue virus entry into cells. *Journal of virology*, 81(9), pp.4819–4827.

Forzan, M., Wirblich, C. & Roy, P., 2004. A capsid protein of nonenveloped Bluetongue virus exhibits membrane fusion activity. *Proc Natl Acad Sci U S A*, 101(7), pp.2100–2105.

Foster, N.M. et al., 1991. Temporal relationships of viremia, interferon activity, and antibody responses of sheep infected with several bluetongue virus strains. *American Journal of Veterinary Research*, 52(2), pp.192–196.

Franchi, P. et al., 2008. Laboratory tests for evaluating the level of attenuation of bluetongue virus. *Journal of Virological Methods*, 153(2), pp.263–265.

Fujiwara, M., Tsunoda, R. & Shigeta, S., 1999. Human Follicular Dendritic Cells Remain Uninfected and Capture Human Immunodeficiency Virus Type 1 through CD54-CD11a. *Journal of* ….

Gambles, R.M., 1949. Bluetongue of Sheep in Cyprus. *Journal of Comparative Pathology and Therapeutics*, 59, pp.176–190.

García-Bocanegra, I. et al., 2011. Role of wild ruminants in the epidemiology of bluetongue virus serotypes 1, 4 and 8 in Spain. *Veterinary Research*, 42(1), pp.1–7.

Gaya, M. et al., 2015. Inflammation-induced disruption of SCS macrophages impairs B cell responses to secondary infection. *Science (New York, N.Y.)*, 347(6222), pp.667–72.

Geisbert, T.W. et al., 2003. Pathogenesis of Ebola Hemorrhagic Fever in Cynomolgus Macaques. *The American journal of pathology*, 163(6), pp.2347–2370.

Gerry, A.C. & Mullens, B. a, 2000. Seasonal Abundance and Survivorship of <I>Culicoides sonorensis</I> (Diptera: Ceratopogonidae) at a Southern California Dairy, with Reference to Potential Bluetongue Virus Transmission and Persistence. *Journal of Medical Entomology*, 37(5), pp.675–688.

Ghalib, H.W., Schore, C.E. & Osburn, B.I., 1985. Immune response of sheep to bluetongue virus: In vitro induced lymphocyte blastogenesis. *Veterinary Immunology and Immunopathology*, 10(2–3), pp.177–188.

Gibbs, E.P., Lawman, M.J. & Herniman, K.A., 1979. Preliminary observations on transplacental infection of bluetongue virus in sheep-a possible overwintering mechanism. *Res Vet Sci*, 27(1), pp.118–120.

Girard, J.-P., Moussion, C. & Förster, R., 2012. HEVs, lymphatics and homeostatic immune cell trafficking in lymph nodes. *Nature Reviews Immunology*, 12(11), pp.762–773.

González, L. et al., 2001. Detection of immune system cells in paraffin wax-embedded ovine tissues. *Journal of Comparative Pathology*, 125(1), pp.41–47.

Gonzalez, R.J. et al., 2015. Dissemination of a Highly Virulent Pathogen: Tracking The Early Events That Define Infection. *PLoS Pathogens*, 11(1), pp.1–18.

Gonzalez, S.F. et al., 2010. Capture of influenza by medullary dendritic cells via SIGN-R1 is essential for humoral immunity in draining lymph nodes. *Nature immunology*, 11(5), pp.427–434.

Gould, A.R. & Pritchard, L.I., 1990. Relationships amongst bluetongue viruses revealed by comparisons of capsid and outer coat protein nucleotide sequences. *Virus Research*, 17(1), pp.31–52.

Grant, C.F. et al., 2012. Assessment of T-dependent and T-independent immune responses in cattle using a B cell ELISPOT assay. *Veterinary Research*, 43(1), p.1.

Gray, E.E. & Cyster, J.G., 2012. Lymph node macrophages. *Journal of Innate Immunity*, 4(5–6), pp.424–436.

Gretz, J.E. et al., 1996. Sophisticated strategies for information encounter in the lymph node: the reticular network as a conduit of soluble information and a highway for cell traffic. *Journal of immunology*, 157(2), pp.495–499.

Gretz, J.E., Anderson, a O. & Shaw, S., 1997. Cords, channels, corridors and conduits: critical architectural elements facilitating cell interactions in the lymph node cortex. *Immunological reviews*, 156, pp.11–24.

Grimes, J.M. et al., 1998. The atomic structure of the bluetongue virus core. *Nature*, 395(6701), pp.470–478.

Gu, X. et al., 2014. Longitudinal study of the detection of Bluetongue virus in bull semen and comparison of real-time polymerase chain reaction assays. *Journal of Veterinary Diagnostic Investigation*, 26(1), pp.18–26.

Guilliams, M. et al., 2010. From skin dendritic cells to a simplified classification of human and mouse dendritic cell subsets. *European Journal of Immunology*, 40(8), pp.2089–2094.

Han, Z. & Harty, R.N., 2004. The NS3 protein of bluetongue virus exhibits viroporin-like properties. *Journal of Biological Chemistry*, 279(41), pp.43092–43097.

Hangartner, L., Zinkernagel, R.M. & Hengartner, H., 2006. Antiviral antibody responses: the two extremes of a wide spectrum. *Nature reviews*.

Immunology, 6(3), pp.231–43.

Hardy, W.T. & Price, D.A., 1952. Soremuzzle of sheep. *Journal of the American Veterinary Medical Association*, 120(898), pp.23–5.

Heesters, B.A. et al., 2015. Follicular Dendritic Cells Retain Infectious HIV in Cycling Endosomes. *PLoS Pathogens*, 11(12), p.e1005285.

Hemati, B. et al., 2009. Bluetongue virus targets conventional dendritic cells in skin lymph. *Journal of virology*, 83(17), pp.8789–99.

Henri, S. et al., 2001. The dendritic cell populations of mouse lymph nodes. *Journal of immunology (Baltimore, Md. : 1950)*, 167(2), pp.741–748.

Herrmann-Hoesing, L.M. et al., 2010. Ovine progressive pneumonia virus capsid antigen as found in CD163- and CD172a-positive alveolar macrophages of persistently infected sheep. *Veterinary pathology*, 47(3), pp.518–28.

Herrmann, L.M. et al., 2003. CD21-Positive Follicular Dendritic Cells. *The American Journal of Pathology*, 162(4), pp.1075–1081.

Hirosue, S. & Dubrot, J., 2015. Modes of antigen presentation by lymph node stromal cells and their immunological implications. *Frontiers in Immunology*, 6(SEP).

Hofmann, M.A. et al., 2008. Genetic characterization of toggenburg orbivirus, a new bluetongue virus, from goats, Switzerland. *Emerging Infectious Diseases*, 14(12), pp.1855–1861.

Holmes, E.C., 2003. Patterns of intra- and interhost nonsynonymous variation reveal strong purifying selection in dengue virus. *Journal of virology*, 77(20), pp.11296–11298.

Hopkins, J., Dutia, B.M. & McConnell, I., 1986. Monoclonal antibodies to sheep lymphocytes I. IDENTIFICATION OF MHC CLASS II MOLECULES ON LYMPHOID TISSUE AND CHANGES IN THE LEVEL OF CLASS II EXPRESSION ON LYMPH-BORNE CELLS FOLLOWING ANTIGEN STIMULATION IN VIVO. , (1981).

Hourrigan, J.L. & Klingsporn, a L., 1975. Bluetongue: the disease in cattle. *Australian veterinary journal*, 51(4), pp.170–4.

Howell, P.G., Kumm, N.A. & Botha, M.J., 1970. The application of improved techniques to the identification of strains of bluetongue virus. *Onderstepoort J Vet Res*, 37(1), pp.59–66.

Howerth, E.W., Greene, C.E. & Prestwood, A.K., 1988. Experimentally induced bluetongue virus infection in white-tailed deer: coagulation, clinical pathologic, and gross pathologic changes. *American Journal of Veterinary Research*, 49(11), pp.1906–1913.

Huismans, H. et al., 1987. Isolation of a Capsid Protein of Bluetongue Virus That Induces a Protective Immune Response in Sheep. *Virology*, 179, pp.172–179.

Huismans, H. & Erasmus, B.J., 1981. Identification of the serotype-specific and group-specific antigens of bluetongue virus. *The Onderstepoort journal of veterinary research*, 48(2), pp.51–58.

Iannacone, M. et al., 2010. Subcapsular sinus macrophages prevent CNS invasion on peripheral infection with a neurotropic virus. *Nature*, 465(7301), pp.1079–1083.

Itano, A.A. et al., 2003. Distinct dendritic cell populations sequentially present antigen to CD4 T cells and stimulate different aspects of cell-mediated immunity. *Immunity*, 19(1), pp.47–57.

Janardhana, V. et al., 1999. The ovine cytotoxic T lymphocyte responses to bluetongue virus. *Research in veterinary science*, 67(3), pp.213–221.

Janowicz, A. et al., 2015. Multiple genome segments determine virulence of bluetongue virus serotype 8. *Journal of virology*, 89(10), pp.5238–49.

Jarjour, M. et al., 2014. Fate mapping reveals origin and dynamics of lymph node follicular dendritic cells. *The Journal of Experimental Medicine*, 211(6), pp.1109–1122.

Jeggo, M.H., 1986. A review of the immune response to bluetongue virus. *Revue scientifique et technique (International Office of Epizootics)*, 5(2), pp.357–362.

Jeggo, M.H. & Wardley, R.C., 1982. Generation of cross-reactive cytotoxic T lymphocytes following immunization of mice with various bluetongue virus types. *Immunology*, 45(4), pp.629–35.

Jeggo, M.H., Wardley, R.C. & Brownlie, J., 1984. A study of the role of cell-mediated immunity in bluetongue virus infection in sheep, using cellular adoptive transfer techniques. *Immunology*, 52(3), pp.403–10.

Jeggo, M.H., Wardley, R.C. & Taylor, W.P., 1984. Role of neutralising antibody in passive immunity to bluetongue infection. *Research in veterinary science*, 36(1), pp.81–6.

Jenckel, M. et al., 2015. Complete coding genome sequence of putative novel bluetongue virus serotype 27. *Genome announcements*, 3(2), pp.16–17.

Jimenez-Clavero, M. a. et al., 2006. High Throughput Detection of Bluetongue Virus by a New Real-Time Fluorogenic Reverse Transcription--Polymerase Chain Reaction: Application on Clinical Samples from Current Mediterranean Outbreaks. *Journal of Veterinary Diagnostic Investigation*, 18(1), pp.7–17.

Johnson, L.A. et al., 2006. An inflammation-induced mechanism for leukocyte transmigration across lymphatic vessel endothelium. *Journal of Experimental Medicine*, 203(12), pp.2763–2777.

Jones, L.D. et al., 1997. Baculovirus-expressed nonstructural protein NS2 of bluetongue virus induces a cytotoxic T-cell response in mice which affords partial protection. *Clinical and diagnostic laboratory immunology*, 4(3), pp.297–301.

Junt, T. et al., 2007. Subcapsular sinus macrophages in lymph nodes clear lymph-borne viruses and present them to antiviral B cells. *Nature*, 450(7166), pp.110–114.

Junt, T., Scandella, E. & Ludewig, B., 2008. Form follows function: lymphoid tissue microarchitecture in antimicrobial immune defence. *Nature reviews. Immunology*, 8(10), pp.764–775.

Kar, A.K., Bhattacharya, B. & Roy, P., 2007. Bluetongue virus RNA binding protein NS2 is a modulator of viral replication and assembly. *BMC molecular biology*, 8, p.4.

Karstad, L. & Trainer, D.O., 1967. Histopathology of experimental bluetongue disease of white-tailed deer. *Canadian Veterinary Journal*, 8(11), pp.247–254.

Kastenmüller, W. et al., 2012. A spatially-organized multicellular innate immune response in lymph nodes limits systemic pathogen spread. *Cell*, 150(6), pp.1235–1248.

Katakai, T., 2012. Marginal reticular cells: A stromal subset directly descended from the lymphoid tissue organizer. *Frontiers in Immunology*, 3(JUL), p.200.

Katakai, T. et al., 2008. Organizer-like reticular stromal cell layer common to adult secondary lymphoid organs. *Journal of immunology (Baltimore, Md. : 1950)*, 181(9), pp.6189–6200.

Kirkland, P.D. et al., 2004. Excretion of bluetongue virus in cattle semen: a feature of laboratory-adapted virus. *Veterinaria italiana*, 40(4), pp.497–501.

Koni, P. a et al., 1997. Distinct roles in lymphoid organogenesis for lymphotoxins alpha and beta revealed in lymphotoxin beta-deficient mice. *Immunity*, 6(4), pp.491–500.

Koni, P. & Flavell, R., 1999. Lymph Node Germinal Centers Form in the Absence of follicular dendritic cell network. *The Journal of experimental medicine*, 189(5), pp.855–864.

Koumbati, M. et al., 1999. Duration of bluetongue viraemia and serological responses in experimentally infected European breeds of sheep and goats.

Veterinary Microbiology, 64(4), pp.277–285.

Kruse, M. et al., 2000. Mature dendritic cells infected with herpes simplex virus type 1 exhibit inhibited T-cell stimulatory capacity. *J.Virol.*, 74(0022–538X (Print)), pp.7127–7136.

Krzyzak, L. et al., 2016. CD83 Modulates B Cell Activation and Germinal Center Responses. *The Journal of Immunology*, 196(9), pp.3581–3594.

Kummer, M. et al., 2007. Herpes simplex virus type 1 induces CD83 degradation in mature dendritic cells with immediate-early kinetics via the cellular proteasome. *J Virol*, 81(12), pp.6326–6338.

Lämmermann, T. & Sixt, M., 2008. The microanatomy of T-cell responses. *Immunological Reviews*, 221(1), pp.26–43.

Lee, F. et al., 2011. Presence of bluetongue virus in the marginal zone of the spleen in acute infected sheep. *Veterinary Microbiology*, 152(1–2), pp.96–100.

Lefevre, E. a et al., 2007. Fibrinogen is localized on dark zone follicular dendritic cells in vivo and enhances the proliferation and survival of a centroblastic cell line in vitro. *Journal of leukocyte biology*, 82(3), pp.666–677.

Letchworth, G.J. & Appleton, J.A., 1983. Passive protection of mice and sheep against bluetongue virus by a neutralizing monoclonal antibody. *Infection and Immunity*, 39(1), pp.208–212.

Libraty, D.H. et al., 2002. Clinical and immunological risk factors for severe disease in Japanese encephalitis. *Trans R Soc Trop Med Hyg*, 96(2), pp.173–178.

Linden, A. et al., 2010. Bluetongue Virus in Wild Deer, Belgium, 2005–2008. *Emerging Infectious Diseases*, 16(5), pp.833–836.

Link, A. et al., 2007. Fibroblastic reticular cells in lymph nodes regulate the

homeostasis of naive T cells. *Nature Immunology*, 8(11), pp.1255–1265.

Maan, S. et al., 2008. Sequence analysis of bluetongue virus serotype 8 from the Netherlands 2006 and comparison to other European strains. *Virology*, 377(2), pp.308–318.

Mackay, F. & Browning, J.L., 1998. Turning off follicular dendritic cells. *Nature*, 395(September), pp.26–7.

MacLachlan, N.J., 2011. Bluetongue: History, global epidemiology, and pathogenesis. *Preventive Veterinary Medicine*, 102(2), pp.107–111.

MacLachlan, N.J. et al., 1994. Detection of bluetongue virus in the blood of inoculated calves: comparison of virus isolation, PCR assay, and in vitro feeding ofCulicoides variipennis. *Archives of Virology*, 136(1–2), pp.1–8.

MacLachlan, N.J. et al., 2008. Experimental reproduction of severe bluetongue in sheep. *Veterinary Pathology*, 45(3), pp.310–315.

MacLachlan, N.J. et al., 2014. The immune response of ruminant livestock to bluetongue virus: From type I interferon to antibody. *Virus Research*, 182, pp.71–77.

MacLachlan, N.J., 1994. The pathogenesis and immunology of bluetongue virus infection of ruminants. *Comparative Immunology, Microbiology and Infectious Diseases*, 17(3–4), pp.197–206.

MacLachlan, N.J. et al., 1990. The pathogenesis of experimental bluetongue virus infection of calves. *Veterinary pathology*, 27(4), pp.223–229.

MacLachlan, N.J. et al., 2009. The Pathology and Pathogenesis of Bluetongue. *Journal of Comparative Pathology*, 141(1), pp.1–16.

Maeda, K. et al., 2002. Immunohistochemical recognition of human follicular dendritic cells (FDCs) in routinely processed paraffin sections. *The journal of histochemistry and cytochemistry : official journal of the Histochemistry Society*, 50(11), pp.1475–1486.

Mahrt, C.R. & Osburn, B.I., 1986. Experimental bluetongue virus infection of sheep; effect of vaccination: pathologic, immunofluorescent, and ultrastructural studies. *American journal of veterinary research*, 47(6), pp.1198–203.

Malhotra, D. et al., 2012. Transcriptional profiling of stroma from inflamed and resting lymph nodes defines immunological hallmarks. … *Immunology*, 13(5), pp.499–510.

Marín-López, A. et al., 2014. VP2, VP7, and NS1 proteins of bluetongue virus targeted in avian reovirus muNS-Mi microspheres elicit a protective immune response in IFNAR(-/-) mice. *Antiviral research*, 110(1), pp.42–51.

Martinez-Pomares, L. & Gordon, S., 2012. CD169 + macrophages at the crossroads of antigen presentation. *Trends in Immunology*, 33(2), pp.66–70.

Matsumoto, M. et al., 1997. Lymphotoxin-alpha-deficient and TNF receptor-I-deficient mice define developmental and functional characteristics of germinal centers. *Immunological Reviews*, 156(1), pp.137–144.

McColl, K.A. & Gould, A.R., 1994. Bluetongue virus infection in sheep: haematological changes and detection by polymerase chain reaction. *Aust Vet J*, 71(4), pp.97–101.

Mecham, J.O. & McHolland, L.E., 2010. Measurement of bluetongue virus binding to a mammalian cell surface receptor by an in situ immune fluorescent staining technique. *Journal of Virological Methods*, 165(1), pp.112–115.

Meltzee, E., 2016. Book of my Life. In *The more I know, the less I understand. Be aware, my friend, of what is really worth and what is not. Enjoy your journey.* pp. 1–36.

Mertens, P.P.C. et al., 1989. Analysis of the roles of bluetongue virus outer capsid proteins VP2 and VP5 in determination of virus serotype. *Virology*, 170(2), pp.561–565.

Mintiens, K. et al., 2008. Possible routes of introduction of bluetongue virus serotype 8 into the epicentre of the 2006 epidemic in north-western Europe. *Preventive Veterinary Medicine*, 87(1–2), pp.131–144.

Mohl, B.-P. & Roy, P., 2014. Bluetongue Virus Capsid Assembly and Maturation. *Viruses*, 6(8), pp.3250–3270.

Morrow, G. et al., 2003. Varicella-Zoster virus productively infects mature dendritic cells and alters their immune function. *Journal Of Virology*, 77(8), pp.4950–4959.

Mortola, E., Noad, R. & Roy, P., 2004. Bluetongue virus outer capsid proteins are sufficient to trigger apoptosis in mammalian cells. *Journal of virology*, 78(6), pp.2875–83.

Mueller, S.N. et al., 2007. Viral targeting of fibroblastic reticular cells contributes to immunosuppression and persistence during chronic infection. *Proceedings of the National Academy of Sciences of the United States of America*, 104(39), pp.15430–15435.

Mueller, S.N. & Germain, R.N., 2009. Stromal cell contributions to the homeostasis and functionality of the immune system. *Nature reviews. Immunology*, 9(9), pp.618–29.

Mwangi, D.M., Hopkins, J. & Luckins, a G., 1991. Immunohistology of lymph nodes draining local skin reactions (chancres) in sheep infected with Trypanosoma congolense. *Journal of comparative pathology*, 105(1), pp.27–35.

Nair, N. et al., 2007. Age-dependent differences in IgG isotype and avidity induced by measles vaccine received during the first year of life. *The Journal of infectious diseases*, 196(9), pp.1339–1345.

Narayan, O. & Johnson, R.T., 1972. Effects of viral infection on nervous system development. I. Pathogenesis of bluetongue virus infection in mice. *The American journal of pathology*, 68(1), pp.1–14.

Neitz, W., 1948. Immunological studies on bluetongue in sheep. *Onderstepoort Journal of Veterinary Science and Animal Industry*, 23, pp.93–136.

Nomikou, K. et al., 2015. Widespread Reassortment Shapes the Evolution and Epidemiology of Bluetongue Virus following European Invasion. *PLoS Pathogens*, 11(8), pp.1–23.

Nunamaker, R.A. et al., 1990. Absence of transovarial transmission of bluetongue virus in Culicoides variipennis: Immunogold labelling of bluetongue virus antigen in developing oocytes from Culicoides variipennis (Coquillett). *Comparative Biochemistry and Physiology Part A: Physiology*, 96(1), pp.19–31.

Nunes, S.F. et al., 2014. A Synthetic Biology Approach for a Vaccine Platform against Known and Newly Emerging Serotypes of Bluetongue Virus. *Journal of virology*, 88(21), pp.12222–32.

Odeón, A.C., Gershwin, L.J. & Osburn, B.I., 1999. IgE responses to bluetongue virus (BTV) serotype 11 after immunization with inactivated BTV and challenge infection. *Comparative Immunology, Microbiology and Infectious Diseases*, 22(2), pp.145–162.

OIE - World Organisation for Animal Health, 2016a. Bluetongue (Infection with Bluetongue Virus). In Intergovernmental Panel on Climate Change, ed. *Manual of Diagnostic Tests and Vaccines for Terrestrial Animals*. Cambridge: Cambridge University Press, pp. 1–30.

OIE - World Organisation for Animal Health, 2016b. Infection with bluetongue virus. In *Terrestrial Animal Health Code*. pp. 1–10.

Olsen, L. et al., 2015. The early intestinal immune response in experimental neonatal ovine cryptosporidiosis is characterized by an increased frequency of perforin expressing NCR1+ NK cells and by NCR1− CD8+ cell recruitment. *Veterinary Research*, 46(28), pp.1–17.

Ortego, J., de la Poza, F. & Marín-López, A., 2014. Interferon α/β receptor

knockout mice as a model to study bluetongue virus infection. *Virus Research*, 182, pp.35–42.

Osburn, B.I., 1994. The impact of bluetongue virus on reproduction. *Comparative Immunology, Microbiology and Infectious Diseases*, 17(3–4), pp.189–196.

Owens, R.J., Limn, C. & Roy, P., 2004. Role of an arbovirus nonstructural protein in cellular pathogenesis and virus release. *Journal of virology*, 78(12), pp.6649–6656.

Pages, N. et al., 2014. Culicoides midge bites modulate the host response and impact on bluetongue virus infection in sheep. *PLoS ONE*, 9(1), p.e83683.

Pérez de Diego, A.C., Sánchez-Cordón, P.J. & Sánchez-Vizcaíno, J.M., 2014. Bluetongue in Spain: from the first outbreak to 2012. *Transboundary and emerging diseases*, 61(6), pp.e1-11.

Phan, T.G. et al., 2009. Immune complex relay by subcapsular sinus macrophages and noncognate B cells drives antibody affinity maturation. *Nature immunology*, 10(7), pp.786–93.

Phan, T.G. et al., 2007. Subcapsular encounter and complement-dependent transport of immune complexes by lymph node B cells. *Nature immunology*, 8(9), pp.992–1000.

Pingen, M. et al., 2016. Host Inflammatory Response to Mosquito Bites Enhances the Severity of Arbovirus Infection. *Immunity*, 44(6), pp.1455–1469.

Pini, A., 1976. Study on the pathogenesis of bluetongue: replication of the virus in the organs of infected sheep. *The Onderstepoort journal of veterinary research*, 43(4), pp.159–164.

Polack, F.P. et al., 2003. A role for nonprotective complement-fixing antibodies with low avidity for measles virus in atypical measles. *Nature medicine*, 9(9), pp.1209–1213.

Polack, F.P. et al., 1999. Production of atypical measles in rhesus macaques: evidence for disease mediated by immune complex formation and eosinophils in the presence of fusion-inhibiting antibody. *Nature medicine*, 5(6), pp.629–34.

Prasad, B.V.V., Yamaguchi, S. & Roy, P., 1992. Three-Dimensional Structure of Single-Shelled Bluetongue Virus. , 66(4), pp.2135–2142.

Pullen, G.R., Fitzgerald, M.G. & Hosking, C.S., 1986. Antibody avidity determination by ELISA using thiocyanate elution. *Journal of Immunological Methods*, 86(1), pp.83–87.

Purse, B. V et al., 2005. Climate change and the recent emergence of bluetongue in Europe. *Nature reviews. Microbiology*, 3(2), pp.171–181.

Randolph, G.J., Angeli, V. & Swartz, M.A., 2005. Dendritic-cell trafficking to lymph nodes through lymphatic vessels. *Nature Reviews. Immunology*, 5(8), pp.617–28.

Randolph, G.J., Ochando, J. & Partida-Sánchez, S., 2008. Migration of dendritic cell subsets and their precursors. *Annual review of immunology*, 26, pp.293–316.

Rantakari, P. et al., 2015. The endothelial protein PLVAP in lymphatics controls the entry of lymphocytes and antigens into lymph nodes. *Nature immunology*, 16(4), pp.386–96.

Rasmussen, L. et al., 2013. Transplacental transmission of field and rescued strains of BTV-2 and BTV-8 in experimentally infected sheep. *Veterinary Research*, 44(1), p.75.

Ratinier, M. et al., 2016. Bluetongue virus NS4 protein is an interferon antagonist and a determinant of virus virulence. *Journal of Virology*, p.JVI.00422-16.

Ratinier, M. et al., 2011. Identification and characterization of a novel non-structural protein of bluetongue virus. *PLoS Pathogens*, 7(12), p.e1002477.

Raymond, I. et al., 1997. CNA.42, a new monoclonal antibody directed against a fixative-resistant antigen of follicular dendritic reticulum cells. *The American journal of pathology*, 151(6), pp.1577–1585.

Reed, L.. & Muench, H., 1938. A simple method of estimating fifty per cent end points. *American journal of epidemiology*, 3(3), pp.493–7.

Renshaw, B.R. et al., 1994. Humoral immune responses in CD40 ligand-deficient mice. *The Journal of experimental medicine*, 180(5), pp.1889–900.

Richards, R.G. et al., 1988. Comparison of virologic and serologic responses of lambs and calves infected with bluetongue virus Serotype 10. *Veterinary Microbiology*, 18(3–4), pp.233–242.

Romero-Palomo, F. et al., 2013. Immunohistochemical detection of dendritic cell markers in cattle. *Veterinary pathology*, 50(6), pp.1099–108.

Roozendaal, R. et al., 2009. Conduits Mediate Transport of Low-Molecular-Weight Antigen to Lymph Node Follicles. *Immunity*, 30(2), pp.264–276.

Roozendaal, R. & Carroll, M.C., 2007. Complement receptors CD21 and CD35 in humoral immunity. *Immunological Reviews*, 219(1), pp.157–166.

Roozendaal, R., Mebius, R.E. & Kraal, G., 2008. The conduit system of the lymph node. *International Immunology*, 20(12), pp.1483–1487.

Ross, R. et al., 2000. Expression of the actin-bundling protein fascin in cultured human dendritic cells correlates with dendritic morphology and cell differentiation. *Journal of Investigative Dermatology*, 115(4), pp.658–663.

Rossi, S. et al., 2014. Bluetongue dynamics in French wildlife: Exploring the driving forces. *Transboundary and Emerging Diseases*, 61(6), pp.e12–e24.

Rossitto, P. V. & MacLachlan, N.J., 1992. Neutralizing epitopes of the serotypes of bluetongue virus present in the United States. *Journal of General Virology*, 73(8), pp.1947–1952.

Rowe, A.K. et al., 1999. Clinical, Virologic, and Immunologic Follow-Up of Convalescent Ebola Hemorrhagic Fever Patients and Their Household Contacts, Kikwit, Democratic Republic of the Congo. *The Journal of Infectious Diseases*, 179(s1), pp.S28–S35.

Roy, P. et al., 1990. Recombinant virus vaccine for bluetongue disease in sheep. *Journal of virology*, 64(5), pp.1998–2003.

Roy, P., Boyce, M. & Noad, R., 2009. Prospects for improved bluetongue vaccines. *Nature reviews. Microbiology*, 7(2), pp.120–128.

Ruscanu, S. et al., 2013. Dendritic Cell Subtypes from Lymph Nodes and Blood Show Contrasted Gene Expression Programs upon Bluetongue Virus Infection. *Journal of Virology*, 87(16), pp.9333–9343.

Ruscanu, S. et al., 2012. The double-stranded RNA bluetongue virus induces type I interferon in plasmacytoid dendritic cells via a MYD88-dependent TLR7/8-independent signaling pathway. *Journal of virology*, 86(10), pp.5817–28.

Russell, H. et al., 1996. Comparative effects of bluetongue virus infection of ovine and bovine endothelial cells. *Veterinary pathology*, 33(3), pp.319–331.

Al Saati, T. et al., 2001. A new monoclonal anti-CD3 antibody reactive on paraffin sections. *Appl Immunohistochem Mol Morphol*, 9(4), pp.289–296.

Saegerman, C., Berkvens, D. & Mellor, P.S., 2008. Bluetongue epidemiology in the European Union. *Emerging Infectious Diseases*, 14(4), pp.539–544.

Sánchez-Cordón, P.J. et al., 2015. Comparative analysis of cellular immune responses and cytokine levels in sheep experimentally infected with bluetongue virus serotype 1 and 8. *Veterinary Microbiology*, 177(1–2), pp.95–105.

Sánchez-Cordón, P.J., Pérez de Diego, A.C., et al., 2013. Comparative study of clinical courses, gross lesions, acute phase response and coagulation disorders in sheep inoculated with bluetongue virus serotype 1 and 8.

Veterinary Microbiology, 166(1–2), pp.95–105.

Sánchez-Cordón, P.J. et al., 2010. Immunohistochemical detection of bluetongue virus in fixed tissue. *Journal of comparative pathology*, 143(1), pp.20–8.

Sánchez-Cordón, P.J., Pedrera, M., et al., 2013. Potential role of proinflammatory cytokines in the pathogenetic mechanisms of vascular lesions in goats naturally infected with bluetongue virus serotype 1. *Transboundary and emerging diseases*, 60(3), pp.252–62.

Santman-Berends, I.M.G.A. et al., 2010. Vertical transmission of bluetongue virus serotype 8 virus in Dutch dairy herds in 2007. *Veterinary Microbiology*, 141(1–2), pp.31–35.

Scandella, E. et al., 2008. Restoration of lymphoid organ integrity through the interaction of lymphoid tissue-inducer cells with stroma of the T cell zone. *Nature immunology*, 9(6), pp.667–75.

Schwartz-Cornil, I. et al., 2008. Bluetongue virus: virology, pathogenesis and immunity. *Veterinary Research*, 39(5), p.46.

Schwickert, T.A. et al., 2009. Germinal center reutilization by newly activated B cells. *The Journal of experimental medicine*, 206(13), pp.2907–14.

Sealfon, R.S. et al., 2015. FRESCo: finding regions of excess synonymous constraint in diverse viruses. *Genome biology*, 16(1), p.38.

Sellers, R.F., Pedgley, D.E. & Tucker, M.R., 1978. Possible windborne spread of bluetongue to Portugal, June-July 1956. *The Journal of hygiene*, 81(2), pp.189–96.

Senechal, B., 2004. Infection of mature monocyte-derived dendritic cells with human cytomegalovirus inhibits stimulation of T-cell proliferation via the release of soluble CD83. *Blood*, 103(11), pp.4207–4215.

Shaw, A.E. et al., 2013. Reassortment between two serologically unrelated

bluetongue virus strains is flexible and can involve any genome segment. *Journal of virology*, 87(1), pp.543–57.

Shepherd, A.J., Swanepoel, R. & Leman, P.A., 1989. Antibody response in Crimean-Congo hemorrhagic fever. *Reviews of infectious diseases*, 11 Suppl 4(June), pp.S801–6.

De Silva, N.S. & Klein, U., 2015. Dynamics of B cells in germinal centres. *Nature Reviews Immunology*, 15(3), pp.137–148.

Singer, R.S., MacLachlan, N.J. & Carpenter, T.E., 2001. Maximal Predicted Duration of Viremia in Bluetongue Virus--Infected Cattle. *Journal of Veterinary Diagnostic Investigation*, 13(1), pp.43–49.

Sixt, M. et al., 2005. The conduit system transports soluble antigens from the afferent lymph to resident dendritic cells in the T cell area of the lymph node. *Immunity*, 22(1), pp.19–29.

Van Der Sluijs, M.T.W. et al., 2013. Transplacental transmission of bluetongue virus serotype 1 and serotype 8 in sheep: Virological and pathological findings. *PLoS ONE*, 8(12), pp.4–12.

Smelt, S.C. et al., 1997. Destruction of follicular dendritic cells during chronic visceral leishmaniasis. *The Journal of Immunology*, 158(8), pp.3813–3821.

Spreull, J., 1905. Malarial catarrhal fever (bluetongue) of sheep in South Africa. *Journal of Comparative Pathology and Therapeutics*, 18, pp.321–337.

Stair, E.L., 1968. *The pathogenesis of bluetongue in sheep: a study by immunofluorescence and histopathology, dissertation,*. Texas A & M University.

Steele, K.E., Anderson, A.O. & Mohamadzadeh, M., 2009. Fibroblastic reticular cell infection by hemorrhagic fever viruses. *Immunotherapy*, 1, pp.187–197.

Stewart, M. et al., 2015. Characterization of a second open reading frame in genome segment 10 of bluetongue virus. *Journal of General Virology*,

96(11), pp.3280–3293.

Stewart, M. et al., 2012. Protective efficacy of Bluetongue virus-like and subvirus-like particles in sheep: Presence of the serotype-specific VP2, independent of its geographic lineage, is essential for protection. *Vaccine*, 30(12), pp.2131–2139.

Stott, J.L. et al., 1982. Clinical expression of bluetongue disease in cattle. *Proceedings of the Annual Meeting of the United States Animal Health Association*, 86, pp.126–131.

Stott, J.L. et al., 1990. Interaction of bluetongue virus with bovine lymphocytes. *Journal of General Virology*, 71(2), pp.363–368.

Sukumar, S., Szakal, A.K. & Tew, J.G., 2006. Isolation of functionally active murine follicular dendritic cells. *Journal of Immunological Methods*, 313(1–2), pp.81–95.

Swartz, M.A., 2001. The physiology of the lymphatic system. *Advanced Drug Delivery Reviews*, 50(1–2), pp.3–20.

Takamatsu, H. et al., 2003. A possible overwintering mechanism for bluetongue virus in the absence of the insect vector. *Journal of General Virology*, 84(1), pp.227–235.

Takamatsu, H. & Jeggo, M.H., 1988. Cultivation of Bluetongue virus-specific ovine T cells and their cross-reactivity with different serotype viruses. *Immunology*, 66, pp.258–263.

Theiler, A., 1907. Inoculation of sheep against Blue tongue and the results in practice. , (l), pp.263–264.

Thorne, E.T. et al., 1988. Bluetongue in free-ranging pronghorn antelope (Antilocapra americana) in Wyoming: 1976 and 1984. *Journal of wildlife diseases*, 24(1), pp.113–119.

Du Toit, R.M., 1944. The transmission of blue-tongue and horse-sickness by

Culicoides. *Onderstepoort Journal of Veterinary Science and Animal Industry*, 19, pp.7–16.

Troxell, M.L. et al., 2005. Follicular dendritic cell immunohistochemical markers in angioimmunoblastic T-cell lymphoma. *Applied immunohistochemistry & molecular morphology : AIMM / official publication of the Society for Applied Immunohistochemistry*, 13(4), pp.297–303.

Turley, S.J., Fletcher, A.L. & Elpek, K.G., 2010. The stromal and haematopoietic antigen-presenting cells that reside in secondary lymphoid organs. *Nature reviews. Immunology*, 10(12), pp.813–825.

Umeshappa, C.S. et al., 2011. A comparison of intradermal and intravenous inoculation of bluetongue virus serotype 23 in sheep for clinico-pathology, and viral and immune responses. *Veterinary Immunology and Immunopathology*, 141(3–4), pp.230–238.

Umeshappa, C.S., Singh, et al., 2010. Apoptosis and immuno-suppression in sheep infected with bluetongue virus serotype-23. *Veterinary Microbiology*, 144(3–4), pp.310–318.

Umeshappa, C.S., Singh, K.P., et al., 2010. Cell-mediated immune response and cross-protective efficacy of binary ethylenimine-inactivated bluetongue virus serotype-1 vaccine in sheep. *Vaccine*, 28(13), pp.2522–2531.

Vakkila, J. et al., 2005. A basis for distinguishing cultured dendritic cells and macrophages in cytospins and fixed sections. *Pediatric and Developmental Pathology*, 8(1), pp.43–51.

Veronesi, E. et al., 2010. Viraemia and clinical disease in Dorset Poll sheep following vaccination with live attenuated bluetongue virus vaccines serotypes 16 and 4. *Vaccine*, 28(5), pp.1397–1403.

Veronesi, E., Hamblin, C. & Mellor, P.S., 2005. Live attenuated bluetongue vaccine viruses in Dorset Poll sheep, before and after passage in vector midges (Diptera: Ceratopogonidae). *Vaccine*, 23(48–49), pp.5509–5516.

Verwoerd, D.W. et al., 1972. Structure of the bluetongue virus capsid. *J Virol*, 10(4), pp.783–794.

Victora, G.D. et al., 2012. Identification of human germinal center light and dark zone cells and their relationship to human B-cell lymphomas. *Blood*, 120(11), pp.2240–2248.

Victora, G.D. & Nussenzweig, M.C., 2012. Germinal centers. *Annu Rev Immunol*, 30, pp.429–457.

Vignuzzi, M. et al., 2006. Quasispecies diversity determines pathogenesis through cooperative interactions in a viral population. *Nature*, 439(7074), pp.344–348.

Vinuesa, C.G. et al., 2010. T cells and follicular dendritic cells in germinal center B-cell formation and selection. *Immunological Reviews*, 237(1), pp.72–89.

Vosdingh, R.A., Trainer, D.O. & Easterday, B.C., 1968. Experimental bluetongue disease in white-tailed deer. *Canadian journal of comparative medicine and veterinary science*, 32(1), pp.382–7.

Wade-Evans, A.M. et al., 1996. Expression of the major core structural protein (VP7) of bluetongue virus, by a recombinant capripox virus, provides partial protection of sheep against a virulent heterotypic bluetongue virus challenge. *Virology*, 220(1), pp.227–31.

Waldvogel, A.S. et al., 1987. Neurovirulence of the UC-2 and UC-8 strains of bluetongue virus serotype 11 in newborn mice. *Vet Pathol*, 24(5), pp.404–410.

Waldvogel, A.S. et al., 1986. Strain-dependent virulence characteristics of bluetongue virus serotype 11. *Journal of General Virology*, 67(4), pp.765–769.

Wang, X. et al., 2011. Follicular dendritic cells help establish follicle identity

and promote B cell retention in germinal centers. *Journal of Experimental Medicine*, 208(12), pp.2497–2510.

Weaver, S.C. et al., 1999. Genetic and fitness changes accompanying adaptation of an arbovirus to vertebrate and invertebrate cells. *Journal of virology*, 73(5), pp.4316–4326.

Weaver, S.C. & Reisen, W.K., 2010. Present and future arboviral threats. *Antiviral Research*, 85(2), pp.328–345.

Wechsler, S.J., McHolland, L.E. & Tabachnick, W.J., 1989. Cell lines from Culicoides variipennis (Diptera: Ceratopogonidae) support replication of bluetongue virus. *Journal of Invertebrate Pathology*, 54(3), pp.385–393.

Whetter, L.E. et al., 1989. Bluetongue virus infection of bovine monocytes. *The Journal of general virology*, 70 (Pt 7), pp.1663–76.

White, D.M. et al., 2005. Studies on overwintering of bluetongue viruses in insects. *Journal of General Virology*, 86(2), pp.453–462.

Willard-Mack, C.L., 2006. Normal structure, function, and histology of lymph nodes. *Toxicologic pathology*, 34(5), pp.409–24.

Wilson, A., Darpel, K. & Mellor, P.S., 2008. Where does bluetongue virus sleep in the winter? *PLoS Biology*, 6(8), pp.1612–1617.

Wilson, A.J. & Mellor, P.S., 2009. Bluetongue in Europe: past, present and future. *Philosophical Transactions of the Royal Society B: Biological Sciences*, 364(1530), pp.2669–2681.

Winkelmann, E.R. et al., 2014. Subcapsular sinus macrophages limit dissemination of West Nile virus particles after inoculation but are not essential for the development of West Nile virus-specific T cell responses. *Virology*, 450–451, pp.278–289.

Wolenski, M. et al., 2003. Expression of CD83 in the murine immune system. *Medical Microbiology and Immunology*, 192(4), pp.189–192.

Worwa, G. et al., 2010. Virological and pathological findings in Bluetongue virus serotype 8 infected sheep. *Veterinary Microbiology*, 144(3–4), pp.264–273.

Xu, G. et al., 1997. VP7: An attachment protein of bluetongue virus for cellular receptors in Culicoides variipennis. *Journal of General Virology*, 78(7), pp.1617–1623.

Yoshida, K., van den Berg, T.K. & Dijkstra, C.D., 1993. Two functionally different follicular dendritic cells in secondary lymphoid follicles of mouse spleen, as revealed by CR1/2 and FcR gamma II-mediated immune-complex trapping. *Immunology*, 80(1), pp.34–9.

Zaba, L.C., Krueger, J.G. & Lowes, M.A., 2009. Resident and 'inflammatory' dendritic cells in human skin. *The Journal of investigative dermatology*, 129(2), pp.302–8.

Zhang, X. et al., 2010. Bluetongue virus coat protein VP2 contains sialic acid-binding domains, and VP5 resembles enveloped virus fusion proteins. *Proceedings of the National Academy of Sciences of the United States of America*, 107(14), pp.6292–6297.